DEVELOPING A NON-INVASIVE TREATMENT FOR TWIN-TWIN TRANSFUSION SYNDROME USING HIGH INTENSITY FOCUSED ULTRASOUND IN AN ANIMAL MODEL

A thesis submitted for the degree of

Doctor of Philosophy

of

Imperial College London

by

Caroline Jayne Shaw

Institute of Reproductive and Developmental Biology

Imperial College London

Submitted July 2017

ABSTRACT

High Intensity Focused Ultrasound (HIFU) is a non-invasive, non-ionising technology which can selectively occlude blood vessels. In Twin-Twin Transfusion Syndrome (TTTS), anastomotic placental vessels in a shared placenta allow uneven blood distribution between the twins. Despite advances in prenatal and neonatal care, TTTS remains the leading cause of death and disability in twins. Invasive fetoscopic laser can divide anastomoses, with risks of miscarriage, placental haemorrhage, extreme prematurity or second trimester rupture of membranes. Fetoscopic laser has undergone improvements in technology and therapeutic protocols over two decades, but it still does not consistently improve survival or decrease severe neurological morbidity in surviving twins. Hence, it is only used in severe cases, where benefits outweigh risks, and over 16-18 weeks gestation, after chorion and amnion fusion. This represents an unmet clinical need, which could be addressed by ultrasound-guided HIFU (USgHIFU).

Selective occlusion of placental vessels using HIFU has not been described. Ultrasound identification of placental vascular anastomoses in humans is described, but is not in routine clinical use. Therefore, we tested the efficacy and safety of using USgHIFU as a non-invasive method of placental vascular occlusion in the pregnant sheep.

An iterative study design in six animal groups was used. Treatment protocols for ultrasound guidance and HIFU delivery were developed in three animal groups. The efficacy and rates of associated direct and indirect iatrogenic harm of each version of the protocol was tested in another three animal groups, using invasive and non-invasive measures.

Overall, transdermal USgHIFU occluded 97% of target placental vessels in the most developed treatment protocol. This persisted for 21 days and showed evidence of permanent vessel occlusion by *fibrosis obliterans*. This was achieved without significant adverse events, although maternal skin (2%), uterine (1%) and fetal skin burns (1%) were observed. There were no long-term effects (up to 21 d) of the technique based on assessment of maternal and fetal cardiovascular, metabolic, endocrine and obstetric outcomes, or evidence of fetal compromise.

This study is proof of principle that USgHIFU can be used to occlude placental vessels in the pregnant sheep. There is a low rate of direct iatrogenic harm and no evidence of indirect harm associated with the technique. As such, this supports the concept of future translational studies to develop USgHIFU as a treatment for TTTS in humans.

This thesis is the result of my own original work, **except as acknowledged in sections 3.7.3.1, 4.2.1.1 and Appendix IV**. In these sections, the work presented results from the collaboration with the Institute of Cancer Research and the University of Cambridge to develop and test this technology. The length of this thesis does not exceed the prescribed word limit

Caroline J Shaw

CONTENTS

LIST OF FIGURES

CHAPTER 1

CHAPTER 2

CHAPTER 3

CHAPTER 4

CHAPTER 5

CHAPTER 6

CHAPTER 7

APPENDICES

LIST OF TABLES

CHAPTER 1

CHAPTER 2

CHAPTER 4

CHAPTER 5

CHAPTER 6

CHAPTER 7

CHAPTER 9

APPENDICIES

ACKNOWLEDGEMENTS

My Ph.D. was undertaken at the Institute of Developmental and Reproductive Biology, Imperial College London. I am grateful to my supervisors, **Dr Christoph Lees** and **Professor Phil Bennett** for giving me this opportunity to carry out this research during my speciality training. Despite my insistence that this thesis was a Sisyphean task, Christoph has been a great mentor on whom I know I can rely for guidance, support and a balanced view of life. I thank you for your faith in me, and your friendship through the highs and lows.

This research project was a collaboration between many people and departments, who have all given freely of their time, knowledge, help and advice, and to who I owe many thanks, and the successful completion of this thesis. I would also like to thank **Action Medical Research**, the **Genesis Research Trust** and the **Isaac Newton Trust** for recognising the potential of this research, and their generous support.

The **Therapeutic Ultrasound Team, Institute of Cancer Research**, under the leadership of **Professor Gail ter Haar,** provided essential HIFU knowledge, support and equipment to this project, without which the concept would never have taken flight. It has been a great pleasure to be a part of their team.

Professor Dino Giussani and his team at the **Department of Physiology, University of Cambridge**, provided an invaluable induction into, and resources from, the world of experimental sheep physiology, without which the project, having taken flight, would have quickly fallen to earth. My three years with your team have shaped me into an academic, and I truly appreciate all the opportunities given to me, and the time invested in my training.

To my co-investigators from the Institute of Cancer Research, **Dr Ian Rivens** and **Dr John Civale**, who spent countless hours at my side learning how to occlude placental blood vessels in sheep, through power-cuts, floods, snow, road closures, sheep revolts and tea shortages, I thank you for your good humour, patience and perseverance (and your on-call computer assistance and biscuits).

To my fellow researchers at the University of Cambridge, **Dr Kim Botting** and **Mr Sage Ford**, who were by my side as I learnt how to wrangle sheep and manage a research project - without your hard work and motivation none of this would have been possible. Your help and support in navigating the day-to-day realities of a research project kept me going. It has been an honour and a privilege.

I have also had the opportunity to spend three wonderful years working with the staff of the **Centre for Fetal Care, Queen Charlotte's and Chelsea Hospital**. Thank you for welcoming me into your department, and teaching me how to scan – your care and dedication to your patients is an inspiration, and I miss you all. To **Dr Gowri Paramasivam**, **Dr Shireen Meher**, and **Dr Bryony Jones**, I have truly valued the time I have spent learning from you, and am glad to count you as my friends.

I would also like to thank:

Dr Beth Allison & Dr Kirsty Brain	For all the hard work that produced the recovery control group raw data made available to this research project
Mr Richard Symonds-Tayler	For his technical assistance with all the electrical components of the HIFU system, and his chats over coffee.
Dr Emily Camm	For teaching me not to fear histology!
Dr Katie Davis	For teaching me how to measure cortisol in fetal plasma.
Dr Yougou Niu	For his help during surgical procedures.
Ms Sharon Gander	For her dedicated care of my experimental sheep.

LIST OF ABBREVIATIONS

AAA	Arterio-arterial anastomoses
AC	Abdominal circumference
ANCOVA	Analysis of covariance
ANOVA	Analysis of variance
ANP	Atrial natriuretic peptide
AVA	Arterio-venous anastomoses
AVM	Arterio-venous malformation
BNCs	Binucleated cells
BPD	Bipareital diameter
CA	California
CamDAS	Cambridge Data Acquisition System
CCO	Combined cardiac output
cCTG	Computerised cardiotocograph
CI	Confidence interval
CO_2	Carbon dioxide
CR	Controlled release
CTG	Cardiotocograph
CV	Coefficient of variation
C-STAR	Cross-sectional treatment area ratio
DICOM	Diagnostic Imaging and Communications in Medicine
DV	Ductus venosus
DVP	Deepest vertical pool
DV-PIV	Ductus venosus venous pulsatility index
EDD	End diastolic diameter
EDTA	Ethylenediaminetetraacetic acid
EDV	End diastolic velocity
EF	Ejection fraction
EFW	Estimated fetal weight
EjT	Ejection time
ELISA	Enzyme-linked immunosorbent assay
ESD	End systolic diameter
ET	Endotracheal tube
EtCO2	End tidal carbon dioxide
EXIT	Ex-utero intrapartum treatment

fCaO2	Fetal arterial oxygen content
FGR	Fetal growth restriction
FHR	Fetal heart rate
FHRV	Fetal heart rate variability
FiO2	Fraction of inspired oxygen
FL	Femur length
FS	Fractional shortening
GA	Gestational age
GUI	Graphical user interface
H&E	Haematoxylin and eosin
Hb	Haemoglobin
HC	Head circumference
HF	High frequency
HIFU	High Intensity Focused Ultrasound
IA	Intra-amniotic
ICR	Institute of Cancer Research
ICT	Isovolumetric contraction time
IM	Intramuscular
IQR	Interquartile range
IRT	Isovolumetric relaxation time
IV	Intravenous
IVC	Inferior vena cava
LF	Low frequency
Ltd.	Limited
LV-MPI	Left ventricular myocardial performance index
MA	Massachusetts
MAC	Minimum alveolar concentration
MAP	Mean arterial pressure
MCA	Middle cerebral artery
MCA-PI	Middle cerebral artery pulsatility index
MCA-PSV	Middle cerebral artery peak systolic velocity
MCDA	Monochorionic diamniotic
MI	Missouri
MoM	Multiples of median
MRI	Magnetic resonance imaging

NaCl	Sodium Chloride
nHF	Normalised high frequency
nLF	Normalised low frequency
NR	Not reported
NSW	New South Wales
NY	New York state
NZ	New Zealand
p_aCO_2	Partial pressure of arterial carbon dioxide
p_aO_2	Partial pressure of arterial oxygen
pH_a	Arterial pH
PI	Pulsatility index
PMSG	Pregnant mare's serum gonadotrophin
PRPA	Peak rarefaction pressure amplitude
PSV	Peak systolic velocity
PTAH	Phosphotungstic acid haematoxylin
PTFE	Polytetrafluoroethylene
PV	Per vagina
PVC	Polyvinyl chloride
RFA	Radio frequency ablation
RMSSD	Root mean square or successive differences
SaO_2	Saturation of oxyhaemoglobin (direct measurement in blood analysis)
SpO_2	Saturation of oxyhaemoglobin (indirect measure from pulse oximetry)
SIR	Society of Interventional Radiology
SC	Subcutaneous
SD	Standard deviation
SDNN	Standard deviation of N-N intervals
SEM	Standard error of the mean
SIVA	Supplemental intravenous anaesthesia
STV	Short term variation
SVFL	Selective vessel fetoscopic laser
TAPS	Twin Anaemia-Polycythaemia Syndrome
TTTS	Twin-Twin Transfusion Syndrome
TX	Texas
UA	Umbilical artery
UA-PI	Umbilical artery pulsatility index

UCA	Ultrasound contrast agent
US	Ultrasound
UK	United Kingdom
USA	United States of America
UtA	Uterine artery
UtA-PI	Uterine artery pulsatility index
UV	Umbilical vein
VLF	Very low frequency
VT	Vermont
VVA	Veno-venous anastomoses
WA	Washington state
[ ]	Concentration of
ca.	Circa
~	Approximately
<	Less than
>	Greater than
≤	Less than or equal to
≥	Greater than or equal to

GLOSSARY OF TECHNICAL TERMS

Attenuation	In ultrasound physics, (acoustic) attenuation describes the loss of energy from the ultrasound wave as it passes through a viscous medium, in our situation, overlying tissues. This is specific to the frequency of the ultrasound wave.
CamDAS	The name of a portable, customised data acquisition system, which samples the output of invasive arterial pressure transducers and flow probes, to transmit information about heart rate, arterial pressure and flow to a visual interface.
C-STAR	A ratio devised for this study. It relates the 2D ultrasound appearance of the cross-sectional area containing the target blood vessel to a simplified cross-sectional area that is exposed to the focal zones of all HIFU exposures in a HIFU exposure series. A ratio of 1 indicates the areas are of equal size. If the ratio is <1, the area around the target vessel is larger than the HIFU treatment area; if the ratio is >1, the opposite is true.
Drive voltage	A nominal setting on our customised HIFU system, which was directly adjusted by the operator to deliver more or less ultrasound energy to the target vessel. It is measured in dBm, a unit which describes the power ratio (e.g. electrical to acoustic) of the measured power to one milliwatt.
Focal zone	The region in which the intensity (incident energy per unit area) of HIFU is high enough to produce tissue damage. Also called the HIFU focus.
Free field intensity	The amount of ultrasound energy (per unit area) which would reach the HIFU focus if there were no energy losses along the path of the ultrasound beam.
HIFU exposure series	Refers to a sequence of HIFU exposures with the same exposure characteristics, placed so that individual lesions are joined into a linear track.

Hyperecho	An ultrasound finding of an area of tissue in which the echoes are stronger than the surrounding, similar, tissue. In HIFU research, de novo development of hyperecho is recognised to denote an area of tissue heating.
In situ intensity	An estimated amount of ultrasound energy (per unit area) which is delivered to the HIFU focus. It is equal to free field intensity minus the estimated energy losses due to acoustic attenuation of the tissue in the path of the ultrasound beam.
Lesion	An area of tissue destruction resulting from exposure to HIFU energy.
Targeting error	A discrepancy between the placement of the HIFU focal zone and the intended vascular target resulting from incorrect planning of the HIFU exposure series (operator error), defined for this study only.
Technical error	A failure of the HIFU system to deliver the HIFU exposure series as planned (system error), defined for this study only.

LIST OF UNITS

%	Percent
$beats.min^{-1}$	Beats per minute
bpm	Beats per minute
$breaths.min^{-1}$	Breaths per minute
cm	Centimetre
$cm.s^{-1}$	Centimetre per second
d	Day
$db.cm^{-1}.MHz^{-1}$	Decibels per centimetre per megahertz
dBm	Decibel milliwatts
G	Needle gauge
g	Gram
$g.dl^{-1}$	Grams per decilitre
h	Hour
Hz	Hertz
IU	International unit
kg	Kilogram
$kg.m^{-2}$	Kilogram per square meter
kHz	Kilohertz
$kW.cm^{-2}$	Kilowatts per square centimetre
$mEq.l^{-1}$	Milliequivalents of solute per litre of solvent
$mg.kg^{-1}$	Milligram per kilogram
$mg.l^{-1}$	Milligram per litre
MHz	Megahertz
min	Minute
ml	Millilitre
ml $O2.min^{-1}$	Millilitres of oxygen per minute
ml O2.ml $blood^{-1}$	Millilitres of oxygen per millilitre of blood
$ml.kg^{-1}$	Millilitre per kilogram
$ml.min^{-1}$	Millilitres per minute
$mlO2.gHb^{-1}$	Millilitres of oxygen per gram of haemoglobin
mm	Millimetre
$mm.cl^{-1}$	Millimetres per centilitre
$mm.d^{-1}$	Millimetres per day

mmHg	Millimetres of mercury
$mmHg.(ml.min^{-1})^{-1}$	Millimetres of mercury per flow in millilitres per minute
$mmol.l^{-1}$	Millimoles per litre
ms	Millisecond
ms^2	Square millisecond
µl	Microliter
$µmol.min^{-1}$	Micromoles per minute
$ng.ml^{-1}$	Nanograms per millilitre
nm	Nanometre
nu	Normalised unit
^{o}	Degree
^oC	Degrees Celsius
rpm	Revolutions per minute
s	Second
$W.cm^{-2}$	Watts per square centimetre

CHAPTER 1: INTRODUCTION

The text in sections 1.1 and 1.2 of this chapter is substantially based on a previously published paper, Shaw et al. 2014 (1).

1.1 Twin to Twin Transfusion Syndrome

1.1.1 Background

Twin to Twin Transfusion Syndrome (TTTS) is an important condition in fetal medicine which affects between 10-15% of monochorionic diamniotic (MCDA) twins (2, 3), and is the most important underlying cause of death and handicap in monochorionic twins (4). MCDA twins are considered high risk pregnancies due to the incidence of this and other complications (3), and prenatal surveillance for sonographic evidence of TTTS is more intense than for singleton or dichorionic twin pregnancies (5).

TTTS is a complication only found in pregnancies where fetuses share a placenta, usually monochorionic twins or dichorionic triplets. It results from unequal sharing of blood supply between twins due to placental vascular anastomoses, present in 95% monochorionic placentae (6, 7) which allow "vascular steal". This is a description of unbalanced blood flow between the circulations of each fetus (8), leading to a relative over- and under-perfusion of the recipient and donor twin respectively. Placental vascular anastomoses may form between the placental arterial vessels of donor twin and recipient twin, the arterial and venous systems, or the venous and venous systems (Figure 1.1).

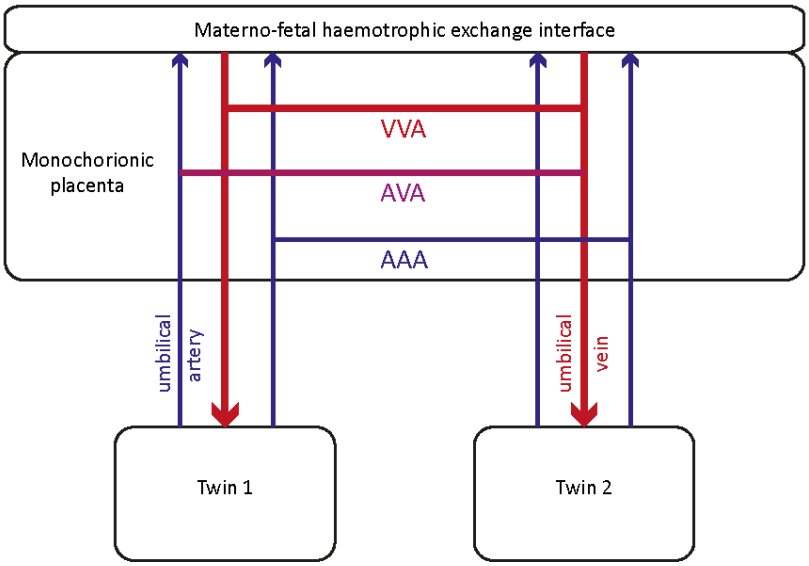

Figure 1.1: Placental vascular anastomoses.
Schematic representation of potential placental vascular anastomoses in a monochorionic placenta. AAA: arterio-arterial anastomoses, AVA: arterio-venous anastomoses, VVA: veno-venous anastomoses.

Fifty percent of monochorionic placentae contain arterio-arterial anastomoses (AAA); 25% contain veno-venous anastomoses (VVA); 5% contain arterio-venous anastomoses (AVA) and

5% contain no anastomoses at all. AAAs and VVAs are superficial and allow bidirectional flow, giving the potential to correct the imbalance of the circulations according to the pressure differential between the circulations of donor and recipient twins. AVAs are deeper, with exchange occurring at the capillary level within a placental lobule, and only allow flow in a single direction, from artery to vein, i.e. from high pressure to low. The diameter of AVAs quoted in published literature is between 0.9 – 2.1 mm (9). Although they can form in either direction (donor to recipient and recipient to donor), this unidirectional flow is believed to give rise to the unbalanced blood flow distribution between the twins' circulations found in TTTS (10). AVAs allow deoxygenated blood flow to be shunted from the umbilical arterial flow returning from the donor twin to the placental bed, into the umbilical venous flow travelling from the placental bed to the recipient twin. This additional blood volume remains in the recipient twin's circulation unless restored to the donor circulation by the action of AAAs, VVAs or AVAs flowing in an opposing direction in the placental bed. The overall sum of blood flow via these anastomoses determines whether the placental circulation is balanced or unbalanced, and the size and direction of the vascular steal.

1.1.2 Diagnosis

As a result of the progressive vascular steal, the donor twin will become under-perfused as its circulating volume is reduced. It will begin by making physiological changes appropriate to its volume depleted status, such as activation of the renin-angiotensin system and renal conservation of fluid, leading to oliguria and oligohydramnios. As the circulating volume reduces further these changes become pathological with the fetus centralising blood flow, ultimately leading to fetal death.

Conversely the recipient twin will be over-perfused and hypervolaemic, and will begin making physiological changes to offload excess circulating volume, releasing atrial natriuretic peptide (ANP), becoming polyuric and leading to polyhydramnios. As the circulating volume increases further the fetus will start to show signs of congestive cardiac failure due to the volume overload and ultimately become hydropic leading to fetal death.

Some of the sequence of changes that take place as TTTS progresses can be monitored via prenatal ultrasound and was standardised into a classification system by Quintero. Under this system there is grading of disease progression as assessed by ultrasound from mild (stage I-II) to severe (stage III-IV) with in utero death of one or both fetuses being stage V (Table 1.1) (11).

Stage	Amniotic fluid discordance	Absent bladder in Donor twin	Abnormal fetal Doppler studies	Fetal hydrops	Fetal demise
I	+	-	-	-	-
II	+	+	-	-	-
III	+	+	+	-	-
IV	+	+	+	+	-
V	+	+	+	+	+
Details of ultrasound criteria	DVP <2cm donor; DVP >8cm recipient		A/REDF in Umbilical artery; Reveresed 'a wave' in ductus venosus; Pulsatile umbilical venous flow.	Ascites; Collection of fluid in 2+ fetal cavities	One or both fetuses

Table 1.1: Quintero staging of TTTS.
Ultrasound-based staging of TTTS, derived from Quintero et al. 1999 (11). Key: + denotes that the criteria is met, - denotes that the criteria is not met.

It is difficult to define the natural history of each Quintero stage of TTTS as the ultrasound staging system was introduced in response to the need for a uniform classification of disease to use with invasive treatments, amniocentesis and fetoscopic laser. Prior to this, cases were typically divided into hydropic (stage IV) and non-hydropic (stage I-III) groups when reporting observational data or the outcome of treatments, and the capability for regular ultrasound surveillance is a relatively recent event. However some retrospective analyses have been published of TTTS cases with no intervention or with amnio-drainage only (which may prolong the pregnancy by reducing uterine stretch, improving survival rates with regard to gestation age at delivery but does not alter the underlying disease pathology) which gives an idea of the heterogeneity of the disease process (Table 1.2) (12).

Stage at Diagnosis	Spontaneous regression or resolution	Stable disease	Progressive disease	In-utero death	Perinatal death
Stage I	27.30%	27.30%	31.80%	18.20%	22.70%
Stage II	53.30%	6.70%	40.00%	13.30%	30.00%
Stage III	21.70%	47.80%	30.40%	26.10%	45.70%
Stage IV	12.50%	62.50%	25.00%	25.00%	56.20%

Table 1.2: Natural history of disease progression and mortality in TTTS.
The numbers represent the percentage of pregnancies in which TTTS will improve, remain stable or worsen, based on TTTS stage at diagnosis. It also shows the percentage of pregnancies which will end in fetal death before delivery, at any gestation (in utero death) or perinatal death (death before delivery at over 24/40 or within 7 days of delivery) based on TTTS stage at diagnosis. Data derived from Dickinson et al. 2004 (12).

This demonstrates that although more advanced stage of disease at diagnosis gives a higher overall risk of perinatal death, delivering an individual prognosis based on stage of disease at diagnosis is far from simple. To this end, many groups have attempted to define features which may quantify the risk of progressive TTTS and perinatal death. AAAs may be protective against developing TTTS, although their presence or absence is not conclusive. VVAs have been suggested to contribute to co-twin rates of death and neurological damage by allowing sudden changes in venous return to create profound hypotension in the surviving co-twin in the event of intrauterine fetal death, usually of the donor twin.

1.1.3 Treatment

The results of the multicentre Eurofetus study, a randomised control trial comparing amnio-drainage with fetoscopic laser for treatment of TTTS, published in 2004, established fetoscopic laser (after 2 decades of development) as the optimum therapy in treatment of TTTS (13). This started a proliferation of centres providing fetoscopic laser, studies reporting incremented technique developments, and affected pregnancies managed by this invasive method.

Fetoscopic laser seeks to ablate the placental anastomoses, essentially separating the fetal circulations, and halting any further vascular steal, though it cannot reverse or redistribute the blood flow distribution imbalance that has already occurred. Amnio-drainage seeks to reduce the risk of preterm labour secondary to polyhydramnios and uterine stretch, particularly at pre-viable or extremely premature gestational ages, but does not alter the underlying disease pathology. The potential disadvantage of fetoscopic laser is that while both are invasive techniques, there is a larger calibre instrument introduced into the intrauterine space with

fetoscopic laser, for a longer duration, leading to a higher complication rate (14). Direct complications of breaching the intrauterine space include amniotic fluid leakage, placental haemorrhage, chorioamnionitis, miscarriage or extreme prematurity, and damage to adjacent fetal or maternal structures.

The Eurofetus trial showed that, especially in severe disease, these higher risks due to intrauterine invasion were offset by the more complete treatment of disease in terms of overall survival. Compared to amnio-drainage, fetoscopic laser demonstrated higher survival rates of at least one twin to six months of age, and thereafter was recommended as the gold standard of care for cases of TTTS stage III-IV. Only Quintero stage III and IV disease was considered for treatment by fetoscopic laser, as in stage I and II disease the overall risk of perinatal death was found to be less than the risk of fetal demise from the procedure.

However, a 2014 Cochrane review found no difference for overall death between pregnancies treated with fetoscopic laser versus amnio-drainage: RR 0.87, 95% CI 0.55-1.38. This meta-analysis included data from only two trials, Eurofetus and NIHCD (15), 182 pregnancies and 364 fetuses. Neither was there any difference in babies alive with major neurological abnormality at 6 years treated by amnio-drainage versus fetoscopic laser: RR 0.97, 95% CI 0.34-2.77. There was, however a reduction in neurodevelopmental delay in children alive at 6 years when treated with fetoscopic laser: RR 1.57 95% CI 1.05-2.34. There was no difference between techniques for: rates of death of one or both twins; preterm labour or rupture of membranes rates within 48 hours of the procedure; the incidence of intraventricular haemorrhage grade III/IV, the need for mechanical ventilation after delivery or blood transfusion within 48 hours of delivery (15). For this reason, fetoscopic laser can still be recommended to pregnancies affected by TTTS to reduce developmental delay, with the caveat that it will not alter survival or rates of major neurological abnormality.

Additionally, complications of fetoscopic laser do not result solely from invasion of the intrauterine space. The “deep” nature of AVAs means that they are not readily visible for identification via the fetoscope on the surface of the placenta as AAA and VVA are; rather unpaired vessels with a difference in blood colouration are seen to perforate the placental surface and an anastomosis at the capillary level is assumed. There is also no real-time method of confirming that complete ablation of all anastomoses has occurred at the time of surgery. Colour Doppler studies post fetoscopic laser treatment describe between 5-30% residual anastomoses, which may result in residual disease in up to 16% of treated cases and is associated with lower rate of survival and neurologically intact infants (16).

Alternatively, smaller calibre residual anastomoses can result in Twin Anaemia-Polycythaemia Syndrome (TAPS). Iatrogenic TAPS is more common after ablation than spontaneously (13% vs. 5%) (2, 17) suggesting that it is within the same disease spectrum as recurrent TTTS. While TAPS has much better outcomes than TTTS it can still result in the need for postnatal transfusion and exchange transfusion, elevated bilirubin levels and ischaemic events in the polycythaemic twin, entailing an increased perinatal hospital stay for the twins and an additional burden on neonatal services.

Attempts to reduce the level of residual anastomoses have been made by trialling an alternative to selective vessel fetoscopic laser (SVFL): SVFL followed by placental bipartition. In this technique the shared area of the placenta is identified and all tissue along that line is ablated, with visible vessels occluded first to reduce the risk of haemorrhage, and then the remaining tissue bipartition to create a functionally dichorionic placenta and ideally occluded any unidentified smaller or deeper vessels (18). Recurrence rates appear to be lower (around 5%), and the incidence of TAPS is also reduced with this technique. However, in a meta-analysis of 531 cases using the new technique, there is no improvement in survival, no significant prolongation of gestation, no reduction in severe morbidity or difference in long-term neurodevelopmental injury compared to SVFL alone (19).

1.2 High Intensity Focused Ultrasound

1.2.1 Background

High intensity focused ultrasound (HIFU) is a clinical therapeutic technique which uses high frequency sound waves (usually, 1-10 MHz), generated by a piezoelectric ceramic transducer outside the body. HIFU is a non-invasive alternative to surgery, in that it has the potential to destroy targeted tissues, without damaging adjacent tissue, as invasive surgical techniques do. The ultrasonic energy generated can be tightly focused and accurately placed to produce localised tissue destruction (referred to as lesions) at depth. HIFU uses a focused source to converge the ultrasonic energy into a tissue volume distant from the transducer. This region is called the focal zone or focus, and is the only position in which the ultrasound intensity (incident energy per unit area) should be high enough to produce changes in the structure of the tissue, and create a lesion. The tissue in the path along which the ultrasound waves pass is ideally exposed to energies too low to produce damage. The lesions formed are ellipsoid in shape, reflecting the shape of the focal region of the beam, and are typically 1-2mm in diameter (orthogonal to the direction of sound travel) and 8-15mm in length (parallel to the direction of sound travel). To destroy larger, clinically relevant, volumes of tissue, this small focal zone is moved systematically throughout the target region by electronic or mechanical means to form a line or a grid of lesions (Figure 1.2). The use of diagnostic imaging allows non-invasive identification of the target and monitoring of response.

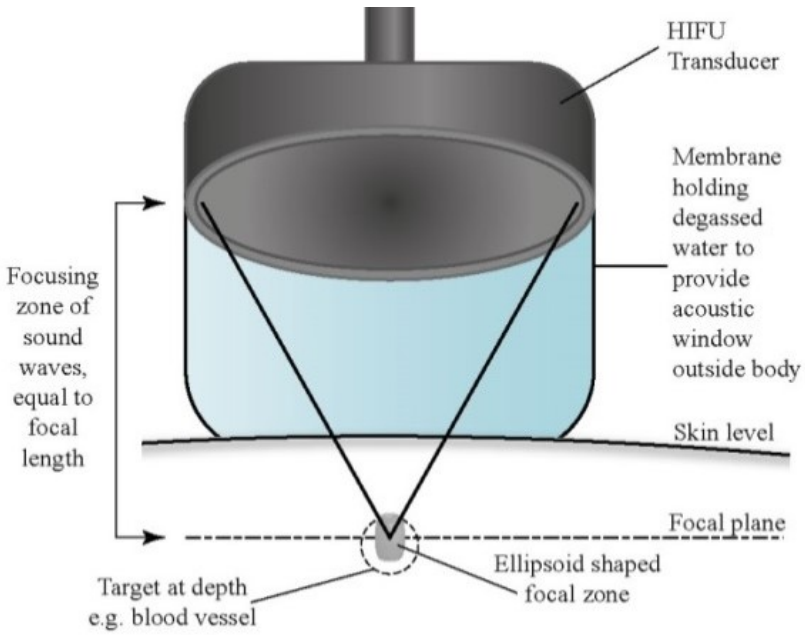

Figure 1.2: Non-invasive set-up of HIFU transducer to produce tissue lesions at depth.
Reproduced from Shaw *et al*. 2014 (1)

HIFU energy can pass through different tissue layers en route to the target. Providing regions of bone and air are avoided relatively little energy should be lost at each tissue interface. The main energy loss is due to attenuation (absorption and scatter) within the tissue layers. The amount of ultrasound energy generated by the transducer is known as the free field intensity, which can be measured, whereas the amount which reaches the target tissue is known as the in situ intensity, which is by necessity an estimated value based on assessment of energy losses, calculated from the free field intensity and energy losses to acoustic attenuation. Alternative techniques such as radio frequency ablation (RFA), laser photocoagulation and microwave energy have poor tissue penetration so use invasive methods to destroy deep tissue, but deliver a more predictable amount of energy to the tissue when properly calibrated and controlled.

HIFU exposure can be continuous (primarily used to induce heating) or pulsed, which may better exploit acoustic cavitation and reduce the need for tissue heating to produce tissue damage (20).

Ultrasound can be converted to thermal energy mainly via a variety of molecular relaxation processes which occur following ultrasound excitation. When temperatures in excess of 56^{o}C are maintained for ≥ 2 s (21, 22) this causes coagulative necrosis due to protein denaturation, cellular destruction (22) and tissue stiffening (23). Coagulative necrosis is a form of unplanned cell death in response to a cellular insult, where tissue architecture is characteristically preserved, cells retain their outline while their proteins coagulate, and metabolic activity ceases (24). In soft tissue, HIFU lesions are characterised histologically by a necrotic centre and a rim of functionally impaired cells (lacking glycogen stores) which fade to ghost outlines leaving a sharp rim between affected and unaffected tissues 48 hours after exposure, with the lesion encapsulated by granulation tissue (25). Detachment of cells from their basement membrane and each other is also observed (26) with evidence of a strong acute inflammatory response and remodelling in a chronic inflammatory response, involving cellular regeneration, proliferation, migration and removal of debris lasting up to three months (20).

Applying pulses of HIFU can cause rapid changes in tissue pressure, described as the peak rarefaction pressure amplitude (PRPA). There is a threshold PRPA for each tissue at which acoustic cavitation occurs, where gas or liquid filled cavities form, usually at points of “weakness”, such as interfaces between different tissue layers or fluid filled structures (27). These bubbles oscillate and exert shear stresses on the surrounding tissue or may expand rapidly and collapse, destroying surrounding tissue structure, in a technique known as histotripsy. This mechanism does not rely on tissue heating to work (20). Histology of tissue

subjected to histotripsy reveals emulsification, and regions filled with acellular debris produced by mechanical fractionation of the tissue (28).

As of 2017, HIFU is an approved method of treatment for uterine fibroids, breast, renal, liver, pancreatic, prostate and thyroid cancers, ablation of brain tissue in essential tremor and Parkinson's disease, and treatment of pain from bony metastases (29). However, these are all applications of HIFU which involve targeted soft tissue ablation, rather than specific occlusion of blood vessels. Purely vascular applications – such as treatment of peripheral arterial disease or arterio-venous malformations in the brain – remain in the conceptual or preclinical stages of development.

1.2.2 Vascular Specific HIFU

The first specific attempts to produce HIFU mediated vascular occlusion were in 1972 and relied upon visual targeting of surface vessels, the auricular artery in rabbits (30). Since then, HIFU has been demonstrated produce a number of vascular changes when applied to blood vessels, suggesting more than one possible mechanisms by which blood flow can be occluded. Each research group also used different strategies to attempt to occlude vessels, so the ideal method of producing selective vascular occlusion is far from apparent from this review of the body of published work. There is a lack of consistent reporting of methodology and outcomes, and as such there is no consensus which can be reached as to the most successful exposure characteristics for vascular occlusion.

The results of this systematic review of are provided in Table 1.3 and Table 1.4 (1). In summary, the effect of HIFU energy on blood vessels can be to:

(i) produce occlusion or arteries and veins by obliteration of the vascular lumen (31-43);
(ii) occlude arteries or veins by generation of persistent thrombus within the lumen leading to fibrosis obliterans (30, 34, 36, 39, 42);
(iii) produce vascular spasm and reduction in blood flow (34, 37, 38, 40, 41, 44-46).

Exposure of blood vessels can also lead to:

(i) arterial rupture (31, 32, 37, 38, 47);
(ii) no change in blood flow seen or impairment in vascular function reported (48-50).

HIFU has also been used to demonstrate haemostasis of experimentally punctured arteries and veins, by sealing the defect or producing occlusive thrombus (51-56).

The majority of studies use continuous HIFU designed to induce vessel heating (Table 1.3), although a smaller number used pulsed HIFU to maximise generation of thrombus without heating (Table 1.4). There is a wide range of in situ intensities described, 0.025 – 8.8 $kW.cm^{-2}$, with the majority clustering around 2.0-4.5 $kW.cm^{-2}$. The duration of exposure varies widely, 0.5-720 s, with most of studies using 5 – 20 s.

There is a single case report of successful treatment in human pregnancy: a TRAP sequence where HIFU was applied to the insertion of the umbilical cord of the acardiac fetus (43). This study did not demonstrate whether selective vascular occlusion or localised soft tissue destruction at the cord insertion point (the established clinical method used by RFA) was performed in the acardiac twin. It is therefore unclear if a vascular-specific or a soft-tissue specific exposure protocol resulted in division of the fetal circulations, although the ultrasound images previously published (57) suggest the latter. This study used an unknown number of 10 s HIFU exposures, in an unknown pattern, at 4.6 $kW.cm^{-2}$ in situ intensity to achieve its effect, which persisted for 20 weeks until delivery of the surviving twin.

Author (year)	Model	Vessel	Animals (n)	Exposures (n)	Vessel Diameter (mm)	Non-invasive?	Targetting	Intensity ($W.cm^{-2}$)	Frequency (MHz)	Focal Length (mm)	Sonications	Exposure Time (s)	Tissue Temp	Cavitation	Vascular Occlusion	Haemostasis	Thrombus	Endothelial Damage	Vascular Spasm	Vascular Rupture	Vascular wall damage	Length of Follow-up
Fallon (1972)	Rabbit	Auricular Artery	12	28	0.7 - 1.0	Yes	Visual	25-1500	1	125	1	0.5-720	38.5-66.7	NR	X	-	o	o	-	-	o	72 hrs
Schultz-Haakh (1989)	Dog	Unspec. vein	19	-	NR	Yes	A-mode	NR	3	NR	multiple	NR	NR	NR	-	-	o	-	-	-	o	Immediate sacrifice
	Man	Varicose leg veins	11	-	NR	Yes	Visual	NR	3	NR	multiple	NR	NR	NR	-	-	o	-	-	-	o	Immediate sacrifice
Yang (1992)	Rabbit	Aorta, IVC	24	-	NR	Surgical exposure	Visual	1500	4	NR	20	5	68.8-80.1	NR	X	-	-	-	X	X	o	6 months
Delon-Martin (1995)	Rat	Femoral vein	6	-	1.5	Surgical exposure	A-mode	167	7.31	20	4-7	3	<45	X	o	-	o	o	-	-	-	28 days
Hynyen (1996)	Rabbit	Femoral art., vein	19	26	1.0 - 1.3	Yes	MRI	4400-8800	1.49	NR	5-8	1	NR	o	o	-	-	-	o	o	-	14 days
Hynyen (1996b)	Rabbit	Renal artery	9	-	0.6	Yes	MRI	2800, 6500	1.5	NR	12-16	10	64	o	o	-	-	-	o	o	-	7 days
Vaezy (1997)	Rabbit	Liver microvasculature*	8	27	<0.5	No	Visual	3000	3.3	40	1	1-2	59-86	o	o	o	X	o	-	-	o	Immediate sacrifice
Vaezy (1998)	Pig	Muscular Arteries*	5	41	3-10	No	Visual	3100	3.5	55	1	10-20	NR	NR	X	o	o	o	o	-	o	Immediate sacrifice
Martin (1999)	Pig	Muscular Arteries*	3	89	3-10	No	Doppler	2000	3.5	55	1	5-20	NR	NR	X	o	-	-	-	o	-	Immediate sacrifice
Vaezy (1999)	Pig	Muscular Arteries	4	76	3-10	No	Doppler	3000	3.5	55	1	17-25	NR	NR	o	o	o	o	-	-	o	Immediate sacrifice
Rivens (1999)	Rat	Femoral art., vein	10	-	0.5-1.5	Surgical exposure	Visual	4660	1.7	150	1	2	NR	NR	o	o	-	-	-	o	-	Immediate sacrifice
Denbow (2000)	Rat	Femoral art., vein	16	-	0.5-1.5	Surgical exposure	Visual	1690-4660	1.7	150	1	5	NR	NR	o	-	-	-	-	o	-	Immediate sacrifice
Fujiwara (2002)	Rat	Femoral artery	18	36	0.5	NR	NR	800	1	NR	1	5-10	46	NR	X	-	-	-	-	-	-	Immediate sacrifice
								10,000	3		1	5-10	98	NR	o	-	-	-	-	-	o	12 days
Hwang (2003)	Rabbit	Auricular Vein*	15	-	1.0	Yes	Visual	750	3.9	35	1-3	3	NR	NR	o	o	o	o	o	-	o	28 days
Ishikawa (2003)	Rat	Femoral artery	23	-	0.5	Yes	Doppler	530-2750	3.3	NR	1	5	98	NR	o	-	o	o	o	-	o	3 days
Nizard (2004)	Sheep	Uterine Artery	7	-	NR	No	Doppler	NR	1.05	100	6-7	8-10	NR	•	X	-	-	o	o	-	o	NR
Zderic (2006)	Rabbit	Femoral Artery	25	-	1.5	No	Visual	3000	9.6	25	Multiple	5-10	NR	NR	o	o	o	o	o	-	o	60 days
Ichizuka (2007)	Rabbit	Umbilical artery	11	-	0.4-0.8	Yes	Doppler	1400-5500	2.26	70	3-15	5	NR	NR	o	-	o	o	-	X	o	Immediate sacrifice
Ichihara (2007)	Rabbit	Renal artery	8	-	0.5	Yes	Doppler	4000	2.2	60	2-10	5	NR	NR	o	-	-	-	o	o	o	7 days
Ichizuka (2012)	Human (in utero)	Umbilical artery	1	-	NR	Yes	Doppler	2300	1.71	NR	NR	10	NR	NR	X	-	-	-	-	-	-	3 weeks
Okai (2013)	Human (in utero)	Umbilical artery	1	-	NR	Yes	Doppler	4600	1.71	60	multiple	10	NR	NR	o	-	-	-	-	-	-	20 weeks
van Breugel (2015)	Human	Tibial AVM	1	5	NR	Yes	MRI	NR	NR	NR	5	8.3 - 19.5	62 - 81	NR	o	-	-	-	-	-	-	13 months
Ichizuka (2016)	Rabbit	Renal artery, vein	3	NR	NR	Yes	Doppler	1940	1.1	60	NR	10	NR	NR	o	-	-	-	-	-	-	Immediate sacrifice

Key: o: Vascular effect observed X: Vascular effect not observed -:Vascular effect not reported/investigated *: lacerated vessels NR: not reported

Table 1.3: Systematic review HIFU vascular occlusion (continuous HIFU).
Summary of the continuous HIFU exposure characteristics used in the 23 studies included in the systematic review, and their associated vascular outcomes.

Author (year)	Model	Vessel	Number animals	Number Exposures	Vessel Diameter (mm)	Non-invasive?	Targetting	Intensity ($W.cm^{-2}$)	PRPA (Mpa)	Frequency (MHz)	PRF (Hz)	Burst length (msec)	Exposure Time (s)	Temp	Cavitation	Vascular Occlusion	Haemostasis	Thrombus	Endothelial Damage	Vascular Spasm	Vascular Rupture	Vascular wall damage	Length of followup	Additional IV therapy
Mahoney (2000)	Rabbit	Auricular artery, vein	22	-	1.0	Yes	Visual	NR	4-37	0.68-2.02	5-20	10	10-180	NR	o	o	-	-	-	o	o	o	3 hours	-
Hwang (2006)	Rabbit	Auricular Vein	16	-	1.0	Yes	Visual	NR	1-9	1.17	1	NR	1-120	NR	o	**X**	-	o	o	-	-	o	I hour	UCA
Yang (2009)	Rat	Aorta, Femoral Artery	9	-	1	No	Doppler	578-1734	NR	1	1	50	6	29-30	o	**X**	**X**	**X**	**X**	o	**X**	**X**	Immediate Sacrifice	UCA
Hwang (2010)	Rabbit	Auricular Vein	21	-	1	Yes	Visual	23	9	1.17	NR	NR	60	NR	o	o	-	o	o	-	**X**	**X**	14 days	UCA + Fibrinogen
Kim (2017)	Worm	Ventral blood vessel	NR	6-20	NR	Yes	Visual	NR	NR	1.1-3.3	1-10	NR	1-600	NR	-	o	-	-	-	-	o	-	Immediate Sacrifice	-

Key: o: Vascular effect observed X: Vascular effect not observed -:Vascular effect not reported/investigated NR: not reported

Table 1.4: Systematic review HIFU vascular occlusion (pulsed HIFU).
Summary of the pulsed HIFU exposure characteristics used in the 5 studies included in the systematic review, and their associated vascular outcomes.

The heterogeneity of these results demonstrates that describing the properties of delivered energy alone is not predictive of the outcome in blood vessels. In some studies, vascular occlusion has been successful at lower energy levels where only non-occlusive endothelial or vascular wall damage has been reported and at higher levels where vascular rupture would be expected. This may be explained by blood vessels forming part of a biological system, with multiple anatomical, physiological, mechanical, thrombotic and inflammatory responses to the absorption of ultrasound energy.

Neither coagulative necrosis nor tissue emulsification alone are likely to be effective mechanisms of vascular occlusion. HIFU can destroy soft tissue microvasculature by coagulative necrosis even when not deliberately targeted at the vessels, occluding vessels up to a diameter of 0.5 mm (58), working with limited efficacy on lacerated vessels of 0.5-2.5 mm and being ineffective on vessels >2.5 mm (54). However, both damaged (59) and undamaged (26) un-occluded blood vessels are often seen surrounding soft tissue HIFU lesions, resulting in circumferential haemorrhage (60), with greater haemorrhage in more vascular regions (61). Changes suggestive of coagulative necrosis are also seen in vessel walls exposed to HIFU without loss of structure or function (48, 54). In emulsified tissue there are also margins which demonstrate circumferential haemorrhage around the lesioned area (62). Pulsed HIFU has been shown to produce oedema and disruption of the extracellular matrix and collagen fibrils of vessels, without occlusion (48, 54, 63), acoustic cavitation in tissue is associated with unintended vascular rupture (27, 64) and may therefore be used to increase vascular permeability.

1.2.3 Proposed mechanisms of HIFU mediated vascular occlusion

1.2.3.1 **Heating and tissue fusion**

Arteries and veins have a common basic structure comprising the tunica intima, an inner layer of endothelium on a basement membrane. The tunica media is an intermediate layer of smooth muscle, thicker in arteries than veins and absent in capillaries. The tunica adventitia is an external supportive layer and may be continuous with surrounding collagenous connective tissue, absent in capillaries. Arteries also contain elastin layers (65). Capillaries, arterioles and venules (d ≤0.3 mm) comprise tissue microvasculature. Theoretical modelling of vascular thermal damage suggests that the first vessel changes are caused by thermal denaturation and shrinkage of collagen fibres while vessel integrity is maintained by elastic laminae, if present, and smooth muscle (66).

Tissue fusion is a common method of therapeutic vascular occlusion. The vessel is mechanically compressed and occluded, while energy is converted to heat at the point of occlusion, which seals the vessel closed by tissue fusion. Tissue fusion requires partial denaturation of collagen (and elastin if present) such that the fractured structure can reform bonds outside the laminar structure (bridging), effectively fusing the many layers of the vessel wall together. Arteries and veins become more difficult to occlude by tissue fusion as their diameter, lumenal blood flow or pulse pressure increases. Collagen is a prominent feature of the tunica media and adventitia. Heating collagen to above its denaturation threshold of 62-67^{o}C (67) unravels its rope-like structure. Collagen undergoes isovolumetric shrinkage of up to 60% of its length when heated above this threshold, the majority of which occurs within 1 second (68). Such vessel shrinkage has been demonstrated ex vivo where the luminal cross-sectional area of a non-perfused vessel was reduced by up to 96% (69, 70), although this effect is much less pronounced in perfused vessels in vivo (45). Heating of collagen beyond this threshold leads to hyalinisation and fracturing of its structure, which contributes to tissue stiffness, and is a possible explanation for why vessels subjected to multiple HIFU exposures stiffen and become prone to rupture (52). During the initial phase of heating (<1 s) collagen is able to form bridging bonds to other partially denatured collagen fibres and fuse tissue (71). However, the free ends of collagen must be physically adjacent to form bridging bonds, usually requiring a form of external compression. Capillaries, arterioles and venules have sufficiently narrow lumen that a combination of collagen shrinkage and cellular dehydration will result in vessel collapse and coagulation with minimal attendant cell damage or haemorrhage (72), the likely mechanism of HIFU-mediated microvascular destruction.

Vascular occlusion does not invariably result from heating a vessel. Heating to temperatures above 100^{o}C with laser or diathermy, where the water in cells vaporises and ruptures cellular membranes, produces a weak coagulum of denatured cells, collagen debris and carbonised tissue, unable to withstand physiological blood pressure (73), and can cause vascular rupture due to vessel wall necrosis and elastin destruction (74). A similar tissue vaporisation is seen in HIFU tissue emulsification, although tissue carbonisation is less likely to occur as desiccated tissue cannot propagate ultrasound, and further heating does not occur beyond this point. Successful vascular occlusion by collagen fusion occurs in temperature range 73-87^{o}C (75), while temperatures below 54^{o}C caused no structural changes in collagen (75).

The electrothermal bipolar vessel sealing system is approved for clinical occlusion of arteries (diameter ≤6 mm) and veins (diameter ≤12 mm) (76). It uses mechanical compression combined with electrical heating to cause collagen bridging between vessel walls (77). The

resultant occlusion has a burst pressure well in excess of physiological pressures (78). The system is computer controlled, monitoring electrical impedance to allow careful control of the energy supplied and prevent tissue under or overheating (77).

While there are no studies on HIFU-mediated vascular occlusion that investigate the presence of tissue fusion, several studies indirectly suggest that it occurs. Disruption of vascular and perivascular collagen has been observed with vascular occlusion using histology and electron microscopy (33-35). The collagen changes can extend beyond the tunica media to the tunica adventitia and adjacent connective tissue, and shrinkage in these outer layers can result in lumenal constriction and occlusion (53, 55). In one study, vascular occlusion was an unintended side effect of HIFU, and fusion of the vessel via collagen was described, along with disruption of the elastic lamina (55). Elastin fragmentation has been demonstrated in occluded vessels using van Gieson staining, changes which were not seen in non-occluded vessels (34).

Other studies have investigated the effects of HIFU specifically on the vascular collagen, using Masson's trichrome stain (79). Although occlusion was not achieved, collagen in the vessel walls was fragmented and took on a corkscrew appearance, creating spaces within the tunica media which corresponded to the vacuolisation seen in the smooth muscle when haematoxylin and eosin (H&E) staining was also performed. Similarly, collagen fibre swelling and vessel wall fracture in response to non-occlusive HIFU exposure (80), and the collapse of collagen in damaged microvasculature has been reported (59).

Successful HIFU-mediated vascular occlusion occurs within the temperature ranges discussed above. Occlusion has been reported in the range of 64^{o}C – 98^{o}C (33, 34, 37, 54), with non-occlusive vascular damage occurring 43^{o}C – 69^{o}C (30, 33, 48) and no damage to the tunica media or adventitia at <43^{o}C (30, 36, 44). This agrees with theoretical modelling of temperature change in vessels that shows that collagen shrinkage would predominate in vessels before tissue necrosis at the temperatures typically achieved by HIFU (66, 71). The duration these temperatures were maintained varies between studies, affecting the overall amount of thermal energy supplied to the tissue, which may explain why the temperature ranges are wide and overlapping.

1.2.3.2 **Thrombogenesis and endothelial damage**

Thrombogenesis may be an appropriate haemostatic response to vascular injury, or a non-haemostatic disease process. Virchow's triad suggests three predisposing factors which may

result in non-haemostatic thrombus formation in vivo: endothelial damage, stasis of blood flow or hypercoagulability of blood (24). With reference to HIFU-mediated vascular occlusion, all three mechanisms appear to be contributory to thrombus formation within vessels. The potential effect of ultrasound exposure and heating on blood constituents must also be considered.

Endothelial damage is an established pathophysiological mechanism by which vascular occlusion occurs. It leads to occlusive thrombus generation in the vessel lumen and permanent stenosis and fibrosis of the vessel in a chronic inflammatory process. This can be achieved by intravascular injection of sclerosing agents, mechanical damage to the tunica intima or can be iatrogenic. Endothelial damage results in exposure of subendothelial collagen, which is an activator of the coagulation cascade. Primary haemostasis is a sequence of activation, aggregation then adherence of platelets to areas of damaged endothelium. This leads to secondary haemostasis with deposition of fibrin around the adhered platelets and organisation into stable thrombus. Widening of gaps between endothelial cells occurs allowing extravasation of plasma proteins and acute inflammatory response cells and the collection of subendothelial oedema. With more extreme damage the endothelial cells die and cease their synthetic function, leading to a failure of vascular relaxation signalling, which may contribute to vascular spasm in addition to thrombogenesis.

Endothelial damage is often observed with vascular occlusion (Table 1.3, Table 1.4), as would be expected given that the endothelium is damaged at the lowest of reported exposures. It is usually accompanied by thrombosis, which can produce an occlusive seal even where incomplete tissue fusion has occurred (73). Transmural vascular damage, including endothelial damage and thrombosis has been demonstrated in studies using both scanning electron microscopy (39) and histology by phosphotungstic acid haematoxylin (PTAH) staining (34). A sequence of changes leading to permanent obstruction has been described in rabbit veins, with transmural thermal injury occurring at day 0, followed by fibrin thrombus deposition, endothelial cell detachment and acute inflammatory response at day 2. By day 7 there was occlusive organised thrombus and chronic inflammatory response (vacuolar degeneration) that persisted until day 28, by which time the vessel had been replaced by fibrous scar tissue without residual inflammatory reaction (39). However, the question of whether HIFU can produce stable thrombus and vascular occlusion by endothelial damage alone remains unanswered.

Isolated endothelial damage has been produced in vivo by HIFU exposure without damage to the tunica media, adventitia or surrounding tissue (36, 79, 81) although this has not resulted in permanent vascular occlusion in the absence of acoustic cavitation or artificially elevated levels

of fibrinogen, which makes the blood hypercoagulable and promotes formation of stable thrombus. It appears that HIFU exposures which do not produce inertial acoustic cavitation can damage the endothelium, but do not sufficiently expose subendothelial collagen to produce a clinically significant primary haemostatic response in vivo. This is supported by in vitro studies which show that though platelet aggregation occurs with HIFU exposure, adherence requires collagen substrate (82). Where inertial cavitation is promoted by ultrasound contrast agent, this results in a higher proportion of the endothelial surface area being damaged than at the same energy level without these microbubbles, and in the generation of thrombus (81). However, even with increased endothelial damage, elevated circulating levels of fibrinogen were required to produce occlusive thrombus (41).

Blood hypercoagulability has been described as the primary cause of “acoustic haemostasis” and has also been suggested as a method of thrombogenesis (82, 83). This describes the expression of adhesion molecules on the surface of platelets (activation) in response to HIFU exposure and clumping (aggregation) in the absence of triggers from endothelial damage, occurring up to 50 s after initial HIFU exposure. It is known that platelets can be activated in the absence of tissue damage by shear stresses on their surface (84), and in the studies by Poliachik, aggregation occurred in response to acoustic cavitation. This is thought to be due to microstreaming causing shear stresses on the surface of the platelets which are sufficient to cause activation and aggregation but insufficient to cause disruption of the membrane (85). However, adherence has not been observed without an artificial collagenous substrate or endothelial damage, meaning the resultant thrombus would be non-adherent in vivo. Given the nature of the continuous flow of the circulatory system, such aggregated platelets are more likely to result in distant emboli than occlusive thrombus.

Heating platelets has not been directly studied with reference to HIFU. It is known that platelets are optimally activated at body temperature, 36-38^{o}C, and are functionally impaired at temperatures >45^{o}C, showing an inability to activate or aggregate (86). Hence it is unlikely that platelets heated by HIFU have any role in vascular occlusion, other than as cellular debris in organised thrombus. Similarly, red blood cells haemolyse at >45^{o}C (87).

Slowing of blood flow has been observed to contribute to HIFU-mediated vascular occlusion as unintended occlusion occurred more commonly at points of vessel compression in one study where the aim was to seal lacerated vessels (55). Stasis of red blood cells is a known effect of low intensity unfocused ultrasound (intensities ≤12 W.cm^{-2}), with separation of blood into bands of cellular aggregates and plasma due to the ultrasound standing waves (88), with normal circulation restored after exposure (89). To form a standing wave, strong reflection of the plane

of the wave is required, which is unlikely to occur *in vivo.* To date this effect has not been observed in vessels exposed to HIFU. This remains an area for further investigation in HIFU.

This evidence suggests that endothelial damage and physiological primary haemostasis are the key features in thrombus generation resulting from HIFU exposure of blood vessels. However, there is minimal evidence that this mechanism alone can produce permanent vascular occlusion. It is more likely that thrombosis has contributory role in maintaining and organising HIFU mediated vascular occlusion.

1.2.3.3 **Blood flow**

Vascular spasm is a recognised response of vessels to injury. The smooth muscle of the vessel contracts, as a physiological method of reducing blood flow, improving the success of primary haemostasis and ultimately reducing blood loss (90). It is seen in vessels exposed to HIFU, both in the presence and absence of vascular damage, and can be monitored non-invasively by Colour Doppler measurements of peak systolic velocity (PSV). Induction of vascular spasm by HIFU to produce temporary cessation of blood flow has been shown (37) although the intensities used were above the threshold for acoustic cavitation causing vascular rupture. Regardless, this represents a means by which lumenal narrowing can occur.

Vascular spasm has been seen in vivo at HIFU intensities which produce transmural vascular damage (37, 38, 40, 46) but also in exposures which do not produce vascular damage (34, 70) and is not reliant on the occurrence of tissue heating (44). Although the effect is described as transient, it persists for sufficient time post HIFU exposure to allow repeat PSV measurements taken by Doppler ultrasonography even in absence of evidence of vascular damage on histology (44).

Vascular spasm is likely augmented by the loss of vascular relaxation in response to endothelial damage and cessation of endothelial cell synthetic function. In a series of ex vivo experiments in canine coronary arteries, vascular relaxation was lost as a result of endothelial damage and disruption of the nitric oxide signalling pathways, but mechanisms of relaxation remain intact in the vascular smooth muscle and can be activated by the administration of exogenous nitric oxide donors, isolating the cause as endothelial damage (91).

The radiation force of high intensity sound waves can create localised streaming of liquids away from the focal point (92), even overcoming the physiological pressure gradient normally controlling blood flow in vessels. This has been observed in practice, where reversal of the

arterial jet and pulsatile flow was observed in lacerated femoral, axillary and carotid arteries in pigs independent of mechanical compression exerted by the transducer being pressed against the vessel, which alone was insufficient to obstruct flow even temporarily (51). The lumens of arteries are maintained patent by the pressure gradient of blood flow through them, with a typical mean arterial pressure (MAP) in the range of 85-125 mmHg in humans. Arteries such as the femoral, axillary and carotid artery will lose lumenal patency when the MAP ≤50 mmHg (93). This suggests the possibility that acoustic streaming could disrupt the local pressure gradient in the artery sufficiently to cause it to collapse. Veins and the microvasculature are much more easily collapsible and so would also be expected to collapse by this mechanism.

A final hypothesised mechanical effect by which HIFU could occlude blood flow is by temporary compression of the vessel due to its acoustic radiation force. When exposed to HIFU, tissue cannot respond fast enough to the changes between positive and negative pressures, meaning its motion becomes out of phase with the acoustic wave and energy is transferred to the tissue. This transfer of momentum to the tissue, in the direction of the wave propagation, results in tissue displacement. The amount of pressure delivered will vary with both the intensity of the HIFU source and the attenuation of the overlying tissue, but will be magnified by the small area over which it is delivered.

Although much speculated upon, acoustic radiation force has not been observed to collapse blood vessels in vivo, however soft tissue deformation and displacement of 1 – 3 mm has been observed in vivo (94). Given the recognised difficulties in making non-invasive in situ pressure measurements (70), it is not unreasonable that in vivo effects of acoustic radiation force have not been fully demonstrated. Synchronised systems to enable use of diagnostic Doppler ultrasound during HIFU exposure have been proposed (95, 96), but these would only demonstrate “no flow” in a vessel, not a definitive cause, and B-mode ultrasound imaging would likely lack the spatial resolution to determine reliable changes in diameter of vessels. In an experimental system to study isolated blood vessels in vitro, acoustic radiation force was sufficient to displace vessels out of the field of view of the microscope intended to monitor changes in vessel diameter (70).

Greater deformation and displacement of the proximal wall of the blood vessel compared to the distal wall would probably be expected, promoting collapse, as the blood within the vessel is much less stiff than surrounding soft tissues. Even without this difference, unidirectional pressure can occlude arterial blood flow at normal pulse pressures (e.g. pressing on a pulse point) and can be likened to the effect of momentum in the direction of HIFU wave propagation. Blood vessels are also maintained patent by the pulse pressure of blood flow, as previously

discussed, and if this pressure has been reduced by acoustic streaming as observed experimentally (51) then lower pressures would be needed to produce such collapse or deformation. This is an area which would benefit from further experimental evaluation as whether compression and deformation of blood vessels by acoustic radiation force occurs is of relevance to the design of HIFU systems.

1.2.3.4 **Inflammation and tissue repair**

There has been minimal work specifically on the contribution of inflammatory responses to vascular occlusion. The harmonic scalpel, an invasive system for producing vascular occlusion which uses ultrasound to create vibrational forces in the tissue, creates a more pronounced acute inflammatory response than electro-cautery, despite resulting in a smaller area of injured tissue (77). HIFU produces extensive oedema, disruption to tissue, inflammatory cell infiltration and activation of the cytokine cascade. Inertial cavitation induced damage produces a comparable activation of the acute inflammatory response, though this response does not convert into a chronic inflammatory response in the absence of tissue damage (20). Extracellular oedema is known to reduce blood flow, especially in smaller vessels, and perivascular oedema resulting from HIFU exposure has been cited as contributing to lumenal constriction (69).

The role of the inflammatory response in controlling and organising the physiological response to vascular damage cannot be discounted. Collateral circulation was seen to arise quickly following vascular occlusion (31), so while a distributing artery may be blocked the area is not automatically devascularised. Ultimately, the nature of the chronic inflammatory response will determine whether the vessel becomes patent again or remains permanently occluded and fibrosed (36, 39).

1.2.3.5 **Strategies to produce HIFU mediated vascular occlusion**

Consideration of the theoretical and experimental evidence of the responses of vessels exposed to HIFU demonstrates that there are many potential mechanisms through which the physical properties of HIFU may interact with a living system that contribute to vascular occlusion. Vascular occlusion cannot be considered simply as a side effect of vessel cellular destruction, and protocols for HIFU-mediated vascular occlusion should be designed to maximise this plethora of effects (Figure 1.3).

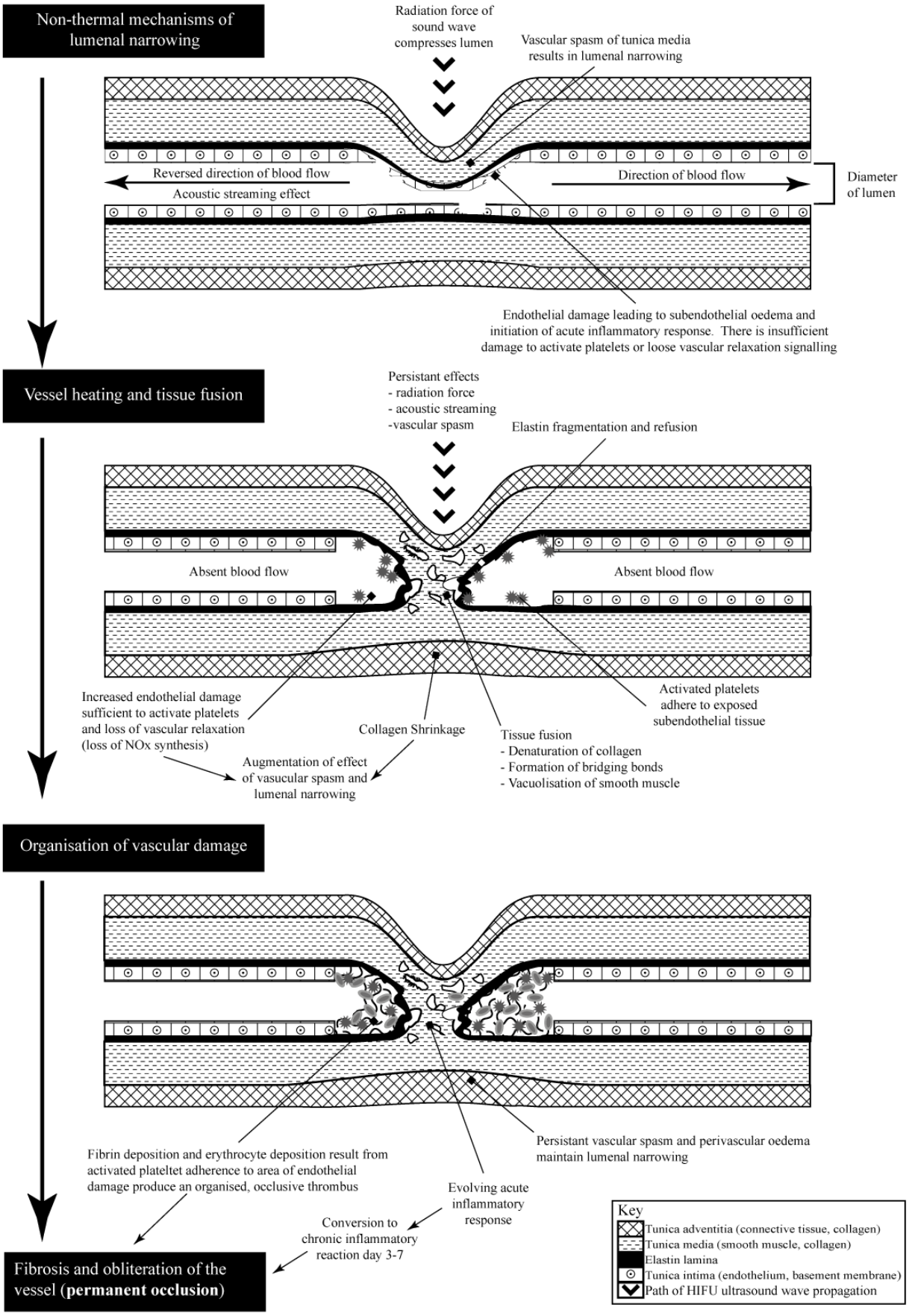

Figure 1.3: A suggested multi-stage integrated mechanism for HIFU-mediated vascular occlusion.
The schema presents the suggested integrated mechanism for HIFU vascular occlusion as a progression through the tissue changes produced by time and temperature changes (1)

There are various ways in which the effects described above could be combined but as time and temperature appears to be important factors in distinguishing acute and more delayed vascular occlusion, a multi-stage process can be envisioned taking place along a typical heating-time curve of HIFU.

In the initial stage, we consider the effects taking place before temperatures reach the 64^{o}C – 98^{o}C range where tissue fusion occurs, which for HIFU could mean from <1 second up to approximately 20 seconds. These effects are temporary, reversible or repairable, and alone have not been shown to produce permanent vascular occlusion. This stage relies on lumenal narrowing achieved through combination of the mechanical effects of ultrasound (tissue displacement and acoustic streaming), with tissue response such as vascular spasm, cell shrinkage, endothelial damage, and accumulation of subendothelial oedema. This stage does not necessarily represent lumenal collapse but features processes through which vessel wall apposition could be produced.

In the next stage, temperatures will reach a range in which tissue fusion can occur, and the energy deposition will be sufficient to produce irreversible damage, with denaturation and shrinkage of collagen and fracturing of elastic laminae. There is also the persistent effect of vascular spasm, obstructed blood flow and the increasing endothelial destruction leads to a loss of vascular relaxation responses and activates platelets.

The final stage is dominated by tissue response that persists beyond the end of the HIFU heating. The mechanical effects of HIFU are removed and so perivascular oedema is the only potential method of weak external compression. In this stage, the strength of tissue fusion and/or thrombotic occlusion is tested by the return of physiological blood pressure. The vessel may be fused in a fully or partially occluded position, or not at all. Activation of secondary haemostatic mechanisms form occlusive, stable thrombus that can withstand the physiological flow pressures involved. Progression from acute to chronic inflammatory responses remodel the damaged vessel, which ultimately determines if permanent occlusion of the vessel occurs over the following period, up to 28 days.

1.2.4 Bioengineering requirements

HIFU treatment is comprised of a number of components – targeting, energy delivery and monitoring of its effects. Targeting is most usually achieved by either ultrasound or magnetic

resonance imaging (MRI). Therapy ultrasound beams are usually generated from a transducer that is focused using either a bowl configuration, a plane transducer/lens combination or a multi-element array with which focussing is achieved by appropriate application of phase and amplitude to each element. Where ultrasound is used to monitor HIFU ablation of soft tissue, a successful treatment is assessed in terms of the appearance of a hyperechoic region, whereas with MRI thermometry sequences are used to estimate thermal dose (97). If the spatial precision of HIFU damage is to be harnessed to its fullest extent, it is important to account for tissue motion when placing the lesions. This presents a major challenge to successful targeting and treatment delivery and may be achieved, for example, by synchronising the HIFU exposure with cardiac or respiratory motion, and specifically for fetal medicine, accounting for movement of the fetus and umbilical cord within the amniotic sac.

In obstetrics, ultrasound image guidance is likely to be the method of choice for reasons of safety, clinical and patient familiarity, targeting efficacy and real-time responsiveness to fetal movement. To successfully occlude a selected blood vessel, it needs to be identified clearly for targeting, currently best done using Doppler ultrasound techniques. Vessels of >1 mm diameter can be identified in the fetus in clinical practise by Doppler ultrasound (98). The main disadvantage of diagnostic ultrasound is that, unlike MRI, it does not permit the measurement of absolute temperature rise during exposure, both due to interference of the therapy beam with the diagnostic information, and a lack of consistent sound speed dependence on temperature. Should accurate thermal dosimetry become a key factor, then MRI guidance for HIFU would be more suitable.

The choice of appropriate HIFU transducer geometry and exposure frequency depends on the clinical application and, more specifically, the depth of vessel to be occluded. In choosing the frequency to be used, a trade-off is necessary between the amount of energy absorbed within the target volume (which increases with frequency) and the ability to get sufficient energy to the target depth (which decreases with increasing frequency due to attenuation by the overlying tissues). It is also important to recognise that vascular specific HIFU applications typically require a higher in situ intensity and a smaller focal zone than for soft tissue applications, which would add additional complexity to transducer design. It has been shown that a “rule of thumb” for determining the optimum frequency is to allow the total attenuation in the overlying tissue to be around 10 dB (99). For typical soft tissues with an attenuation of 0.7 $dB.cm^{-1}.MHz^{-1}$ this would imply an optimum frequency of around 2.6 MHz for a target depth of 5 cm and 1.4 MHz for 10 cm. It should also be remembered that the focal region is smaller at higher frequencies, if all other source geometries remain the same. The inclusion of a central aperture in the HIFU

transducer design allows an US imaging probe to be inserted into the treatment head, thus ensuring a fixed geometry between targeting and treatment components, most efficiently with coincident acoustic axes. This also facilitates the monitoring of a treatment immediately after cessation of the HIFU exposure. Therefore, design of a HIFU transducer to meet the specific requirements of the vascular application in question is ideal.

1.2.5 Potential complications

The main specific complication of vessel exposure to HIFU are rupture and haemorrhage. Exposure to higher intensities in the experimental range has been associated with rupture of vessels, potentially due to acoustic cavitation (31, 32, 37, 47, 100) as has multiple exposures of the vessel wall which cause overheating and tissue stiffening by a cumulative effect (38, 45, 55). This effectively represents an upper exposure limit above which the application of HIFU becomes counterproductive. Therefore, HIFU appears to differ from several other occlusive techniques, particularly laser and electrocautery, which rely on multiple exposures of blood vessels to ensure permanent and stable occlusion. It is possible that it would be unsafe to use HIFU in this manner, although varying the exposure site in larger vessels may mitigate this effect.

Paradoxically, the non-invasive nature of HIFU also represents a risk of complications. Invasive methods have greater control over where the energy (thermal and mechanical) they supply is delivered as they are visually targeted and controlled. Excessive soft tissue destruction, thermal spread to adjacent structures, or heating in front of and behind the focal zone can cause pre- and post-focal damage to structures adjacent to the focus, and therefore complications. This is of particular significance where the targets are small, or hard to locate, and the margin of error is limited. Injuries to bowel (37, 61), nerves (31) or adjacent vessels (36) have been reported in fetal and vascular HIFU experiments, with or without associated vascular occlusion. Mistargeting is also an issue as not only does it fail to occlude the target vessels, but repeat exposure may also be precluded until such time as tissue healing has been allowed to occur. However, accuracy of vascular targeting has been shown to be improved with the use of colour flow Doppler ultrasound over even surgical exposure and visual targeting in the application of HIFU (52).

There are also general complications related to HIFU usage. If an inappropriate acoustic window is used, or there are elements in the acoustic window which scatter or reflect, rather

than transmitting, the ultrasonic energy, heating to unpredictable locations may occur, causing burns, typically on the skin because this has a higher absorption coefficient compared to most other soft tissues, although any tissue in the path of the ultrasound energy may be affected. The abdominal skin is particularly vulnerable as thermal energy has a tendency to accumulate in the subcutaneous tissue due to its greater ability to absorb heat (101) that surrounding tissue, its insulator properties (101-103) and the relatively poorer blood supply compared to surrounding tissue that prevents it from dissipating heat (104, 105). The air-skin interface is also the most likely area at which acoustic reflection can occur.

While the use of HIFU in pregnancy has only reached the stage on anecdotal evidence, there is safety data regarding the use of HIFU to ablate solid tissue structures in the non-pregnant uterus. Such adverse events are classified by according to the Society of Interventional Radiology guidelines, in which type A-B events are reported as minor complications, and type C-F events are significant complications (106).

A recent retrospective review of approximately 9,988 patients treated with HIFU for conditions such as uterine fibroids, adenomyosis, placenta accreta, abdominal wall endometriosis and caesarean scar pregnancy reported an 10.6% rate of adverse events, 2.4% which were significant complications (class C-D). The most common complication was excessive vaginal discharge or bleeding (8.9%), followed by abdominal or buttock pain (3.5%); 2/9988 patients experience pain lasting more than 2 months secondary to sciatic nerve injury. The rate of abdominal skin burns was 0.3% (26/9988); 4/26 patients with skin burns required surgical removal of necrotic tissue as a result of skin burns. There were 16 cases of urinary retention, 3 cases of acute renal failure, which required dialysis, but recovered, and 1 case of bowel perforation, which required surgery (107).

These rates of complications reflect the use of a commercially available HIFU therapy system and an established treatment protocol: they also rely on patient reporting of adverse events. The rates quoted in the above study are lower than reported in smaller scale prospective studies, focused on developing treatment protocols, with planned follow-up of patient outcomes. Skin burn rates are between 4% (108-110) and 10% (111). Burns could be any severity from skin reddening (111) to full thickness third degree burns (107, 112). Cooling of the maternal skin to around 20^{o}C during HIFU exposures is a method currently under investigation to reduce the risk of maternal skin damage (113).

Similarly, many of the published studies report a patient with chronic leg pain secondary to sciatic nerve injury (107, 109-111, 114), which is now a recognised significant complication of applying HIFU in the pelvic region.

1.3 Fetal sheep model

The chronically instrumented fetal sheep model is a well-recognised method of studying non-stressed, non-anaesthetised fetal physiology, endocrine and metabolic responses in utero. It allows assessment of fetal responses to challenges such acute and chronic hypoxia, reduction or occlusion of umbilical and uterine artery blood flows. As such, there is a broad range of reference data available regarding normal ovine fetal physiology, which has contributed to the knowledge base available to obstetric medicine (115). Current methods of fetal sheep instrumentation allow surgical insertion of indwelling catheters and flow probes using aseptic techniques. Indwelling catheters in the fetal circulation allow continuous monitoring of fetal heart rate and blood pressure as well as intermittent sampling of fetal blood for arterial blood gas, acid-base status, metabolic and endocrine measurements. Indwelling flow probes allow continuous monitoring of fetal heart rate, heart rate variability and blood flow in a vessel, which combined with blood sampling from that vessel allows calculation of substrate (notably oxygen and glucose) delivery to different vascular beds. These methods of monitoring allow detection of recognised parameters of fetal distress, namely changes in fetal heart rate patterns, acid-base and metabolic status and redistribution of fetal blood flow from peripheral to central vascular beds, the so called “brain sparing effect”. The fetal sheep model can also be used as an acute model to capture physiological, endocrine and metabolic responses in utero to anaesthesia, surgery or surgical experimentation, but this has the disadvantage that the effect of anaesthesia must be considered in the results obtained. Fetal sheep models have also been used to test HIFU techniques for ablation of solid tissue and for ablation of maternal uterine arteries (46, 60, 61).

1.3.1 Relevance to human pregnancy

No animal model can ever truly represent human pregnancy, but the pregnant sheep and fetus form a good model for human pregnancy, both in terms of suitability for experimentation and comparative anatomy and physiology.

In terms of experimental suitability, unlike other experimental animals, sheep tend to have only singleton or twin pregnancies and the birth weight of the lambs are similar to those of human babies, although the lamb is comparatively more developed at birth than the human. The gestational length of the ewe is also 145-150 days, around 50% of the human gestational period, longer than many other experimental animals, meaning that techniques, timing and

duration of experimentation are more easily translated between a research and clinical context, and vice versa.

The sheep also tolerates uterine surgery well. Unlike humans and primates, the ovine uterine musculature is thinner and does not contract as vigorously when incised. Some local contraction does occur, but the lack of generalised contraction results in an easier surgical procedure, requiring less manipulation and stimulation of the fetus, less interruption of uterine and umbilical blood flows secondary to uterine contraction, and lower rates of post procedure miscarriage and placental abruption or separation (116).

Both factors allow the successful placement and maintenance of flow probes and catheters on both the maternal and fetal sides of the feto-placental unit.

The sheep conforms to the general pattern of mammalian circulation, and fetal sheep have a similar cardiovascular system to human fetuses, including present ductus venosus and arteriosus and foramen ovale (117). These three shunts make the human and sheep fetal circulations adaptive to intra-uterine challenges by allowing redistribution of blood from the peripheral to central circulation (118). The mean arterial pressure and oxygen saturation at defined points in blood vessels, acid-base endocrine and metabolic status in sheep are comparable to human values. Both the sympathetic and parasympathetic nervous systems mature during the last third of fetal life (119-121), producing characteristic reduction in fetal heart rate and increase in mean fetal arterial blood pressure approaching term (122). Accordingly, the late gestation fetal sheep has functional chemo- and baroreceptors as well as adrenergic and cholinergic receptors to mediate homeostatic and regulatory responses. This allows fetal sheep to make responses to fetal stress by redistribution of blood flow in a comparable manner to human pregnancy. Adult sheep have similar cardiovascular parameters to man if allowances are made for smaller weight of the average sheep (123).

1.3.2 Heart rate variability analysis

The fetal heart rate (FHR) fluctuates under the influence of centrally mediated sympathetic and parasympathetic tone, producing variability, which alters with increasing gestational age as these systems mature, and between different fetal behaviour states, the prevalence of which also changes with gestational age (124). Diurnal variation in fetal heart rate variability (FHRV) is also seen (125), as well as intrinsic variability (126). The variability in fetal heart rate can be assessed in a number of ways.

The most familiar method from human pregnancy is via the cardiotocograph (CTG) or computerised cardiotocograph (cCTG, Figure 1.4). Unlike clinical assessment of FHRV on a traditional cardiotocograph (CTG), which has well acknowledged intra-observer variability (127), and does not alter perinatal mortality (128), computerised cardiotocography (cCTG) produces objective measures of FHRV based on the Dawes-Redman criteria previously published (129). One such measure, short term variation (STV), is a statistical summary measure of the variation interbeat intervals of 3.75 s epoch of averaged fetal heart rate recordings, excluding pronounced accelerations and decelerations. A persistent reduction of STV to below 3 ms within 24 hours of delivery has been shown to be predictive of an increased risk of metabolic acidosis and early neonatal death (130). As such, interpretation of cCTG based on STV is recommended for prenatal surveillance of fetuses with suspected fetal growth restriction to detect acute fetal distress requiring delivery (131). Increases in normal values for STV are seen with advancing gestational age (132), likely representing a gradual increase in sympathetic rather than parasympathetic tone in the pre-term fetus (133, 134), with lower variability in FGR fetuses resulting from sympathetic suppression (133, 135-138).

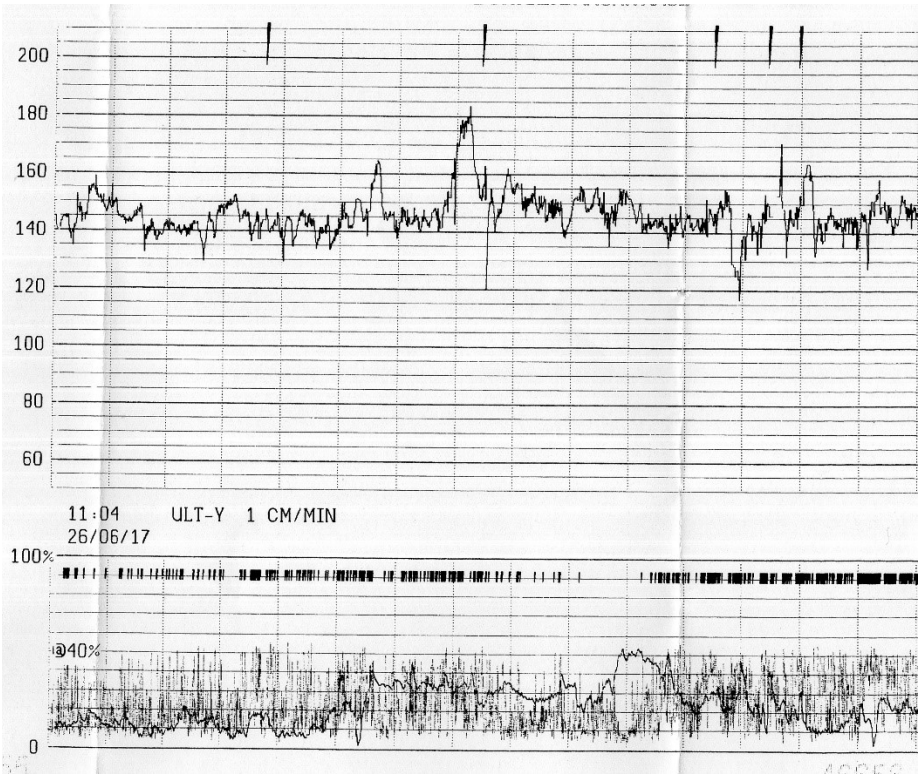

Figure 1.4: Computerised Cardiotocograph (cCTG).
The image shows a section of a cCTG from a human patient at 36 weeks' gestation. The upper part of the image shows the fetal heart rate varying between 130 – 180 bpm, in a normal pattern of active sleep. The STV was 6.8 ms. The lower part of the image shows the fetal movements (an active fetus) and the uterine activity (no coordinated activity).

Overall heart rate variability, as well as the contribution of the sympathetic and parasympathetic nervous system to the variability can also be estimated by time domain and frequency spectrum analysis of heart rate recordings. Time domain analyses are statistical summary measures of the inter-beat intervals in milliseconds of successive waveforms of the heart rate (the R-R or N-N interval, Figure 1.5). The standard deviation of the NN intervals (SDNN) reflects all the cyclic components responsible for heart rate variability in the period of recording, and estimates the overall variability of the heart rate. It is affected by length of recording, so comparison of short term variability over standardised 5 minute samples is recommended (139). The root mean square of the successive differences (RMSSD) is a further time domain measure, which reflects the parasympathetic control of heart rate and is strongly correlated with high-frequency variation of the heart rate (139).

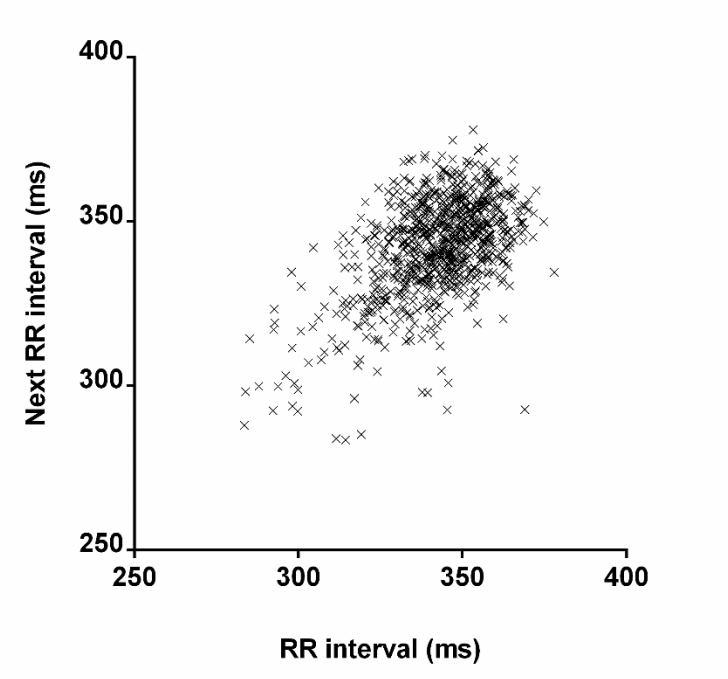

Figure 1.5: Poincaré plot of successive R-R intervals.
The graph shows each R-R interval plotted against the successive R-R interval in a 5 min sample of heart rate in a chronically instrumented fetal sheep in the active sleep state (126 d GA). The clustering of the points gives a qualitative indication of the variability of the fetal heart rate.

Power spectral analysis of the heart rate variability determines the energy in specific frequency components of heart rate variability and allows a more precise evaluation of the sympathovagal balance than time domain measures (Figure 1.6). The low frequency component (LF; 0.04-0.15Hz) reflects predominantly sympathetic control of heart rate variability but a proportion of the variation results from parasympathetic activity (126). The high frequency component (HF; 0.15 – 0.4 Hz) reflects parasympathetic control of heart rate variability (140). The physiological explanation of the very low frequency component (VLF; 0-0.04Hz) is less well defined, but is

thought to relate to thermoregulation, peripheral chemoreceptor activity and fluctuations in the renin-angiotensin system (141). VLF, LF and HF contribute to total power, which is affected by the absolute heart rate (142). Therefore, in longitudinal studies where fetal heart rate changes with gestation (132) normalised LF and HF (LF or HF as a proportion of total power) should also be presented to detect changes in relative LF and HF power which can otherwise be masked by changes in total power (143).

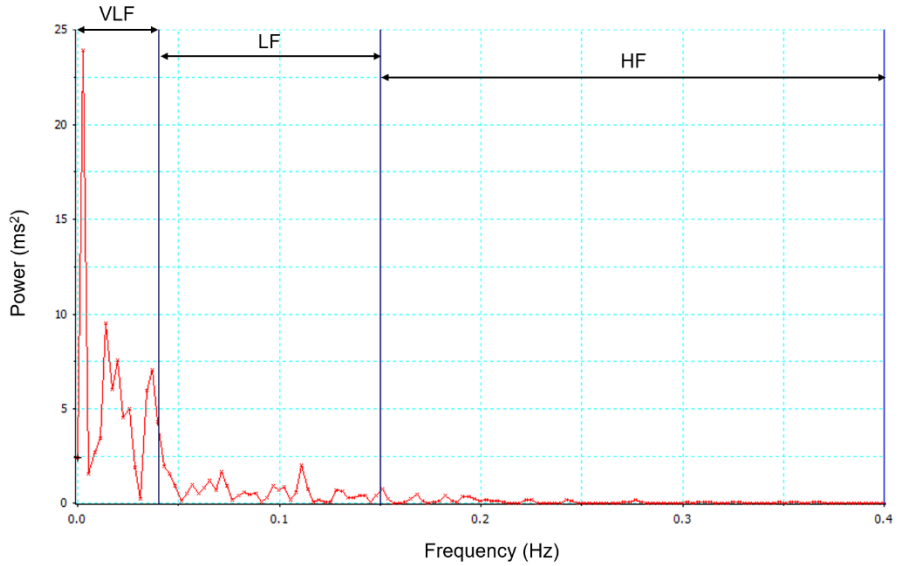

Figure 1.6: Spectrum plot of specific frequency components of heart rate variability.
The graph shows the total power of the heart rate variability divided into VLF, LF and HF components. This is the same 5 min sample of heart rate in a chronically instrumented fetal sheep in the active sleep state (126 d GA) shown in Figure 1.5. Comparison of the area under the curve in the LF and HF bands indicates the relative activity of the sympathetic and parasympathetic nervous systems.

Spectral analysis of FHR variability requires the FHR to be acquired on a beat-to-beat basis for reliable results (144). Non-invasive Doppler ultrasound monitoring, as used in computerised and traditional CTG, cannot measure beat-to-beat variation because FHR is implicitly averaged by correlation based techniques that are used to calculate it (129). Auto regression techniques can be used to obtain FHR on a beat-to-beat basis from Doppler ultrasound derived FHR (135) (125), however they can only be considered reliable for frequencies less than half the frequency at which the averaging takes place (143). As the sampling frequency of average heart rate produced by CTG machines which typically report every 2.5 s is 0.4Hz (145) this limits analysis to VLF and LF domains (i.e. <0.2 Hz). Fetal MRI has also been used to measure R-R intervals in human fetuses (146, 147), however studies of FGR fetuses in the antenatal period are few in number, and this technique is not widely accessible.

Data on normal values and changes with gestation in fetal HRV measured by time domain and power spectra are relatively sparse and the relative contributions of the sympathetic and

parasympathetic nervous system remain under debate. While there is broad agreement that SDNN, total power, LF and HF power increase with gestational age and fetal maturity, alterations in the LF/HF ratio relative to gestational age, fetal activity/sleep state or fetal compromise follow an unclear pattern (126, 143, 145-153).

1.3.3 Sheep placentation

Unique to this project is the requirement for a model of placental vascular anastomoses, ideally in a singleton pregnancy. The ovine placenta is a specific type of chorioallantoic placenta classified as a synepitheliochorial placenta, which is unique to ruminant species. It is organised into discrete regions of maternal and fetal tissue called placentomes: the maternal portion is the uterine caruncle and the fetal portion which develops is the cotyledon. Uterine caruncles are specialised projections of non-glandular areas of the uterine epithelium (154) to which the fetal trophectoderm can first attach, then interdigitate and allow binucleated cells (BNCs) derived from the fetal trophectoderm to migrate into the uterine epithelium. The feto-maternal syncytium is formed by fusion of fetal trophectoderm binucleated cells (BNCs) with maternal uterine epithelial cells, and the fetal BNCs have the ability to deliver hormones and effectors into the maternal circulation. The placentomes are therefore formed of enmeshed maternal and fetal villi, where feto-maternal haemotrophic exchange takes place (155), and fetal allantoic vessels arise from this area of the placentome to emerge into the amniotic sac. These vessels are small in diameter (1-3 mm), and run between placentomes before joining together into larger vessels, which ultimately form the two umbilical arteries and vein and umbilical cord (Figure 1.7). In the human placenta, fetal cotyledons are recognised, with discrete villous trees of fetal blood flow, despite the externally continuous nature of the placental surface. The villous tree of both placentae is similar in that they contain stem, intermediate and terminal villi of comparable structure and size (156). Vascular anastomoses between allantoic circulations in multiple pregnancy in sheep are rare (157). Hence while the presentation of the human and sheep placental initially appear very different they are functionally comparable and their vasculature is anatomically similar: the key difference being the exposed vessels which mimic vascular anastomoses in monochorionic placentae.

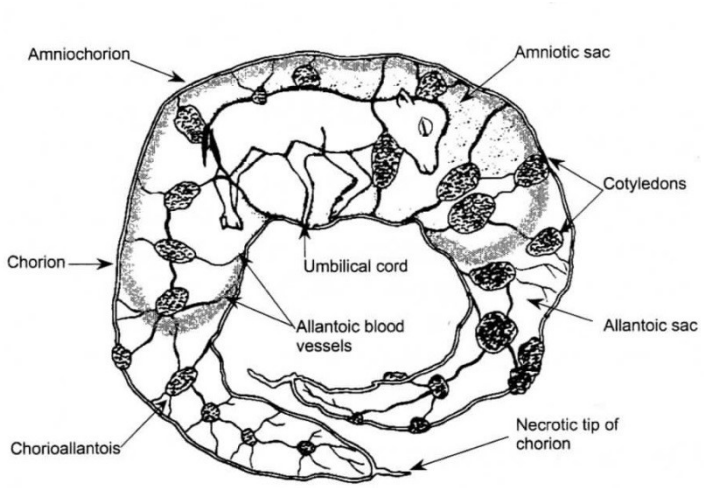

Figure 1.7: Diagram of sheep placentation.
The image shows the relative arrangement of placentomes, allantoic vessels (which will be targeted as they emerge from placentomes in this study) and the formed umbilical cord. Reproduced from Hafez 2000 (157).

In sheep, 4 different classes of placentomes (type A-D) are recognised based on their morphology, although they are histologically not different, and although type D have been suggested to be more efficient than type A (158) they are also larger, and size rather than morphology influences vascularity and nutrient transfer (159). Type A are concave, type D are convex, and types B and C are intermediate stages between concave and convex (160) (Figure 1.8).

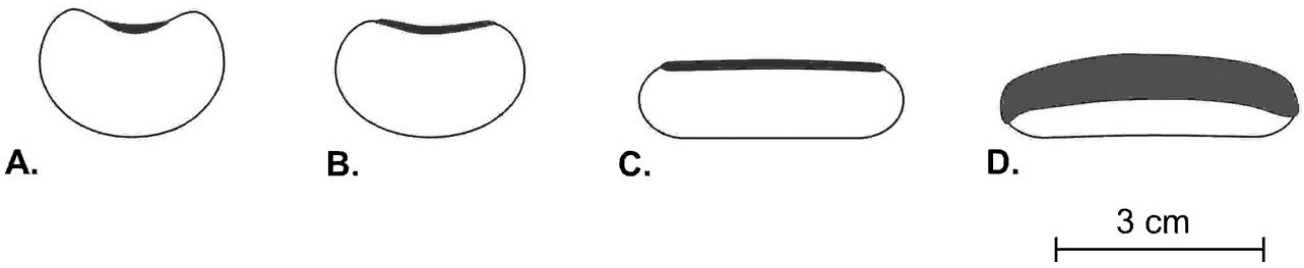

Figure 1.8: Placentome types.
A diagrammatic representation of cross-sectional appearance of sheep placentomes morphology by type, reproduced from Vatnick *et al.* 1991 (160).

Regardless of type, the organisation of the sheep placenta into placentomes increases the surface area of feto-maternal exchange surfaces by 5-10 fold per gram of fetus compared to human placentae (161). Placental mass increases until around 70-90 days post conception in sheep (term ~150 days post conception) and the surface area of the villi continue to increase until around 120-125 days post conception to meet the increasing demand of the growing fetus. This increase in surface area is achieved by ongoing branching of the maternal and fetal villi and reduction of the intervening connective tissue until the two blood vessel systems are very

closely placed with little separation. Typically, placentomes are type A and B until around 100 days post conception, and a variable proportion become type C and D after this time (155). If there is a restricted placentome number, such as where uterine caruncles have been removed pre-pregnancy, there is a shift towards larger, convex placentomes (162).

There are a limited number of caruncles per uterus, not all of which are formed into placentomes during pregnancy. The Welsh Mountain breed normally have 70-80 placentomes in pregnancy. Multiple pregnancies have more placentomes than singletons, but the overall amount of placentomes per fetus remains reduced compared to singletons. There is a close correlation in sheep between total placentome mass and birthweight (163), majority of maternal caruncles need to be removed pre-pregnancy to produce an placental insufficiency or a model of growth restriction in pregnancy (164). The effect of reduction in placental mass in the third trimester has not been reported.

This makes the sheep placenta a suitable for a model of placental vascular anastomoses. Even in singleton pregnancy there are placental blood vessels connecting areas of placental tissue which can be identified with Doppler ultrasound and targeted for HIFU mediated vascular ablation. The organisation of the placenta, particularly the large reserve in surface area of feto-maternal haemotrophic exchange and the capacity to increase the efficiency of remaining placentomes in cases of placental insufficiency mean that a clinically relevant number of vascular ablations can be performed without the expectation of causing fetal compromise.

1.3.4 Effect of anaesthesia in ewes and fetuses

In pregnant women, regional anaesthesia is usually preferred for surgical procedures where possible due to the lower associated maternal risks of hypoxia, aspiration pneumonia and mortality when compared to general anaesthesia (165, 166). However it is recognised that general anaesthesia produces less hypotension, less cardiovascular instability and better control over ventilation than regional anaesthesia (167). Inhalational anaesthetics of the halogenated ether class, including isoflurane, sevoflurane and desflurane, are typically used for maintenance of anaesthesia, with or without supplemental IV anaesthesia (SIVA). The concentration of anaesthetic vapour in oxygen required to produce a given level of sedation varies between drugs used, but can be standardised as the minimum alveolar concentration (MAC). A MAC of 1.0 represents the concentration of an anaesthetic vapour in the lungs which prevents motor responses to noxious stimuli in 50% of subjects. SIVA reduces the required

concentrations of inhalational anaesthetics in humans (168) and sheep (169), but in sheep any potential benefit from this is negated by the increased recovery times from SIVA. Ruminants are at significant risk of regurgitation and bloat when recumbent (170) and that the highest risk period of this is during recovery (171) hence prolonging recovery increases morbidity in ruminants. For isoflurane, the blood:gas, blood: brain and fat: blood coefficients are 1.4, 1.6 and 48 respectively. Despite these values being on paper inferior to newer agents such as sevoflurane and desflurane (172), in practise anaesthetic maintenance and recovery from anaesthesia in pregnant sheep is unaltered between the three anaesthetic agents (170).

The 1.0 MAC value of isoflurane in pregnant sheep has been determined as between 0.86-1.14% inhaled isoflurane (167, 173, 174). Isoflurane appears in the fetal circulation within 2 minutes of maternal administration, but remains lower (50-80%) than maternal levels throughout the duration of anaesthesia, with the uptake curve of mother and fetus following the same pattern (175). Fetal 1.0 MAC has estimated in sheep as 0.34% inhaled content (174) and measured as 0.5% inhaled content in newborn lambs (176) so it is reasonable to consider that the fetus achieves an equivalent or greater depth of anaesthesia as the mother.

In humans, for maternal procedures low to moderate concentrations of halogenated ether inhalational anaesthetics can be used (0.5-1.0 of MAC) can be used to maintain anaesthesia. For procedures which require uterine relaxation, such as non-obstetric abdominal surgery (for avoidance of intra-operative uterine contraction) or hysterotomy for open fetal surgery, higher concentrations are required (2.0-3.0 MAC) (177-180). Isoflurane is recognised as a potent vasodilator which has a dose and duration dependant effect on maternal and fetal physiology during the period of anaesthesia, which have been well described in the fetal sheep model. Some studies date from the 1980s when isoflurane emerged as a novel anaesthetic agent; however there has been renewed interest in the past decade as the increasing success rates of fetal ex utero intrapartum treatment (EXIT) procedures has led to pregnant women being exposed to general anaesthesia for longer periods at higher concentrations, with the added complication of a compromised fetus undergoing a surgical procedure. There are currently 6 published works which report ovine maternal and fetal cardiovascular and metabolic responses to isoflurane anaesthesia at 0.8 gestational age (summary tables of results provided for reference in Appendix I).

Regardless of stage of gestation, pregnant ewes show and initial bradycardia and arterial hypotension combined with decreased uterine blood flow (173-175, 181-184). This response is both dose and time-dependant as these effects are only observed at 1.5-2.0 MAC and above (167, 173) and all parameters recover to baseline within 120 minutes of start of anaesthesia

(181, 182), or within 6 minutes of extubation (167, 170). Maternal hypotension can be corrected with intravenous fluids or inotropic drugs; however this does not alter the degree of cardiovascular compromise observed in the fetus (168). At MAC 1.5-2.0 there is also a trend to increasing arterial carbon dioxide content (p_aCO_2) in the maternal blood, despite tight control of end tidal carbon dioxide ($EtCO_2$) and a corresponding decrease in arterial pH (pH_a)(167, 173, 175, 181, 182). Maternal ventilation responses are supressed at ≥1.0 MAC but automated ventilation with an high fraction of inspired oxygen (FiO_2) ensure that maternal oxygenation remains high (167).

The fetus shows a dose dependant reduction in fetal heart rate and mean arterial blood pressure with left ventricular systolic dysfunction at 1.5-2.0 MAC, which unlike maternal responses persisted for the duration of the anaesthetic administration and rapidly recovered on extubation. This was accompanied by increase in fetal p_aCO_2 and decrease in pH_a, although the acidosis was fully reversible within 24 hours (167, 173, 175, 181, 182). A marked elevation of fetal arterial oxygen content (p_aO_2) is consistently observed due to maternal ventilation with a high FiO_2, so cerebral oxygenation is either maintained at baseline levels (182) at (ca. 0.6 of gestation) or increased in late gestation (ca. 0.8 gestation) (181). This gestational difference is likely due to the development of cerebral blood flow autoregulatory pathways, which mature at different gestational ages (185, 186). The effect of hypercapnia on increasing cerebral blood flow may also contribute to maintained or increased oxygenation. Isoflurane sedation does not alter the capacity of fetal sheep to redistribute cerebral – systemic blood flow in response to reduced uteroplacental flow or development of acidosis (184), and fetal sheep maintained their cerebral blood flow when fetal MAP varied 20-48 mmHg (187).

1.3.5 Effect of uterine manipulation

The effect of uterine manipulation on fetal wellbeing and physiology has not been well documented. There is currently no little available in humans regarding the physiology of the mother and fetus in response to uterine manipulation while under anaesthesia, although what there is suggests the fetus initiates cardiovascular defence mechanisms and redistributes blood to the brain, despite normal oxygenation (188). Fetal cardiovascular defence responses have been described in sheep fetuses to reduced uterine blood flow (189) primarily mediated by the sympathetic nervous response to fetal acidosis (190) and perpetuated by endocrine mediated fetal stress responses (191). Elevation of intra-abdominal pressure secondary to gas insufflation in laparoscopy has been demonstrated in animal models to decrease uterine blood flow and

cause marked respiratory acidosis in the fetus (192). The impact of these insults in terms of fetal brain oxygenation depends on the developmental maturity of fetal compensatory mechanisms from the early third trimester onwards, which are not impaired by general anaesthesia (184). Severe functional brain hypoxia is observed in second trimester sheep fetuses (193), but there is preserved brain oxygenation in the third trimester (192). In humans, epidemiological data suggests there is a negative impact of undergoing laparoscopy or laparotomy between 4-20 weeks gestational age, reported as a statistically increased relative risk of growth restriction, low birth weight and premature delivery, although there was no control in the data to account for the impact of maternal disease on obstetric outcomes. Cumulative survival to one year of age was unaffected; however there was insufficient data to analyse outcomes for operations in the second and third trimester (194).

1.4 Doppler Ultrasound

1.4.1 Principles of action

Doppler ultrasound is a non-invasive technique which allows assessment of moving structures, notably the flow of blood through a vessel or heart valve. It exploits the fact that movement will scatter ultrasound energy more than still tissue, and produce a frequency shift in the reflected ultrasound energy that is detected by the ultrasound transducer. This frequency shift, or Doppler effect, can be used to calculate the speed and direction (though not absolute volume) of blood flow in a vessel relative to the ultrasound transducer. Unlike time-transit ultrasonic flow probes, Doppler ultrasound results are altered by angle of insonation, with the error increasing as the angle between direction of flow and path of the ultrasound beam increases. Speed and direction information can be visually represented to the operator as (among others) colour Doppler, where information is presented as a colour-coded overlay on top of 2D B-mode imaging. Pulsed wave Doppler displays velocity information from a subsection of the B-mode image (defined by the "Doppler gate") mapped against time to create a waveform of blood flow through a vessel. From this, values such as peak systolic velocity (PSV), mean velocity and end diastolic velocity (EDV) can be measured (Figure 1.9). Pulsatility index (PI) may then be calculated as (PSV-EDV)/MV.

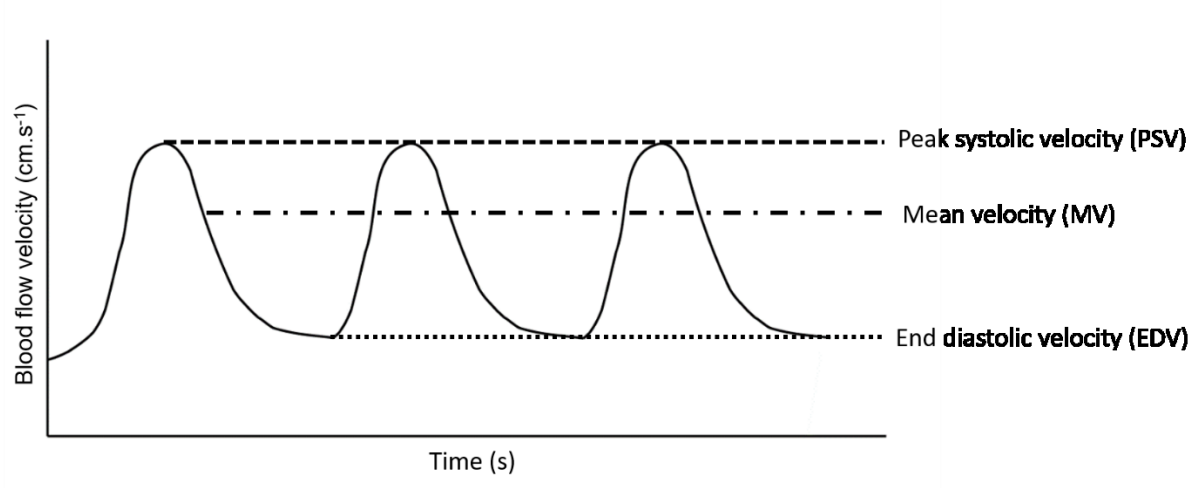

Figure 1.9: Pulsed Doppler representation of a monophasic arterial waveform.
The diagram shows an illustration of blood flow over three cardiac cycles, measured with pulsed wave Doppler. Common metrics (PSV, MV, EDF) which can be derived from these waveforms are shown. Pulsatility index (PI) is then calculated as (PSV-EDV)/MV.

1.4.2 Mapping of placental anastomoses

Arterio-arterial and arterio-venous anastomoses in human monochorionic placentae have been successfully identified on ultrasound. Both are located within the placenta using colour Doppler waveform interrogated with pulsed wave Doppler to identify the type of vascular anastomoses. Arterio-arterial anastomoses appear easier to locate with a sensitivity of 85% and specificity of 97.3% when compared to placental injection studies (195). Arterio-venous anastomoses are more challenging, with sensitivity of between 25-50% when compared to placental injection studies (196-198). In all cases, identification was easier with larger vessels and anterior placental positioning.

1.4.3 Placental mapping in sheep

There has been limited work characterising placental vessels in sheep although vessels are readily apparent on colour Doppler as they emerge from the fetal aspect of the placentomes (Figure 1.10). 3D quantification of utero-placental flow has been validated *in vivo* using the pregnant sheep model (199) demonstrating a high degree of accuracy can be obtained in imaging and quantification of ovine placental vessels.

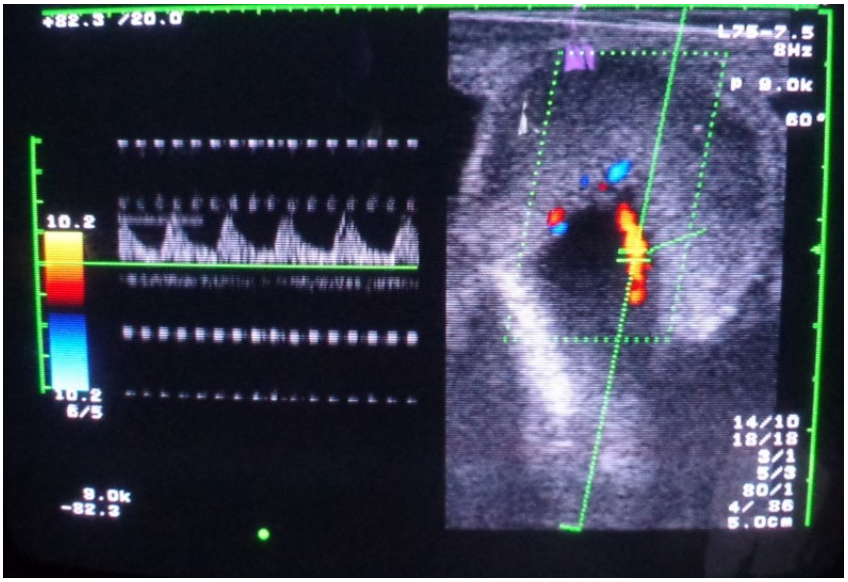

Figure 1.10: Doppler ultrasound of a placental vessel emerging from a placentome.
This is a representative ultrasound image obtained during the study of placental vasculature, using a 3.75 MHz convex abdominal probe (PVK-357AT, PowerVision 7000, Toshiba Medical Systems). Sheep: OR585, 116 d gestational age.

1.5 Ultrasound assessment of fetal wellbeing in humans

The following section considers the evidence for assessment of fetal wellbeing in the antenatal period and excludes consideration of intrapartum evidence.

1.5.1 Fetal growth rate

Fetal weight cannot be measured directly, only estimated, from ultrasound derived fetal biometry. The most commonly used fetal measurements for this purpose are the biparietal diameter (BPD), head circumference (HC), abdominal circumference (AC) and femur length (FL). Typically, the Hadlock formula is used to estimate fetal weight, with a mean error of 10-15% (200), and serial measurements of fetal biometry and estimated fetal weight can be used to calculate the change in size or weight of the fetus over time.

The human growth rate is rapid during fetal life, and deviation from a consistent pattern of growth can be associated with placental insufficiency, metabolic and genetic/chromosomal abnormalities or infection. Fetal growth restriction (FGR) is defined as the failure of a fetus to achieve a genetically pre-programmed size while in utero. FGR is an important predictor of perinatal morbidity and mortality, but increasingly failure to maintain a consistent fetal growth rate growth rate, rather than estimated fetal weight has been recognised as the more important predictor of poor outcomes in this group of small fetuses (201).

As in human pregnancy, ultrasound derived measurement of fetal biometry can be performed in utero, except for HC, due to the altered shape of the sheep skull compared to humans. BPD, AC and FL have all been reported to increase in a linear fashion with increasing gestational age in sheep until term (202), and to correlate to size at birth (203), although the estimation of fetal weight based on these parameters is less accurate than in humans when using the Hadlock formulae (203).

Fetal growth restriction in sheep is defined as a birth weight or size more than 2 standard deviation (SD) below the mean of the breeding flock for that season (204). FGR can be induced in fetal sheep by simulation of utero-placental dysfunction (carunclectomy, placental embolization, single umbilical artery ligation), maternal hyperthermia, hypoxia or nutritional manipulation (205) and is associate with adult cardiac and metabolic dysfunction (206).

1.5.2 Umbilical artery Doppler

Currently, based on a systematic review and meta-analysis of published studies, including more than 10,000 pregnancies, Doppler studies of the umbilical artery (UA) are recommended to be incorporated into the assessment of fetuses at risk of placental insufficiency (207).

The waveform of the fetal umbilical artery, as measured by pulsed wave Doppler, reflects the fetal cardiac contraction, vessel wall elasticity, afterload in fetal vessels and impedance of blood flow from the fetal to the placental vessels (a marker of placental resistance). The maximum velocity (PSV) is related to blood flow from fetus to placenta during ventricular contraction and peak systolic arterial pressure; the minimum velocity (EDV) represents blood flow during ventricular relaxation and the nadir of diastolic arterial blood pressure. Forward blood flow is expected for the entire duration of the cardiac cycle in a low-resistance system with normal placental function (208). The umbilical artery pulsatility index (UA-PI) shows a progressive decline with advancing gestation, as a result of increases in fetal diastolic arterial blood pressure, from a mean of 1.07 (95% confidence interval (CI) 0.79 – 1.45) at 28 weeks' gestation to 0.74 (95% CI 0.55 – 1.00) at full term (40 weeks), adjusted for estimated fetal weight (209).

UA-PI is estimated to show elevation when 60-70% of placental vasculature has become high resistance (210). Waveform changes may include absent or reversed end diastolic flow (211, 212) which indicate forward blood flow is no longer possible for the entire cardiac cycle, denoting an even more pronounced degree of placental failure. Abnormal waveform patterns predict fetal compromise and precede acute fetal deterioration by up to 12 days (213). The UA-PI can be altered by the position of the cord from which the measurement is taken (214), fetal activity (215), but does not show diurnal variation (216).

Despite the differences in sheep and human placentation, once in the coiled umbilical cord, umbilical artery blood flow in the sheep has a similar waveform to that of humans, with continual forward flow throughout the cardiac cycle. However, there are no longitudinal studies of UA-PI throughout gestation. Additionally, due to the nature of the experimental work being performed, many values of UA-PI are taken in anaesthetised animals. While the trends of UA-PI changes correlate well with changes measured by invasive measures of blood flow in the umbilical artery, quantitative values for blood flow cannot be predicted base on Doppler studies alone (199, 217).

In un-anaesthetised animals UA-PI is reported as 0.70 – 0.90 at ca. 115-120 d gestation (205, 218, 219), falling to around 0.50 at 135 days gestation (220). Just as in humans, hypoxia,

hypertension and impaired placental function result in elevation or UA-PI (205, 218, 220). Under anaesthesia, the umbilical PI can increase by 1.5 - 2-fold (221).

1.5.3 Middle cerebral artery Doppler

Doppler assessment of the fetal middle cerebral artery (MCA) can be used to assess fetuses at risk developing anaemia, or for evidence of cerebral vasodilation, which may indicate preferential redistribution of blood to the fetal brain as part of a fetal cardiovascular stress response.

The peak systolic velocity of the middle cerebral artery (MCA-PSV) waveform as measured by pulsed wave Doppler increases with gestational age from a median of 40.5 $cm.s^{-1}$ (± 1.5 multiples of median (MoM), 20.3 – 60.7) at 30 weeks' gestation to 64.4 $cm.s^{-1}$ (± 1.5 MoM, 32.2 – 96.6) at 40 weeks' gestation in normal pregnancy (222) as a result of increasing systolic blood pressures. Elevation of MCA-PSV above 1.5 MoM is known to result from fetal anaemia (223) but can also result from severe acute or chronic hypoxia (224, 225).

The pulsatility index of the middle cerebral artery (MCA-PI) Doppler also decreases with gestation from a mean of 1.94 (90% CI 1.45 – 2.47) at 28 weeks' gestation to a mean of 1.35 (90% CI 0.83 – 1.93) at 40 weeks' gestation in normal pregnancy (226) as a result of increasing diastolic blood flow. A reduction in PI below the normal range for that gestational age is a marker of cerebral vasodilation, and may therefore represent an early sign of hypoxia in fetuses (227-229), although its predicative power for adverse outcomes is low (230, 231). An elevation in MCA-PSV has been suggested show cerebral redistribution more consistently and to predict perinatal morbidity better than a low MCA-PI in IUGR fetuses (225).

There are no reported measurements of the middle cerebral artery Doppler in fetal sheep, although the anatomy of the circle of Willis in the human and sheep brains is comparable.

1.5.4 Cerebro-placental ratio

The cerebro-placental ratio (CPR) relates the PI of the UA Doppler to that of the MCA Doppler (UA-PI/MCA-PI). In normal pregnancy, the value of CPR rises to a maximum around 34 weeks' gestation, mean 2.35 (95% CI 1.63 – 3.29), before falling towards term, mean 1.97 (95% CI 1.29 – 2.88). A ratio of <1 has long been recognised to fetal brain sparing (232), conferring an 11-fold increased risk of adverse perinatal outcomes in growth restricted fetuses (233).

There are no reported measurements of the cerebro-placental ratio in fetal sheep.

1.5.5 Ductus venosus

The ductus venosus (DV) is fetal venous shunt which in normal pregnancy allows between 30-55% oxygenated blood in the umbilical vein (UV) to bypass the hepatic circulation and pass directly in to the inferior vena cava (IVC), thereafter to the right atrium (234). Flow through the DV increases with gestation to increase until 31 weeks' gestation, after which time is remains stable despite increases in umbilical blood flow and liver size (235, 236).

The diameter of the DV is around one third of the UV and it connects to the IVC at a steep upward angle: both of these features increase the velocity of blood flow within the DV and cause it take on a triphasic waveform pattern. The ductus venosus pulsatility index for veins (DV-PIV) decreases with gestation from a mean of 0.56 (95% CI 0.31 – 0.81) at 28 weeks' gestation to a mean of 0.45 (95% CI 0.21 – 0.71) at 39 weeks' gestation in normal pregnancies (235), reflecting changes in fetal pre- and after-load with increasing maturity.

In growth restricted fetuses, up to 60% of UV blood flow bypasses the hepatic circulation (234). As such, changes in the DV-PIV and characteristics of the waveform, notably absent or reverse 'a' wave, reflect atrial pressure-volume changes during the cardiac cycle. Elevations of DV-PIV have been shown to be associated with the presence of markers of biochemical dysfunction (237). A reversed 'a' wave results from increased afterload and/or preload (238), and denotes the onset of pre-terminal fetal compromise (239). As such, DV is recommended for timing of delivery in early onset fetal growth restriction (131).

Just as in the human, in the fetal sheep DV shunting of oxygenated blood accounts for 45 – 60% of umbilical vein blood flow, which is increased during hypoxia or reduced umbilical vein flow (234). In the event of cardiac decompensation, reversal of the 'a' wave has been reported (240). There is a single longitudinal study in un-anaesthetised ewes of changes in DV-PIV with gestation: akin to humans, there is no significant change between a mean of 0.52 (± 0.02 standard error of mean (SEM)) at 115 d gestational age to a mean of 0.58 (± 0.03 SEM) at 136 d gestational age (240).

1.5.6 Uterine artery Doppler

In the non-pregnant state, uterine arterial (UtA) blood flow is low, with high resistance in arteries characterised by low end diastolic flow velocities and an early diastolic notch reflecting the elasticity of the vessel. In normal early pregnancy, maternal uterine arteries are remodelled by the action of extra-villous trophoblastic tissue to allow high flow, low resistance maternal arterial blood flow to the placental bed. These changes are characterised by pulsed wave Doppler by an increase in end diastolic velocities, which reduces the pulsatility index (UtA-PI) and a loss of the early diastolic notch. Persistent notching or elevation of UtA-PI beyond 24 weeks' gestation is an indicator of high pressure blood flow in the arterial lumen and poor arterial relaxation, which are markers of inadequate spiral artery remodelling (241, 242), although vasoconstriction alone can increase the PI of blood flow through that vessel so long as flow is maintained (243, 244).

The UtA-PI falls markedly from early pregnancy until the end of the second trimester, thereafter it falls more slowly with a mean of 0.81 (95% CI 0.56 – 1.17) at 28 weeks' gestation and a mean of 0.65 (95% CI 0.47 – 0.89) at 40 weeks' gestation (245). An elevation in the UtA-PI, even in the third trimester, can be used to predict adverse perinatal outcome in the presence of growth restriction (246).

In sheep, the presence or absence of notching in ovine uterine arteries has not previously been reported. There is a single longitudinal study which reports the decline of the UtA-PI in sheep from a mean of 1.0 (± 0.3 SEM) at 112 d gestation to a mean of 0.66 (± 0.1 SEM) at 140 d gestation, although this does not reach significance due to the small numbers in the study (247).

1.5.7 Cardiac function

Fetal echocardiography can be used to assess of the fetal heart function in addition to structure. In the fetus, due to the presence of the ductus arteriosus which passes the pulmonary circulation, both the left and right ventricle pump blood into the systemic circulation and work in parallel to produce the combined cardiac output (CCO). Maintenance of adequate cardiac output depends on the adequate venous return, fetal heart rate and stroke volume, myocardial contractility and the afterload of the systemic circulation. In utero, fetal cardiac function may be measured by direct measurements of cardiac dimensions to calculate fractional shortening (FS) or ejection fraction (EF) (2D B- or M-mode ultrasound) or ventricular volume (4D ultrasound). Function can also be assessed indirectly by qualitative measurements of blood flow (cardiac

output), tissue excursion (myocardial contraction force) or time intervals during the cardiac cycle (myocardial performance index) (248).

The left ventricular myocardial performance index (LV-MPI) in normal pregnancy is stable through gestation with a mean of 0.36 (95% CI 0.28 – 0.44) (249-252). Elevation is recognised as an early marker of cardiac dysfunction in complicated pregnancy (253, 254).

Similarly, left ventricular fractional shortening is reported to be constant throughout gestation with a mean of 0.33 (95% CI 0.26 – 0.41) (255), with a reduction indicating fetal cardiac compromise (256). Ejection fraction is also gestational age independent, with a mean of 0.74 (95% CI 0.61 – 0.87); again, reduction indicates fetal cardiac compromise (251).

While right heart dominance is usual in fetal life, with the right ventricle pumping 55-60% of the CCO to the peripheral circulation (257, 258), the balance is changed in hypoxia with the left ventricle pumping comparatively more blood to the central rather than the systemic circulation (259). During acidaemia the fetal left ventricle can increase contractility in response to an inotropic stimulus – angiotensin II – even in the presence of increased peripheral resistance (260), maintaining its systolic function longer than its diastolic function (261). The left ventricle is also more sensitive to progressive acidaemia than the right ventricle (261).

Again, there are no longitudinal studies of fetal cardiac indices at different gestational ages in fetal sheep, and no relevant values are reported in un-anaesthetised sheep.

CHAPTER 2: EXPERIMENTAL DESIGN IN RELATIONSHIP TO HYPOTHESES, AIMS AND OBJECTIVES

2.1 **The unmet clinical need**

Twin to Twin Transfusion Syndrome is a condition where there remains scope for improving the treatments available. SVFL has been used over the last two decades to treat TTTS by ablating the abnormal placental anastomoses which cause the disease. While this can be successful in preventing the worsening of TTTS, based on meta-analysis of SVFL used to treat TTTS, there is no overall increase in perinatal survival (15). Recent developments in technology and technique, while showing a trend to improvement, have yet to show the anticipated improvement in survival rates (19). Meta-analysis of different invasive methods of treating fetal vascular disease in utero suggest that while survival relates to the efficacy of the method of vascular occlusion, complication rates (preterm labour or rupture of membranes) increase with increasing calibre of the instrument introduced into the uterus (14). Even with improving technology, fetoscopes of 2-3 mm in diameter in use, and fetal demise rates of 5-25% are still quoted (262).

It could be argued that the invasive nature of fetoscopic laser has prevented it from becoming a treatment available to all pregnancies with TTTS, such as those identified at an early stage (<III) or early gestation (<16-18 weeks' gestation). These are both areas of unmet clinical need in the management of TTTS.

Any new treatment to ablate placental vasculature would need to address two key areas: firstly, it would be non-invasive and secondly it would include a method of confirmation of anastomotic occlusion or complete placental equatorial division.

HIFU may be an alternative to invasive fetoscopic laser in TTTS. The energy levels needed to ablate placental vasculature (263) and the focal depths required are within the HIFU range of operation, and the reduction in complication rate may allow treatment of less severe disease. Either selective vascular occlusion or equatorial division of the placenta could be performed, as points or confluent planes of ablation can be achieved with HIFU (31). HIFU may be able to reduce rates of recurrent TTTS and TAPS, as residual anastomoses would be identified by Doppler ultrasound (196) integrated into the HIFU system for targeting. This could potentially allow HIFU to be used to treat TTTS more widely and at an earlier stage which may confer an additional survival benefit beyond that achieved from the non-invasive nature of the technique.

However, while HIFU has previously been used in pregnancy to successfully treat TRAP, this was a soft tissue application, and the area of specifically occluding placental vasculature non-invasively with HIFU remains unexplored. Given that there currently exists a treatment modality for TTTS that improves the prognosis for affected fetuses, any novel therapy would need to be

thoroughly tested for efficacy and safety in a pre-clinical development phase before the technology could be considered for a clinical trial.

2.2 **Hypotheses**

1. (a) It is possible to occlude placental vasculature in the pregnant sheep using non-invasive, ultrasound guided HIFU.

   (b) The resulting vascular occlusion is a permanent effect.

2. (a) HIFU mediated placental vascular occlusion can be achieved without significant direct iatrogenic harm to mother or fetus in the pregnant sheep model.

   (b) HIFU mediated placental vascular occlusion can be achieved without significant short or long term materno-fetal cardiovascular, metabolic, endocrine compromise or evidence of abnormal fetal growth or physiological maturation (indirect iatrogenic harm).

2.3 **Experimental design & aims**

This project had two main aims: first, to perform an ultrasound energy delivery study which would establish the efficacy, and potential for direct iatrogenic harm, of using ultrasound guided HIFU to occlude placental vasculature. This would enable us to develop an ultrasound guided HIFU treatment protocol for selective occlusion of placental vasculature in the pregnant sheep, to inform either further animal or human studies. It was not expected that this treatment protocol would be optimised, but would, if successful, serve as a proof of concept for this application of HIFU.

Second, we aimed to investigate the obstetric, cardiovascular, metabolic and endocrine responses of the mother and fetus to HIFU mediated placental vascular occlusion, both short and long term, providing evidence regarding the maternal and fetal tolerance of, and recovery from HIFU treatments. It would also identify the risk of indirect harm, if any, associated with the technique.

The design of a series of experiments to meet these two, seemingly simple, aims was instead complicated by a number of difficulties. The study design deviated significantly from the one

originally planned, and for this reason, the logic behind the experimental design is explained below.

2.3.1 Efficacy and safety of placental vascular occlusion

To meet the first aim, from an experimental point of view, it was not necessary to perform any monitoring of mother or fetus beyond confirmation of maternal and fetal survival to the end of the planned HIFU exposure and a careful post-mortem examination. The development of an HIFU treatment protocol from the minimal foundations of knowledge described in section 1.2.2, however, would require an iterative approach, where successive HIFU treatment protocols were experimentally evaluated and refined over time and multiple animal groups.

This approach clashed with directly with the second aim, to evaluate maternal and fetal responses to the "challenge" of HIFU mediated placental vascular occlusion. Typically, in any experimental protocol to assess the response to a particular "challenge", the challenge itself is standardised, an event with fixed characteristics, repeated in multiple subjects. However, the nature of the HIFU treatment protocol development part of this study was that the HIFU treatment protocol could change from one experimental subject to the next, based on the information gained. Therefore, the HIFU treatment protocol could not be tested against maternal and fetal responses and altered in the same animal.

This necessitated an experimental design where the HIFU treatment protocol was refined to a certain level, then tested (unchanged) in multiple subjects (even if flaws were apparent in the protocol before the end of testing), then further refined, then tested (unchanged), through as many cycles as needed or possible (Figure 2.1).

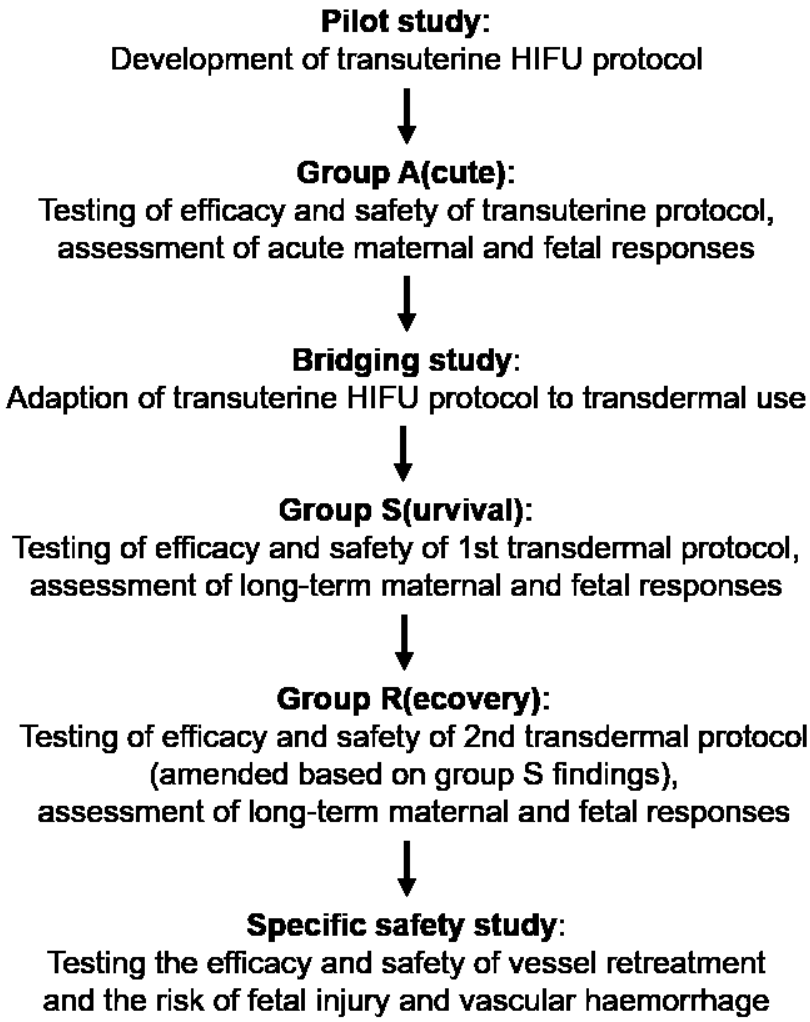

Figure 2.1: Animal groups.
This schema shows the progression of animal groups used in this thesis with the key priorities of each group summarised.

Given this iterative design, and that the project had finite resources, time and numbers of animals, certain adjustments to the experimental protocols were required. Essentially, the most refined HIFU treatment protocol was not tested in all animals, so the outcome data from each animal group is not necessarily directly comparable between groups.

Additionally, as early treatment protocols were weighted more to efficacy than safety, collating data regarding efficacy or safety from all phases of the study may not be valid either. The process of developing the HIFU treatment protocol will be discussed more fully in chapter 4.

2.3.2 Maternal and fetal responses to HIFU placental vascular occlusion

To meet the second aim, the ideal way to structure these experiments would be to place a pregnant ewe under general anaesthesia, surgically implant maternal and fetal vascular catheters and flow probes, then recover the ewe. Once both ewe and fetus had recovered from the effects of anaesthesia and surgery, and returned to a baseline of normal physiology, typically after around 5 days, then HIFU experiments could commence. This would allow both the short-term reaction to, and longer-term recovery from, HIFU placental vascular occlusion to be measured. As the ewe would ideally be un-anaesthetised, this would separate the effects of HIFU from those of surgery and anaesthesia. Maternal and fetal recovery could then be monitored until term, when a post-mortem examination could be conducted.

However, it was not possible to organise the experiments in such a way because of practical considerations. These are summarised in Table 2.1. Overall, it was not possible to separate the timing of the application of HIFU from general anaesthesia and materno-fetal surgery. For this reason, the maternal and fetal responses to, and recovery from HIFU were tested in 3 separate animal groups (A, S and R: Figure 2.1, and described further in the next section). Each group contributed to the overall analysis of the short and long term materno-fetal cardiovascular, metabolic, endocrine and obstetric responses to HIFU mediated placental vascular occlusion.

2.3.3 Animal groups

These requirements on the experimental design necessitated a stepwise progression through six animal groups (Figure 2.1). Two developed the HIFU treatment protocol: the pilot study and transdermal bridging study. Three tested progressive iterations of the HIFU treatment protocol for efficacy and safety: Groups A, S and R. The final group addressed specific safety concerns for which insufficient data had been collected in the preceding 5 groups. These names for the animal groups will be used consistently throughout the thesis to denote to which animal group results refer, and a summary of the animal groups is shown in.

Requirement	Original plan	Problem	Solution
The abdomen of the ewe must be still during HIFU exposures	HIFU exposures to be applied to un-anaesthetised ewes restrained in dorsal recumbency	(i) It was not possible to restrain an un-anaesthetised animal to a sufficient degree; (ii) Maternal respiratory movement sufficient to cause mistargeting.	HIFU exposures applied: (i) General or regional anaesthesia required to prevent maternal movement, (ii) General anaesthesia would allow a mechanical ventilation pauses to prevent respiratory movement.
The abdomen of the ewe must be exposed and near-horizontal during HIFU exposures	Ewes restrained in dorsal recumbency during HIFU (sitting at 45^{o})	Not possible to restrain an un-anaesthetised animal in fully recumbent position	HIFU exposures applied in animals under general or regional anaesthesia, with ewe fully recumbent.
Maternal recovery from HIFU should not be compromised by surgical / anaesthetic procedures	HIFU to be applied after recovery from surgery/anaesthesia (5 days)	Fully recumbent pregnant ewe at risk of aspiration of gastric contents	(i) Ewe fasted for 24 h pre-procedure (ii) General anaesthesia was preferred to regional anaesthesia as it allowed the maternal airway to be protected with cuffed endotracheal tube
Maternal blood pressure should be stable	HIFU to be applied after recovery from surgery/anaesthesia (5 days)	Fully recumbent pregnant ewe at risk of auto-caval compression, and vasodilator effect of isoflurane anaesthesia	(i) A 30^{o} left tilt introduced to theatre table while ewe recumbent (ii) Continuous intravenous crystalloid infusion used to support maternal blood pressure (iii) General anaesthesia was preferred to regional anaesthesia as blood pressure control better
The abdomen of the ewe should be unscarred to preserve acoustic window	HIFU to be applied after recovery from surgery/anaesthesia (5 days)	The healing scar would interrupt the acoustic window	HIFU exposures to be applied: (i) transuterine (**Group A**: allows air to be excluded and foreign bodies to be moved away, but not non-invasive); (ii) before surgery on the maternal abdomen (**Group R:** prevents measurement of materno-fetal responses to acute application of HIFU, only allows measurement of recovery); (iii) without surgery on the maternal abdomen (**Group S:** restricts assessment of materno-fetal responses to and recovery from HIFU to non-invasive techniques).
The path between the maternal skin and anterior surface of the uterus should be free of foreign bodies to preserve the acoustic window	HIFU to be applied after recovery from surgery/anaesthesia (5 days)	Intravascular catheters and flow probe cables could migrate to cross the acoustic window during recovery. Damage to vascular catheters could cause fetal haemorrhage.	
The intra-abdominal space of the ewe should be free of air to preserve acoustic	HIFU to be applied after recovery from surgery/anaesthesia (5 days)	Free air will be introduced at the time of laparotomy and can take up to 18 d to fully clear (264)	
Maternal and fetal physiological status before HIFU exposures should be representative of normality	HIFU to be applied after recovery from surgery/anaesthesia (5 days)	Need for HIFU exposures to be performed under general anaesthesia	(i) Duration of anaesthesia was minimised wherever possible, and kept to < 5 h in all cases (ii) Control groups were exposed to anaesthesia ± surgery

Table 2.1: Adjustments to original experimental design.
The table lists the experimental requirements of the study, the original experimental plan to meet these requirements, the practical problems which emerged during and the solutions implemented which required adjustment of the experimental protocol.

		Pilot NON-RECOVERY *Demonstration of initial feasibility*	Group A(cute) NON-RECOVERY *Acute responses to HIFU*	Transdermal Bridging NON-RECOVERY *Adaption of transuterine to transdermal application*	Group S(urvival) RECOVERY *Chronic responses to HIFU (non-invasive monitoring)*	Group R(ecovery) RECOVERY *Chronic responses to HIFU (invasive monitoring)*	Specific Safety NON-RECOVERY *Collection of data regarding outstanding safety concerns*
	Gestational age	115 ± 2 d	116 ± 1 d	115 ± 0 d	115 ± 10 d	116.5 ± 1.5 d	110.5 ± 5.5 d
SURGICAL PROCEDURES & ANAESTHESIA	Treatment applied	HIFU	HIFU / Sham	HIFU	HIFU / Sham	HIFU / Control	HIFU
	Number of sheep	5	5 / 6	2	6 / 6	10 / 6	4
	Isoflurane anaesthesia	Yes	Yes	Yes	Yes	Yes	Yes
	Laparotomy	Before HIFU (n = 4) None (n = 1)	Before HIFU	None	None	After HIFU	Before HIFU (n = 1) None (n = 3)
	Hysterotomy	None	Before HIFU	None	None	After HIFU	None
INVASIVE MONITOING	Arterial Catheters - arterial blood pressure - heart rate - blood sampling (metabolic / endocrine)	None	Fetal descending aorta Fetal ascending aorta Maternal descending aorta	None	None	Fetal descending aorta Maternal descending aorta	None
	Blood samples	None	Immediately before, during and after HIFU / sham	None	Cord blood sampled at post-mortem	Daily after HIFU	None
	Flow probes - volume of blood flow - heart rate	None	Fetal femoral artery Fetal carotid artery Maternal uterine artey	None	None	Fetal femoral artery	None
	Heart rate variability analysis	n/a	No	n/a	n/a	Yes	n/a
NON-INVASIVE MONITORING	Fetal ultrasound biometry	None	None	None	Every 5th day after HIFU	None	None
	Utero-placental and fetal Doppler studies	Intermittent FHR checks	None	Intermittent FHR checks	Daily for 5 days after HIFU, then every 5th day	None	Intermittent FHR checks
	Intraoperative maternal pulseoximetery and end tidal CO_2	Yes	Yes	Yes	Yes	Yes	Yes
	Inspection for maternal distress, injury or obstetric complications	n/a	n/a	n/a	Daily after HIFU	Daily after HIFU	n/a
FOLLOW-UP	Baseline for comparison established	n/a	30 min before HIFU commenced	n/a	24-48 h before GA / HIFU	Day 5 post surgery	n/a
	Follow-up post HIFU / sham treatment completion	< 15 min	30 min	< 15 min	21d	21 d	< 15 min
	Number of sheep which completed followup	5	5 / 6	2	6 / 6	6 / 6	4
	Post mortem examination	Placental tissue Iatrogenic damage	Placental tissue Iatrogenic damage	Placental tissue Iatrogenic damage	Placental tissue Fetal biometry Organ weights Iatrogenic damage	Placental tissue Fetal biometry Iatrogenic damage	Placental tissue Iatrogenic damage

Table 2.2: Summary of animal groups.
The table shows a summary of the demographics of animals included in each group, and the surgical procedures, method of invasive and non-invasive follow-up used to assess maternal and fetal wellbeing. The timing and nature of post-mortem examination for each group is also summarised.

CHAPTER 3: EXPERIMENTAL ANIMAL METHODS

3.1 Sheep Husbandry

All experiments were conducted on Welsh Mountain ewes, with singleton pregnancies of known gestational age. All procedures were licensed by the Home Office (Scientific Procedures) Act 1986 and were approved by the University of Cambridge Ethical Review Board. All animal experiments were conducted at the large animal facility at the University of Cambridge.

3.1.1 Breeding cycles

The Welsh Mountain sheep is a highland domesticated breed. An average mature ewe weighs 35-45 kg (265). In temperate zones such as England, sheep are seasonally polyoestrous, and their sexual and ovarian characteristics follow a pattern determined by day length, breed and nutrition. During the breeding season ewes have an oestrous cycle of between 14-19 days and ovulate 1-3 eggs per cycle (157). Welsh mountain ewes have a high singleton pregnancy rate with a gestational period of 145-150 days (265, 266), however the photoperiodicity of the breeding season effectively limits the reproductive rate of the ewe to one delivery per year. The length of the breeding season can be extended into the typical period of anoestrous (April – July) using hormonal control methods of ovine reproduction. Regardless of season, timing of ovulation can be synchronised between ewes by vaginal insertion of progesterone-impregnated sponges (20 mg Flugestone acetate, controlled release, PV, Chronogest® CR, Intervet UK Ltd., Walton, UK) for 14 days which mimics the luteal phase. Removal of these sponges leads to a rapid fall in progesterone levels analogous to corpus luteum regression, and in the natural breading season ovulation will occur 48-72 hours later. In the anoestrous season, ovulation rates can be increased by injection of exogenous gonadotrophins at time of sponge removal (500 IU, IM, PMSG-Intervet®; Intervet UK Ltd., Walton, UK) although there is a highly variable tendency to multiple ovulation in response to dose administration, which increases the rate of multiple pregnancy in our population of sheep (unpublished data). In this study, both natural breeding and anoestrous season pregnancies were used.

3.1.2 Tupping and dating of pregnancy

The Welsh Mountain ewes were mated on site by one of the seven rams kept for the breeding programme. Ewes were placed with these rams immediately following removal of sponges (± exogenous gonadotrophins) and insemination was noted to have occurred on the day when

fresh raddle-ink marks were present on the rumps of ewes. If pregnancy was confirmed by trans-abdominal ultrasound approximately 60 days later, then the pregnancy was dated from the date of insemination. Fetal number was also determined at this ultrasound examination, and confirmed by ultrasound scan at 80 days gestational age.

3.1.3 Management and maintenance of pregnant ewes

Prior to inclusion in the study, when weather conditions permitted, pregnant ewes could graze on open pasture. At other times were housed in stock-holding pens with *ad libitum* access to hay, sheep nuts, mineral lick and water. Standard veterinary practise was used for treatment of any routine conditions.

3.2 Surgical procedures

3.2.1 Pre-operative preparation

To reduce the risk of intraoperative regurgitation of intestinal contents or bloat developing, which can occur in up to 6% of general anaesthetics in sheep (123), pregnant ewes had food but not water withdrawn for 24 hours prior to induction of anaesthesia (171). During this time, the ewe was held in an individual holding pen in the experimental facility in the sight of other sheep. Immediately prior to operation the ewe was weighed and transferred to the anaesthetic room, where a trans-abdominal ultrasound scan was performed to confirm fetal number and viability.

3.2.2 Induction and maintenance of anaesthesia

Induction of anaesthesia was by maternal intra-jugular injection of alfaxalone 3mg.kg^{-1} (Alfaxan®, Jurox, UK). The ewe was intubated with a size 7.0 – 9.0 cuffed endotracheal (ET) tube dependent on maternal weight (Portex® Tracheal tube, Smiths Medical International Ltd., Luton, UK) in the dorsal recumbent position with neck extended under the guidance of an illuminated laryngoscope. Successful placement of the ET tube was confirmed by auscultation of breath sounds through the chest wall and end tidal CO_2 ($EtCO_2$) monitoring. Anaesthesia was maintained with isoflurane (1.5-2.5% in 4:1 O_2:N_2O) administered by positive pressure

ventilation (Flomasta ventilator, M & I.E. Dentsply, Exeter, UK.) throughout the operation. Depth of anaesthesia was monitored by observing the jaw tension and eye blink reflexes. The ewe was ventilated in a slight head down position to reduce the chance of aspiration of regurgitated stomach contents. A left lateral tilt on the operating table was maintained for reduction of autocaval compression by the gravid uterus.

Carprofen (1mg.kg^{-1}, Rimadyl^{TM}, Pfizer, Sandwich, UK) a veterinary non-steroid anti-inflammatory drug, was given at 50% total anaesthetic time to aid maintenance of anaesthesia.

Maternal hydration was maintained to counteract the cardiovascular depressant effects of isoflurane (173) with a 0.9% Sodium Chloride (NaCl) infusion (5ml.kg^{-1}.hr^{-1} IV, Aquapharm®, Animalcare Ltd., York, UK). This was commenced once the maternal femoral vein catheter was inserted, or via an intravenous (IV) cannula (16G Intraflon 2®, Vygon, Swindon, UK) placed in the maternal jugular vein if no catheterisation for experimental purposes was performed.

Non-invasive maternal monitoring and recording of heart rate, oxygen saturation and $EtCO_2$ was performed throughout the period of anaesthesia (total time taken for surgery and experimental protocol to be completed) with a veterinary anaesthetic monitor (VM-2500, Viamed, Keighley, UK). Values for each parameter were recorded every 8 s and exported to VM-2500 PC software, converted into CSV files and were available for offline data analysis postoperatively.

3.2.3 Preparation of maternal skin

In all animals, wool was shaved from the maternal abdomen and three iodine washes (Vetasept: 7.5% povidone iodine, Animalcare Ltd., York, UK) were performed to remove dirt and excess lanolin following induction of anaesthesia. Prior to incision, the abdominal skin was washed with a chlorhexidine solution (4% chlorhexidine gluconate, 96% ethanol) which was allowed to evaporate before skin incisions were made. Additional measures were taken to prepare maternal skin in animals exposed to transdermal HIFU, and these will be discussed where indicated in the HIFU-specific methods sections (chapter 4).

3.2.4 Maternal surgery

Surgery was performed under aseptic conditions using routine techniques in our laboratory (267-269). Drapes, instruments, ligatures and equipment were sterilised by autoclave. Heat sensitive items (catheters, flow probes, plastic protective covers) were gas sterilised (ethylene

oxide, H. W. Andersen Products Ltd., Clacton-on-Sea, UK) with a minimum 24 hours between completion of sterilisation and use. Unprepared areas of the ewe were covered with sterile drapes, the abdomen was covered with a sterile plastic sheet cut where incisions were required (Buster Op Cover, Kruuse, Langeskov, Denmark).

3.2.4.1 **Maternal descending aorta and IVC catheters**

The skin of the medial aspect of the upper hind limb was incised to expose the *Sartorius* and *Adductor* muscles. Blunt dissection of the plane between these muscles allowed visualisation of the maternal femoral artery and vein, which were then cannulated with Polytetrafluoroethylene (PTFE) and Polyvinyl chloride (PVC) catheters (described in more detail in section 3.2.6) using the technique described by Hecker (123). In short, the vessel was occluded distally by a thick linen ligature to prevent backflow, and forward flow temporarily occluded by elevation of the vessel by a second proximal ligature. The vessel was incised between these two points and a suitable catheter advanced via the femoral artery or vein into the descending aorta or inferior vena cava, respectively. The proximal ligature was used to seal the vessel around the catheter to prevent blood leakage and the suture tails of the distal ligature was then used to anchor the catheter in place against the vessel. The catheter was tested by withdrawing blood and flushing it with sterile saline immediately following insertion.

3.2.4.2 **Maternal laparotomy**

A 15-20 cm ventral midline incision was made in the skin of the maternal abdomen, avoiding mammary veins. Blended monopolar diathermy was used to divide subcutaneous fat and expose the rectus sheath. The abdominal cavity was opened along the *linea alba* to expose the pregnant uterus. A main branch of the maternal uterine artery was identified and followed back to as close to the common origin of the uterine artery as possible, which was isolated carefully at this point. A transit time probe (4mm aperture, S-series, Transonic Systems Inc., Ithaca NY, USA) was placed around the uterine artery and secured in place by closure of the visceral peritoneum around the body of the flow probe. An acoustic coupling agent was used to fill the resultant pocket and exclude air from the acoustic window of the flow probe to allow immediate use (270).

3.2.5 Fetal surgery

The exposed pregnant uterus was exteriorised. Fetal number and position was confirmed by palpation. For insertion of fetal femoral catheters and flow probes, an hysterotomy was performed adjacent to the rear fetal hooves, with the incision made in an area of uterine wall relatively free of placentomes of vessels. The edges of the incision and fetal membranes were grasped with Babcock forceps and the fetal hind limbs were exteriorised. The Babcock forceps were then also used to also grasp the fetal skin to conserve amniotic fluid during instrumentation of the fetus, as described elsewhere (123). Incisions made bilaterally with blended monopolar diathermy in the fetal skin to expose the *Sartorius* and *Adductor* muscles. Blunt dissection between these muscles allowed access to the femoral artery which was isolated on both sides along the exposed length. On one side, the femoral artery was cannulated with a PVC fetal arterial catheter. On the contralateral side a 2mm aperture time transit time flow probe (R series, Transonic Systems Inc., Ithaca, USA) was placed around the femoral artery and secured to the surrounding tissue with silk sutures (5-0 Mersilk, Ethicon Ltd., Livingston, UK) inserted through the plastic flange. An acoustic coupling agent was used to eliminate air from the acoustic window. The fetal skin was closed with thin linen suture and the catheter and flow probes cable were exteriorised through the skin incision and secured with ligatures to the fetal skin to prevent accidental removal. A third catheter was secured to the fetal hind limb for monitoring of the amniotic cavity pressure. The fetus was then returned to the uterine cavity and the fetal amnion and chorion were secured around the trailing catheters and cables with thin linen ligatures. The uterine incision was closed with a non-locking continuous suture (2/0 Surgicryl® PGA, SMI AG, St. Vith, Belgium) with additional figure-of-eight sutures inserted as required to ensure adequate haemostasis.

If required for insertion of fetal carotid arterial catheters and flow probes, a second hysterotomy was then performed and the fetal head and neck were exteriorised using Babcock forceps to secure the fetal membranes and wall to the fetal skin to preserve amniotic fluid. A ventral midline incision was made in the skin of the fetal neck and blunt dissection performed between the *sternocleidomastoid* and *scalene* muscles to expose the carotid artery bilaterally. The artery was isolated along its exposed length, and a fetal arterial catheter was advanced via the carotid artery into the ascending aorta using the technique described for the fetal femoral artery. On the contralateral side a 2mm aperture transit time flow probe (R-series, Transonic Systems Inc., Ithaca NY, USA) was placed around the carotid artery and secured with silk sutures inserted through the plastic flange of the probe and surrounding tissue. Acoustic coupling agent was again used to exclude air. The fetal skin was closed with thin linen ligature and the catheter and

cable exteriorised through the skin incision. The fetal head was then returned to the uterine cavity and the fetal amnion and chorion and uterine incision closed as previously. If there was intraoperative loss of amniotic fluid an approximate equivalent volume of warmed sterile saline was transfused via the fetal amniotic catheter prior to the commencement of the experimental protocol and all vascular catheters were heparinised at this time.

In Group A animals, the operative procedures were complete at this point and the fetal and maternal catheters and flow probes were connected to data acquisition and recording software in preparation for the start of the acute HIFU experimental protocol.

In Group R animals, the fetus was given antibiotics following uterine closure (600mg benzylpenicillin IA, Crystapen, Genus Pharmaceuticals, Newbury, UK). The *rectus* sheath was repaired with polyglycan sutures (2 Vicryl, Ethicon Ltd., Livingston, UK). The maternal skin was closed with non-absorbable sutures (2/0 Ethilon, Ethicon Ltd., Livingston, UK.). Vascular catheters were exteriorised via a keyhole incision on the maternal flank; flow probe cables were exteriorised through the contralateral flank. Inhalational anaesthesia was withdrawn and the animal was extubated when spontaneous respiratory effort was re-established.

3.2.6 Catheter specifications

To make maternal arterial catheters a 1.5 m lengths of PTFE clear thin wall sleeving was used (bore 1.00 mm, external diameter 1.60 mm, product number 01-96-1725, Altec, Bode, UK). A cuff of wider bore PTFE was adhered to the catheter at 15 cm from the tip to gauge of distance of insertion at surgery and allow anchoring at the insertion point to the vessel (Figure 3.1). Stiff materials such as PTFE provide higher fidelity pressure recordings than softer catheter materials, but have a higher rate of vessel perforation and are vulnerable to mechanical occlusion when kinked. PTFE catheters are more suitable for catheterising larger arterial vessels (116).

Maternal vein and amniotic catheters were made from 1.5 m length of PVC clear laboratory tubing (bore 1.00mm, external diameter 2.00m, product number 01-94-1561, Altec, Bode, UK). Maternal vein catheters were marked at 8 cm intervals to assess the distance of insertion during surgery and for ease of identification when exteriorised. Fetal amniotic catheters had round windows cut into the tip to ensure patency in the amniotic space and allow anchoring (Figure 3.1).

Fetal arterial catheters were made by joining a 7 cm tip of PVC clear single lumen tubing (bore 0.86 mm, external diameter 1.52mm, Critchley Electrical, NSW, Australia) to a 1.5 m length of coloured PVC laboratory tubing (bore 1.00 mm, external diameter 1.60mm, Altec, Bode, UK) using cyclohexanone. During surgery catheter tips were shortened to an appropriate length and a 30-40^0 bevel angle cut to the end to facilitate entry into a smaller vessel (Figure 3.1). Colour coded outer tubing was used for ease of identification of fetal vessels. PVC is softer and so less likely to perforate vessels, but retains adequate stiffness to advance into vessels and produce phasic pressure recordings of acceptable accuracy and is not overly susceptible to mechanical obstruction. Additionally, blood does not clot readily in PVC, although fibrin will adhere to it, more so in fetal than adult preparations. The benefit of joining a small tip to a wide bore is that sampling of blood is easier and better quality phasic pressure recordings. PVC catheters are more suitable for catheterising smaller vessels and veins (116).

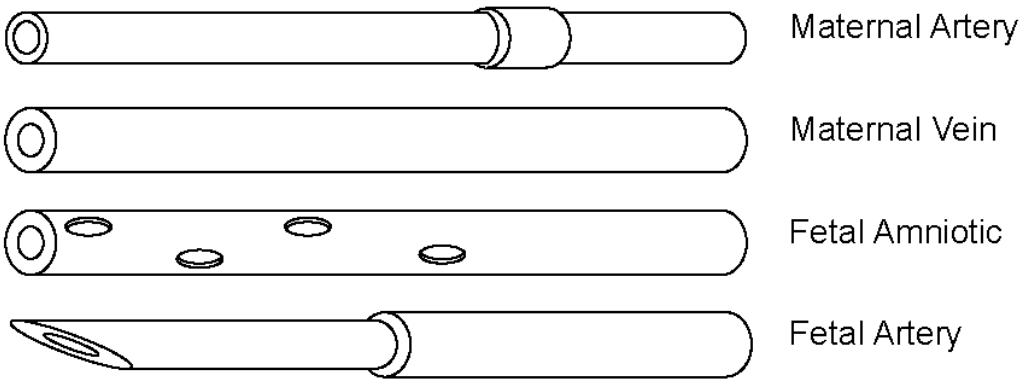

Figure 3.1: Surgical catheter tips.
The diagram shows the different types of maternal and fetal catheter tips used in the instrumented pregnant sheep.

3.2.7 Post operative care

Following invasive surgery, if animals were to be recovered, ewes were housed in individual floor pens with a 12 hour light and dark cycle with *ad libitum* access to hay, nuts and water. Maternal antibiotics (Procaine Benzylpenicillin 15 mg kg-1 I.M., Depocillin®, Intervet UK Ltd., Milton Keynes, UK) were administered for 5 days following surgery and fetal antibiotics (600mg benzylpenicillin I.A., Crystapen, Genus Pharmaceuticals, Newbury, UK) were administered daily until the end of the experiment. Maternal analgesia (Carprofen 1.4 mg kg-1 S.C., Rimadyl^{TM}, Pfizer Ltd., Sandwich, UK) was administered for 3 days postoperative, and as required if signs

of maternal pain were evident based on behaviour, facial expressions, stance and feeding patterns. Animals were checked daily for signs of maternal pain and distress, problems with mobility, bladder or bowel function, preterm labour or rupture of membranes or vaginal bleeding.

3.3 Invasive assessment of materno-fetal cardiovascular status

3.3.1 Invasive blood pressure monitoring

Intra-arterial catheters were used for the acute and chronic measurement of arterial blood pressure in maternal and fetal sheep. A blunt 18 G needle was inserted into the end of each catheter, connected to a 3-way tap and the catheter was filled with a volume in excess of the catheter dead space for transmission of phasic pressure changes. A solution of 0.08 IU Heparin (Wockhardt, Wrexham, UK) per ml 0.9 % NaCl (Aquapharm®, Animalcare Ltd., York, UK) was used.

The catheters were connected to pressure transducers (ArgoTrans™ Transducer, Argon Medical Devices Inc., Plano TX, USA) positioned at the level of the maternal heart. The pressure transducers convert the arterial pressure waveform into an electrical signal which is sampled by the CamDAS system at a rate of 500 kHz (private communication). Phasic arterial pressure recordings were corrected for atmospheric pressure (maternal) or amniotic cavity pressure (fetal). For maternal pressure transducer recordings, atmospheric pressure at the level of the heart was regarded as zero.

3.3.2 Invasive blood flow monitoring

Transit time flow probes were used for the acute and chronic measurement of arterial flow rates in maternal and fetal sheep. They are non-constrictive flow probes which can be placed around an isolated vessel and secured to adjacent tissues to prevent mechanical irritation or occlusion of the vessel by shifting of the flow probe (Figure 3.2). They are able to measure absolute blood flow rates in the vessel they surround, and this is independent of the diameter, shape and angulation of the vessel, as well as the flow profile of the blood within (271). Further details of how this is achieved are given in Appendix II. The transit time flow probes convert the rates of arterial blood flow into an electrical signal which is sampled by the CamDAS system at a rate of 500 kHz (private communication).

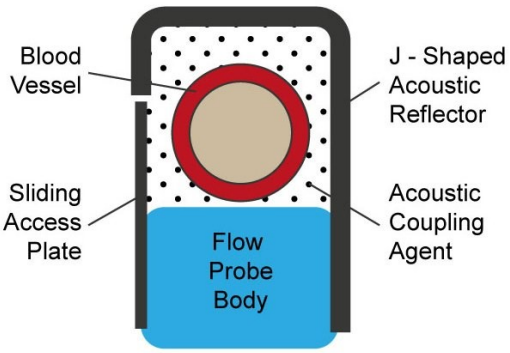

Figure 3.2 Transonic flow probes.
The diagram shows a cross sectional representation of a blood vessel positioned within the time-transit flow probe.

3.3.3 Data Recording System

Physiological values were obtained and recorded using a customised data acquisition system, the Cambridge Data Acquisition System (CamDAS) (268, 269). This is an ambulatory system, housed in a protective jacket worn by the pregnant ewe (Figure 3.3). It makes use of a battery-powered pressure and PASAQ boxes to continuously transmit digitised pressure and flow information to a laptop running IDEEQ (Maastricht Instruments, Maastricht, Netherlands). Recorded data were available thereafter for offline analysis (Figure 3.4).

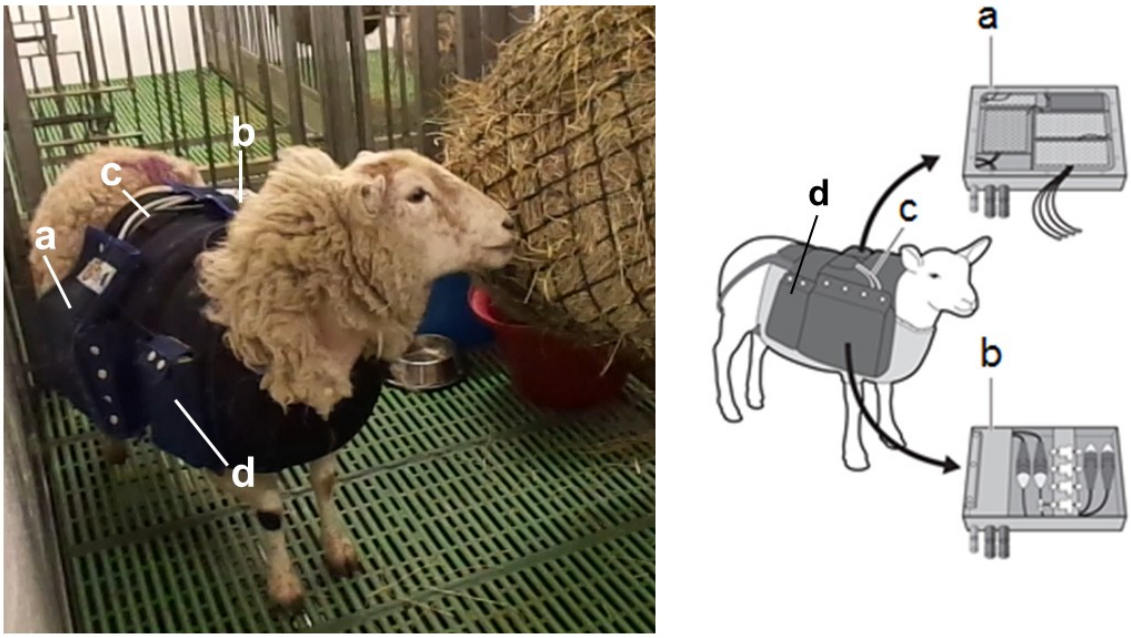

Figure 3.3: Cambridge Data Acquisition System (CamDAS).
The photograph shows one of the pregnant ewes ('Spot') in Group R wearing the CamDAS jacket. (a) Box for flow probe attachment and Bluetooth transmission; (b) box containing pressure transducers; (c) data cables connecting pressure box to flow box; (d) battery packs. Illustration adapted with permission from Allison et al. (269).

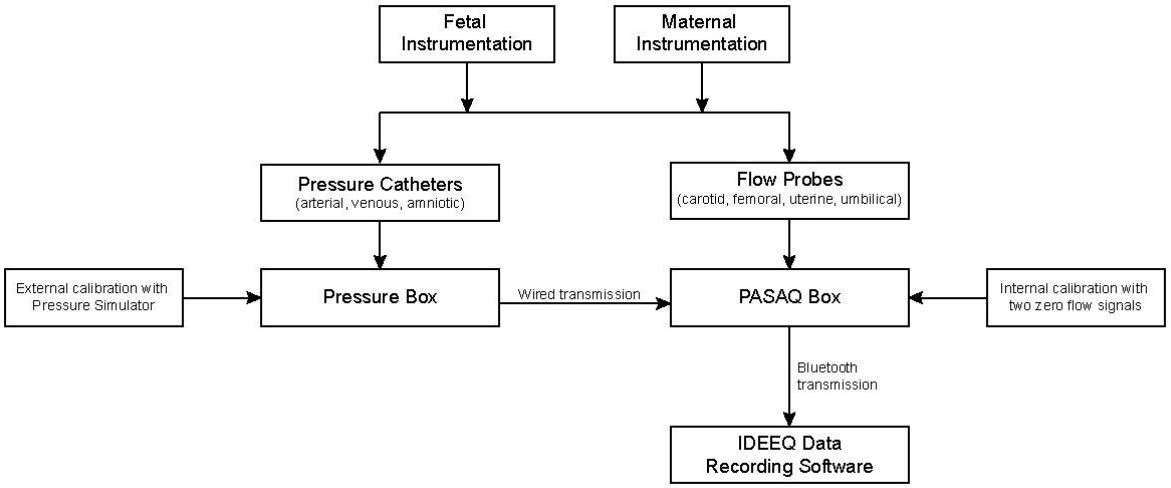

Figure 3.4: Schema of CamDAS data transmission.
The diagram shows the collection and transfer of maternal and fetal cardiovascular data through CamDAS system to recording software, where digitised data was stored for further analysis offline.

3.3.4 Data processing

Cardiovascular data for arterial blood pressure and blood flows were consolidated into files containing either 90 minutes (Group A) or 24 hours of data (Group B, 00:00:00 to 23:25:59) and were uploaded into a data analysis program (Labchart 7 Pro, AD Instruments Ltd., NZ). Using this software, mean values for sequential one minute epochs ("minute means") were generated for the systolic peak, diastolic nadir, and amplitude of maternal and fetal arterial blood pressures. Minute means for mean arterial flow rate and mean amniotic cavity pressure were also generated by this method. A maximum of 1440 numerical values for each cardiovascular parameter per 24 hours, or 90 per 90 minutes, were exported to a customised spreadsheet (Excel ®, Microsoft Corporation, Redmond WA, USA). Values were first logic checked by the customised spreadsheet for data which was non-physiological and produced due to catheter blockage or equipment error ("artefact data", logical arguments detailed further in Appendix III). Following the exclusion of "artefact data", calculations for mean arterial pressure and vascular resistance were applied to the remaining minute means. For Group A, minute means are reported directly. For Group R, minute mean values within any given hour were then averaged to give hourly means, and hourly means were further averaged to give the daily means reported in this chapter. This method of using time epochs and sequential averaging is recognised to prevent time periods with greater periods of excluded "artefact data" being under-represented in the overall average (272).

3.4 **Heart rate variability**

Continuous values of fetal heart rate were recorded using a customised data acquisition system (CamDAS) described in section 3.3.3. In animals in Group R, fetal heart rate was recorded from the immediately post-operative period until post-mortem, and converted into files containing 24 hours of data (00:00:00 to 23:25:59) in Labchart (Labchart 7 Pro, AD Instruments Ltd., Dunedin, NZ). The electrical signals produced by the pressure transducers and flow probes were sampled at 500 kHz (500,000 readings per second) which is more than sufficient to acquire fetal heart rate on a beat-to-beat basis, and measure inter-beat variability in the fetal heart rate.

The fetal heart rate was sampled daily in six, five-minute blocks spaced evenly between 00:00 and 06:00 using the waveform derived from fetal descending aorta catheter signals. Mean values for fetal heart rate during sequential 2.5 second epochs throughout each block were generated for cardiovascular data using Labchart and these values were plotted chronologically to create a CTG-like representation of fetal heart rate (Figure 3.5). Blocks were visually identified as FHR patterns A-D, and quiet sleep was defined as FHR pattern A and active sleep as FHR pattern B. If no suitable FHR pattern was acquired, resampling was performed within the same time period for that day, offset by 15 minutes.

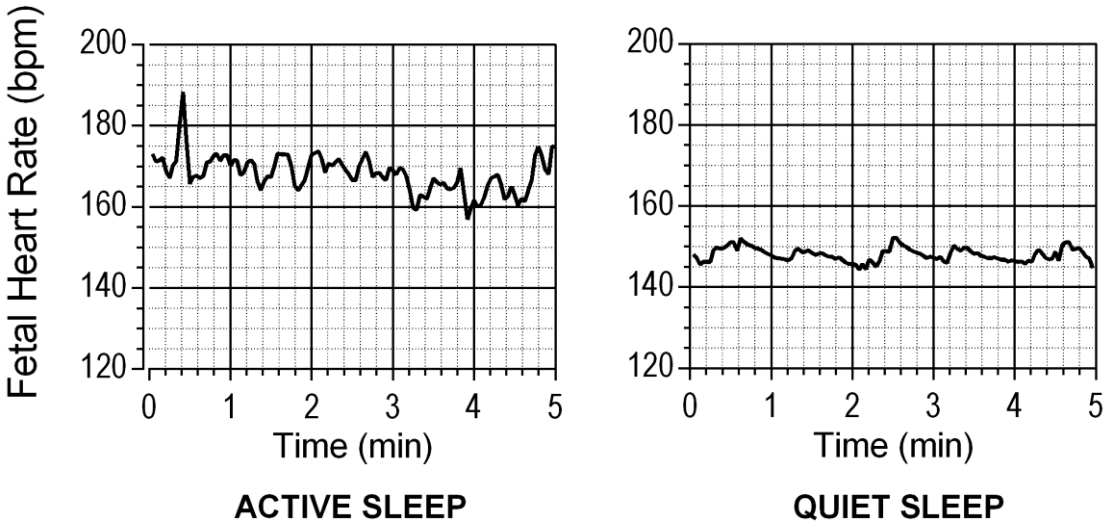

Figure 3.5 Fetal Heart Rate Variability Patterns.
A representative example of active sleep (left) and quiet sleep (right), which can be categorised by visual identification.

In blocks defined as active or quiet sleep, the R-R intervals were identified using an automated program in Labchart 7 Pro; each block was manually checked for accuracy of R wave

identification and missed R waves were manually marked. Time domain and power spectral analysis was then performed; based on previous published literature the frequency boundaries used were: VLF 0-0.04 Hz, LF 0.04-0.15 Hz, HF 0.15-0.4 Hz (151, 273, 274). Mean daily values for average heart rate, SDNN, RMSSD, absolute and normalised LF and HF, LF/HF ratio and total power were calculated daily from the five-minute samples. Baseline values represent the average of the mean values obtained on days three to five following exposure to HIFU or sham occlusion of placental vasculature.

STV was calculated using R-R intervals in a customised excel spreadsheet, as previously published (153): first average heart rate was used to calculate the baseline R-R value; second the baseline R-R value was used to exclude values representing accelerations or decelerations as these are excluded by STV calculation software (129). The remaining values were averaged in 3.75 s (1/16th minute) epochs and the mean difference between 16 sequential periods (1 minute mean difference) was calculated as per published STV calculation algorithms (272). Final STV values are the mean of the 5-minute mean difference values.

3.5 Invasive assessment of metabolic and endocrine status

3.5.1 Blood sampling

A closed system for management of maternal and fetal catheters was connected under aseptic operative conditions using sterile components to reduce the risks of fetal and intrauterine infection during regular catheter use. The ends of maternal and fetal catheters were disinfected with immersion in a chlorhexidine solution (4% chlorhexidine gluconate, 96% ethanol) immediately following exteriorisation and connected to three-way taps. One connection of the three-way tap was to the pressure transducer described in section 3.3.1; the other connection was to a polyethylene extension catheter (Lectro-cath®, Vygon, Swindon, UK) capped with a push-fit adaptor containing an one-way bacteriostatic membrane (Bionector 2®, Vygon, Swindon, UK), from which blood samples could be drawn using aseptic non-touch techniques without opening the closed circuit to the atmosphere. Bionectors were changed at least every seven days as per manufacturer recommendations. Catheters were maintained patent with daily flushing with heparinised saline (100 IU.ml^{-1} heparin sodium in 0.9% NaCl solution, 5 mL flush daily).

In Groups A and R, blood samples were taken from the maternal and fetal descending aortic catheters, and in Group A also from the fetal ascending aorta catheter (0.3 mL each) were drawn into sterile syringes at pre-defined time points. These were used to determine pH, arterial base excess, concentration of bicarbonate, partial pressures of oxygen and carbon dioxide (ABL5 Blood Gas Analyser, Radiometer, Copenhagen, Denmark). Blood glucose and lactate concentrations were obtained from an automated analyser (YSI 2300 Stat Plus, Yellow Springs Instruments, Ohio, USA). In Group A the haemoglobin, haematocrit and oxygen saturation of the blood were determined using an ABL80 Flex analyser (Radiometer, Copenhagen, Denmark). In the HIFU exposed animals of Group R haemoglobin and oxygen saturation of the blood were determined using the ABL80 Flex analyser. In the control group R animals, the haemoglobin and oxygen saturation of blood were determined using an OSM3 analyser (Radiometer, Copenhagen, Denmark). Results obtained by these two methods have been previously been compared internally at time of machine replacement and are highly comparable (private communication).

The maternal arterial blood oxygen content (C_aO_2; in ml O_2.ml blood^{-1}), oxygen (ml O_2.min^{-1}) and glucose (µmol.min^{-1}) delivery to the uterus were calculated using the following equations:

$$\mathbf{C_aO_2 = (([Hb] \times S_aO_2)/100)(\mathit{k}/100) + (\mathit{d} \times P_aO_2)}$$

$$\mathbf{Oxygen\ delivery = C_aO_2 \times blood\ flow}$$

$$\mathbf{Glucose\ delivery = [glucose] \times blood\ flow}$$

where [Hb] (g.dl^{-1}) is the concentration of haemoglobin in arterial blood, S_aO_2 (%) is the saturation of haemoglobin with oxygen. Assuming that one molecule of adult haemoglobin binds four molecules of oxygen, *k* is the capacity of haemoglobin to carry oxygen (mlO_2.gHb^{-1}), usually quoted as 1.34-1.36 at sea level. The coefficient *d* is the solubility of oxygen in blood, usually quoted as 0.003 at body temperature, and P_aO_2 is the partial pressure of arterial oxygen (mmHg), and this section of the equation accounts for the contribution of dissolved oxygen. The concentration of arterial glucose is given in mmol.L^{-1}. Oxygen delivery is therefore given in ml O_2.min^{-2}, and glucose delivery in µmol.min^{-1} where uterine blood flow is measured in ml.min^{-1}.

The fetal arterial blood oxygen content (*f* C_aO_2; in mmol.L^{-1}) was calculated using and adaption of the standard equation above which accounts for the changes in oxygen carriage by fetal

haemoglobin, converts the quantity of oxygen dissolved into the molar form, but treats dissolved oxygen as negligible (267):

$$f\,C_aO_2 = (([Hb] \times S_aO_2)/100) \times 0.62$$

Oxygen and glucose deliveries were calculated by multiplying the arterial concentration of each in by the flow in the corresponding vessel at the same time, as previously. The flow value used was the mean flow during the period in which the sample was taken, which varied in duration (Figure 3.6).

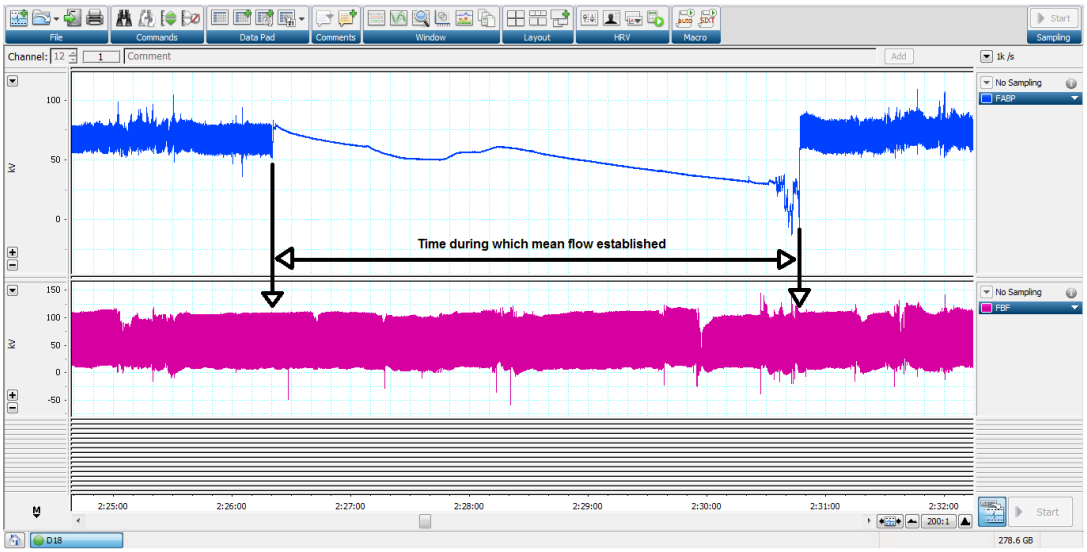

Figure 3.6: Arterial pressure artefact (denoting the duration of sampling).
The screen capture of Labchart software shows the non-pulsatile artefact that occurs when the three-way tap is closed to the pressure transducer during blood sampling, which indicates the time during which mean flow should be calculated for the substrate delivery equation.

3.5.2 Plasma cortisol assay

For Group R animals, maternal and fetal blood was collected under basal conditions, with the ewe unrestrained in her usual enclosure, by the method described above. On the fifth day post HIFU (baseline) and the day of post-mortem (day 20), in addition to the 0.3 ml required for daily analysis, a further 5 ml of maternal and fetal blood was collected into EDTA and centrifuged (5000 rpm, 4^0C, 5 min) for plasma extraction. All samples were then frozen at -80^{o}C for later analysis. Samples for the HIFU and control animals of Group R were analysed at the same time, by the method below.

The concentration of fetal cortisol in plasma was quantified using a commercially available cortisol indirect enzyme-linked immunosorbent assay (ELISA) kit according to the product

instructions (RE52061, IBL International, Hamburg, Germany). This assay has previously been validated for use in fetal ovine plasma (275).

Duplicate 20 µl plasma aliquots (undiluted) were taken from previously unthawed EDTA-treated samples for use in the cortisol assay. Each microtiter plate was also populated with manufacturer-provided standard concentrations of cortisol in duplicate (0, 20, 50, 100, 200, 400, 800 $ng.ml^{-1}$), manufacturer-provided control solutions, and stripped plasma. Standard and control solutions were placed at opposite ends of the plate to minimise the effect of intra-assay variation on the extrapolation of cortisol concentrations. To make stripped plasma activated charcoal was added to fetal plasma at a ratio of 1 g:50 ml, mixed and centrifuged (2996 rpm, 4^0C, 10 mins). This process was repeated and the resulting supernatant was filtered, and used in the assay without further dilution. The samples were incubated with enzyme conjugate at room temperature for 1 hour and then washed with buffer, before substrate and stop solutions were applied to complete the immunofluorescence reaction. The optical density of the wells was then read at a wavelength of 450 nm (ELx800 Absorbance Reader, Biotek, Winooski VT, USA) within ten minutes of the end of the assay.

A standard curve for interpretation of the results of each plate was produced by plotting the mean optical density of manufacturer-provided standard concentrations of cortisol against their known concentrations, expressed as a natural logarithm. The equation of the resulting line of best fit was used to extrapolate cortisol concentrations from measured optical densities. Using this method, all control solution values fell within the manufacturer specified ranges; the stripped plasma values concentrations of cortisol were 3.2 – 3.6 $ng.ml^{-1}$, which was the lower limit of detection for the assay. The inter-assay coefficient of variation (CV) for the 2 control samples (mean concentrations 68 ± 27 and 206 ± 61 $ng.ml^{-1}$) was 6.3% and 4.2% respectively, giving and overall inter-assay CV of 5.2%. The intra-assay coefficient of variation for the fetal samples reported (n=60) is 5.0% and for the maternal samples reported (n=48) is 8.3%; the overall intra-assay CV is 6.0%. The stated cross-reactivity of the cortisol assay with other cortisol related compounds is cortisone 4.2%, corticosterone 1.4%, 17α-OH-progesterone 0.4%, desoxycorticosterone 0.9%, 11-desoxy-cortisol 7.0%.

3.6 **Non-invasive assessment of fetal growth and wellbeing**

All ultrasound scans were carried out by a single operator (CJS) using a 3.75 MHz convex abdominal probe (PVK-357AT, PowerVision 7000, Toshiba Medical Systems, Crawley, UK). Animals were held in a dorsal recumbent position by an experienced handler and restrained

with the minimum force required in order to expose their abdomen, which was shaved and depilated at the time of HIFU or sham application and did not require further hair removal following this. All ultrasound examinations were limited to a maximum length of 30 minutes in un-anaesthetised sheep. In all cases, confirmation of fetal heart pulsations was sought before proceeding with the rest of the examination.

Ultrasound measurements were repeated until a minimum of three representative values were obtained. B-mode images were optimised for depth, focus and gain and Doppler assessments were performed with appropriate adjustment of pulse repetition frequency and wall motion filter for the vessel under examination. Images could not be saved for offline examination due to the basic nature of the ultrasound machine available, therefore assessment for inter-observer variability was not possible.

3.6.1 Ultrasound measurement of fetal biometry

Based on descriptions in published literature, biparietal diameter (BPD) was estimated as the widest linear distance between parietal bones behind the proximal end of the supra-orbital processes with the fetal head in axial view (202)(Figure 3.7a). The abdominal circumference (AC) was measured using in a transverse circular view of the fetal abdomen at the level of the 12th thoracic rib, just above the insertion of the umbilical cord, using an ellipse (203)(Figure 3.7b). The femur length (FL) was measured as the calcified length of the bone with the angle of insonation perpendicular to the shaft of the bone (202)(Figure 3.7c). Amniotic fluid was measured as the deepest vertical pool (DVP) within the pregnant horn which did not contain fetal parts.

Figure 3.7: Ultrasound assessment of fetal biometry.
The ultrasound images show (A) axial section of fetal head; (B) transverse circular view of fetal abdomen; (C) fetal femur. These are representative ultrasound images of the type collected in group S animals, using a 1.9 – 6.0 MHz convex sector array, (PVT-375BT, i700, Toshiba Medical Systems UK). Sheep: BL11, 109 d gestational age.

Estimated fetal weight was calculated using a sheep specific formula suggested by Carr *et al*. (203) and the Hadlock (BPD-AC-FL) formula optimised for use in human pregnancy (276). The formula used to calculate fetal growth rates was:

Fetal growth rate = (Day 21 value – baseline value) / 21

3.6.2 Fetal Doppler studies

The methods used for Doppler evaluation of maternal and fetal vessels are based on good practice guidelines published for use in human pregnancy (277).

The umbilical cord was identified with colour flow Doppler and the arterial pulsatility index (PI) was measured with pulsed-wave Doppler, with the PI based on auto-tracing of the best three consecutive waveforms. Umbilical artery Doppler was performed in all cases in a free loop of umbilical cord near the cord insertion (Figure 3.8a). This was done to ensure the sampling was performed in the full umbilical cord after all the allantoic vessels had joined. Although in humans there is variation of values for PI within the umbilical cord, with higher values found nearer the cord insertion, this technique was the only way to ensure reproducibility between animals and samples.

Middle cerebral artery Doppler was performed in an axial section of the fetal head at the level of the sphenoid wings with colour flow mapping used to identify the circle of Willis (Figure 3.8b). Sampling was undertaken by pulsed-wave Doppler within the proximal third of the vessel; no angle correction was applied and the angle of insonation was kept as close to 0^0 as possible. A restriction of ± 20^0 angle of insonation was imposed and values were not recorded when this section was not achieved. PI was measured by auto-tracing of the best three consecutive waveforms; peak systolic velocity (PSV) was measured with manual calliper application of the same three waveforms.

Ductus venosus Doppler was performed in either an oblique transverse section through the upper abdomen or in the mid-sagittal longitudinal section, depending on fetal positioning. The vessel was first identified with B-mode imaging between the umbilical vein and the inferior vena cava, confirmed as having characteristic aliasing on colour flow Doppler (Figure 3.8c), and sampled with pulsed-wave Doppler. PI was measured by auto-tracing of the best three consecutive waveforms without contamination from other vessels.

The maternal uterine artery was identified with colour flow Doppler where it crossed the external iliac artery, and the pulsed-wave Doppler gate was placed within 1 cm of this crossover point

(Figure 3.8d). Measurements were taken bilaterally and PI was measured by auto-tracing of the best three consecutive waveforms. Values quoted are an average of both sides.

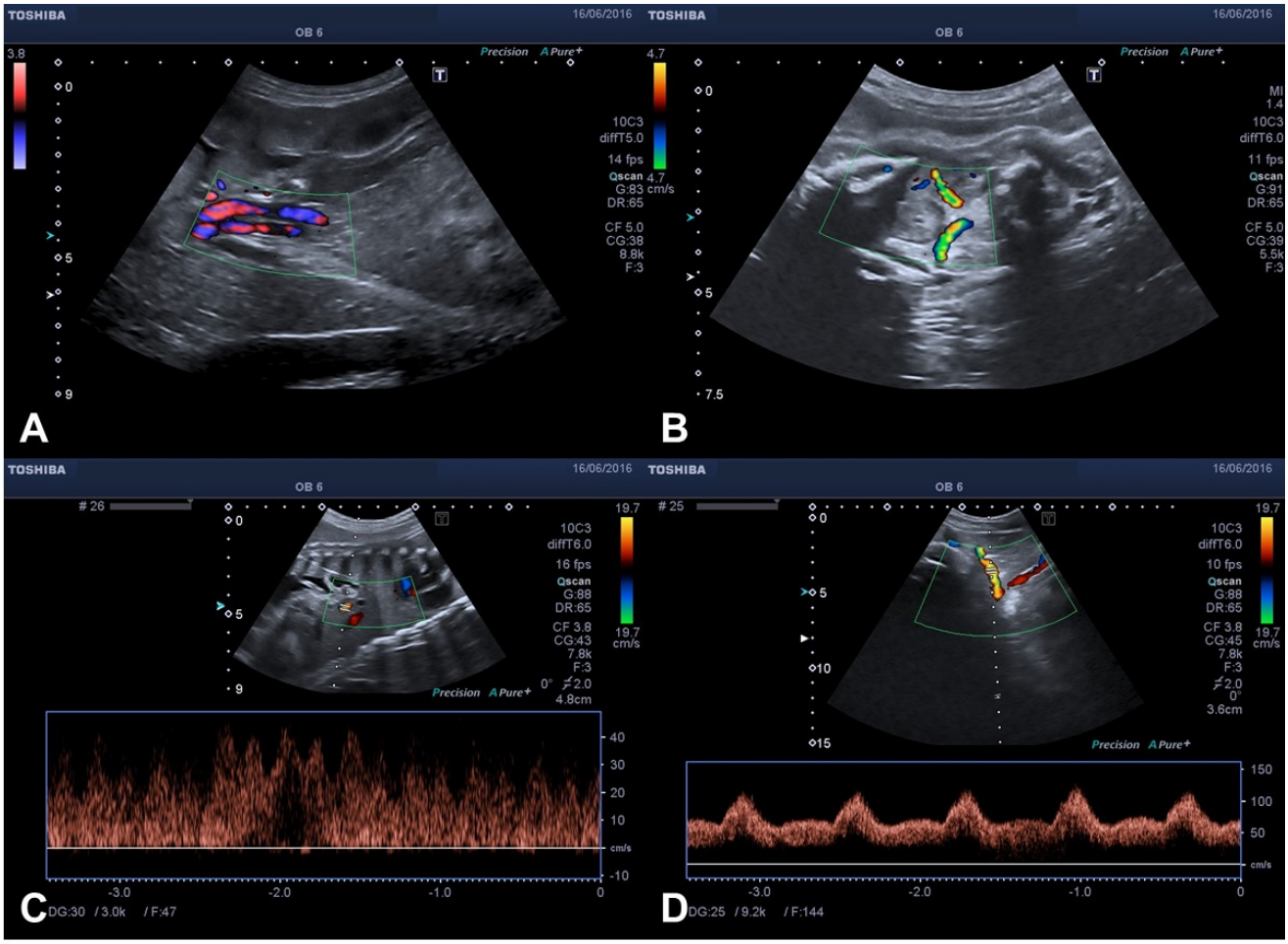

Figure 3.8: Fetal Doppler studies in sheep.
The colour flow Doppler images show (A) the insertion of the umbilical cord, (B) the middle cerebral arteries and the pulsed wave Doppler images show in (C) the waveform of the ductus venosus and (D) the maternal uterine artery. These are representative ultrasound images of the type collected in group S animals, using a 1.9 – 6.0 MHz convex sector array, (PVT-375BT, i700, Toshiba Medical Systems UK). Sheep: BL11, 109 d gestational age.

3.6.3 Fetal cardiac function

The methods used for evaluation of fetal cardiac function are based on good practice guidelines published for use in human pregnancy (248).

In the four-chamber view of the heart, the M-mode axis line was placed perpendicular to the intraventricular septum at the tip of the mitral valve leaflets. One dimensional measurements were taken of the ventricular maximum diameter in systole (ESD) and minimum diameter at the end of diastole (EDD) over three consecutive beats. These values were used to calculate fractional shortening (FS), ventricular volumes using the Teichholz formula (the end diastolic volume (EDV) and end systolic volume (ESV)), and the ejection fraction (EF):

FS = (EDD-ESD)/EDD

EF = (EDV-ESV)/EDV

In the apical four chamber view, the sample gate of the pulsed-wave Doppler function was placed just beneath the atrio-ventricular valves, with the angle of insonation maintained to ± 20^0 to the direction of blood flow through the valve. The isovolumetric contraction time (ICT), ejection time (EjT) and isovolumetric relaxation time (IRT) were measured over three consecutive beats and used to calculate the myocardial performance index (MPI):

MPI = (IRT + ICT)/EjT

3.7 Group-specific experimental protocols

3.7.1 Group A(cute)

Eleven singleton Welsh Mountain sheep fetuses at 116 ± 1 d gestational age (term ~148d) were used (HIFU n=5; Sham n=6). Under general anaesthesia, maternal laparotomy was performed and arterial catheters were placed in the maternal descending aorta and the fetal ascending and descending aorta; arterial flow probes were placed around the maternal uterine artery and the fetal femoral and carotid arteries (section 3.2.4, 3.2.5). The uterine incisions were closed and the anterior uterine surface was left exposed; the maternal and fetal arterial catheters and flow probes were connected to the CamDAS system and calibrated (sections 3.3.1, 3.3.2, 3.3.3). Once completed and ready to record, this time point was taken to be the start of the experimental protocol ("-30 min"). The median duration of anaesthesia at the start of the experimental protocol ("-30 min") was 145 min (range 128-180 min) in the sham group and 138 min (range 125-157 min) in the HIFU group (ns, p=0.14).

The experimental protocol took place over 90 minutes. Cardiovascular variables were recorded though-out and divided into three, 30 minute periods for analysis (baseline, HIFU/sham exposures, recovery, Figure 3.9). HIFU was applied trans-uterine to occlude between five and seven placental vessels using the protocol for group A described later (section 4.3.1.3). At the end of the recovery protocol ("60 min") cardiovascular monitoring was stopped, but in some animals further HIFU exposures were delivered as part of the dose-delivery study to maximise animal usage. All animals were euthanised (section 4.3.1.2) for post-mortem examination within one hour of the end of the recovery protocol (sections 4.3.1.4, 4.3.1.7).

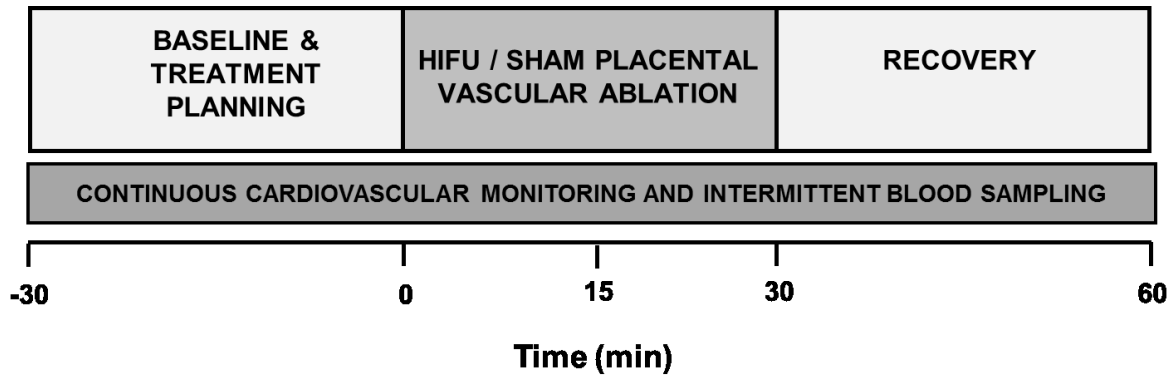

Figure 3.9: Group A experimental timeline.
Schema of experimental timeline divided into the baseline, HIFU/sham exposures, and recovery periods.

3.7.2 Group S(urvival)

Twelve singleton Welsh Mountain sheep fetuses at 115 ± 10 d gestational age were used (HIFU n=6; sham n=6). Prior to HIFU or sham exposure of placental vasculature, materno-fetal ultrasound was performed in un-anaesthetised animals to establish a physiological baseline (section 3.6). Between 24-48 h later, animals were placed under general anaesthesia to allow prone positioning and control maternal movement, however no invasive surgical procedures were performed. Materno-fetal ultrasound was performed shortly after induction of anaesthesia, during the HIFU planning period, then at the midpoint and end of HIFU or sham exposures of placental vasculature (Figure 3.10). The median duration of anaesthesia was 147 min (range 142 – 161 min) in the control group and 144 min (range 128 – 165 min) in the HIFU groups (not significant, p = 0.45).

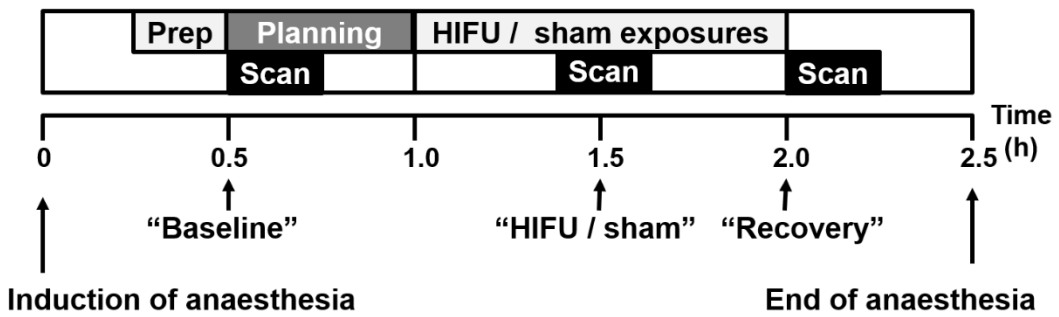

Figure 3.10: Group S experimental timeline.
Schema of anaesthesia and acute experimental timeline for group c animals, divided into periods of experimental preparation ("prep"), planning of vascular exposures, exposure to HIFU, materno-fetal ultrasounds and length of anaesthesia.

HIFU was applied through intact maternal abdominal skin to occlude four to six placental vessels using the Group S HIFU protocol (section 4.5.1.3). Animals were recovered from anaesthesia and monitored for 21 days by ultrasound until approaching term (Figure 3.11), when they were euthanised for post-mortem examination (section 4.5.1.2, 4.5.1.4, 4.5.1.7). In addition, fetal weight and biometry was measured; fetal brain, heart, lungs, kidneys, livers, adrenal glands, pancreases were weighed.

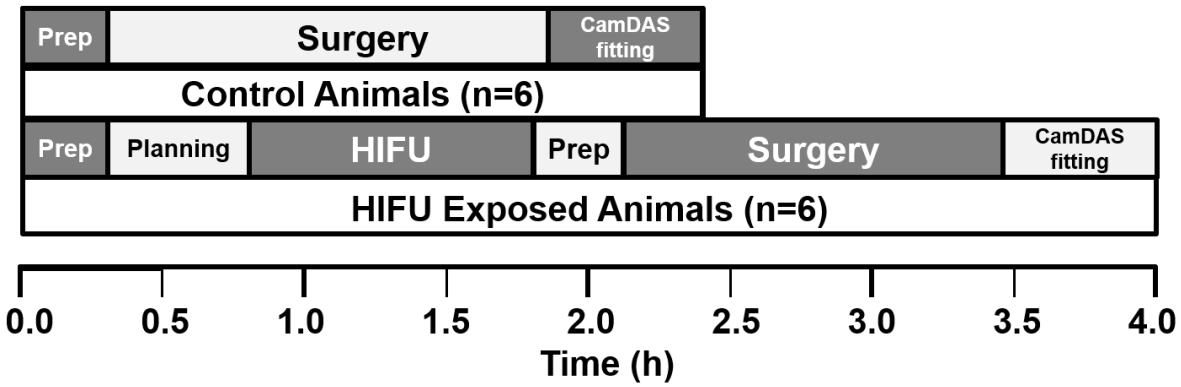

Figure 3.11: Group S post exposure monitoring timeline.
The schema shows the relative frequency and timing of daily inspections, materno-fetal ultrasound and post mortem examination.

3.7.3 Group R(ecovery)

3.7.3.1 **Control animals**

All experimental procedures and raw data collection in the animals forming the Group R control animals had been completed prior to the onset of this study. This work was performed by Professor Giussani, Dr B Allison, Dr N Yiu and Dr K Brain at the large animal facility, University of Cambridge. Professor Giussani provided the raw data (IDEEQ files of cardiovascular data, Home Office records of animals, laboratory records of surgical procedures, timings and recovery, unprocessed tables of daily blood results, records of post mortem biometry and organ weights, and frozen fetal plasma for cortisol assays) for comparison to the HIFU exposed animals as part of the collaboration between Imperial College London and the University of Cambridge to conduct this study. All subsequent analysis presented in chapters 5-7 of this raw data is my own work, and performed as described in the relevant methods sections.

Six singleton Welsh Mountain sheep fetuses at 116 ± 2 d gestational age were used. Under general anaesthesia, a maternal laparotomy and uterine hysterotomy were performed. Arterial catheters were placed in the maternal descending aorta and the fetal ascending and descending aorta; arterial flow probes were placed around the maternal uterine artery and the fetal femoral and carotid arteries (section 3.2.4, 3.2.5). The uterine and abdominal incisions were closed, catheters and flow probe cables were exteriorised through the maternal flank, the CamDAS jacket was fitted to the sheep, and catheters and flow probes were connected to the CamDAS system (section 3.3) (Figure 3.12). The median duration of anaesthesia was 145 min (range 133 – 170 min). Animals were recovered from anaesthesia (section 3.2.7), and 24-hour cardiovascular recording was commenced and continued for 21 days until approaching term, with daily blood sampling at a consistent time of day (Figure 3.13), after which animals were euthanised for post-mortem examination. Records of fetal biometry, organ weights, placentome number, type and weights were available for these animals.

3.7.3.2 **HIFU exposed animals**

Ten singleton Welsh Mountain sheep fetuses at 116 ± 1 d gestational age were used. Under general anaesthesia, HIFU was applied through intact maternal abdominal skin to occlude six placental vessels in each animal using the Group R HIFU protocol (section 4.6.1.3). Following this, maternal and fetal surgery was started. A maternal laparotomy and uterine hysterotomy were performed. Arterial catheters were placed in the maternal and fetal descending aortas and an arterial flow probes was placed around fetal femoral artery (section 3.2.4, 3.2.5). A reduced amount of fetal and maternal surgical instrumentation was performed compared to the Group A and the control Group R animals to keep the anaesthetic time below 5 hours. The uterine and abdominal incisions were closed, catheters and flow probe cables were exteriorised through the maternal flank, the CamDAS jacket was fitted to the sheep, and catheters and flow probes were connected to the CamDAS system (section 3.3) (Figure 3.12). The median duration of anaesthesia was 238 min (range 211 – 293 min) in these animals. This was significantly longer than the control animals (student's t test, $p < 0.001$). Animals were recovered from anaesthesia (section 3.2.7), and 24-hour cardiovascular recording was commenced and continued for 21 days until approaching term, with daily blood sampling at a consistent time of day (Figure 3.13), after which animals were euthanised for post-mortem examination (section 4.6.1.2, 4.6.1.4, 4.6.1.7).

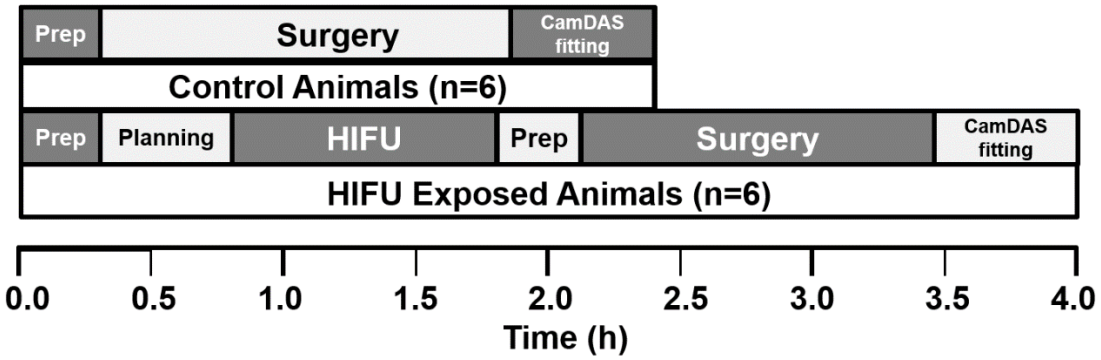

Figure 3.12: Group R surgical and experimental timeline.
Schema of surgical and acute experimental timeline for group R animals, divided into periods of surgical preparation ("prep"), planning of vascular exposures, exposure to HIFU, maternal and fetal surgical procedures and fitting and connection of CamDAS system.

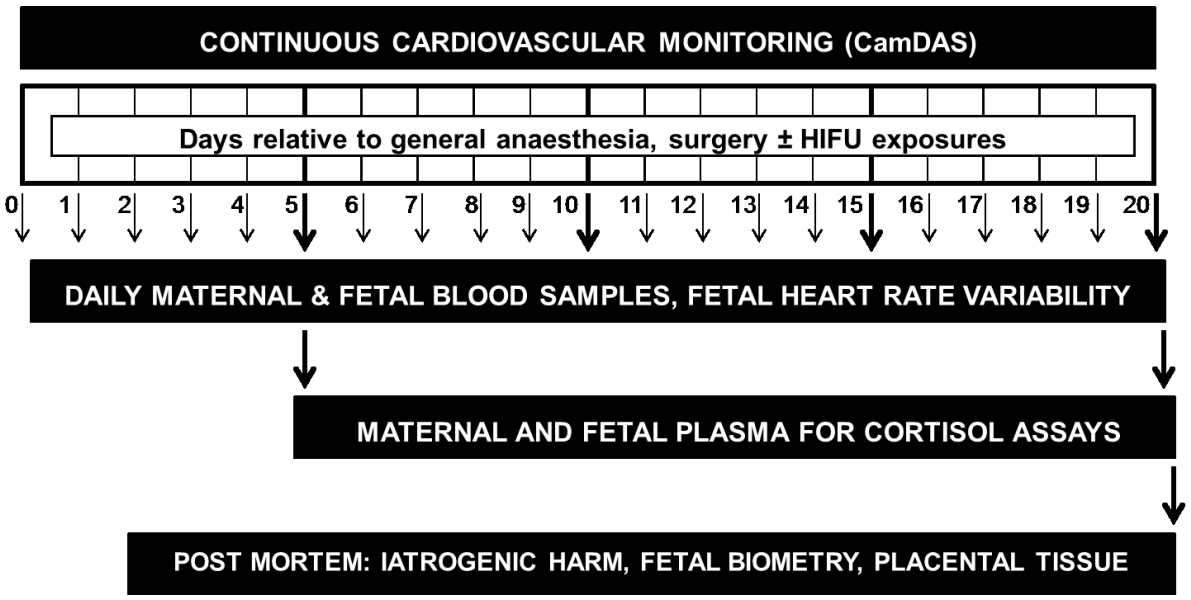

Figure 3.13: Group R postoperative monitoring timeline.
The schema shows the relative frequency and timing of cardiovascular monitoring, blood sampling for metabolic and endocrine analysis, sampling of the fetal heart rate for analysis of variability, and post mortem examination.

3.8 **Statistical analysis**

All statistical analysis was performed in SPSS (version 22, IBM, NY, USA). Graphs were drawn in GraphPad Prism (version 6, GraphPad Software, Inc., San Diego CA, USA). Statistical significance was accepted when $p < 0.05$ for all tests, although where applicable individual *p* values are presented in graphs and tables.

3.8.1 Descriptive and comparative statistics

3.8.1.1 **Continuous data**

Data were assessed for normality using the Shapiro-Wilkes test. Descriptive analysis was performed using mean ± standard error of the mean (SEM) for normally distributed physiological and metabolic data; mean ± standard deviation (SD) was used for normally distributed ultrasound data. Median ± 95% confidence intervals (95% CI) were used for non-parametric continuous data, unless otherwise stated. A two-tailed Student's *t*-test was used to compare means (normally distributed) or a Mann-Whitney U-test was used to compare medians (non-parametric data).

To assess the effect of HIFU treatment on a continuous dependent variable when additional independent variables needed to be considered, two-way ANOVA testing was used. A repeated measures two-way ANOVA was used to investigate the change in the dependent categorical variable due to the interaction of time with HIFU treatment; a standard two-way ANOVA was used if the second independent categorical variable was not time. If a significant effect or interaction was identified post hoc testing as applicable was performed to identify the source of variation.

3.8.1.2 **Area under the curve analysis of cardiovascular data**

In Group A, the experimental protocol was divided into three, 30 minute periods, baseline, HIFU or sham exposures, and recovery. Absolute cardiovascular values in the exposure and recovery periods were first compared to the mean of the baseline period, and then the magnitude of change from the baseline (in absolute and percentage terms) was calculated. To investigate these comparisons further, a summary measure of analysis, area under the curve, was applied to the absolute values, and the values for absolute and percentage change from baseline for cardiovascular indices in each of these time periods. This is a recognised method of generating values suited to statistical analysis from detailed short-term physiological data (278).

3.8.1.3 **Categorical data**

Proportions of categorical data are described as numerator over denominator, with a percentage value given. A chi-squared test was used for univariate analysis of categorical data, with additional calculation of odds ratios and relative risks and their associated 95% confidence intervals.

3.8.1.4 **Gestational age**

Gestational age is expressed as the mid-range value of the data set ± half the range.

3.8.2 Modelling statistics

3.8.2.1 **Correlation**

To compare ultrasound to necroscopy measurement of fetal biometry, Pearson correlations were performed normally distributed data and Spearman rank correlations were performed for non-parametric data. Bland-Altman correlations were performed to examine the limits of agreement between the techniques: percentage differences quoted were calculated as (100*(USS-PM)/average of USS and PM).

3.8.2.2 **Linear regression**

Linear regression was performed to model the relationship between scalar dependent and independent continuous variables. Analysis of covariance (ANCOVA) testing was used to test the effect of exposure to HIFU on the relationship of the dependant variable to the independent variable where a significant relationship was found by linear regression.

3.8.3 Establishment of a baseline in Group R

Following the experimental protocol recovery from surgery was monitored for 21 days. Daily values for maternal and fetal cardiovascular indices and metabolic status were generated. As it was not possible to establish a pre-operative baseline, the baseline was taken to be on day five postoperative. This is when postoperative recovery is traditionally understood to be complete in

the fetal sheep model and has recently been supported by work published from our laboratory (269). Absolute daily cardiovascular and metabolic values were first compared to the day five baseline, and then the magnitude of change from the baseline (in absolute and percentage terms) was calculated.

3.8.4 Power calculations

Testing for indirect iatrogenic harm (Groups A, S and R):

These phases of the study were powered to detect a difference in means of quantitative data as follows:

Difference in means ≥ 2.5

Alpha = 0.05

Power = 80%

Minimum sample size required = 5

The expected difference in means was based on published cardiovascular, metabolic and endocrine data of chronically instrumented fetal sheep responses to intrauterine challenges causing chronic hypoxia, growth restriction or stress (269, 270, 279, 280).

Testing for direct iatrogenic harm (pilot, bridging and specific safety studies):

These phases of the study were not powered for sample size as there were no quantitative outcomes.

CHAPTER 4: DEVELOPING AND TESTING A TREATMENT PROTOCOL FOR ULTRASOUND-GUIDED HIFU PLACENTAL VASCULAR OCCLUSION

4.1 Introduction

The purpose of this study was to test the feasibility, efficacy and safety of HIFU mediated selective placental vascular occlusion in a large animal model (as described in Chapter 2). It was a preclinical phase of developing a non-invasive method of placental vascular occlusion, with the ultimate intent of providing an alternative method of treatment for conditions arising from abnormal placental vasculature, such as TTTS.

As described in section 1.2.2, at the inception of this study, there was little consensus based on published literature relating to the amount of ultrasound energy (in situ intensity), or the number, timing, duration or placement of HIFU exposures, required to achieve specific vascular occlusion. Neither was there any conclusive evidence regarding the likely mechanism of vascular occlusion, the persistence of that occlusion, if achieved. The potential rates and types of iatrogenic harm for any given set of HIFU exposure variables selected remained unknown.

As a result, the experimental HIFU treatment protocol used in this study was based on HIFU femoral arterial occlusion experiments performed previously in a rodent model by co-investigators at the Institute of Cancer Research (ICR)(31, 32). This protocol had not previously been tested in large animal models, humans or pregnancy in any species. To date, there remain no reported cases of selective occlusion of placental blood vessels by HIFU with which to modify or further inform our experimental design. Additionally, the ultrasound guided HIFU laboratory system used was originally designed and built by researchers at the ICR for soft tissue ablation, not vascular occlusion. As described in section 1.2.2, the theory, methods and bioengineering requirements of producing HIFU soft tissue ablation can differ greatly from those of specific vascular occlusion. Therefore, as testing in humans was not ethically justifiable, or practically possible given the early stage of development, the pregnant sheep model was selected to use in preclinical testing. This model met both the anatomical requirements of the study (a consistent model of placental anastomoses, section 1.3.3), and also provided a recognised model of maternal and fetal physiology (section 1.3.1) in which to study potential direct and indirect side effect of the technique.

Due to the constraints on the experimental design discussed in chapter 2, refinement of the HIFU treatment protocol occurred in an iterative fashion, towards a treatment protocol which combined acceptable levels of efficacy and safety in sheep pregnancy. In this chapter, successive iterations (Figure 2.1) of the methods and to develop and test treatment protocols for ultrasound-guided HIFU occlusion of placental vasculature will be described. This chapter will describe and discuss how our techniques for applying HIFU evolved based on the results of

each previous phase of the study. Where relevant, it will also explain how the methods were influenced by other features of experimental design which aimed to assess the impact of HIFU placental vascular occlusion on maternal and fetal physiology. However, the results of this assessment of maternal and fetal physiology will be presented in chapters 5-7 and discussed in chapter 8.

4.2 **Pilot study**

In this first phase of the HIFU study, we sought to:

(i) establish if it was feasible to use ultrasound guided HIFU to occlude placental vessels in the pregnant sheep model;
(ii) establish if this was an immediately survivable insult for mother and fetus while under general anaesthesia.

To achieve this, it was necessary to demonstrate that:

(i) placental vessels could be identified by ultrasound in sheep pregnancy using colour flow Doppler, when also integrated with a HIFU transducer, suspended in a waterbag;
(ii) integrated colour flow Doppler could be used to target the HIFU focal zone relative to placental vessels with sufficient accuracy to achieve occlusion;
(iii) integrated colour flow Doppler could be used to confirm vascular occlusion;
(iv) sufficient HIFU energy could be delivered to the placental vessels to produce occlusion;
(v) confirm survival of mother and fetus to the planned end of HIFU exposures (up to 4 h from the first occlusions).

At this stage, while there was no deliberate attempt to cause harm, there was also no attempt to compromise potential efficacy to avoid harm to mother or fetus. No safety protocols were imposed on the treatment protocols beyond what was required for safe operation of the HIFU equipment by the researchers.

4.2.1 Methods

4.2.1.1 **HIFU therapy system**

The equipment for the HIFU therapy system was provided by the Therapeutic Ultrasound team at the ICR. The equipment was brought to the large animal facility at the University of Cambridge, set up and used in collaboration with 1 - 3 members of the ICR for experiments when HIFU (rather than sham HIFU) was used. The equipment was calibrated (Appendix IV), maintained, adapted and repaired by staff at the ICR.

The HIFU therapy system was a collection of separate pieces of equipment, some of which was custom designed and built at the ICR, not a commercially available, integrated system. The components are shown in outline in Figure 4.1, and as labelled photographs in Figure 4.2. HIFU was applied to animal tissue through a degassed water filled plastic polythene bag (the 'waterbag'), in contact with the anterior surface of the maternal uterus (transuterine) or abdominal skin surface (transdermal), suspended from an arm on the mechanical gantry arm. The tap water in the waterbag was degassed before the start of the HIFU exposures using a custom built portable degassing system from the ICR. The degassing system was comprised of a ceramic filter (2.5x8 Extra flow Liqui-Cel®, 3M Industrial Group, Bracknell, UK) and a vacuum pump (FB65540, Thermoscientific UK, Rugby, UK) to allow degassing, a water filter (RS Pro DWFK 10, RS Components Ltd., Northampton, UK) to filter the water, and a water pump (SB30 secondary circulating pump, Wilo UK, Stafford, UK) to circulate water between the waterbag and the degassing system. Water temperature and oxygen content were monitored ad hoc. The waterbag was only degassed before the end of the experiment if cavitation was evident in waterbag on ultrasound imaging during exposures

The HIFU transducer (H148MR, Sonic concepts, Inc., WA, USA) had a frequency of 1.66 MHz; its diameter was 64 mm, with a 19 mm circular central aperture to allow diagnostic ultrasound imaging parallel to the direction of the path of HIFU energy. The focal length of the HIFU transducer was 63 mm, and the dimensions of the focal zone are diameter 1.2 mm (x axis), diameter 1.2 mm (y axis) and length 8.9 mm (z axis) (private communication). The diagnostic ultrasound probe was a 4-10 MHz phased sector array transducer (P10-4, Z.one Zonare ultrasound system, Mindray, Shenzen, China), which supported B mode, colour flow, power and pulsed wave Doppler, tissue harmonic and compound B-mode imaging. This probe was designed for paediatric echocardiography and neonatal applications, but was used here because its small size allowed it to image through the 19 mm central aperture in the HIFU transducer.

The diagnostic ultrasound probe was aligned to the HIFU transducer by means of a customised plastic housing which fitted around the diagnostic ultrasound probe and interlocked with the upper surface of the HIFU transducer. This alignment ensured that the HIFU focal zone was along the of the ultrasound image at all times. The centre of the HIFU focal zone was fixed at 70 mm from the top of the ultrasound image due to the slight offset of the leading edge of the diagnostic transducer behind the leading edge of the HIFU transducer.

Both transducers were held in position within the water bag by the movable arm of a mechanised 3D positioning gantry. This gantry arm prevented accidental rotation or angulation

of the diagnostic/therapeutic transducers. The only planned movements allowed were up and down in the path of sound travel/along the midline of the ultrasound image (z axis), or orthogonal to the direction of sound (x and y axes, also at right angles to each other). The precision of the position system was reported by the ICR team to be better than 1 mm (private communication). A laptop computer was used to run a custom coded graphical user interface (GUI) in MATLAB (MATLAB R2013a, Mathworks, MA, USA) to control and record the 3D position of the mechanised gantry arm for each exposure.

This GUI also controlled the signal generator settings and the firing (switching on/off) of the HIFU transducer. The HIFU exposure conditions which could be varied using the GUI were: (i) the drive voltage (a nominal setting, see Appendix IV), (ii) the duration of a HIFU exposure, (iii) the time interval between one HIFU exposure and the next in a series of exposures, (iv) the distance between one HIFU exposure and the next in a line of exposures, and (v) the number of HIFU exposures in a series or line. In addition, the GUI logged the signal generator voltage setting, and the start time and duration of each HIFU exposure, which were exported as a text file, available for review after experiments.

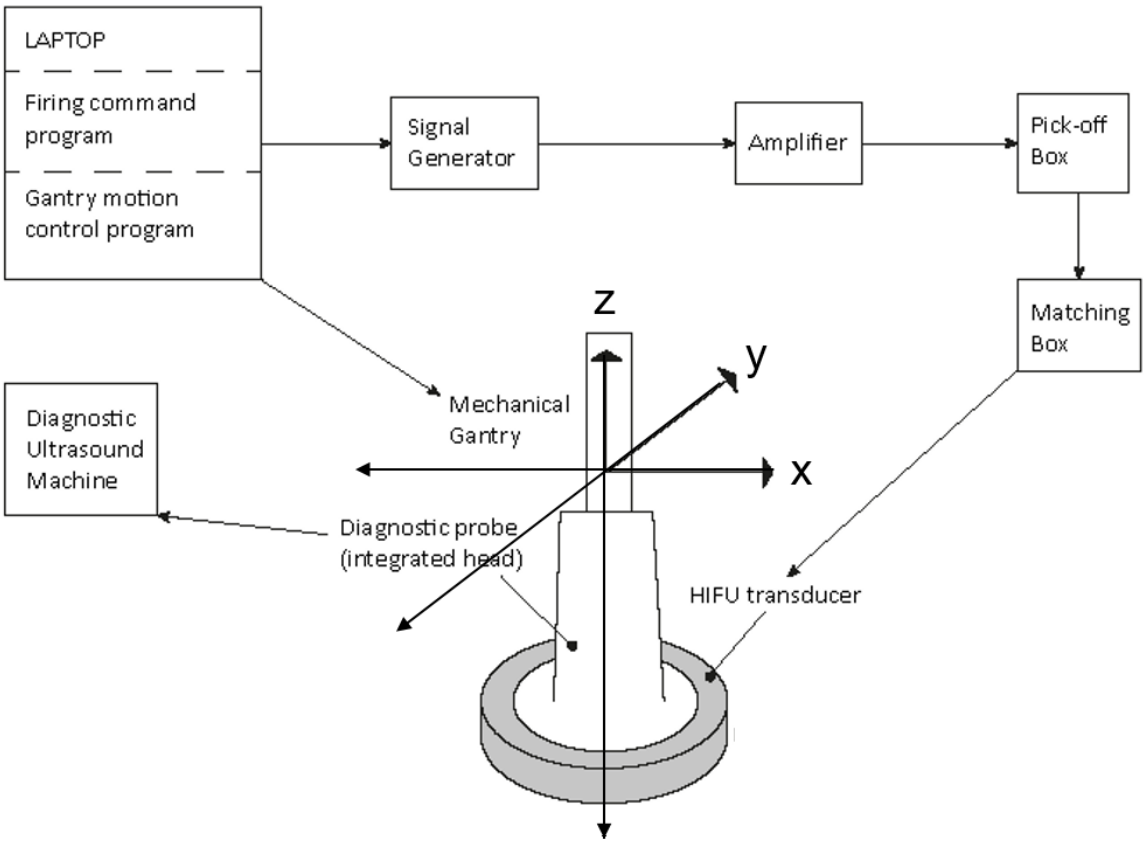

Figure 4.1: HIFU therapy system components.
The schema shows the connections of the HIFU transducer in relation to the laptop based control interface, mechanical gantry arm, diagnostic ultrasound transducer and other equipment. The arrows x, y and z denote the three directions in which the mechanical gantry arm was able to move (orthogonal to each other). The z axis is also the direction of sound, or the path along which HIFU energy travels, away from the transducer.

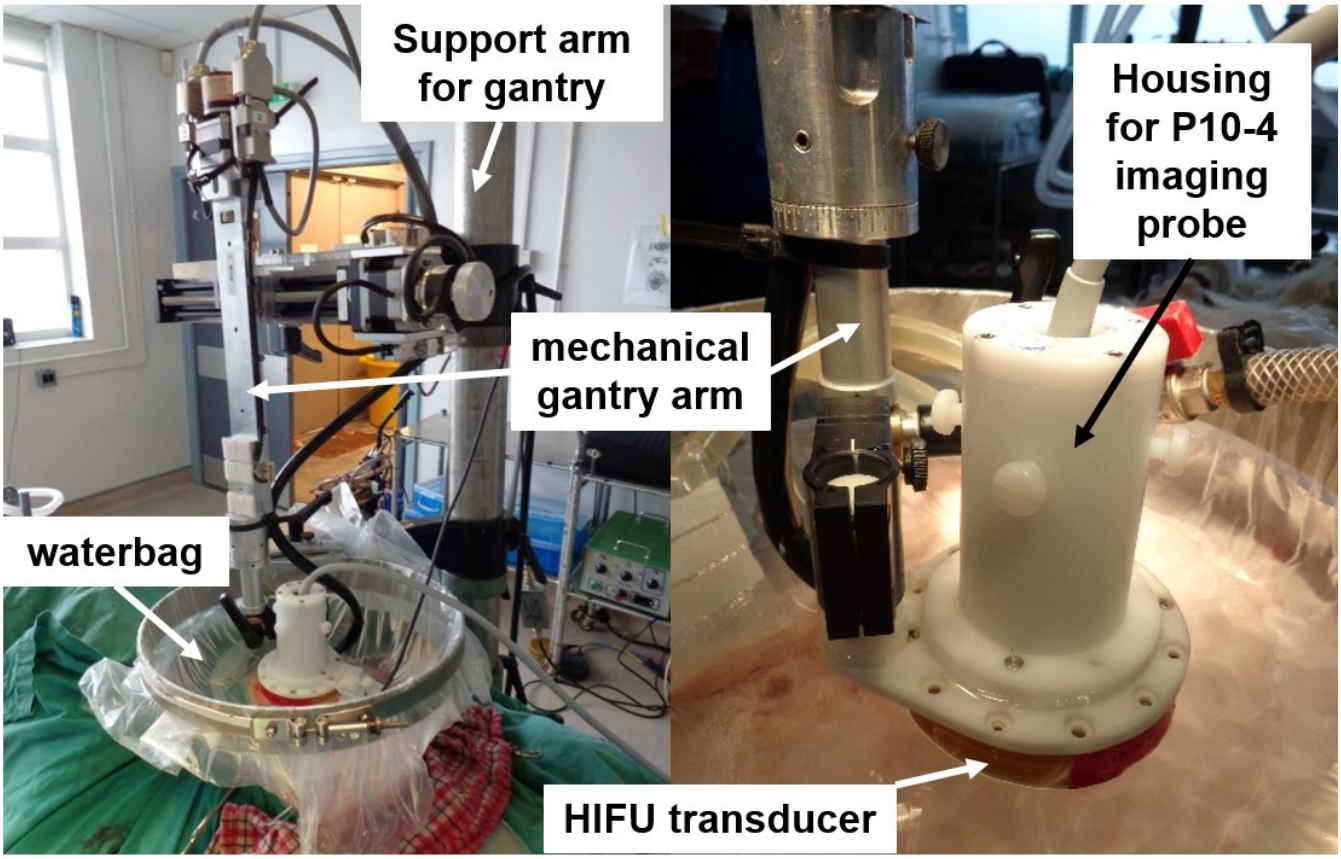

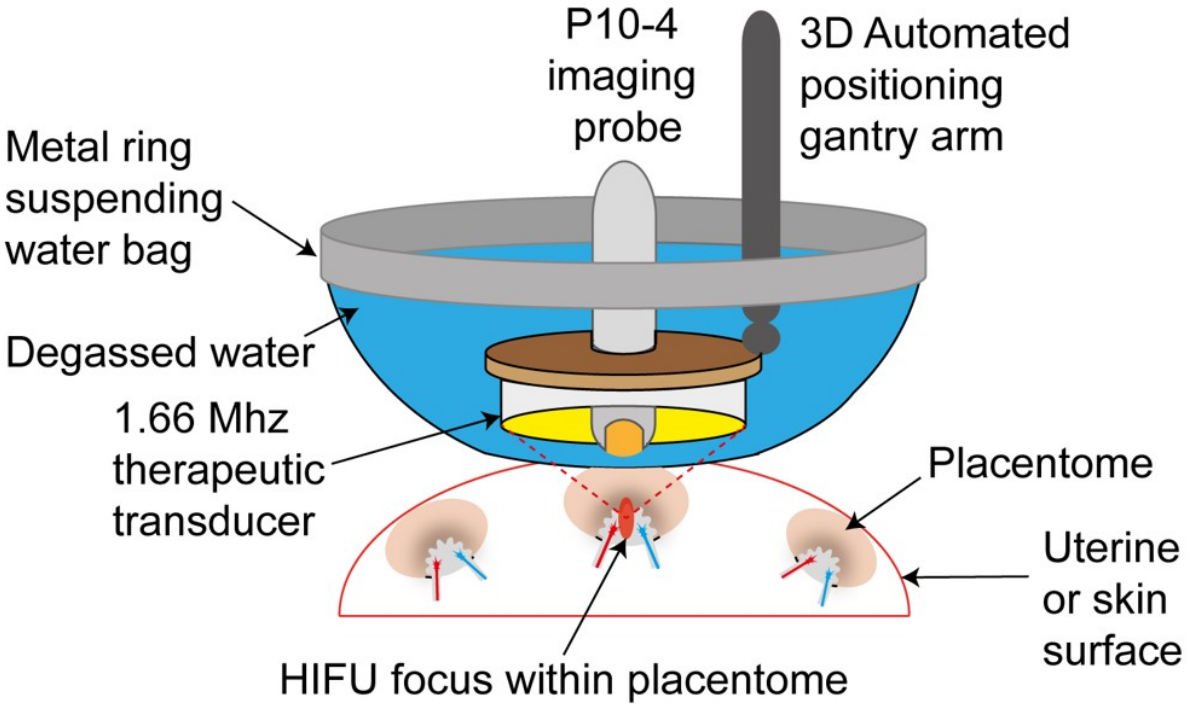

Figure 4.2: HIFU therapy system setup.
Top left: the picture shows the mechanical gantry arm and associated support structures in relationship to the waterbag, HIFU and diagnostic ultrasound transducers. Top right: the picture shows an enlargement of the HIFU therapy transducer and the housing of the diagnostic transducer which allow integration of the two transducers, and their attachment to the mechanical gantry arm. Bottom: the diagram shows the arrangement of diagnostic and HIFU transducers in relationship to the gantry arm, the water bag, degassed water, and the maternal uterine or skin surface (not to scale).

4.2.1.2 **Animals and surgical preparation**

Five ewes pregnant with singleton Welsh mountain fetuses at 115 ± 2 days of gestation (term ~ 145 d) were used. Under general anaesthesia, a maternal midline laparotomy was performed to expose the uterine surface in four animals, and the maternal skin was left intact in a fifth animal (sections 3.2.1-3.2.4).

If the uterus was exposed, the surface of the uterus was first wet with degassed water, then the waterbag was placed in direct contact with that area. Any pockets of trapped air between the plastic of the waterbag and the surface of the uterus were smoothed out.

In the animal where the skin remained intact, the maternal abdominal skin was prepared first by shaving with clippers to remove wool, then washed with iodine scrub solution (Vetasept: 7.5% povidone iodine, Animalcare Ltd., York, UK) to remove dirt and lanolin, and washed again with tap water. The remaining hair was chemically depilated (Nair ® hair removal cream, Church & Dwight Co., Kent, UK) and the skin was washed for a final time with tap water, then wet with degassed water. The waterbag was placed in contact with the maternal skin and trapped air between the plastic and the skin was smoothed out.

Mechanical ventilation of the ewe was paused during HIFU exposures to reduce respiratory movement which would lead to mis-targeting, referred to in this thesis as a “breath hold”. Non-invasive monitoring of maternal of cardiac and respiratory function was performed to ensure correct maintenance of anaesthesia (section 3.2.2). During breath holds, ventilation was recommenced either when the HIFU exposure series was completed, or if maternal oxygen saturation (measured by non-invasive pulse oximetry) fell to below 94%, or if maternal end tidal CO_2 rose to >8%, whichever occurred sooner.

All fetuses were assessed with ultrasound at the planned end of the HIFU exposures to determine presence or absence of fetal heart pulsations, and confirm fetal survival or death. Non-invasive maternal recording of maternal heart rate was used to confirm maternal survival to the planned end of the experimental procedure.

On completion of all planned HIFU exposures the ewe and fetus were euthanised without recovery from general anaesthesia under schedule one of the UK Animals (Scientific Procedures) Act 1986. A slow IV injection into the maternal jugular vein of 120 $mg.kg^{-1}$ pentobarbitone sodium (Pentoject®, Animalcare Ltd., York, UK) was used for this purpose. Air embolus into the jugular vein was used as a secondary confirmation of death. Maternal cardiac activity was auscultated with a stethoscope and death was confirmed on cessation of cardiac

and respiratory activity. Cessation of fetal cardiac activity was confirmed with diagnostic ultrasound.

4.2.1.3 **Vascular targets and HIFU treatment protocol parameters**

Between 1 and 5 placental vessels (1 vessel per animal, n=1; 3 vessels per animal, n=3; 5 vessels per animal, n=1) were targeted with colour flow Doppler in each animal, using the HIFU transducer, diagnostic ultrasound, control and positioning system described above.

The initial drive voltage used was the maximum power that was not anticipated to cause damage to the HIFU system electrics (-4 dBm), based on advice from the ICR team. After three sheep, this did have to be reduced to -5 dBm to protect the transducer impedance matching box from electrical damage. No further alterations were made to drive voltage in this pilot study, nor was there any attempt to correct for depth of the target beneath the surface to maintain a constant in situ intensity (Appendix IV).

The exposure conditions investigated in this study were the time interval (5, 10 or 20 s) and distance (1 or 2 mm) between HIFU exposures in a series. The duration of each exposure was kept constant at 5 s, based on previous experience that this was the shortest duration allowable to achieve occlusion (31, 32). Extrapolating from these studies of occluding femoral arteries in rats, the initial intention was to place a linear track of HIFU exposures orthogonal to the direction of sound, from one edge of a placentome to the opposite one. This linear track was designed to pass through the targeted vessel. The group of HIFU exposures which comprised the planned linear track are called an “exposure series” from here onwards. A gap of 1 – 2 mm between exposures was suggested as the width of the HIFU focus was known to be 1.2 mm; a 1 mm spacing should therefore produce overlap, a 2 mm spacing should leave a small gap between exposures.

This meant the width (orthogonal to the direction of sound) of each individual placentome and spacing of exposures should have determined the number of HIFU exposures in an exposure series. However, the number of exposures required in an exposure series was also investigated in these pilot studies, comparing “maximal” with “limited” exposure series (Figure 4.3). It is apparent from these images that a maximal exposure series (Figure 4.3d,e,f) may need to be placed higher within the placentome to take advantage of the greatest width of tissue. The limited exposure series were more directly localised to the vascular target and tended to sit closer to the point at which the vessels emerged from the placentome tissue. Even

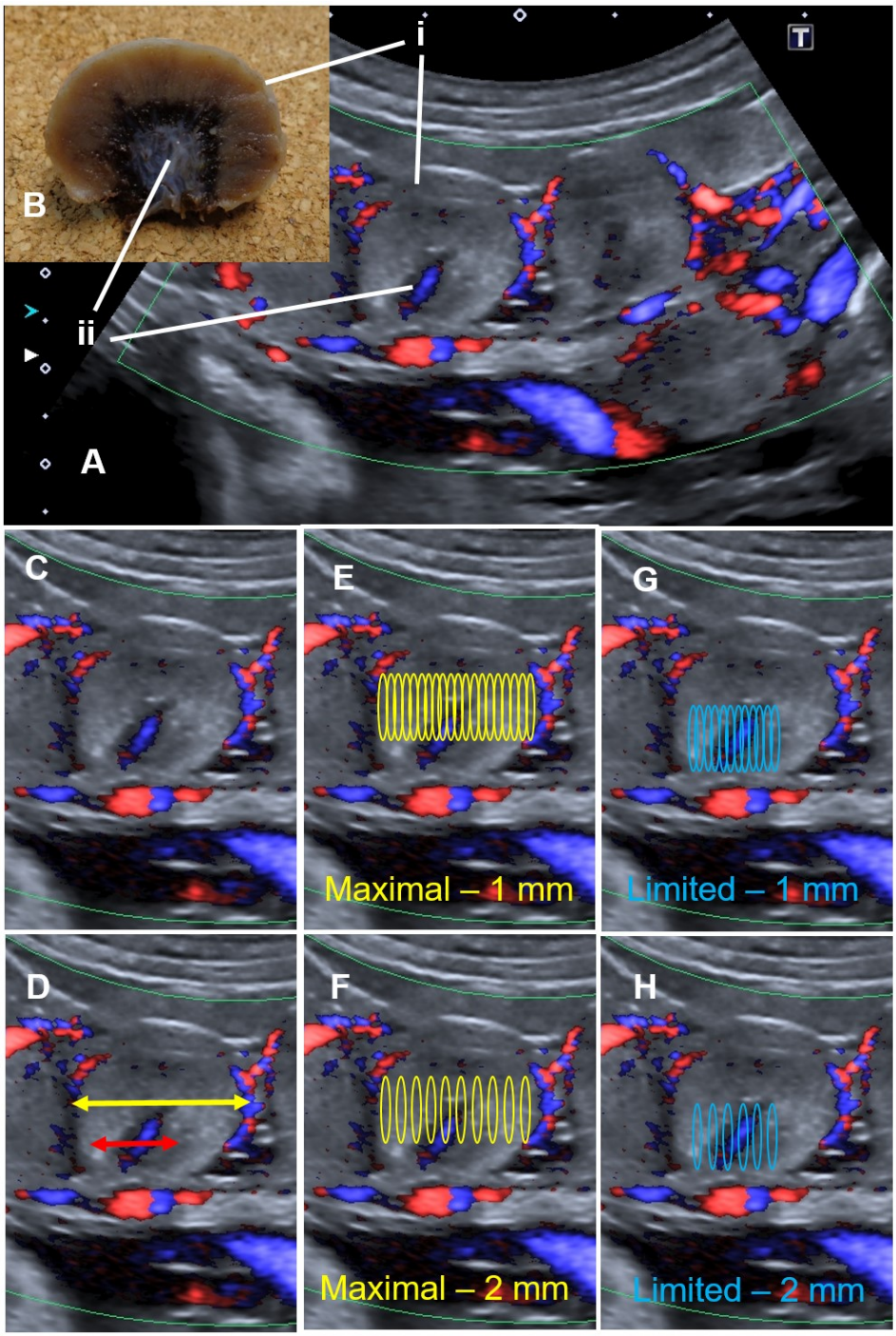

Figure 4.3: Types and planning of HIFU exposure series.
(A) Ultrasound image with colour flow Doppler showing (i) the outline of a placentome, and (ii) the colour flow signal indicating the origin of vessels from the fetal portion of the placentome. (B) The photograph shows corresponding landmarks in a bisected placentome at post mortem examination. (C) Shows an enlargement of the same placentome annotated in image A. This enlargement is used in panels D-H to illustrate planning of different types of HIFU exposure series. (D) The yellow arrow denotes the maximum width of placental tissue within this placentome, the red arrow measures the minimum width of HIFU exposures that could cross the echolucent area from which the target vessel arises, and still start and finish in soft tissue. (E) The yellow ovals (drawn to scale) represent the overlapping placement of 1 mm spaced HIFU exposure series, covering the full width of the placentome, the "maximal pattern" (total of 20 ovals). (F) The yellow ovals represent the non-overlapping, 2 mm spaced, placement of HIFU exposures across the full width of the placentome (total of 10 ovals). (G) The blue ovals represent the overlapping placement of 1 mm spaced HIFU exposures from the one soft tissue border of the echolucent area to the other, the "limited pattern" (12 ovals), (H) the blue ovals represent the non-overlapping placement of 2 mm spaced HIFU exposures from the one soft tissue border of the echolucent area to the other (6 ovals). Ultrasound image obtained using a 1.9 – 6.0 MHz convex sector array, (PVT-375BT, i700, Toshiba Medical Systems UK). Sheep: BL11, 109 d gestational age.

so, in a limited exposure series, an arbitrary decision was made that the minimum of the first and last HIFU exposure series were placed entirely in placental soft tissue (Figure 4.3d,g,h).

4.2.1.4 **Assessment of treatment success**

Treatment success was planned to be assessed using two measures, which could be correlated to each other.

The primary measure was the comparison of pre- and post-HIFU exposure colour Doppler imaging of the target vessel, because this is the non-invasive measure available clinically to judge success and guide therapy. If there was no colour flow Doppler signal detectable after HIFU exposures in the target vessel, this was determined to be “no flow”, indicative of a successful vascular occlusion. If there was preserved colour flow Doppler signal detectable after HIFU exposures in the target vessel, this was determined to be “residual flow”, indicative of a failed vascular occlusion. Pre- and post-exposure colour Doppler images were taken from the same 3D location, as controlled by the mechanised gantry arm, with precision of at least 1 mm as previously described. During post-HIFU exposure imaging the colour flow velocity scale was increased to its maximum (-6.3 – 6.3 $cm.s^{-1}$) to aid detection of residual blood flow.

“No flow” was first recorded, real time, in the experimental record; pre- and post-HIFU exposure saved imaging was examined after the end of the experiment to verify these findings (“offline analysis”). If there was a discrepancy between the finding of “no flow” in real-time and offline analysis of saved imaging, the finding from the saved imaging was used in preference.

The secondary measure was identification and histological examination of damaged placentome vessels and at post-mortem examination (same day). Exposed placentomes were tagged with green dye under ultrasound guidance after completion of each exposure series, for ease of identification at post mortem (Figure 4.4). A map of relative placentome positions was retained for differentiation of specific dye-tagged placentomes.

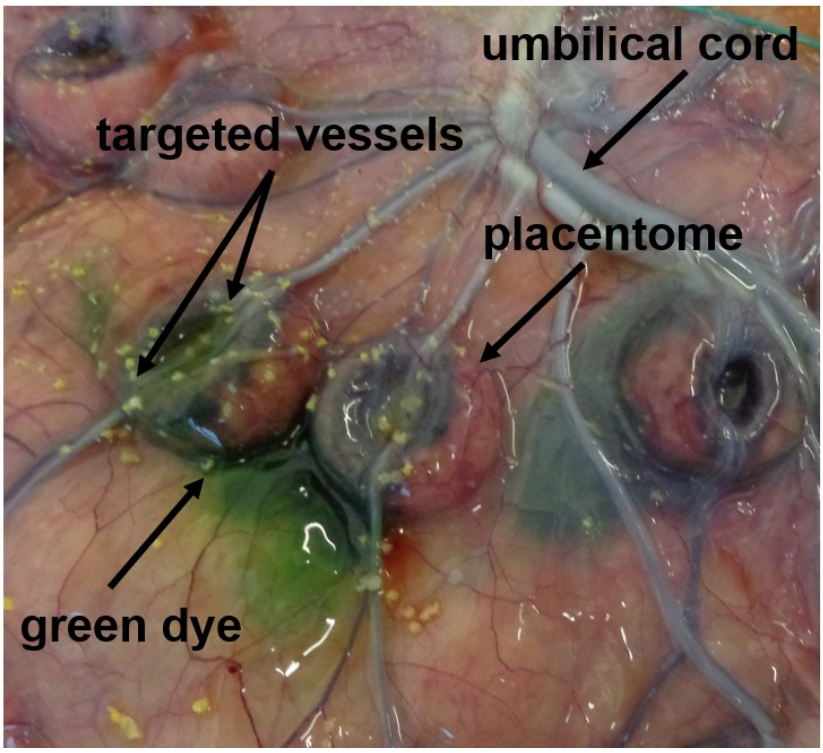

Figure 4.4: Dye tagging of targeted placental vessels.
The picture shows intact placentomes on the inner surface of the maternal uterus inverted at post mortem examination. Areas of green dye mark the placentomes in which vessels have been exposed to HIFU energy.

After euthanasia, a post-mortem examination of mother and fetus was conducted to recover tagged (exposed) placentomes. All placentomes, tagged with dye or not, were excised from the uterus and allantoic membranes, bisected and inspected for damage at this time. All tagged and/or damaged placentomes and two apparently un-tagged and undamaged placentomes were retained for histological examination. Damaged and tagged placentomes were photographed. The visual appearance and location of damage was recorded in the post-mortem examination record.

Collected tissues were immersion fixed in 10% neutral buffered formalin for five days before being washed and stored in phosphate buffered saline for up to six months at 4-6^{o}C. Placentomes were re-photographed after 24 h of immersion in formalin, as tissue damage appeared accentuated at this time.

Tissues were dehydrated through four solutions of increasing concentrations of ethanol before being cleared in three immersions of a histological clearing agent (Histo-clear II, National Diagnostics, Atlanta, USA) and infiltrated with paraffin wax. A minimum of four, 8 µm sections were taken from areas of interest within placentomes (not serial sections) and were mounted on glass microscope slides (Superfrost® Plus, Thermoscientific, MA, USA) ready for histological staining.

Sections were cleared of paraffin using Histo-clear II and rehydrated through four solutions of decreasing concentrations of ethanol before being stained with Harris haematoxylin solution (Sigma-Aldrich, MI, USA). Washing was performed with running tap water, differentiation with 1% acid-alcohol and bluing with Scott's tap water at room temperature, before counterstaining with an eosin Y 1% stock solution (Eosin Y, Sigma-Aldrich, MI, USA). Tissues were washed in running tap water, then dehydrated through four solutions of increasing concentrations of ethanol, cleared in two changes of Histo-clear II, before being cleared in xylene. Coverslips were mounted with synthetic resin mounting media (DPX, Sigma-Aldrich, MI, USA). Sections were examined histologically for evidence of tissue change or damage, and evidence of vascular occlusion or rupture. Findings of individual placentomes were correlated to colour flow Doppler findings for that placentome.

4.2.1.5 **Treatment monitoring**

Real-time tissue responses during HIFU exposures were planned to be monitored either by colour flow Doppler ultrasound, aiming to identify cessation of colour flow signal if it occurred before the end of the planned exposure series, or by tissue B-mode imaging, aiming to identify areas of hyperecho. Initially, single freeze-frame images were saved during exposures, but by the end of the third sheep experiment it was apparent that this would not provide sufficient material for offline analysis of HIFU exposures.

After this, 3 s video clips (8-10 Hz, ~30 frames) of each HIFU exposure in a series were recorded for offline analysis. Clips were limited to a maximum of 3 s by the ultrasound machine settings, and exported as compressed DICOM files. Each DICOM file was converted into a series of still images (one for each frame) using Image J (version 1.49m, public domain licence) and a customised script created by the ICR using MATLAB (MATLAB R2013a, Mathworks, MA, USA).

All the still images / frames from a video clip were examined offline. The linear depth of the HIFU focal plane (marked by the ultrasound machine cursor when set at a depth of 7.0 cm) and the target vessel beneath the skin or surface of the uterus (parallel to the direction of sound, or the central line of the ultrasound image) was measured using onscreen measuring software (Screen Calipers v4.0, Iconico, NY, USA). The linear depth of any overlying amniotic fluid was also measured. These values were used in the calculation of in situ intensity as described in Appendix IV. The position of the ultrasound cursor was checked to be over the intended target vessel (when compared to the pre-HIFU colour flow Doppler image) and the on-screen reading

of the depth was checked to determine it fell between 6.95 – 7.05 cm (expected 7.0 cm). If the cursor was away from the midline, too shallow or too deep compared to the intended target, or there was any other discrepancy in positioning of the focal zone relative to the target vessel, this was determined a potential "targeting error".

The drive voltage, transducer frequency, duration, start time and position of the transducer (x, y, z coordinates, reflecting position of the mechanical gantry arm) was recorded by the GUI software and exported to a text file. The report of gantry positions at each exposure in a series was compared to each other to confirm the planned spacing of exposures had occurred. The settings for each exposure were also checked to ensure an exposure of the planned drive voltage and duration had been delivered. Times of the start of each HIFU exposure in a series were checked and compared to ensure the planned interval had elapsed between HIFU exposures in a series. If the HIFU control or movement system had failed to deliver the planned exposure this was determined a potential "technical error".

To calculate the time taken to deliver a HIFU treatment, the onscreen time of the start of the first HIFU exposure was read off the saved image of the ultrasound screen (shown to the nearest second). The time of the first adequate image that demonstrated no flow or residual flow was also read from the ultrasound screen and recorded as the end of the treatment. The difference between these times was calculated as the treatment duration.

Maternal respiratory rate was recorded by the veterinary anaesthetic monitor and the data was exported as described in section 3.2.2. The number and duration of breath holds – where respiratory rate fell to zero – was read from the capnography data for each HIFU exposure series. The capnograph reports averaged data every 8 s, so breath hold duration is given to the nearest multiple of 8 s.

4.2.1.6 **Management of treatment failure**

If real-time colour flow Doppler imaging demonstrated residual flow, no retreatment was attempted in the pilot study. This was to preserve tissues unaltered after a failed occlusion attempts for further visual and histological examination to help identify why occlusion had failed. If a targeting or technical error, as defined above, was identified, this was recorded as a potential cause of treatment failure. All other failed occlusions were otherwise initially categorised as having an unknown cause.

4.2.1.7 **Assessment of iatrogenic harm**

The HIFU transducer was lifted after each completed exposure series to examine the surface of the skin or uterus for evidence of burns through the waterbag. If found, the area was photographed at the time of discovery, through the waterbag.

A systematic inspection of tissues was performed at post mortem examination and a photographic record was compiled of damage to: (i) maternal skin (if exposed), (ii) maternal rectus sheath (if exposed), (iii) anterior and posterior surface of the uterus, (iv) fetal skin (dorsal, ventral, left and right lateral views), and (iv) maternal bladder and bowel. Areas of maternal and fetal skin, rectus and uterus with visual changes suggestive of iatrogenic damage were also collected for histological examination, fixed in formalin, sectioned and stained with H&E as described in section 4.2.1.4.

4.2.2 Results

4.2.2.1 **Feasibility of using colour flow Doppler to target placental vessels**

In this phase of the study we were able to demonstrate the feasibility of using colour flow Doppler to identify placental blood vessels in the sheep. Figure 4.3a shows an example of the high quality of imaging of placental vessels possible in the sheep using a typical probe used for obstetric ultrasound (1.9 – 6.0 MHz convex sector array, PVT-375BT) applied intraoperatively directly to the maternal abdominal surface, using a loaned modern ultrasound machine (i700, Toshiba Medical Systems UK, Sussex, UK).

The clarity of this imaging was reduced by the requirement to use a paediatric echo probe small enough to image through the central (19 mm) aperture of the HIFU transducer, as described in section 4.2.1.1. However, there was still sufficient image quality to identify and target placental blood vessels as they emerged from the fetal side of placentomes, and demonstrate presence or absence of blood flow post HIFU exposures. Figure 4.5 shows an example of good transuterine colour Doppler imaging of placental blood vessels before and after HIFU treatment, with no residual colour flow in the target vessel evident on the post-exposure imaging, indicative of a successful occlusion.

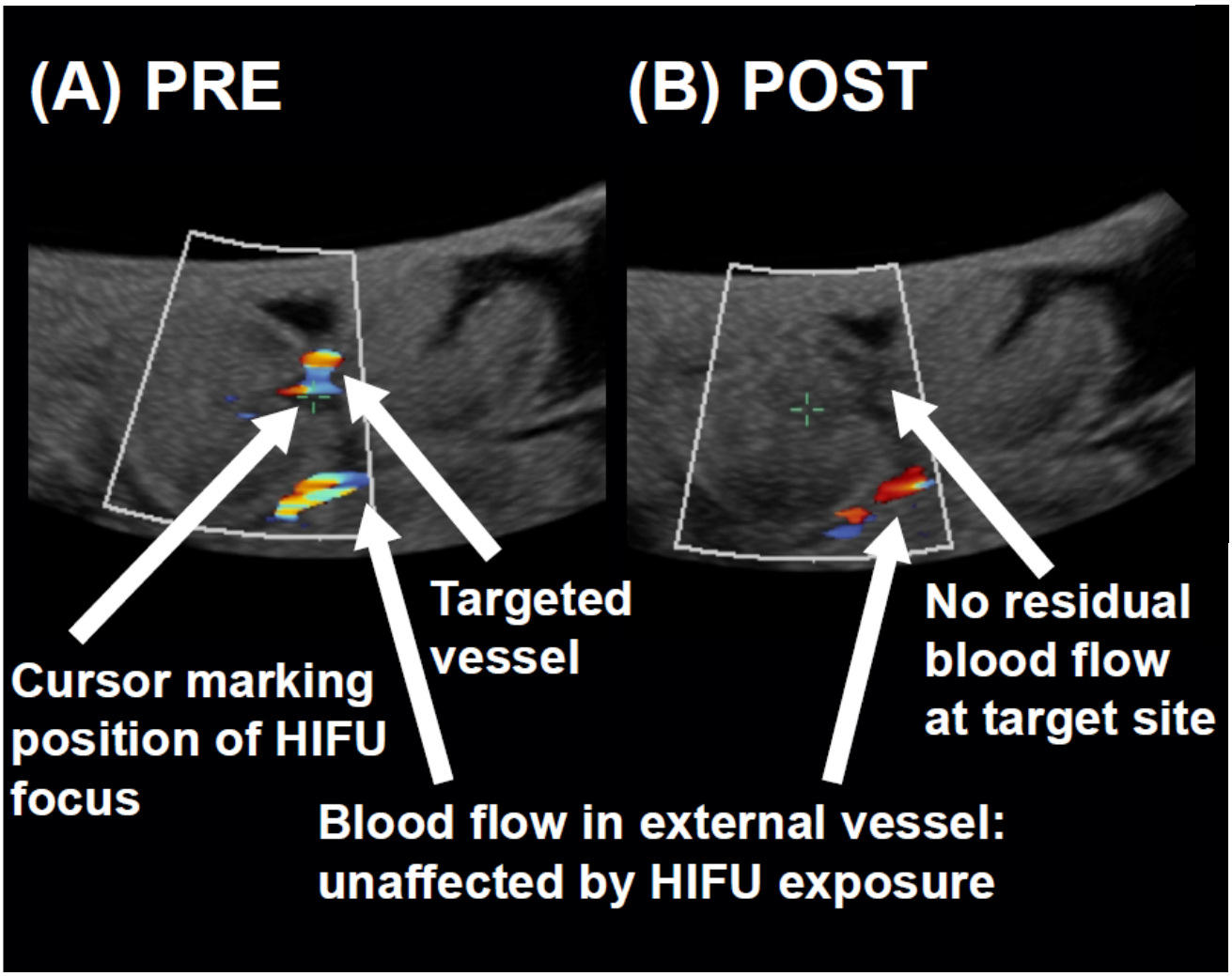

Figure 4.5: Colour flow Doppler ultrasound imaging of placental vascular occlusion (good quality).
(A) Pre-exposure colour flow Doppler imaging of a placentome. (B) Post-HIFU exposures colour flow Doppler imaging of the same placentome demonstrating no colour flow Doppler signal within the targeted vessel, reproduced from Shaw *et al.* (281). The HIFU exposure series was comprised of 9 transuterine exposures, 2 mm spaced, duration 5 s, interval 20 s, in situ intensity 6.3 $kW.cm^{-2}$. Obtained using a 4-10 MHz phased sector array transducer (P10-4, Z.one Zonare ultrasound system) in sheep OR616, 110 d gestational age.

Even with less clear imaging, it was still possible to identify and target placental blood vessels, and demonstrate post-HIFU "no flow" denoting successful occlusion, as shown in Figure 4.6.

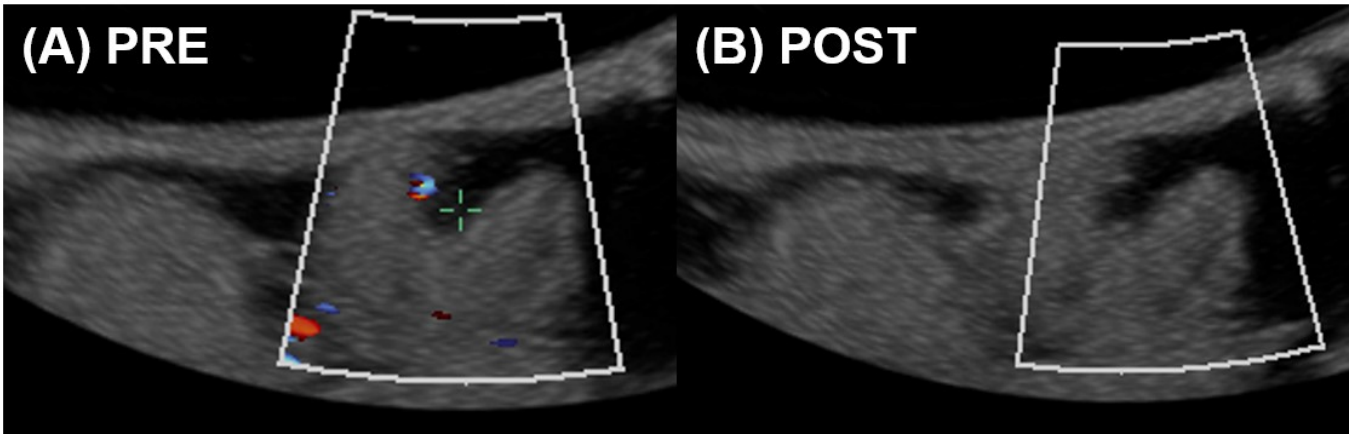

Figure 4.6: Colour flow Doppler ultrasound imaging of placental vascular occlusion (satisfactory quality).
(A) Pre-exposure colour flow Doppler imaging of a placentome. The intended vascular target is beneath the ultrasound cursor (blue cross). (B) Post-HIFU exposure colour flow Doppler imaging of the same placentome demonstrating no residual colour flow Doppler signal within the targeted vessel. The HIFU exposure series was comprised of 6 transuterine exposures, 2 mm spaced, duration 5 s, interval 20 s, in situ intensity 7.0 $kW.cm^{-2}$. Obtained using a 4-10 MHz phased sector array transducer (P10-4, Z.one Zonare ultrasound system) in sheep OR616, 110 d gestational age.

It was also possible to demonstrate failure to occlude a placental vessel by comparison of colour Doppler imaging, with preserved colour flow Doppler signal at the target vessel, as shown in Figure 4.7.

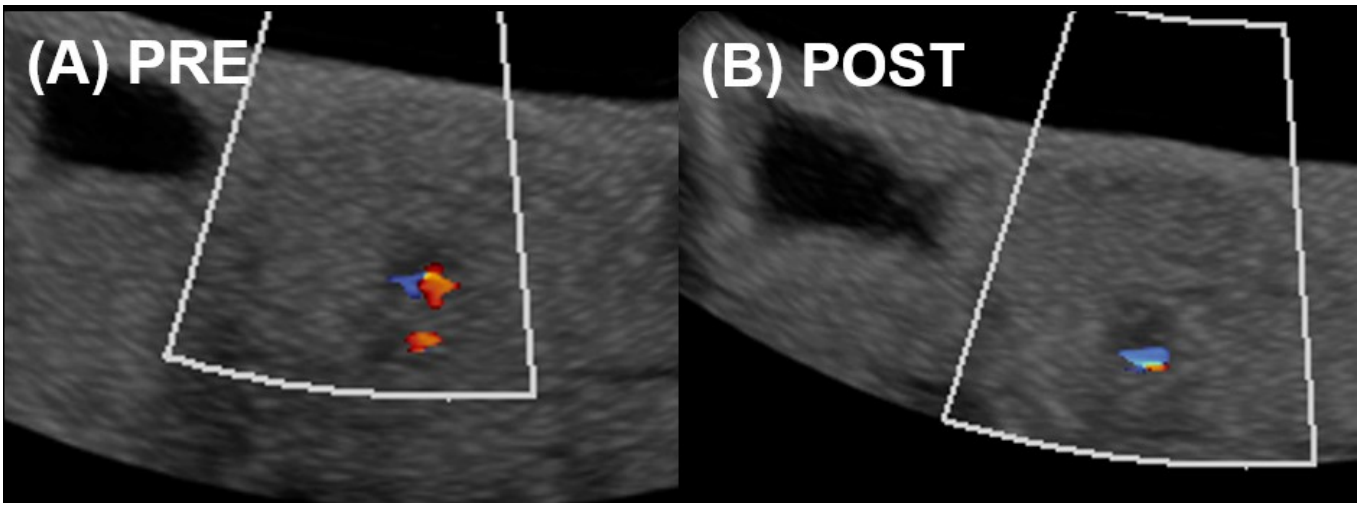

Figure 4.7: Colour flow Doppler imaging of unsuccessful placental vascular occlusion.
(A) Pre-exposure colour flow Doppler imaging of a placentome through intact maternal skin. (B) Post-HIFU exposure colour flow Doppler imaging of the same placentome demonstrating residual flow within the targeted vessel. The HIFU exposure series was comprised of 13 transdermal exposures, 2 mm spaced, duration 5 s, interval 20 s, in situ intensity 5.8 $kW.cm^{-2}$. Obtained using a 4-10 MHz phased sector array transducer (P10-4, Z.one Zonare ultrasound system) in sheep OR610, 110 d gestational age.

Treatment monitoring of tissue responses during HIFU exposures with colour flow Doppler, however, was not possible with our equipment. There was interference between the HIFU and diagnostic ultrasound systems to a sufficient degree that the artefact rendered imaging uninterpretable during HIFU exposures. This meant that the only time in which colour flow Doppler could be used was before, between or after HIFU exposures. However, there was artefact for around 3-4 diagnostic ultrasound frames (~0.5 s at a typical frame rate of 8 Hz) following the end of a HIFU exposure, before the presence or absence of colour flow signal in the targeted vessel could be interpreted. An example of this is shown in Figure 4.8. In these images the white arrow is aligned to the same 2D position within the ultrasound image for ease of comparison: in Figure 4.8a the vascular target is clearly visible before HIFU exposures; in Figure 4.8b interference from the active HIFU transducer causes uninterpretable artefact; Figure 4.8c-f shows persistence of this artefact after the HIFU exposure ends, before in Figure 4.8g it is possible to see that there is still colour flow signal in the vascular target despite the single HIFU exposure. The quality of colour flow Doppler imaging was also reduced while the motorised gantry arm was moving the transducers to their next position, due to disturbance of water in the water-bag. This effectively meant that when the interval between exposures was 10 or 20 s there was around 7-17 s to interpret the image on the screen; when the interval between HIFU exposures was reduced to 5 s, this time was at most 2.5 s, which increased the possibility of human error in interpreting findings. Additionally, due to the planned movement of the gantry arm, imaging was not being collected from the same 3D position as pre-exposure imaging, making the findings less reliable.

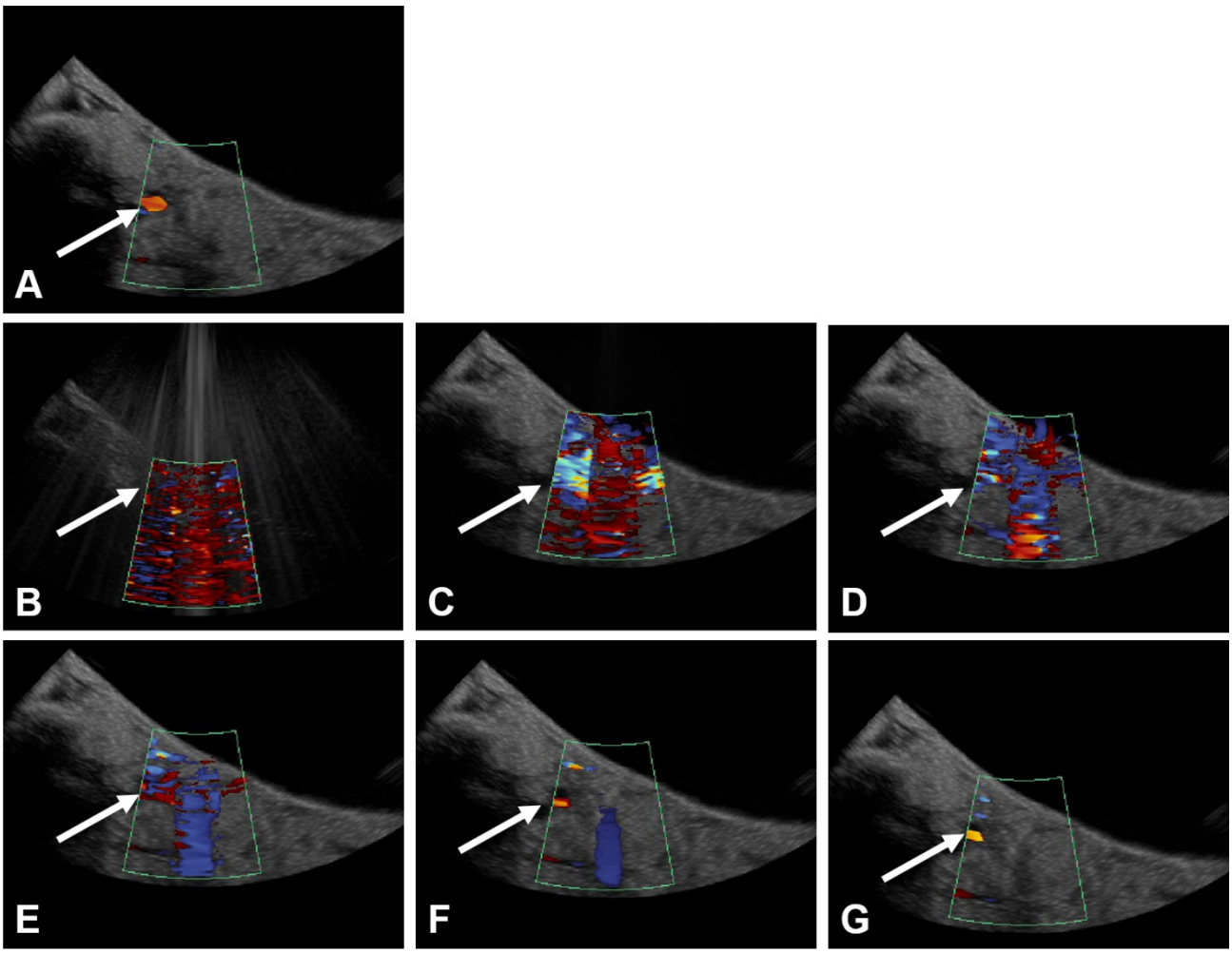

Figure 4.8: Colour flow Doppler artefact during and after HIFU exposures (8Hz frame rate).
(A) Pre-exposure colour flow Doppler ultrasound imaging of a placentome, the white arrow marks the colour flow signal of the targeted vessel. (B) Colour flow Doppler imaging of the same placentome during a transuterine HIFU exposure (5 s duration, in situ intensity 5.6 $kW.cm^{-2}$) demonstrating artefact in the colour Doppler signal. Colour flow Doppler imaging of the same placentome after HIFU energy source turned off in (C) first frame, (D) second frame, (E) third frame, (F) fourth frame, and (G) fifth frame. Artefact is present until the fifth frame (0.5 s post exposure, G), at which time it is evident that there is residual flow within the target vessel. Obtained using a 4-10 MHz phased sector array transducer (P10-4, Z.one Zonare ultrasound system) in sheep OR624, 117 d gestational age.

By comparison, it was possible to interpret B-mode imaging during HIFU exposures, even in the presence of artefact. Before, during and after HIFU exposures it was possible (although difficult) to visually identify the outline of the placentome (Figure 4.9, white arrows) containing the targeted vessel and the echolucent area in which the vessel ran (Figure 4.9, blue arrow); hyperechoic events could also be identified with B-mode imaging (Figure 4.9, yellow arrows).

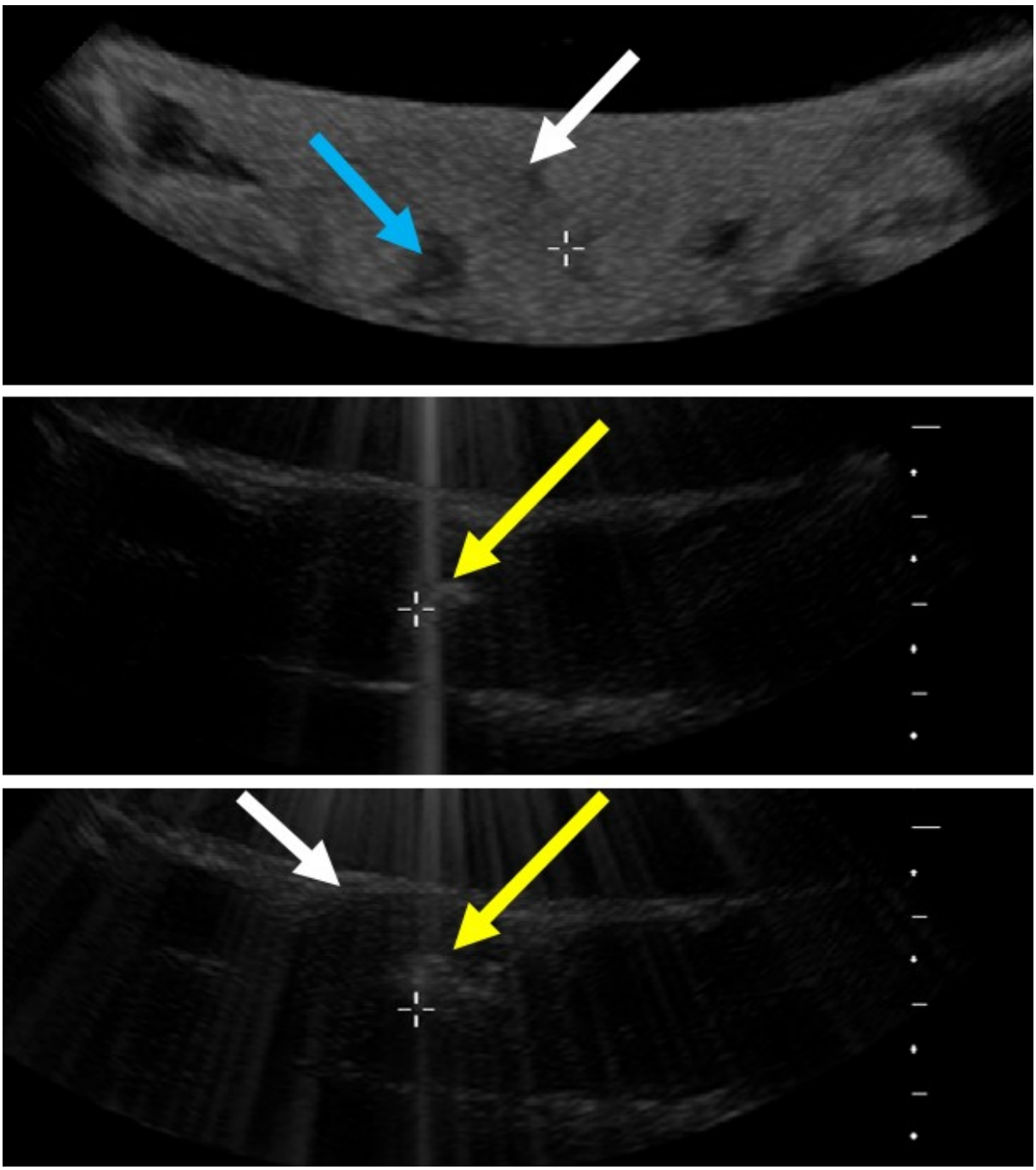

Figure 4.9: Hyperecho development during HIFU exposures.
Top panel: B-mode ultrasound imaging of placentome before HIFU exposures. The white arrow denotes the border of the placentome and the blue arrow points to the echolucent area in the centre of the placentome in which the targeted vessels are typically found. The white cross is the ultrasound cursor marking the position in the tissue where the centre of the HIFU focal zone will be positioned – the HIFU exposure series is a maximal one, which will progress from the right-hand border of the placentome to the left. Central panel: The B-mode ultrasound image now shows the artefact produced by HIFU energy; the white cross again shows the centre of the HIFU focal zone during this exposure (the 5th in a series of 13 transuterine HIFU exposures, 5 s duration, 20 s interval, 2mm spaced, 6.4 kW.cm^{-2} in situ intensity, target depth 15 mm). The yellow arrow shows an area of hyperecho involving the tissue currently being exposed to HIFU and spreading to the previous exposed locations (to the right of the focus). Bottom panel: The B-mode ultrasound imaging again shows the artefact due to the HIFU energy, the white arrow shows the border of the placentome, and the yellow arrow shows the hyperecho, which has expanded after the 8th of 13 exposures, following the track along which the HIFU exposure series has travelled. Obtained using a 4-10 MHz phased sector array transducer (P10-4, Z.one Zonare ultrasound system) in sheep OR616, 110 d gestational age.

4.2.2.2 **Feasibility of placental vascular occlusion**

Overall, in the pilot study, 15 placental vessels were targeted with colour flow Doppler. Based on a comparison of pre- and post-HIFU colour Doppler imaging of targeted vessels, 12 out of 15 (80%) were successfully occluded.

Secondary confirmation of successful or failed occlusion was obtained in 11 of the 15 vessels based on histological examination of exposed vessels (Figure 4.10). In 9 of the 11 vessels which it was possible to examine histologically, there was evidence of trapped erythrocytes within vessel lumen, suggestive of occlusive clot. These 9 vessels were all predicted by colour flow Doppler to be occluded. In the other 2/11 vessels, there was no evidence of trapped erythrocytes; failed occlusion had been predicted in these vessels by colour flow Doppler. There was no evidence of trapped erythrocytes in the vessel lumen of control placentomes which had not been exposed to HIFU. Therefore, at this stage, there was complete correlation between colour flow Doppler and histological findings, where histological examination was possible.

In 4 of 15 exposed placentomes, it was not possible to perform histological examination of the vessels due to difficulties in preparing tissues for examination. This was likely a direct result of the degree of tissue damage produced by HIFU exposures making the tissue difficult to dehydrate and impregnate with paraffin wax, rendering sectioning not possible.

There was visual evidence of soft tissue damage in all the tagged placentomes, regardless of whether occlusion had failed or succeeded. This served as confirmation that the soft tissue, although not necessarily the vessels, had been exposed to HIFU energy. As a method of detecting vascular occlusion, based on these 15 vessels, the specificity of this method was only 50%.

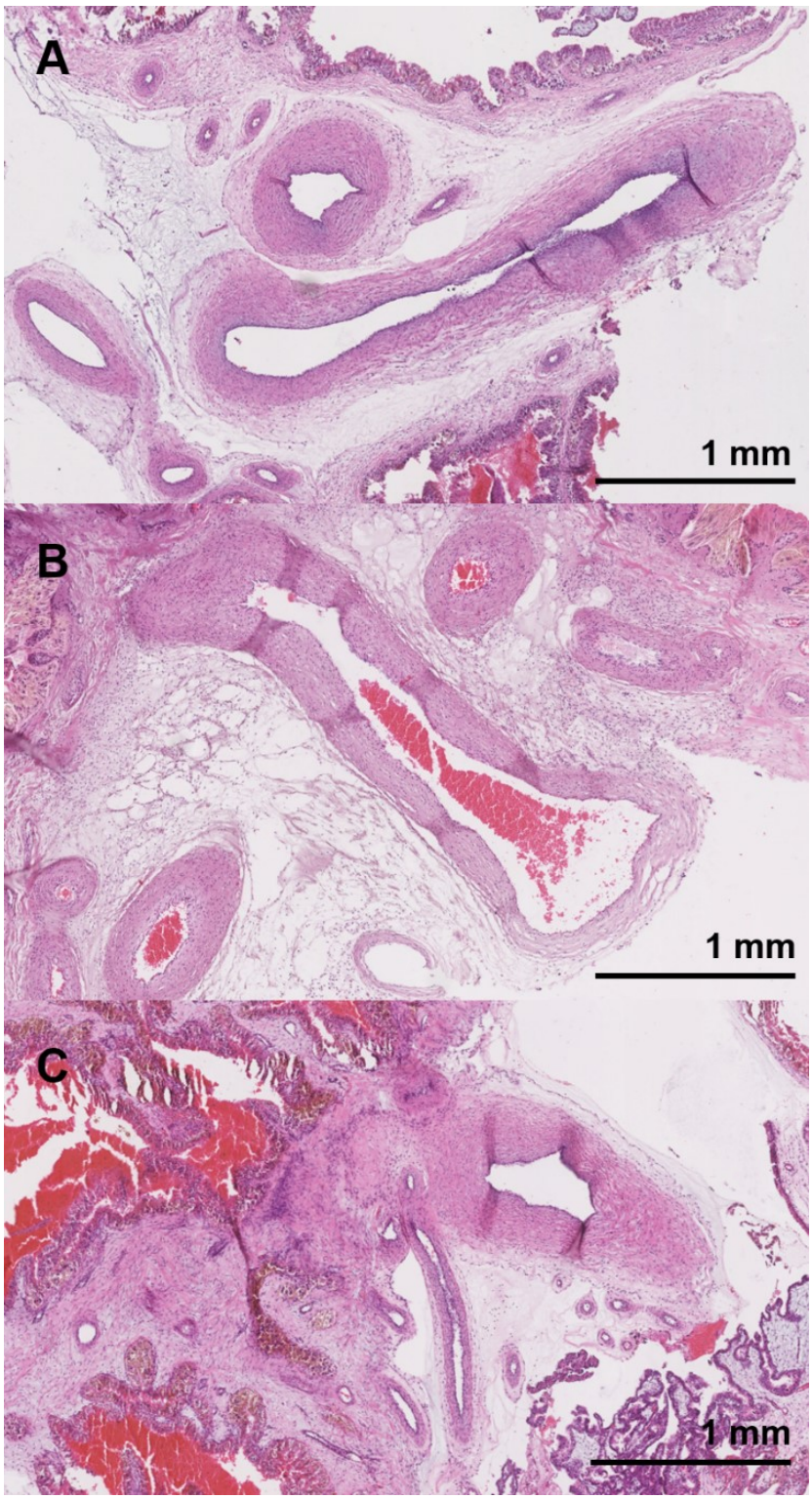

Figure 4.10: Histological outcomes (acute) in vessels following exposure to HIFU.
(A) H&E stain of fetal vessels in a control placentome. The lumen of the vessels are open and unobstructed, suggesting they remain patent. There is no extravasion of blood in the other tissues. (B) H&E stain of fetal vessels in an exposed placentome where colour Doppler imaging suggested occlusion. While the vessel lumen is not collapsed, there are trapped erythrocytes within the lumen suggestive of occlusive clot. (C) H&E stain of fetal vessels in an exposed placentome where colour Doppler imaging suggested failed occlusion. As in the control placentome, these vessel lumen are open and unobstucted, without trapped erythrocytes, however, there is extravasation of blood suggestive of some degree of tissue damage which did not result in vessel occlusion.

Table 4.1 shows a comparison of which exposure conditions produced successful vascular occlusion based on colour flow Doppler findings.

	Successful occlusions	Failed occlusions
Vessel characteristics		
Number	12	3
Depth of vascular target (mm)	13 ± 5	16 ± 6
Diameter (mm)	0.5 - 2.4	0.6 - 0.9
Exposure characteristics		
Drive voltage (dBm)	-4 or -5	-4 or -5
In situ intensity ($kW.cm^{-2}$)	4.3 - 7.0	4.5 - 4.6
Spacing (mm)	1 or 2	2
Interval between exposures (s)	5, 10, 20	20
Number of exposures in series	6 - 20	6 - 20
Planning of exposure series		
Maximal (n=10)	8 (80%)	2 (20%)
Number of breatholds (maximal)	3 - 13	4 - 5
Treatment time (maximal, s)	380 - 1300	NR
Limited (n=5)	4 (80%)	1 (20%)
Number of breatholds (limited)	1 - 2	2
Treatment time (limited, s)	130 - 290	410
Delivery of exposure series		
Transuterine (n=12)	11 (92%)	1 (8%)
Transdermal (n=3)	1 (33%)	2 (67%)

Table 4.1: Pilot study vessel and exposure characteristics.
The table shows the characteristics of vessels and HIFU exposure series in the pilot study, divided by those which resulted in successful of failed occlusion. The depth of the vascular target is given as the mean ± SD; other characteristics are given as ranges or absolute numbers with percentages in brackets where indicated. NR = not recorded.

Based on this comparison, delivering exposure series transuterine, rather than transdermal, was the most effective characteristic in improving rates of successful occlusion: 92% of exposures delivered transuterine were successful in producing occlusion, compared to only 33% delivered transdermal.

This did not appear to be a result of the ability to deliver sufficient acoustic energy through the maternal skin and rectus sheath. The reduction of the drive voltage from -4 to -5 dBm made no appreciable difference to the success rates of occlusion, and the range of estimated in situ intensities for successful and failed occlusions overlapped. The depths of the vascular targets beneath the skin or uterus similarly overlapped

Successful occlusion could be achieved with intervals of 5, 10 or 20 s between exposures, but in the 3 occlusions which failed there was an interval of 20 s between exposures, despite in situ intensities and exposure numbers comparable to other exposure series.

Exposure series were formed of between 6 and 20 exposures; it was possible to achieve occlusion with as few as 6 HIFU exposures in a series (a 2mm spaced, limited exposure series, example in Figure 4.3h), or fail to occlude a vessel with 20 HIFU exposures in a series (2mm spaced, maximal exposure series, example in Figure 4.3e).

There was no obvious benefit of using 1 mm spaced exposure series compared to 2 mm spaced exposure series, however 1 mm spacing increased the number of exposures required in a series, the number of breath holds, and the total duration of time and total acoustic energy delivery required to occlude a vessel which were all potentially harmful to the ewe and fetus (data not shown).

There was no obvious benefit of using “maximal” or “limited” exposure series, and using a “maximal” exposure series also increased the number of exposures required in a series the number of breath holds, and the total duration of time (Table 4.1), and energy delivery required to occlude a vessel (data not shown).

4.2.2.3 **Survival and iatrogenic harm**

All mothers and fetuses survived to the planned end of the experimental procedures.

While visual identification of tissue damage was not specific as a method of confirming vascular occlusion, some appearances were suggestive of over-exposure of tissues with HIFU energy. There was visual evidence of extensive extravasation of blood into the soft tissues and tissue heating when placentomes were bisected (Figure 4.11) in all 15 of the exposed placentomes, regardless of whether occlusion had succeeded or failed. When visual appearances were compared with histological damage, evidence of heat fixation of tissue, extravasation of blood into extracellular spaces, tissue boiling and discrete tissue haemorrhage were evident (Figure 4.12).

At this stage, evidence of tissue boiling or discrete tissue haemorrhage were classified as excessive, unwanted, tissue damage; whether a degree of heat fixation and extravasation was unavoidable was unclear. Histological evidence of excessive tissue damage was found in 7 of the 11 placentomes it was possible to examine, and none of the control placentomes. In 4 of 11 placentomes, however, while there was heat fixation of tissues and extravasation into extracellular spaces, this was the extent of the damage (Figure 4.13). Visually, there appeared to a lesser degree of tissue damage in these placentomes (Figure 4.14). Both discrete tissue haemorrhage and extravasation of blood into intracellular spaces were different to vascular haemorrhage, which is presented below.

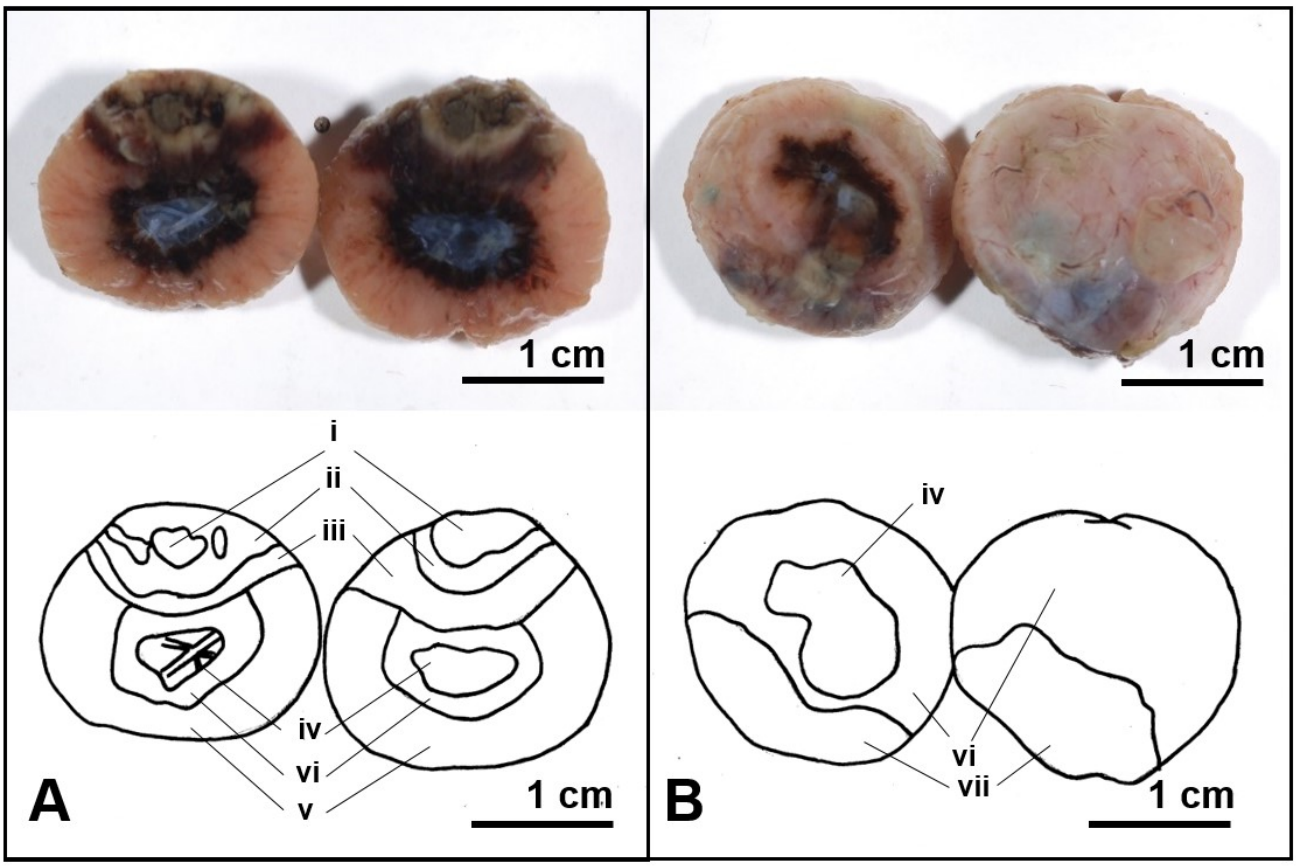

Figure 4.11: Excessive placental soft tissue damage (visual).
The photographs show a placentome bisected after exposure to HIFU (16 exposures, in situ intensity 5.3 kW.cm^{-2}, 2 mm spaced, 10 s interval between exposures, target depth 12 mm) and fixed in formalin for 24 h. The photograph in (A) shows the inner surface of the placentome where it has been bisected, and in (B) the outer surface of the placentome with allantoic membranes removed. In the line diagrams, there are (i) areas of severely damaged tissue and areas of both (ii) tissue pallor, suggestive of heating, and (iii) darkening, suggestive of extravasation, adjacent to the (iv) fetal vessels, (v) region of materno-fetal exchange, involving much of the (vi) placental soft tissue; (vii) show soft tissue discolouration extending to, but contained within, the outer capsule of the placentome, suggestive to tissue boiling.

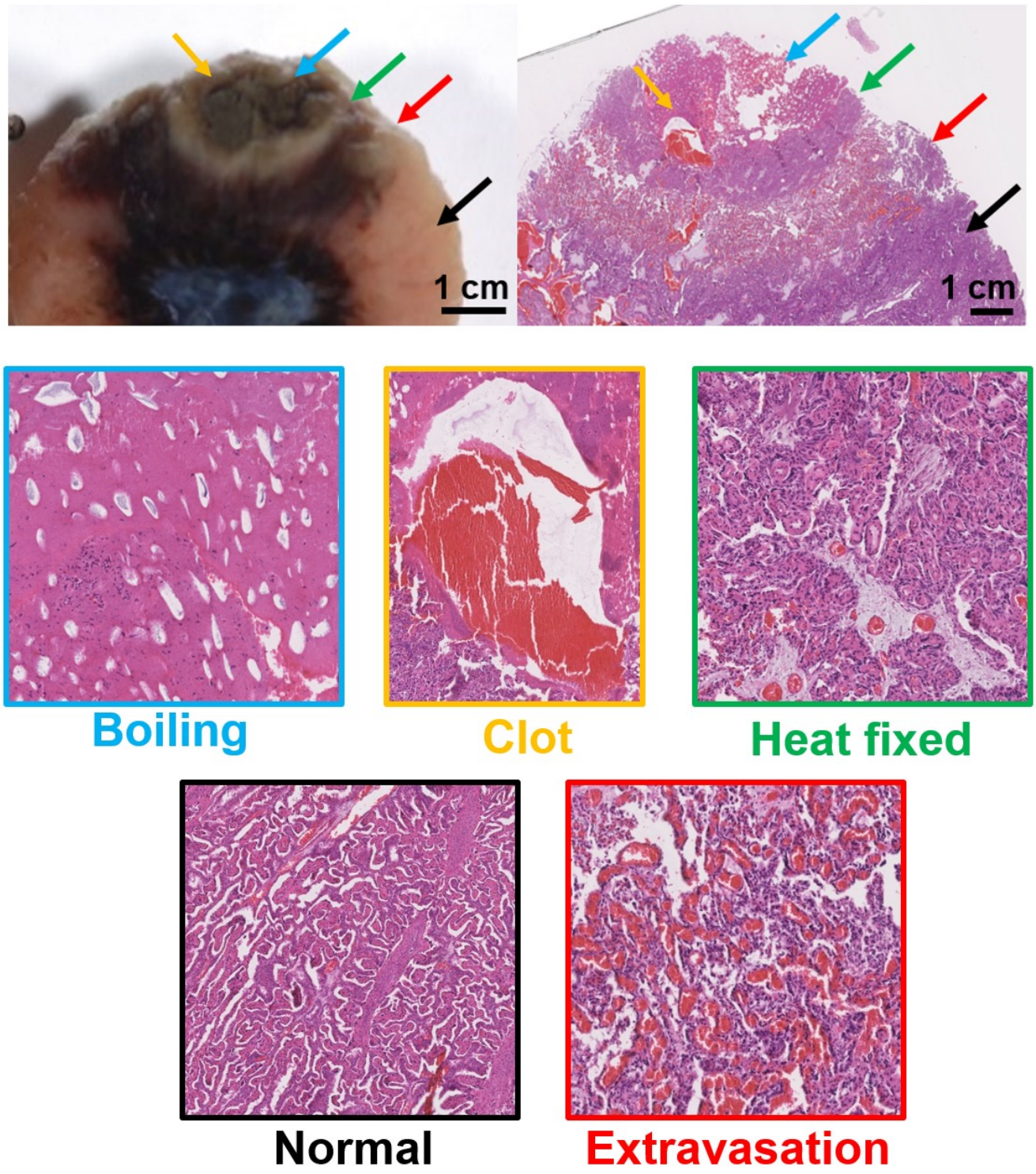

Figure 4.12: Excessive placental soft tissue damage (histology).
The photograph on the upper left is a close-up of the placentome shown in Figure 4.11. The image on the upper right is a H&E stained section of tissue from the same placentome. The black arrow points to normal tissue, the red arrow shows the region where there is extravasation of blood into the intracellular spaces, the green arrow denotes a region of homogenised tissue suggestive of heat fixed tissue, and the blue arrow points to the area where tissue boiling damage has occurred, with loss of tissue architecture and large, regular intracellular spaces. The yellow area is a section of extracellular erythrocytes within a cavity, suggestive of discrete tissue haemorrhage resulting in an area of clot within the tissue. Magnified sections are displayed in beneath, in colour-coded boxes, to match the arrows.

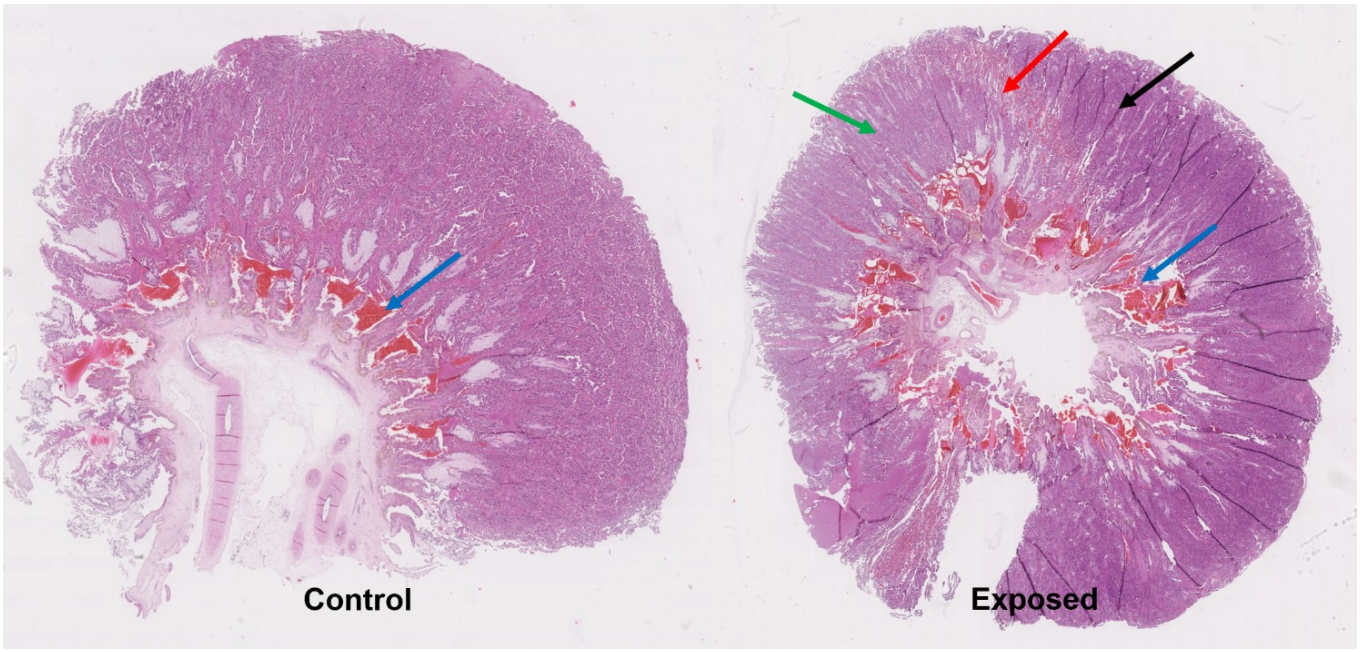

Figure 4.13: Non-excessive placental soft tissue damage (histology).
The image on the left is a H&E stained section of a control placentome. The blue arrow points to areas of extravasation around the materno-fetal interface, despite not being exposed to HIFU. These are potentially an artefact of the process of bisecting the placentome at post-mortem. The un-occluded lumen of the target vessels can be seen. The image on the right is of an placentome exposed to HIFU (6 exposures, in situ intensity 5.0 $kW.cm^{-2}$, 2 mm spaced, 5 s interval between exposures, target depth 14 mm, visual appearances shown in Figure 4.14). The black arrow points to normal tissue, the red arrow shows the region where there is extravasation of blood into the intracellular spaces, the green arrow denotes a region of homogenised tissue suggestive of heat fixed tissue. The blue arrow shows extravasation at the materno-fetal interface, such as seen in the control placentome. There are no regions of clot in the tissue, or evidence of boiling.

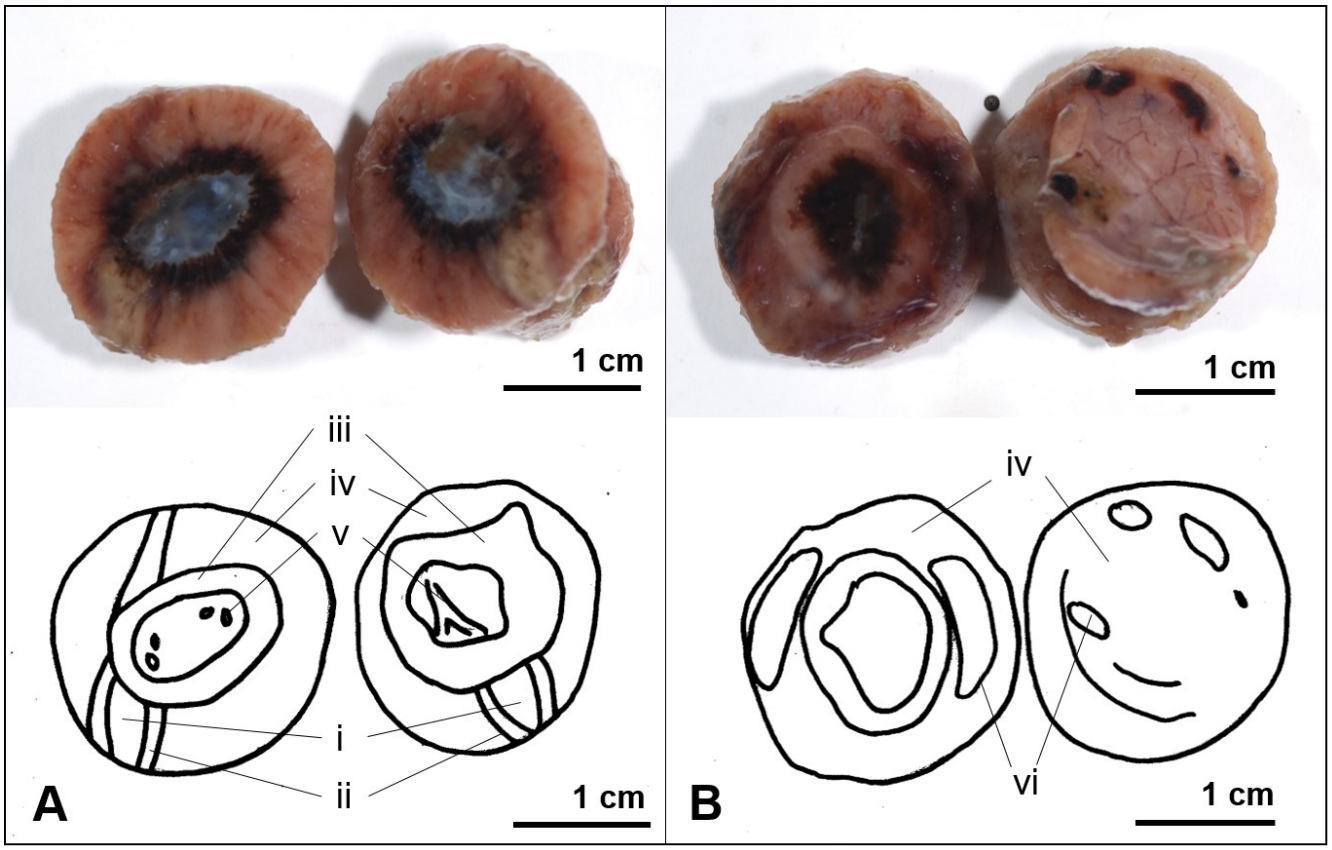

Figure 4.14: Non-excessive placental soft tissue damage (visual).
The photographs show a placentome bisected immediately after exposure to HIFU (6 exposures, in situ intensity 5.0 kW.cm^{-2}, 2 mm spaced, 5 s interval between exposures, target depth 14 mm) and fixed in formalin for 24 h. The photograph in (A) shows the inner surface of the placentome where it has been bisected, and in (B) the outer surface of the placentome with allantoic membranes removed. In the line diagrams, there are areas of (i) tissue pallor, suggestive of heating, and (ii) darkening, suggestive of extravasation, adjacent to the (iii) region of materno-fetal exchange, involving a portion of the (iv) placental soft tissue and crossing the (v) origin of targeted vessels. On the outside of the placentome there is no evidence of capsule damage, the regions marked (vi) are green dye adherent to the surface, discoloured by formalin.

A comparison of targets and exposure characteristics which resulted, or not, in excessive tissue damage is given in Table 4.2.

	Excessive tissue damage	No excessive tissue damage
Vessel characteristics		
Number	7	4
Depth of vascular target (mm)	12 ± 4	19 ± 3
Successfully occluded	7	2
Exposure characteristics		
Drive voltage (dBm)	-4 or -5	-4 or -5
In situ intensity ($kW.cm^{-2}$)	5.3 - 7.0	4.3 - 5.0
Spacing (mm)	1 or 2	2
Interval between exposures (s)	5, 10, 20	5, 20
Number of exposures in series	6 - 20	6 - 20
Planning of exposure series		
Maximal (n=7)	4 (57%)	3 (43%)
Limited (n=4)	3 (75%)	1 (25%)
Delivery of exposure series		
Transuterine (n=8)	7 (87%)	1 (13%)
Transdermal (n=3)	0 (0%)	3 (100%)

Table 4.2: Excessive tissue damage (pilot study).
The table shows the exposure and vessel characteristics in the 11/15 placentomes which were examined histologically, divided into those with and without excessive tissue damage. The depth of the vascular target is given as the mean ± SD; other characteristics are given as ranges or absolute numbers with percentages in brackets where indicated.

Based on this comparison, excessive tissue damage appeared more likely to occur in placentomes exposed to higher in situ intensities, as there was no overlap in these ranges, although numbers were too small to draw a definitive conclusion. While drive voltage had no effect of the degree of tissue damage, the shallower targets, particularly if exposed transuterine, were more prone to excessive tissue damage. Both of these factors contributed to higher in situ intensities. Neither the time interval between, nor the spacing between, HIFU exposures in a series appeared to affect the likelihood of excessive tissue damage. Number of exposures in a series similarly did not discriminate between groups; maximal and limited exposure series both produced excess tissue damage if the in situ intensities were high enough.

There were 2 placentomes in which blood was coagulated in the allantoic membranes (Figure 4.15a-c), initially thought to be possible instances of vascular haemorrhage from the target

vessels. In situ intensities of 6.4 and 7.0 kW.cm^{-2} were delivered to these placentomes, and tissue boiling and discrete tissue haemorrhage reaching the edge of the placentome tissue was seen histologically. It was not, however, possible to identify the vascular haemorrhage histologically, and in both these placentomes there was also evidence of occluded vessels. It is possible that the blood seen was an extension of the discrete tissue haemorrhage seen, and not a haemorrhage as a result of wall damage in the targeted vessel.

There were two uterine burns (Figure 4.15d); both were related to placentomes in which boiling and discrete haemorrhage occurred and reached the edge of the placentome tissue. In situ intensities of 6.4 kW.cm^{-2} (13 exposures, 2mm spacing and 20 s interval) and 5.6 kW.cm^{-2} (7 exposures, 2mm spacing and 5 s interval) were delivered to the vascular targets at 8 and 9 mm depth respectively beneath the uterine surface. As such, these burns may be the result of pre-focal damage, but other high intensity exposures were delivered at similar depths without resulting in a burn.

There were two fetal burns. In one, the fetal back was 12 mm beneath the vascular target, which was exposed to a series of 20 exposures of 4.5 kW.cm^{-2} in situ intensity, 2 mm spacing and 20 s interval between exposures (Figure 4.15e). In the second, the fetus was 19 mm beneath a vessel exposed to 20 exposures at 5.5 kW.cm^{-2} in situ intensity, 2 mm spacing and 20 s interval between exposures (Figure 4.15f). As such, these burns may have been the result of post-focal damage. The fetus was not visible in saved ultrasound images during the treatment of any other placentomes, meaning it was at least 40 mm away from the HIFU focus, dependant on the depth of the target vessel and the ultrasound screen settings.

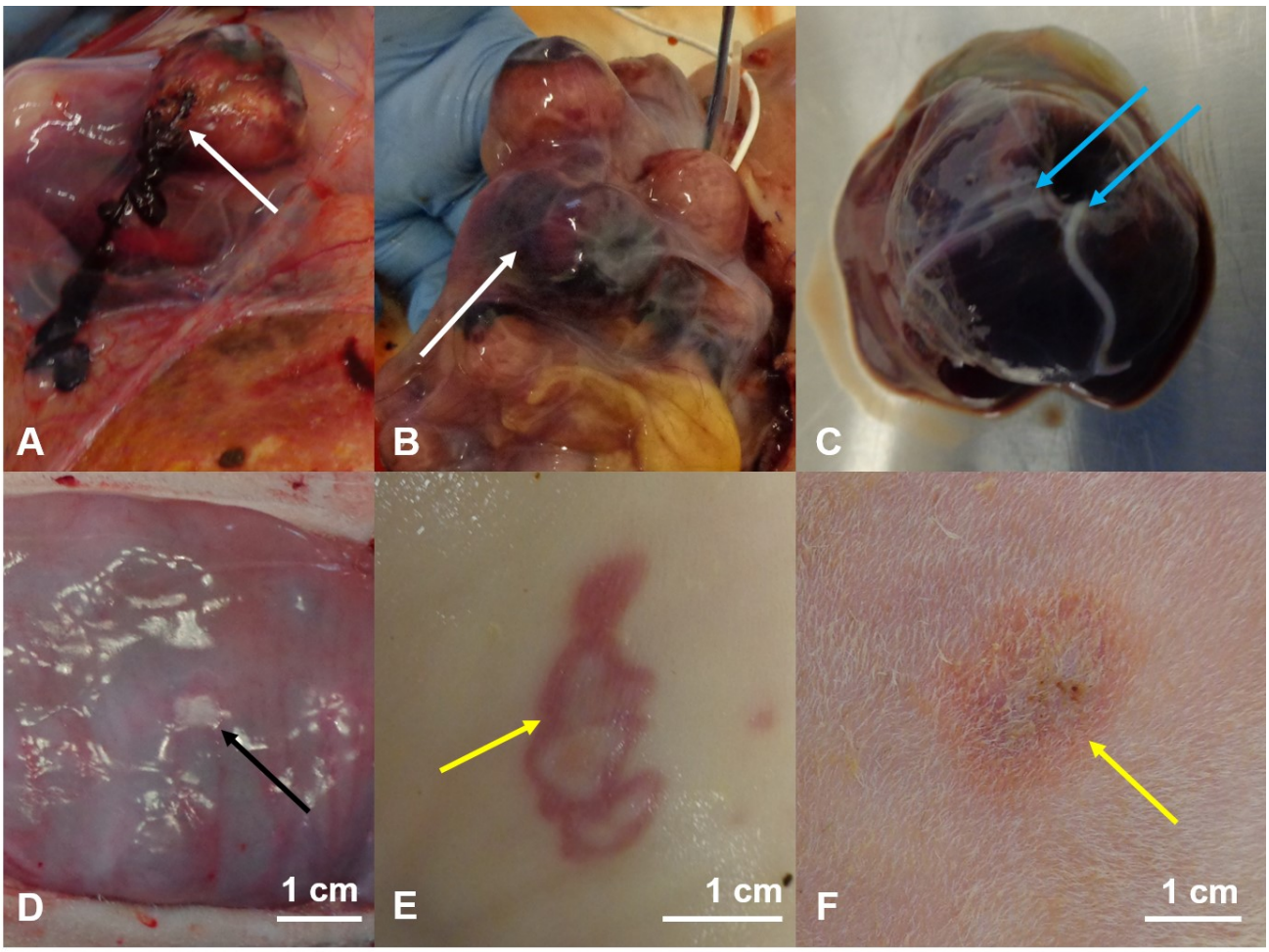

Figure 4.15: Iatrogenic damage (pilot study).
The photographs show (A) a placentome from which a string of clots (white arrow) is visible in the allantoic membranes, and (B) a diffuse blood trapped in the allantoic membranes (white arrow) surrounding a placentome. (C) shows the placentome in (B), once it was excised from the allantoic membranes; the clotted blood is adherent to the surface of the placentome and the target vessels can still be seen emerging from the placentome (blue arrows) although they have a shrunken appearance. (D) shows a uterine burn on the serosal surface of the uterus (black arrow). (E, F) show areas of burn on the fetal skin (yellow arrows).

4.2.3 Pilot study: discussion

The HIFU exposure series in the pilot study demonstrated it was possible to use HIFU to occlude placental blood vessels non-invasively. This was the first time, based on a review of published literature (1), that this had been demonstrated, and validated in principal the basic premise of the study.

At this early stage, the capacity of the mother and fetus to tolerate a period of HIFU placental vascular occlusion was unknown, although there were prior reports of fetal sheep surviving HIFU ablation of fetal soft tissue targets in the short term (60, 61). In this series of 5 sheep, all mothers and fetuses survived the HIFU exposures, suggesting that at least in the short term,

HIFU mediated placental vascular occlusion of 1-5 blood vessels was a survivable procedure in sheep.

Using a drive voltage of -5 dBm, we showed that it was possible to deliver sufficient HIFU energy to the target tissues, through the surface of the uterus or skin, to result in vascular occlusion. However, at least 65% of these exposure series also resulted in excessive tissue damage, i.e. tissue boiling and discrete tissue haemorrhage (given that there were 4 histologically unexamined placentomes which also had macroscopic evidence of significant tissue damage). It appeared that the possibility of excessive tissue damage was relative to the in situ intensity of HIFU energy delivered to the tissues (Table 4.2). Based on this small sample, there was no evidence that reducing the number of exposures, spacing exposures further apart, or allowing a longer cooling time did not protect the tissues from the high in situ intensities, if used. The threshold above which excessive tissue damage occurred following HIFU exposures appeared to be between 5.0 – 5.3 $kW.cm^{-2}$.

It appeared that more widespread tissue and/or vessel haemorrhage, and uterine burns could also result from in situ intensities resulting in excessive tissue damage, although the composite rate of this was lower than for excessive tissue damage (3/15, 20%). There was limited data available, but the estimated in situ intensity threshold above which fetal and uterine burns or vessel haemorrhage into allantoic membranes should be anticipated appeared to be 5.6 – 7.0 $kW.cm^{-2}$. Exposures at these high in situ intensities have previously been associated with vessel rupture (37, 45). It was, however, possible to achieve vascular occlusion without excessive tissue damage or iatrogenic harm, using an in situ intensity of 4.3 $kW.cm^{-2}$. This is consistent with other published studies which have achieved vascular occlusion with in situ intensities of 2.0 – 4.0 $kW.cm^{-2}$ (Table 1.3).

There were a total of 3 HIFU exposure series which resulted in failed occlusion. In one (transuterine, drive voltage -5 dBm, in situ intensity 5.8 $kW.cm^{-2}$, 6 exposures, “limited” pattern, 20 s intervals between exposures, 2 mm spaced) there was a failure of the mechanical arm of the gantry to move along the 10 mm track and only 2 mm movement was recorded. As such, this was defined as a technical failure, and was the first indication that the linear track was an important feature of successful occlusion, although gave no suggestion as to what the mechanism of this could be. It was possible that the length of the linear track corrected for any small (<5-10 mm) targeting errors; it is also possible that the cumulative effect of tissue heating surrounding vessels in addition to within the vessel walls and lumen was of benefit, potentially by producing tissue oedema (section 1.2.3.4) or shrinkage of connective tissue surrounding the vessels (section 1.2.3.3).

The other 2 exposure series which failed were applied through intact maternal skin. There were no obvious targeting or technical errors to account for the failure and as shown in Table 4.3, the only difference in exposure conditions from successful occlusions was the interval between exposures of 20 s. However, given that other exposure series with 20 s intervals between exposures also produced occlusion, the significance of this was uncertain.

The pilot study results also showed it was possible to use integrated colour flow Doppler ultrasound to identify and target placental vessel in the pregnant sheep model with sufficient accuracy to occlude them non-invasively. Colour Doppler was suggested to be a sensitive and specific method to determine if occlusion had occurred or not following a HIFU exposure series, as these results correlated well with histological findings of occlusion in target vessels. While the use of Doppler ultrasound has previously been reported to target blood vessels and demonstrate occlusion in other animals and human fetuses (section 1.2.2) this was the first time this had been demonstrated in sheep placental vessels. This validated using colour flow Doppler as the primary outcome measure of treatment success for subsequent animal groups in our study.

However, interference between the HIFU ultrasound energy and the diagnostic ultrasound meant that there was artefact on both the B-mode and colour Doppler imaging while the HIFU source was in use. The degree of artefact and distortion of the image for this system when colour Doppler was selected as the monitoring method meant it could not be used during a HIFU exposure to monitor the progress of the treatment, and was not easy to use in the intervals between exposures. Artefact was also present during B-mode imaging during HIFU exposures, but with adjustment to the gain it was still possible to interpret the images acquired. Although the imaging cycle of diagnostic transducer (~30 Hz) can be synchronised to on/off pulses of the HIFU transducer to negate this interference, so that the HIFU transducer is off when the diagnostic ultrasound is acquiring an imaging frame, (282) this is a significant software engineering project which was not planned for this study. It also required pulsing of the HIFU energy when we had planned for continuous exposures. Therefore, during HIFU treatments, a decision was made that tissue responses were monitored by B-mode ultrasound imaging (real-time). An additional finding, which had not initially been part of the plan to monitor treatment responses or assess success was the development of hyperecho during HIFU exposures. The significance of hyperecho during exposures was identified as an area requiring further study in subsequent animal groups.

Given that the principle of using Doppler ultrasound guided HIFU to occlude placental vessels in sheep had been shown feasible, the next stage based was to attempt to quantify the acute

impact of ultrasound guided HIFU placental vascular occlusion on maternal and fetal physiology.

It was important that the magnitude of the potential intrauterine insult – namely the number of placental blood vessels occluded, and the length of time this was carried out over – was both a fixed magnitude of insult and comparable to any potential human treatment to make results more directly translatable.

A relatively wide range for the number of anastomoses ablated by fetoscopic laser (per patient) is quoted in published literature: Ierullo et al. (283) report a mean of 4 (range 1-11); Lopriore et al. (284) report a mean of 6-7 (range 3-12) and Slaghekke et al. (19) report a mean of 8 (range 5-11). Typical total treatment times are in the range of 5 - 25 minutes (19, 283).

We also need to limit the total exposure time of the fetus to general anaesthesia, so that physiological responses to HIFU vascular occlusion, and not pathological responses due to prolonged anaesthesia would be assessed. For these two reasons, it was decided to: (i) limit the HIFU treatment time to 30 min, and (ii) aim to target 6-7 placental vessels during the 30 minutes. Therefore, the target time to identify, plan, deliver HIFU and confirm successful or failed occlusion was a maximum of 5 minutes. Based on the findings of the pilot study, "limited" series of HIFU exposures with a 5 s interval, 2 mm spaced were the only type of exposure series which could be reliably delivered, and occlusion success assessed, in less than 5 minutes. This was predominantly due to the fact, they could be completed in a single breath hold. This was also hypothesised to be of benefit in stabilising maternal anaesthesia and oxygenation intraoperatively and so improving fetal condition.

Three "limited" exposure series with the characteristics suggested for Group A animals were delivered in the pilot study: drive voltage -5 dBm, in situ intensities 5.0 – 5.7 $kW.cm^{-2}$, 6-9 exposures in a series, target depth 8 – 14 mm. All 3 produced successful vascular occlusion, and were delivered and assessed in < 5 minutes.

From an experimental design perspective, there was a necessity to apply HIFU directly to the uterine surface in order to record acute fetal physiological responses to HIFU mediated placental vascular ablation (section 0). Given the lower rate of successful occlusion in transdermal application of HIFU compared to transuterine application at the stage, a decision was made to refine the HIFU treatment protocol for transuterine application, where targeting was quicker and easier (as the uterus could be manipulated) and energy losses were lower, before attempting a transdermal approach.

4.3 Transuterine efficacy and safety study: Group A(cute)

In this second phase of the study, we sought to:

(i) establish if HIFU could be used as a method to consistently occlude placental blood vessels (transuterine);
(ii) assess the rates and types of iatrogenic harm to mother and fetus (transuterine);
(iii) assess acute changes in materno-fetal physiology in response to HIFU mediated placental vascular occlusion (methods, results and discussion in chapter 3, 5, 6 and 8).

Establishing HIFU as a consistent method of occluding placental vessels without imposing an excessive burden of iatrogenic harm on the mother and fetus were prerequisites to moving to the phase of the study in which animals were recovered from anaesthesia and longer term follow-up was planned, due to ethical and financial constraints.

The results of the pilot study had enabled the development of a transuterine HIFU treatment protocol in which exposure conditions did not vary, and in the pilot study had a 100% successful occlusion rate, although only based on 3 vessels. The characteristics of this standard transuterine protocol should also enable the planned HIFU exposure series to meet the requirements of the experimental protocol for quick vascular occlusions. By standardising the exposure conditions, we anticipated that we would be able to deliver a consistent challenge to ewes and fetuses, and also better compare the characteristics of exposure series which resulted in successful and failed occlusions.

4.3.1 Methods

4.3.1.1 HIFU therapy system

No changes were made to the system described in section 4.2.1.1.

4.3.1.2 Animals and surgical methods

In brief, 5 pregnant ewes carrying singleton fetuses at 116 ± 1 d gestational age were placed under general anaesthesia (section 3.2.1, 3.2.2); maternal and fetal surgical instrumentation (sections 3.2.4, 3.2.5) was performed for the purpose of monitoring acute maternal and fetal cardiovascular, acid-base and metabolic responses to HIFU mediated placental vascular

occlusion. The uterus was left exposed through a midline laparotomy following the completion of surgery.

This animal group was the first in which maternal and fetal cardiovascular, acid-base and metabolic responses to HIFU mediated placental vascular occlusion were to be monitored in the acute setting. The results of the acute changes in materno-fetal physiological responses to HIFU or sham mediated placental vascular occlusion will be presented and discussed in chapters 5-8, where groups A, S and R can be compared.

Following the completion of surgery, the experimental protocol was divided into three 30 minute periods. The first 30 minutes (-30 to 0 min) was the time allowed to identify vascular targets and plan HIFU exposure series, followed by a 30 minute treatment phase (0-30 min) during which HIFU or sham exposures were performed, then a 30 minute recovery phase (30-60 min, Figure 3.9). During the planning time, the uterus was scanned with B-mode and colour flow Doppler imaging, but not manipulated. At the end of the planning time, the surface of the uterus was wet with degassed water, then the waterbag was placed in direct contact with that area. Pockets of trapped air between the plastic of the waterbag and the surface of the uterus were smoothed out.

During the HIFU treatment time, if required, the uterus was manipulated gently to facilitate good access to placental vessels in areas of the uterus away from the fetus, and the waterbag repositioned and smoothed accordingly. HIFU exposures were delivered according to the protocol described in the next section. Breath holds were used to pause respiratory movement as described in section 4.2.1.2.

Once the experimental protocol was completed, additional HIFU exposure series were performed as part of a dose de-escalation protocol, also described during the next section. This was to examine the effect of reducing drive voltage and to maximise the use to which each experimental animal was put, during which time no monitoring of fetal physiology was performed.

On completion of all the planned HIFU exposures the ewe and fetus were euthanised without recovery from general anaesthesia under schedule one of the UK Animals (Scientific Procedures) Act 1986. A slow intravenous injection into the maternal femoral vein catheter of 120 $mg.kg^{-1}$ pentobarbitone sodium (Pentoject®, Animalcare Ltd., York, UK) was used for this purpose. Air embolus into the femoral vein was used as a secondary confirmation of death. Maternal cardiac activity was auscultated with a stethoscope and death was confirmed on

cessation of cardiac and respiratory activity. Cessation of fetal cardiac activity was confirmed with diagnostic ultrasound.

4.3.1.3 **Vascular targets and HIFU treatment protocol parameters**

HIFU was applied transuterine to between 4 and 7 placental vessels per animal in the time-limited experimental protocol (7 per animal, n=2; 6 per animal, n=2; 4 per animal, n=1). HIFU exposure conditions were: drive voltage -5 dBm, 5 s exposure duration, 5 s intervals between exposures, 2 mm spacing between exposures.

HIFU was applied transuterine to between 1 and 4 placental vessels per animal in the dose de-escalation protocol (4 per animal, n=2; 3 per animal, n=1; 1 per animal, n=1). HIFU exposure conditions were: drive voltage -5 to -8 dBm, 5 s exposure duration, 5 s intervals between exposures, 2 mm spacing between exposures.

In both cases, the “limited” model was used to plan exposure series and determine exposure number (Figure 4.3h). However, unlike in the pilot study, there was no requirement to place at least the first and last exposure in a series in the soft tissue of the placentome adjacent to the echo-lucent area. This was a non-evidence based limit imposed in the pilot study and its necessity was unknown, so it was not included in this phase of the study.

The planning of a HIFU exposure series was limited to information available from B-mode and colour Doppler ultrasound imaging: the size of the placentome (height, width, cross sectional area); the size of the echo lucent area from which vessels arise (height, width, cross sectional area); and the depth of the colour signal beneath the surface of the uterus (linear target depth, Figure 4.16). The diameter of the targeted vessel or the rate/volume of blood flow within it could not be reliably assessed with colour flow or pulsed wave Doppler.

The cross-sectional area of the echo lucent region (in 2D) was used as a simple marker of the area of the size of the region containing target vessel(s), in lieu of being able to measure the vessels themselves. The height and width of the echo-lucent area were converted into a simplified cross-sectional area using the standard formula for the surface area of a regular ellipse:

$$\textbf{Cross sectional echolucent area} = \pi(\text{height}/2)(\text{width}/2)$$

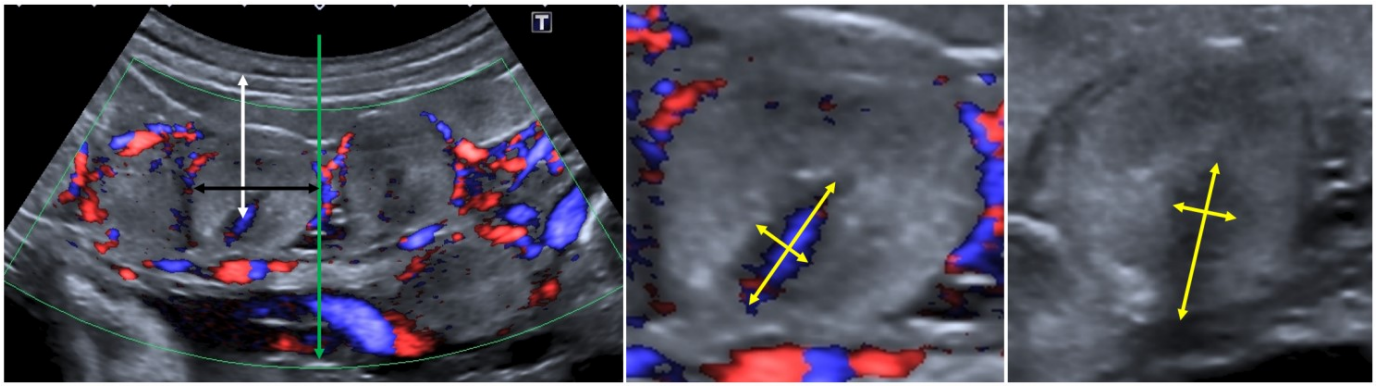

Figure 4.16: Ultrasound information for planning of HIFU exposure series.
The panel on the left shows the same colour flow Doppler image of placentomes and vascular targets as in Figure 4.3. In the left panel, the green arrow shows the direction of sound, along the midline of the image. The black arrow shows the width of the placentome, and the white arrow shows the linear distance between the surface of the uterus to the centre of the targeted vessel, parallel to the direction of sound (the linear target depth). The central panel shows the maximum height and width of the colour flow Doppler signal of the targeted vessels. The right hand panel shows the equivalent maximum height and width of the echolucent area of the placentome in B-mode imaging (where the colour flow Doppler signal had previously been seen). Images obtained using a 1.9 – 6.0 MHz convex sector array, (PVT-375BT, i700, Toshiba Medical Systems UK). Sheep: BL11, 109 d gestational age.

The cross-sectional area of tissue exposed to HIFU energy in an exposure series was also hard to assess accurately. As a crude measure, the known length of movement of the gantry arm orthogonal to the direction of sound, and the size of the HIFU focus were used to estimate the cross-sectional area of the blue outline, using the formula below (Figure 4.17):

Cross sectional HIFU treatment area = (length of HIFU focal zone x orthogonal gantry movement) + π(length of HIFU focal zone/2)(width of HIFU focal zone/2)

As the length of the HIFU focus in the direction of sound is known to be 8.9 mm, and the width of the focus is 1.2 mm, this can be simplified as:

HIFU treatment area (mm^2) = (8.9 x orthogonal gantry movement) + 8.4

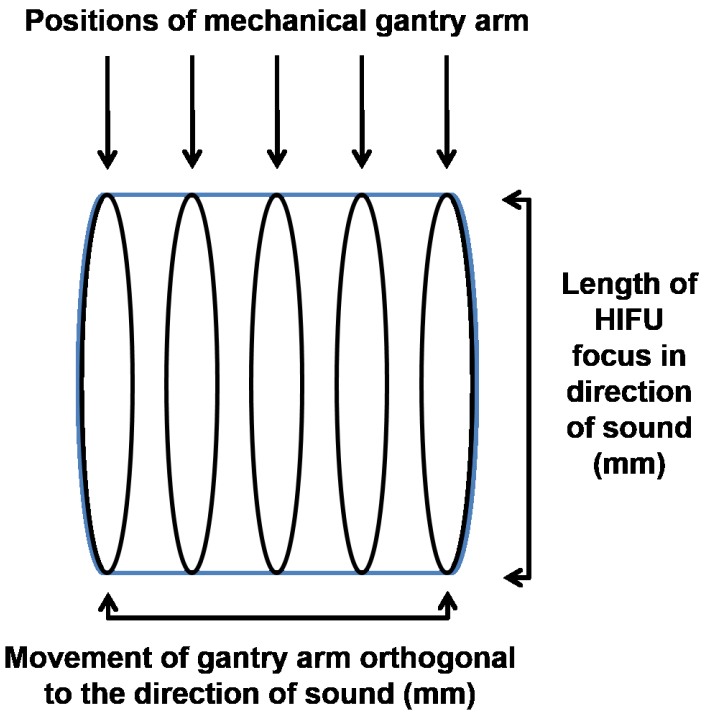

Figure 4.17: Estimation of HIFU treatment area.
The diagram shows the basis of the formula used to estimate the area of tissue exposed to HIFU. The ovals (each scaled to 1.2 x 8.9 mm) represent the position of the HIFU focus in an exposure series of 5 HIFU exposures, 2 mm spaced. The area calculated by the formula *8.9 x orthogonal gantry movement + 8.4* is outlined in blue.

These approximations of the cross-sectional area of (i) the region to be treated and (ii) the area exposed to HIFU were created for this project.

When the HIFU treatment area is divided by the echolucent area:

- a ratio = 1 would indicate they were of the same 2D size;
- a ratio > 1 would indicate the HIFU treatment area was bigger than the target area, a potential spatial over treatment;
- a ratio < 1 would suggest the treatment area was smaller than the target area, a potential spatial under-treatment.

This ratio of echolucent cross sectional area to HIFU treatment cross sectional area is henceforth referred to as the "cross-sectional treatment area ratio" or C-STAR for brevity.

In these animals, the suggested morphology of the placentome was also considered (Figure 4.18). Type A/B placentomes were selected in preference to type C/D placentomes based on ultrasound appearances, as the inverted shape of type A/B placentomes provided a discrete target based on colour Doppler. It was also hypothesised that the position of vessels running through a narrow tissue passage before emerging into the allantoic membranes would assist to hold vessels in a fixed position and provide a better mimic of vascular anastomoses in human

placentae, which are predominantly fixed in tissue, not free to move in the chorio-amniotic membranes.

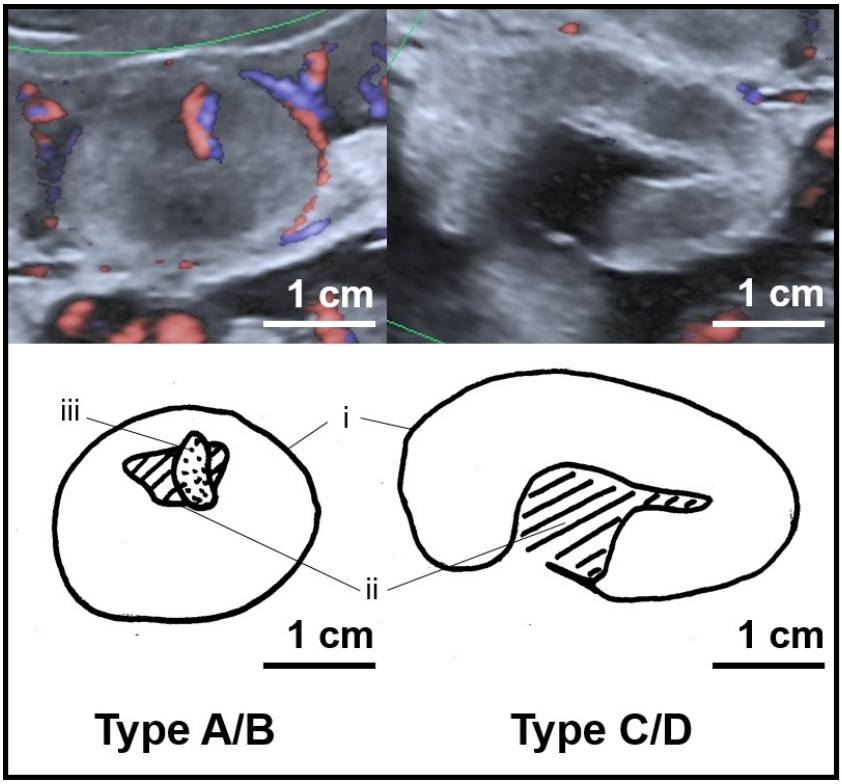

Figure 4.18: Placentome morphology (ultrasound appearances).
The colour flow Doppler ultrasound image shows a placentome and target vessels, which on the upper left panel appears to be type A or B, and on the upper right panel appears to be type C or D. The corresponding line diagrams beneath indicates the position of (i) the border of the placentome, (ii) the border of the echo lucent area and (iii) the colour flow Doppler signal indicating the position of target vessels (only seen in the type A/B placentome). Images obtained using a 1.9 – 6.0 MHz convex sector array, (PVT-375BT, i700, Toshiba Medical Systems UK). Sheep: BL11, 109 d gestational age.

4.3.1.4 **Assessment of treatment success**

Primary confirmation: comparison of pre- and post-HIFU exposure colour flow Doppler imaging for evidence of “no flow” or “residual flow” as described in section 4.2.1.4.

Secondary confirmation: histological examination of exposed placentomes for evidence of occlusion within vessel lumen as described in section 4.2.1.4. In addition, 6 placentomes per animal (n=6) were collected at the post mortem examination of sham exposed control animals and examined histologically for comparison. Vessel diameters were not corrected for shrinkage as heat fixed tissue is known to shrink by a lesser degree than undamaged vessels.

4.3.1.5 **Treatment monitoring**

Real-time tissue responses during HIFU exposures monitored with B-mode imaging, aiming to identify areas of hyperecho. These were logged in the experimental record.

A new safety feature was introduced to the treatment monitoring protocol in this phase of the study. Ultrasound imaging was checked before the start of each HIFU exposure series for the presence of the fetus in the post-focal region. The depth of the ultrasound image was increased to maximum to perform this check, before being decreased again to improve the quality of the imaging of the vascular target.

Three second video clips (8-10 Hz, ~30 frames) of each HIFU exposure in a series were recorded for offline analysis. Analysis of images, the records of exposures generated by the GUI and maternal respiratory rate from the capnography were as described in section 4.2.1.5. In addition, video clips were assessed for the appearance of hyperecho during HIFU exposures.

4.3.1.6 **Management of treatment failure**

If colour flow Doppler imaging demonstrated preserved blood flow after a HIFU exposure series then this was termed a failed occlusion. At the outset of this phase of the study, it was unclear if retreatment would be safe and/or beneficial, so a decision was made to place limits on retreatments.

After a HIFU exposure series resulting in a failed occlusion, a single retreatment could be attempted, unless as a result of the previous exposure series: (i) there was evidence of a uterine burn; (ii) there was suspicion of fetal or other maternal injury; (iii) there was an identified targeting and/or technical error which could not be corrected.

If retreatment was not contraindicated, one further HIFU exposure series was re-planned and delivered to attempt to achieve successful vascular occlusion. If successful vascular occlusion was not achieved after a maximum of two HIFU exposure series, no further attempts to achieve vascular occlusion were made.

4.3.1.7 **Assessment of iatrogenic harm**

The HIFU transducer was lifted after each completed exposure series to examine the surface of the uterus for evidence of burns through the waterbag. If found, the area was photographed at the time of discovery, through the waterbag.

A systematic inspection of tissues was performed at post mortem examination and a photographic record was compiled of damage to: (i) anterior and posterior surface of the uterus, (ii) fetal skin (dorsal, ventral, left and right lateral views), and (iii) maternal bladder and bowel. Tissue listed with visual changes suggestive of iatrogenic damage were also collected for histological examination, fixed in formalin and stained with H&E as described above.

4.3.2 Results

4.3.2.1 **Efficacy of vascular occlusion: time-limited protocol**

HIFU mediated vascular occlusion was attempted in 30 placental vessels during the time-limited experimental protocol. The mean depth of the vascular target beneath the uterine surface was 13.4 mm (SD ± 3.9 mm). The range of estimated in situ intensities delivered to the target tissue was 4.0 – 5.7 $kW.cm^{-2}$. The median number of exposures to complete a series was 5.5 (range 4 – 10); the median duration of the mechanical ventilation pause was 52 s (range 40 – 96 s) and the median time require to perform an exposure series and confirm occlusion or failure was 102.5 s (range 70 – 483 s).

Using the standardised transuterine protocol in which exposure conditions did not vary (although vessel characteristics did), 28/30 vessels were successfully occluded (93%) based on comparison of pre- and post-exposure colour flow Doppler imaging, with 27/30 occluded in a single exposure series. There were two retreatments attempted in the three un-occluded vessels, one of which resulted in successful occlusion, giving a total of 32 exposure series. Hyperecho following two or more successive exposures was associated with successful occlusion in 28/28 exposure series and was only seen in 1/4 unsuccessful exposure series.

Histological evidence of erythrocytes trapped within the vessel lumen, suggestive of clot was found in 24/28 placentomes where occlusion was indicated by “no flow” on post exposure colour flow Doppler imaging. In 4/28 where occlusion was indicated by “no flow” post HIFU exposures, the tissue was either too friable to allow sectioning or there were no vessels visible in the only sections which could be obtained. Again, this difficulty in obtaining adequate sections for

histological examination was likely related to the degree of damage and tissue destruction within the placental tissues. In the two placentomes where colour flow Doppler predicted occlusion had failed, there was no histological evidence of trapped erythrocytes. There was again complete correlation between the colour flow Doppler and histological findings of vascular occlusion.

There was no evidence of trapped erythrocytes in the vessels of sham exposed placentomes (n = 36/36).

The mean vessel diameter measured histologically in vessels where occlusion had occurred (not corrected for shrinkage) was 1.2 mm (range 0.4 – 2.4 mm).

A comparison of vessel characteristics and in situ intensities of successful and failed occlusions – based on first HIFU exposure series of a vascular target only, using colour flow Doppler comparisons as the measure of successful occlusion – is made in Table 4.3:

	Successful occlusions	Failed occlusions
Vessel characteristics		
Number	27	3
Depth of vascular target (mm)	13 ± 4	16 ± 3
Echolucent area (mm^2)	30 ± 20	40 ± 10
Diameter (mm)	1.2 ± 0.5	1.9 ± 0.6
Exposure characteristics		
In situ intensity ($kW.cm^{-2}$)	5.2 (4.0 - 5.4)	5.0 (4.5 - 5.3)
Number of exposures in series	4 - 7	5 - 6
HIFU treatment area (mm^2)	90 ± 30	20 ± 10
C-STAR	5.3 ± 3.8	0.5 ± 0.2

Table 4.3: Group A vessel and exposure characteristics (time-limited transuterine protocol).
The table shows the characteristics of vessels and HIFU exposure series, divided by those which resulted in successful or failed occlusion based on comparison of pre- and post-HIFU colour flow Doppler imaging. The depth of the vascular target, the echolucent and HIFU treatment areas, the C-STAR, and the diameter of vessels are given as the mean ± SD; estimated in situ intensity is quoted as the median, with the full range given in brackets.

There was no difference in the depth, diameter or echolucent area of the vascular targets in which HIFU exposures resulted in a successful or failed occlusion. Similarly, there was overlap in the range of in situ intensities or numbers of exposure delivered to target vessels which

resulted in successful or failed occlusion. However, when the HIFU treatment areas were compared there was a potential difference. In two of these failed occlusions, the gantry arm did not perform the planned movement due to a technical error; in the third target, the only direction of movement planned was in the z axis. Both these circumstances greatly increased the overlap of the HIFU exposures in a series and decreased the area of the placentome that was exposed to HIFU energy. This appeared to contribute to failure of the exposure series to produce occlusion. In agreement with this, the C-STAR in failed occlusions was lower than in successful occlusions (t-test, $p < 0.001$).

4.3.2.2 **Efficacy of vascular occlusion: dose de-escalation protocol.**

In the dose de-escalation study, a further 12 vascular targets were exposed to HIFU, and 9/12 (75%) were occluded. Eight vessels were occluded in a single exposure series; the ninth was occluded after a retreatment. In 2/3 un-occluded vessels, a retreatment was attempted, but this also failed to produce occlusion.

In these placentomes, histological examination was possible in all 12 exposed placentomes. Secondary confirmation of occlusion was obtained histologically (trapped erythrocytes seen within vessels) in all 9 vessels where occlusion was identified by colour flow Doppler. There were no trapped erythrocytes seen within vessel lumen in the 3/12 vessels where colour flow Doppler had shown residual flow post-HIFU exposures.

When vessel characteristics and estimated in situ intensities of successful and failed occlusions – based again on first HIFU exposure series only – are compared for these placentomes, there are no clear differences between groups (Table 4.4).

There was, again, no differences in depth, diameter or echolucent area of the vascular targets between successful and failed occlusions. The range of estimated in situ intensities was overlapping between successful and failed occlusion. It was possible to achieve occlusion with estimated in situ intensities as low as 2.4 $kW.cm^{-2}$, although occlusions at higher intensities also failed. One exposure series which failed to produce occlusion delivered 5.2 $kW.cm^{-2}$ estimated in situ intensity to the target tissue, but only 3 exposures were used: The C-STAR was 1.0 in this placentome. Otherwise there were no targeting or technical errors identified in these HIFU exposure series.

	Successful occlusions	Failed occlusions
Vessel characteristics		
Number	8	4
Depth of vascular target (mm)	11 ± 2	8 ± 3
Echolucent area (mm^2)	0.2 ± 0.1	0.3 ± 0.1
Diameter (mm)	0.9 ± 0.3	1.6 ± 0.7
Exposure characteristics		
In situ intensity ($kW.cm^{-2}$)	4.1 (2.4 - 5.5)	3.0 (2.2 - 5.2)
Number of exposures in series	5 - 6	3 - 6
HIFU treatment area (mm^2)	0.8 ± 0.2	0.7 ± 0.2
HIFU : echolucent areas ratio	4.6 ± 1.8	3.7 ± 2.2

Table 4.4: Group A vessel and exposure characteristics (dose de-escalation transuterine protocol).
The table shows the characteristics of vessels and HIFU exposure series in the pilot study, divided by those which resulted in successful or failed occlusion. The depth of the vascular target, echolucent and HIFU treatment areas, C-STAR, and diameter of vessels are given as the mean ± SD; estimated in situ intensity is quoted as the median, with the full range given in brackets.

4.3.2.3 **Iatrogenic harm: time limited and dose de-escalation transuterine protocols**

There was a single instance of vessel haemorrhage in the 42 vascular targets exposed to HIFU in the time-limited and dose de-escalation protocols used in these animals (1/42, 2%). This occurred in a placentome in which there was a technical error with the movement of the gantry arm and 4 of 5 HIFU exposures in the series were delivered into the same 3D position. There was evidence of extensive bleeding into the allantoic membranes surrounding this placentome at the time of post mortem examination and fetal anaemia preceding post-mortem examination.

Excessive placental soft tissue damage was noted in 23/38 placentomes which could be examined histologically (26 from the time-limited group, 12 from the dose de-escalation group). Again, estimated in situ intensity appeared to be the main determinant of the amount of tissue damage that occurred (Table 4.5). This comparison indicates the upper threshold for this type of damage to occur is an estimated in situ intensity of 5.1 – 5.2 $kW.cm^{-2}$ delivered to the placental tissue.

	Excessive tissue damage	No excessive tissue damage
Vessel characteristics		
Number	23	15
Depth of vascular target (mm)	12 ± 3	11 ± 5
Successfully occluded	22	14
Exposure characteristics		
In situ intensity ($kW.cm^{-2}$)	5.4 (5.2 - 5.7)	4.1 (2.2 - 5.1)
Number of exposures in series	3 - 7	4 - 7

Table 4.5: Excessive tissue damage (Group A).
The table shows the characteristics of vessels and HIFU exposure series, divided by those with and without excessive tissue damage to the placentome soft tissue. The depth of the vascular target is given as the mean ± SD; estimated in situ intensity is given as median and full range. The exposure characteristics of the 4/42 placentomes which could not be examined histologically are excluded from this table.

There was a single maternal uterine burn associated with an exposure series which resulted in excessive tissue damage (drive voltage -5 dBm, in situ intensity 5.5 $kW.cm^{-2}$, 5 exposures, 10 mm target depth). There were no fetal burns.

4.3.3 Transuterine efficacy and safety study: discussion

In these animals, by using a standardised protocol, we were able to demonstrate that it was possible to achieve a consistently high rate (93%) of transuterine HIFU placental vascular occlusion in sheep, in vessels with clinically relevant diameters. This suggested that the treatment protocol which had been selected due to the fact it was able to deliver treatment quickly was also an effective method of achieving vascular occlusion. This spacing and timing of HIFU exposures within a series was therefore adopted for subsequent animal groups, although some modification to energy levels and the spatial pattern of exposures was required.

Estimation of the in situ intensities delivered to the target vessels suggested that high amounts of acoustic energy were being delivered to the tissues, even compared to published studies of vascular applications of HIFU (Table 1.3). The presence of hyperecho linked to successful occlusions suggests that tissue heating was occurring, and that accumulation of thermal energy is an important feature of achieving occlusion.

Histologically, while there was evidence of occlusive clot within vessel lumen, there was no evidence of vessel wall fusion seen. Similarly, there was no evidence of vessel wall oedema,

collagen shrinkage (although no specific collagen stains were performed), and the endothelium of vessels was not examined. Therefore, while it appeared that vascular occlusion had been achieved, this had not occurred via the integrated mechanism suggested in Figure 1.3. Therefore, there remained the possibility that the vascular occlusion produced by occlusive clot would be a transient effect, and that the vessels could recanalise over time if the lumen was not fused closed. As animals were euthanised within 4 hours of HIFU exposures, no further comment regarding this can be made based on the current evidence.

This possibility needs to be balanced against the findings of excessive tissue damage to placental tissue (which has an important synthetic function) which occurred at the same time as HIFU exposures of placental vasculature. However, when the highest and lowest in situ intensities at which occlusion was achieved in this group are compared, there is just over a two-fold difference (Table 4.4). While this underlines the potential overexposures of tissue which may have occurred, and that this may have been the reason for the high efficacy of occlusion, it also indicates that a lower, safer estimated in situ intensity can also produce vascular occlusion in this animal model. These findings from the dose-delivery study, however, justify further investigation. These results also suggest that even with the additional attenuation of overlying maternal skin, fat and rectus sheath, adequate HIFU energy can be delivered into the intrauterine space. This has been demonstrated using different HIFU systems in humans and baboons, without maternal or fetal iatrogenic damage (43, 285, 286). The next phase of the study is planned to be transdermal, and the additional attenuation provided by the maternal skin and rectus sheath should reduce the estimated in situ intensity below the 5.0 $kW.cm^{-2}$ threshold suggested to prevent excessive tissue damage, even when using the maximum drive voltage.

Despite its efficacy, the standard transuterine protocol used did not achieve occlusion in every target, the integration of colour flow Doppler imaging with the therapeutic ultrasound source meant it was possible to identify failed occlusion in real-time and plan for immediate retreatment. In Group A animals, retreatment was attempted in 4 vascular targets, 2 of which were successfully occluded as a result. Retreatment was not associated with evidence of uterine or fetal burns, or risk of haemorrhage. Given the rate of excessive tissue damage, it was not possible here to assess the impact of retreatment on excessive tissue damage. Residual anastomoses are identified in 15-30% of cases following fetoscopic laser (16) and may lead to recurrent disease with a worse overall prognosis (16) or a threefold greater incidence of TAPS (17). Hence, a method to identify residual anastomoses and provide a retreatment is an important feature of any HIFU treatment protocol developed. Currently, residual anastomoses are only identified after completion of fetoscopic laser procedures, and further treatment to

coagulate them may be contraindicated. Technique changes in fetoscopic laser designed to overcome this limitation, namely a move from selective coagulation of visualised placental anastomoses to the Solomon technique in which the entire "vascular equator" is coagulated, have reduced recurrent TTTS and TAPS rates without improving perinatal survival or decreasing procedure-related complications (19).

A low C-STAR was also possibly associated with a risk of vascular haemorrhage. Based on previously published studies, vascular occlusion typically requires higher levels of HIFU energy compared to ablation of soft tissues (1) and this carries with it potential complications of vessel rupture and haemorrhage, attributed to rapid changes in tissue pressure (31, 32, 37) or accumulation of excessive thermal energy in the vessel wall (38, 45, 55). Haemorrhage had occurred in the pilot study in association with gross over-exposure (both in terms of estimated in situ intensity and C-STAR) of the tissues and vessels. However, in Group A, both estimated in situ intensity and the number of HIFU exposures had been reduced by the use of -5 dBm drive voltage and moving to the "limited" exposure pattern, 2 mm spaced. Despite this, there was still an instance of vessel haemorrhage in the group A animals.

This haemorrhage was associated with unintentional non-movement of the mechanical gantry arm due to a software error. In the pilot study, "limited" exposure series were designed to have 1-2 HIFU exposures in the soft tissue surrounding the echo-lucent area containing vessels. This was not done in Group A animals, resulting in a number of exposure series where the C-STAR < 1, a spatial undertreatment, despite the estimated in situ intensity remaining high. This was the only feature which was found to contribute to failed occlusions in this animal group. Based on this fining, the restriction of placing the first and last HIFU exposure in placental tissue was reintroduced for subsequent animal groups. This may be of benefit by inducing heating in the soft tissues surrounding the target vessel. This could reduce the diameter of the vessel lumen be either inducing collagen shrinkage in connective tissues, or external compression of the vessel as a result of tissue oedema, however no histological evidence of either was seen.

4.4 Transdermal bridging study

In this third phase of the study, we sought to investigate if HIFU could be used non-invasively to occlude placental vasculature, by applying it through intact maternal skin, incorporating and extending the treatment protocols used in Group A animals.

In the pilot study, 3 HIFU exposure series had been attempted in one animal through intact maternal skin: difficulties were encountered in targeting and occluding placental blood vessels, with only a 33% successful occlusion rate and a fetal burn. Additionally, the time required to plan and deliver each HIFU exposure series was over an hour. However, the transuterine study had provided experience in targeting and occluding placental blood vessels, and the HIFU treatment protocol used had been streamlined since the pilot study, suggesting the possibility that quicker planning and delivery of transdermal occlusions would now be possible.

Therefore, once again it was necessary to assess:

(i) If it was feasible to use colour flow Doppler integrated with the therapeutic transducer and suspended in a waterbag to identify, target and confirm post-exposure outcome through intact maternal skin.

(ii) If sufficient HIFU energy could be delivered into the intrauterine space to result in vascular occlusion.

(iii) The rates and types of iatrogenic harm to mother and fetus.

4.4.1 Methods

4.4.1.1 HIFU therapy system

No changes were made to the system described in section 4.2.1.1.

4.4.1.2 Animals and surgical methods

Two pregnant ewes carrying singleton fetuses at 115 d gestational age were placed under general anaesthesia (sections 3.2.1, 3.2.2). No invasive surgical procedures were performed, and maternal abdominal skin remained intact.

The maternal abdominal skin was prepared first by shaving with clippers to remove wool, then washed with iodine scrub solution (Vetasept: 7.5% povidone iodine, Animalcare Ltd., York, UK) to remove dirt and lanolin, and washed again with plain water. The remaining hair was chemically depilated (Nair ® hair removal cream, Church & Dwight Co., Kent, UK) and the skin was washed for a final time with plain water, then wet with degassed water. The waterbag was placed in contact with the maternal skin and trapped air between the plastic and the skin was smoothed out. If the waterbag was repositioned, the layer of degassed water on the skin was replaced, and air pockets were smoothed out again.

Breath holds were performed during each HIFU exposure series (section 4.2.1.2).

All fetuses were assessed with ultrasound at the planned end of the HIFU exposures to determine presence or absence of fetal heart pulsations. Non-invasive maternal recording of maternal heart rate was used to confirm maternal survival to the planned end of the experimental procedure.

On completion of the HIFU exposures the ewe and fetus were euthanised without recovery from general anaesthesia under schedule one of the UK Animals (Scientific Procedures) Act 1986, as per section 4.2.1.2.

4.4.1.3 **Vascular targets and HIFU treatment protocol**

HIFU was applied trans-dermally to occlude 4-5 vessels per animal (5 per animal, n=1; 4 per animal, n=1).

HIFU exposure series were based on the transuterine time-limited protocol from Group A, but allowed for a reduction in drive voltage in order to avoid delivering in situ intensities > 5.0 $kW.cm^{-2}$: drive voltage -5 to -6 dBm, 5 s exposure duration, 5 s intervals between exposures, 2 mm spacing between exposures, placement of exposure following the “limited” pattern.

The C-STAR was planned to be > 1 in all cases, based on the results shown in Table 4.3, and the possible associated risk of haemorrhage. This required that all exposure series were planned to start and finish in placental soft tissue bordering the echo lucent area from which vessels arise. The movement of the mechanical gantry arms was restricted to axes orthogonal to the direction of sound (i.e. x or y only) as the GUI software could not reliably support movement in 2 or more axes, and this restriction would reduce the risk of technical error. As in the Group A study, HIFU exposure series were not planned in vascular targets where the fetus was seen in the post focal region.

4.4.1.4 **Assessment of treatment success**

Primary confirmation: comparison of pre- and post-HIFU exposure colour flow Doppler imaging for evidence of “no flow” or “residual flow” as described in section 4.2.1.4.

Secondary confirmation: histological examination of exposed placentomes for evidence of occlusion within vessel lumen as described in section 4.2.1.4. No control tissues were obtained.

4.4.1.5 **Treatment monitoring**

Tissue responses (real-time): as described in section 4.3.1.5.

Offline analysis of saved imaging: as described in section 4.3.1.5.

Identification of fetal position relative to HIFU focus: as described in section 4.3.1.5.

4.4.1.6 **Management of treatment failure**

There were no failed occlusions in this phase of the study.

4.4.1.7 **Assessment of iatrogenic harm**

To monitor for maternal skin burns the maternal abdominal skin was photographed before the start of HIFU exposure series and at the end of all HIFU exposure series without the waterbag in situ. These images were compared offline to examine for the appearance of additional skin trauma between the beginning and the end of the HIFU exposure series, as in some cases clipping and chemical depilation had caused prior superficial skin trauma. Between HIFU exposure series the maternal skin was examined and photographed through the waterbag. Changes in maternal skin colouration suggestive of erythema or burns and their location were recorded real time in the experimental record and photographed. These areas were examined again at the end of all HIFU exposure series to determine if they had faded (erythema) or were still present (burns)

A systematic inspection of tissues was performed at post mortem examination and a photographic record was compiled of damage to: (i) maternal skin, (ii) maternal rectus sheath, (iii) anterior and posterior surface of the uterus, (iv) fetal skin (dorsal, ventral, left and right lateral views), and (iv) maternal bladder and bowel. Areas of maternal and fetal skin, rectus and uterus with visual changes suggestive of iatrogenic damage were also collected for histological examination, fixed in formalin, sectioned and stained with H&E as described previously.

4.4.2 Results

4.4.2.1 **Feasibility of placental vascular occlusion**

Overall, in this transdermal bridging study, 9 placental vessels were targeted with colour Doppler. Based on a comparison of pre- and post-HIFU exposure colour flow Doppler imaging, all 9 of 9 targeted vessels were successfully occluded. Hyperecho was seen in the placental tissue surrounding of all 9 of the targeted vessels. Both mothers and fetuses survived to the end of the planned HIFU exposure series.

Estimated in situ intensities of 3.0 – 3.9 $kW.cm^{-2}$ were delivered to the target tissue, using between 5 and 7 exposures in a series. The reduction in drive voltage from -5 to -6 dBm made no difference to the success rates of occlusion, although numbers are too small to draw a definitive conclusion. The mean distance of the target vessel beneath the surface of the maternal skin was 17.5 mm (SD ± 6.6 mm). All planned exposure series were successfully completed moving in the y axis alone, without the need to correct for angulation of tissue by moving in the z axis.

The median time to complete a treatment was 101 s (range 71 – 141 s) which was comparable to the median time in the transuterine study, with a median breath-hold duration of 56 s (range 48 – 64 s). However, treatment planning time was extended, such that for the first animal it took 3 hours to plan and occlude 5 vessels; in the second animal it took 1 hour 10 minutes to plan and occlude 4 vessels.

Retained erythrocytes within vessel lumen, suggestive of occlusive clot, were identified histologically on H&E stain in all 9 placentomes examined. Once again, the occluded vessels were of clinically relevant dimensions: 0.8 – 2.9 mm. As in previous phases of the study, the colour flow Doppler finding of “no flow” correlated completely with the histological findings of occluded vessels. There was no evidence of tissue boiling or discrete clots within any of these

9 placentomes histologically (markers of excessive placental soft tissue damage) although heat fixation and extravasation were still noted.

There were no instances of vascular haemorrhage, nor were there any uterine of fetal burns noted. There were 4 maternal skin burns recorded, all in the second animal exposed to HIFU; in the first animal there were no maternal skin burns. There was also skin irritation in both animals evident following shaving and chemical depilation of the skin (Figure 4.19). This was a new finding, as previous animals had only been shaved, except for the one animal in the pilot study, which had also been shaved and chemically depilated, but this skin reaction had not been noted.

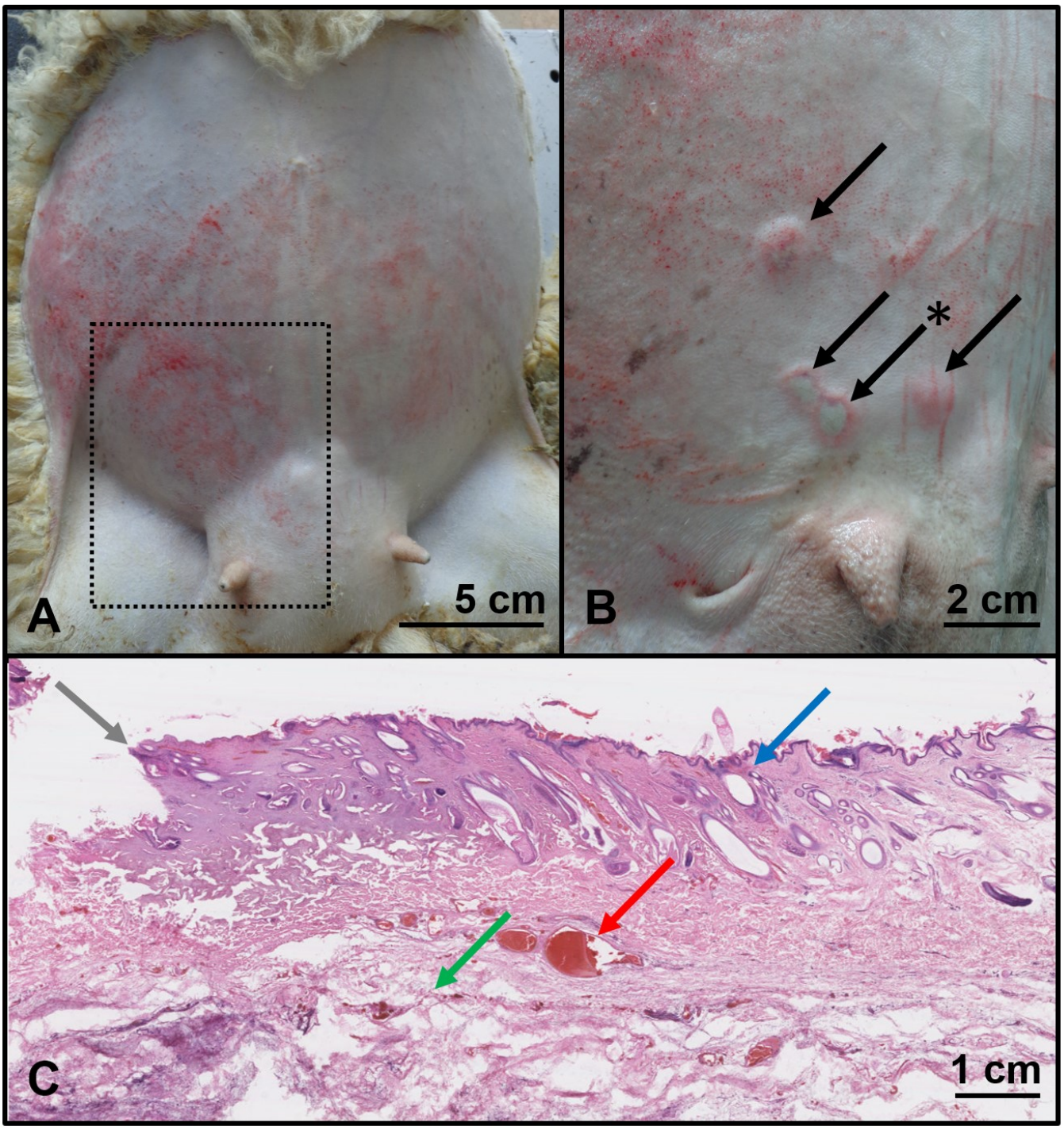

Figure 4.19: Maternal skin burns (transdermal bridging study).
(A) The image shows the condition of the maternal skin following shaving and chemical depilation before any HIFU exposures were made. The skin appears to show irritation. The black dotted rectangle is the region enlarged in (B) showing the condition of maternal skin following HIFU exposures. The areas of burns are indicated with black arrows, and skin irritation can still be seen additional to these areas of burns. The black arrow marked with an asterisk shows the burn presented in (C) as a H&E stained section of a full thickness maternal skin burn. The blue arrow shows normal epidermis, the grey arrow shows burned epidermal cells. The red arrow shows a clot within the subdermal tissue and the green arrow shows the border with the connective tissue, which is not disordered.

4.4.3 Transdermal bridging study: discussion

This transdermal bridging study showed that it was still possible to maintain a consistently high occlusion rate for placental vasculature when HIFU was applied through intact maternal skin. This agrees with the findings of other studies (43, 285, 286) which demonstrate that it is possible to deliver sufficient transdermal energy into the intrauterine space to perform soft tissue ablation. However, these experiments were the first to indicate that sufficient energy for selective vascular occlusion could also be delivered into the intrauterine space. This was possible even with the additional attenuation of the maternal skin and rectus sheath.

The lower range of estimated in situ intensities delivered to the tissues in these animals compared to Group A shows that the high rate of vascular occlusion in Group A was unlikely to be due to overexposure. These experiments showed that lower levels of in situ intensity could be consistently successful in occluding placental vasculature, confirming the findings from the additional exposures in the dose de-escalation transuterine study (Table 4.4).

The HIFU treatment protocol had been modified in this study to include additional safety features. These did not appear to reduce efficacy, but avoided the incidence of vessel or tissue haemorrhage or excessive tissue damage, although number of exposure series on which to base this comment remained small. Given that all the estimated in situ intensities fell beneath the 5.0 $kW.cm^{-2}$ upper threshold instituted following the Group A transuterine study, this was an expected, but also a useful confirmation.

These animals also showed that it was still possible to use colour flow Doppler to identify, target and confirm successful occlusion of placental blood vessels through skin, although the process was slower than in the transuterine studies. It was also possible to identify hyperecho during HIFU exposures through intact maternal skin, at greater treatment depths.

These two animals also demonstrated the possibility of maternal skin burns, although from the data it was difficult to draw any supported conclusions. In one of the animals there were maternal abdominal skin burns as a result of each HIFU exposure series; in the other animal there were none. With such a small sample, the significance of this was hard to interpret.

The animal without burns had a lower maternal weight – 32 kg – compared to the animal with burns – 54 kg – suggesting the could be an influence of subcutaneous maternal fat, potentially in propagating thermal spread from the target vessel to the skin. However, in the case or either pre-focal heating or thermal spread, there would have been damage to the uterus, fat and

rectus sheath in the path between the burn and the vascular target, none of which was observed.

Both animals were shaved and washed with iodine scrub 5-10 min before being chemically depilated with the same agent (Nair). In the second animal, the depilatory cream was washed off with water and liquid soap before being washed again with water; in the first animal only water was used. In the second animal, we had not recorded whether there was degassed water and/or removal or pockets of air between the abdominal skin and the waterbag, suggesting the protocol had not been followed. This non-adherence to protocol was a potential cause of skin burns. Interestingly, each of the burns was also associated with a successful vascular occlusion. Had the burn been the result of poor acoustic coupling between the skin and the waterbag and the resultant deposition of acoustic energy onto the skin, the transmission of sufficient acoustic energy to occlude the vascular target would have been unlikely. This reduced the likelihood that the presence of liquid soap, air pockets or the absence of degassed water was a major contributory factor to the burns, as their main action would have been to reduce the quality of the acoustic coupling between skin and waterbag. The temperature of the water in the waterbag and the oxygen content of the degassed water were not measured during the HIFU exposures, so cannot be commented on. For these reasons, the rate of maternal burns could only be quoted as 0 – 100%, with unclear evidence as to what the contributory factors were at this stage.

However, as there were no fetal or uterine burns, no evidence of haemorrhage or excess tissue damage, a decision was made to proceed into recovery studies. Maternal skin burns are a known side effect of HIFU treatments, and as such were described as a potential adverse effect in the study plan approved under the UK Animals (Scientific Procedures) Act 1986 and the Ethical Review Committee of the University of Cambridge. Hence, the occurrence of maternal skin burns was unlikely to present a sufficient welfare issue that animals would need to be culled for humane reasons before the end of the planned follow-up. Additionally, further investigation of the exposure conditions and contributory factors which promoted the occurrence of maternal skin burns would be useful information should the technique ultimately be translated into human use.

4.5 **Transdermal survival study: Group S(urvival)**

Based on the transdermal bridging study, we had an indication that it was possible use HIFU through intact maternal skin to occlude placental vasculature, and that the protocol adapted from the transuterine study appeared effective.

However, while fetal survival under general anaesthesia, with and without surgical procedures, to the end of planned HIFU exposures was established, fetal survival and rates of obstetric complications beyond reversal of anaesthesia remained unknown. It remained unknown what the effect of an unrecognised uterine burn or placental vascular haemorrhage (as the maternal skin would remain intact during the treatments) could be on the progress of the pregnancy. At this stage our lack of familiarity with the transdermal protocol, particularly targeting, rendered it too slow to be integrated with the planned recovery studies in chronically instrumented maternal and fetal sheep preparations designed to assess this (Figure 3.12).

In addition, while maternal recovery following reversal of anaesthesia was anticipated, and post-mortem examination in previous non-recovery animals suggested no significant maternal injury had occurred to bladder, bowel, major blood vessels in the maternal abdomen or pelvis, there had been no opportunity to make a functional assessment of this, as all previous ewes had been euthanised while under general anaesthesia. Maternal skin burns were anticipated, but the rate and the severity of these was also uncertain, as were ways to prevent them.

Therefore, this phase of the study sought to:

(i) demonstrate longer term fetal survival following HIFU exposures of placental vasculature without any additional surgical procedures;
(ii) establish if HIFU could be used as a method to consistently occlude placental blood vessels (transdermal)
(iii) assess the rates and types of maternal and fetal iatrogenic harm, and identify procedural modifications or safety limits that could prevent harm;
(iv) reduce the total HIFU treatment time sufficiently to allow the planned recovery studies in chronically instrumented sheep to proceed.

4.5.1 Methods

These animals (n=6) were the first in which were recovered from anaesthesia following HIFU exposures of placental vasculature. To assess the quality of fetal recovery, they were paired

with sham-exposed animals (n=6) who underwent general anaesthesia, but were not exposed to HIFU. Utero-placental function, fetal survival and growth, cardiovascular function and initiation of cardiovascular defence mechanisms were measured with non-invasive ultrasound and materno-fetal Doppler studies before, during and after HIFU exposures (section 3.6). These results will be reported and discussed separately in chapters 5-8. These 12 animals will be referred to as 'Group S'.

4.5.1.1 **HIFU therapy system**

The system described in section 4.2.1.1 was used. However, after 3 animals, the protocol for degassing the water in the water bag was changed and a new provision to cool the water was introduced.

In the first 3 of 6 animals in this group, the water in the water bag was taken cold from the tap and not cooled further; it was degassed before the start of HIFU exposures and only again if cavitation was seen in the water on ultrasound during exposures. In the last 3 of 6 animals in this group the water in the water bag was cooled with ice sealed in plastic (so the melting ice water did not mix with degassed water in the bag) and was degassed before each HIFU exposure series. The water was cooled to between 19.7 – 26.3^{o}C and degassed to contain dissolved oxygen between 0.8 – 2.8 mg.l^{-1} in these exposure series.

4.5.1.2 **Animals and surgical methods**

Six pregnant ewes carrying singleton fetuses at 115 ± 10 d gestational age were placed under general anaesthesia (sections 3.2.1, 3.2.2). No invasive surgical procedures were performed, and maternal abdominal skin remained intact.

The maternal abdominal skin was shaved, washed and chemically depilated as described in section 4.4.1.2, with the exception that a different chemical depilatory was used (Veet ® hair removal cream, Reckitt Benckiser, Slough, UK) in an attempt to reduce skin irritation. When this did not work in the first animal, the interval between shaving and chemical depilation was changed from 5 – 10 min in the first of the 6 animals, to 24 – 48 h in the remaining 5 of 6 ewes. Following depilation, the skin was washed for a final time with plain water and wet with degassed water. The waterbag was placed in contact with the maternal skin and trapped air between the plastic and the skin was smoothed out. If the waterbag was repositioned, the layer of degassed water on the skin was replaced, and air pockets were smoothed out again.

Breath holds were performed during each HIFU exposure series (section 4.2.1.2).

Following completion of planned HIFU exposure series, animals were recovered from anaesthesia and monitored for 21 days. Animals were checked daily for signs of maternal pain or distress, infection or poor healing of skin burns, problems with mobility, bladder or bowel function, preterm labour, rupture of membranes or vaginal bleeding. Maternal analgesia (Carprofen 1.4 $mg.kg^{-1}$ S.C., Rimadyl™, Pfizer Ltd., UK) was administered if signs of maternal pain or distress were evident based on behaviour, facial expressions, stance or feeding patterns.

Following recovery, animals were housed in individual pens in an outdoor barn (light and dark cycle dependent on seasonal variation) with ad libitum access to hay, nuts, mineral lick and water. After five days, animals were transferred to communal pens in an outdoor barn with access ad libitum to hay, mineral lick and water; nuts were provided daily.

After the completion of 21 days follow-up, the ewe and fetus were euthanised under schedule one of the UK Animals (Scientific Procedures) Act 1986. A slow intravenous injection into the maternal jugular vein of 120 $mg.kg^{-1}$ pentobarbitone sodium (Pentoject®, Animalcare Ltd., UK) was used for this purpose. Air embolus into the jugular vein was used as a secondary confirmation of death. Maternal cardiac activity was auscultated with a stethoscope and death was confirmed on cessation of cardiac and respiratory activity. Cessation of fetal cardiac activity was confirmed with diagnostic ultrasound.

4.5.1.3 **Vascular targets and HIFU treatment protocol**

HIFU was applied trans-dermally to occlude 4-6 vessels per animal (6 per animal, n=5; 4 per animal, n=1).

HIFU exposure series were based on the protocol used in the transdermal bridging study, but allowed for greater reductions in drive voltage. This was an attempt to reduce the rate of skin burns: drive voltage -5 to -9 dBm, free field intensity 2.5 – 6.7 $kW.cm^{-2}$, 5 s exposure duration, 5 s intervals between exposures, 2 mm spacing between exposures, placement of exposure following the “limited” pattern.

The following safety limits were adopted from the bridging study: (i) all exposure series were planned to start and finish in placental soft tissue bordering the echo lucent area from which vessels arise; (ii) the C-STAR was planned to be >1; (iii) movement of the mechanical gantry arms was restricted to one direction on an axis orthogonal to the direction of sound; and (iv)

predicted in situ intensities above 5.0 $kW.cm^{-2}$ were not planned. As in Group A, vascular targets were not selected if there were fetal parts in the post-focal region, at any distance.

No safety limits on exposure conditions specifically to reduce the rate of maternal skin burns were planned at the outset of this animal group as none had been identified.

4.5.1.4 **Assessment of treatment success**

Primary confirmation: comparison of pre- and post-HIFU exposure colour flow Doppler imaging for evidence of "no flow" or "residual flow" as described in section 4.2.1.4.

Secondary confirmation: as these were survival studies, with 21 days between HIFU exposures and collection of tissue at post-mortem examination, direct secondary confirmation of occlusion for each placentome could not be sought from visual identification and histological examination of damaged tissue. The dye that had previously been used to tag placentomes was not permanent and there was no known safety data regarding intra-uterine use of permanent tissue dyes. Therefore, while it was possible to identify and retrieve placentomes with evidence of HIFU damage at the time of post-mortem, these could not be directly correlated to any specific exposure series performed in that animal. However, given the strong correlation between Doppler and histological findings in previous phases of the study, a finding of the same number of damaged placentomes with histologically occluded vessels as predicted by colour flow Doppler would serve as secondary confirmation of persistent vascular occlusion.

Following euthanasia of ewe and fetus, at post mortem examination, all placentomes were bisected and examined for evidence of tissue damage, weighed and classified by morphological type. In HIFU exposed animals, all placentomes with evidence of tissue damage were retained for histological examination. In addition, 2 placentomes per animal without any evidence of HIFU damage in HIFU exposed animals were retained for histological examination. One placentome was taken from the same region in which the exposed placentomes were found, and the second placentome was taken from a distant region. An additional 6 placentomes, randomly selected, were retained from each sham-exposed animal. Retained placental tissues were fixed, sectioned and stained with H&E as described in section 4.2.1.4, with the exception that histological findings could not be correlated to specific colour Doppler findings.

The 21 day interval between HIFU exposure and tissue collection allowed for the first time allowed the possibility of examining vessels for evidence of persistent vascular occlusion. As the suggested method of occlusion to this point was occlusive clot, in addition to H&E staining,

Phosphotungstic Acid-Haematoxylin (PTAH) staining, which stains organised fibrin, was planned. From each animal in which had been exposed to HIFU the two placentomes which showed the clearest evidence of occluded vascular lumen on H&E staining were selected for PTAH staining; from sham exposed animals one randomly selected placentome was used. All placentomes could not be stained due to financial restrictions on provision of PTAH staining materials. Sections were cleared of paraffin using Histo-clear II and rehydrated through four solutions of decreasing concentrations of ethanol before being washed with distilled water. Slides were incubated in a preheated zinc chloride solution (80-90ºC, Abcam, Cambridge, UK) before being washed in running tap water and rinsed in distilled water. Slides were then immersed in ferric ammonium sulphate aqueous solution (80-90ºC, Abcam, Cambridge, UK) and heated before being washed in running tap water and rinsed in distilled water. Finally, slides were incubated in preheated PTAH stain solution (80-90ºC, Abcam, Cambridge, UK) before being differentiated in 95% reagent alcohol and dehydrated in three changes of absolute ethanol and cleared in two changes of Histo-clear II and one of xylene. Coverslips were mounted with DPX mountant. Slides were examined and the findings were correlated to H&E findings from the same placentome.

4.5.1.5 **Treatment monitoring**

Tissue responses (real-time): as described in section 4.3.1.5.

Offline analysis of saved imaging: as described in section 4.3.1.5.

Identification of fetal position relative to HIFU focus: as described in section 4.3.1.5.

4.5.1.6 **Management of treatment failure**

If colour flow Doppler imaging demonstrated preserved blood flow after a HIFU exposure series (“residual flow”) then this was termed a failed occlusion. Based on the limited data from the transuterine study that retreatment was beneficial and safe, a plan was made to retreat unsuccessful occlusions. After a failed occlusion, retreatment could be planned, unless as a result of the initial exposure series: (i) there was evidence of a maternal skin burn; (ii) there was suspicion of fetal or other maternal injury; (iii) there were targeting or technical errors which could not be overcome at that time.

If retreatment was not contraindicated, one further HIFU exposure series was re-planned and delivered to attempt to achieve successful vascular occlusion. If successful vascular occlusion was not achieved after a maximum of two HIFU exposure series, no further attempts to achieve vascular occlusion were made.

Failed occlusions were classified as targeting or technical errors as described as in section 4.2.1.5. Failed occlusions were also correlated with the presence or absence of maternal skin burns or erythema, and the suspicion of uterine or fetal burns (recorded as burns).

4.5.1.7 **Assessment of iatrogenic harm**

Maternal skin burns: These were monitored intraoperatively as described in section 4.4.1.7. These areas were examined again at the end of all HIFU exposure series and daily thereafter. Any area of skin reddening which resulted from a HIFU exposure series but faded fully within 24 h of exposure was classified as erythema; other areas of damage resulting from HIFU exposure which persisted > 24h were classified as skin burns. These were photographed daily for the first 5 days and then every 5th day to record healing.

A systematic inspection of tissues was performed at post mortem examination and a photographic record was compiled of damage to: (i) maternal skin, (ii) maternal rectus sheath, (iii) anterior and posterior surface of the uterus, (iv) fetal skin (dorsal, ventral, left and right lateral views), and (iv) maternal bladder and bowel. Blood samples were drawn into sterile syringes from the umbilical artery and vein (0.5 ml each). The haemoglobin concentration of the blood was determined using an ABL80 Flex analyser (Radiometer, Denmark). Areas of maternal and fetal skin, rectus and uterus with visual changes suggestive of iatrogenic damage were also collected for histological examination, fixed in formalin, sectioned and stained with H&E as described previously.

4.5.2 Results

4.5.2.1 **Efficacy of vascular occlusion**

HIFU mediated vascular occlusion was attempted in 34 placental vessels. The mean depth of the target vessels was 26 mm (SD ± 9 mm), which was deeper than in either the transuterine or transdermal bridging studies. Drive voltage ranged from -5 to -9 dBm, and estimated in situ intensities from 1.3 – 4.4 kW.cm^{-2}. The median number of exposures required to complete a

series was 6 (range 4 – 7); the median duration of the mechanical ventilation pause was 56 s (range 24 – 64 s) and the median time to complete an HIFU exposure series and determine if occlusion had occurred was 103 s (range 49 – 1087 s). The median maternal weight was 36.5 kg (range 33 – 53 kg).

Based on comparison of pre- and post-HIFU exposure colour flow Doppler imaging 31/34 vessels were successfully occluded (91%). Of these, 29/31 vessels were occluded in a single exposure series; 2/31 vessels were occluded following retreatment with a further exposure series, giving a total of 36 exposure series, 5 of which resulted in failed occlusion. Hyperecho during B-mode ultrasound treatment monitoring was seen in 26/31 (84%) HIFU exposure series resulting in successful vascular occlusion and 2/5 HIFU exposure series resulting in failed vascular occlusion.

In 2/5 HIFU exposure series which resulted in failed occlusion, the planned exposure series were curtailed by problems with control of movement of the mechanised gantry arm (1 software crash, 1 trapped cable preventing movement). In both cases this was recognised and the HIFU exposure series was manually stopped before multiple HIFU exposures could be delivered to the same location, to reduce the risk of vessel haemorrhage. These were the only 2 exposure series where the C-STAR was below 1 (a spatial undertreatment). However, in both, retreatment was contraindicated by maternal skin damage.

In a further 2/5 HIFU exposure series which resulted in a failed occlusion there was a mistargeting of 10-14 mm which resulted in failure of occlusion. In 1 of these a maternal skin burn prevented retreatment; in the other correction of the targeting error resulted in successful occlusion.

In the final 1/5 HIFU exposure series which resulted in a failed occlusion there was no immediate cause of failure which could be identified. The planned exposures were delivered correctly by the system (5 exposures, drive voltage -6 dBm, 3.0 $kW.cm^{-2}$ estimated in situ intensity, 17 mm target depth, 8 mm gantry movement). The subsequent retreatment, which was successful in producing occlusion, had only a 2 mm difference in depth of the HIFU focal plane (5 exposures, drive voltage -6 dBm, 3.1 $kW.cm^{-2}$, 15 mm target depth). The C-STAR was >1 in both the original exposure series and subsequent retreatment. There was no skin damage or evidence of cavitation in the waterbag during the exposure series; the appearance of hyperecho during the first HIFU exposure series at the site of the intended target suggested that acoustic energy was reaching the intended target initially.

As such, there was only one HIFU exposure series in which the exposure conditions, rather than operator or equipment error, could have resulted in failure of occlusion, making a comparison of successful and failed exposure conditions trivial. However, the larger number of exposure series, including more exposures at lower drive voltages, provided further information about where the minimum threshold of in situ intensity to achieve placental vascular occlusion may lie. Figure 4.20 shows the distribution of estimated in situ intensities which produced successful occlusions in Group S animals. There were no estimated in situ intensities > 4.4 $kW.cm^{-2}$, nor were there any successful occlusions <2.3 $kW.cm^{-2}$. The majority of successful occlusions were produced with estimated in situ intensities 2.5 – 3.5 $kW.cm^{-2}$, suggesting that this is could be the therapeutic window in which HIFU exposure series should be planned. However, the exposure series discussed above, which failed for unknown reasons delivered 3.0 $kW.cm^{-2}$ estimated in situ intensity to the target tissues, so this is not an absolute guarantee of successful occlusion.

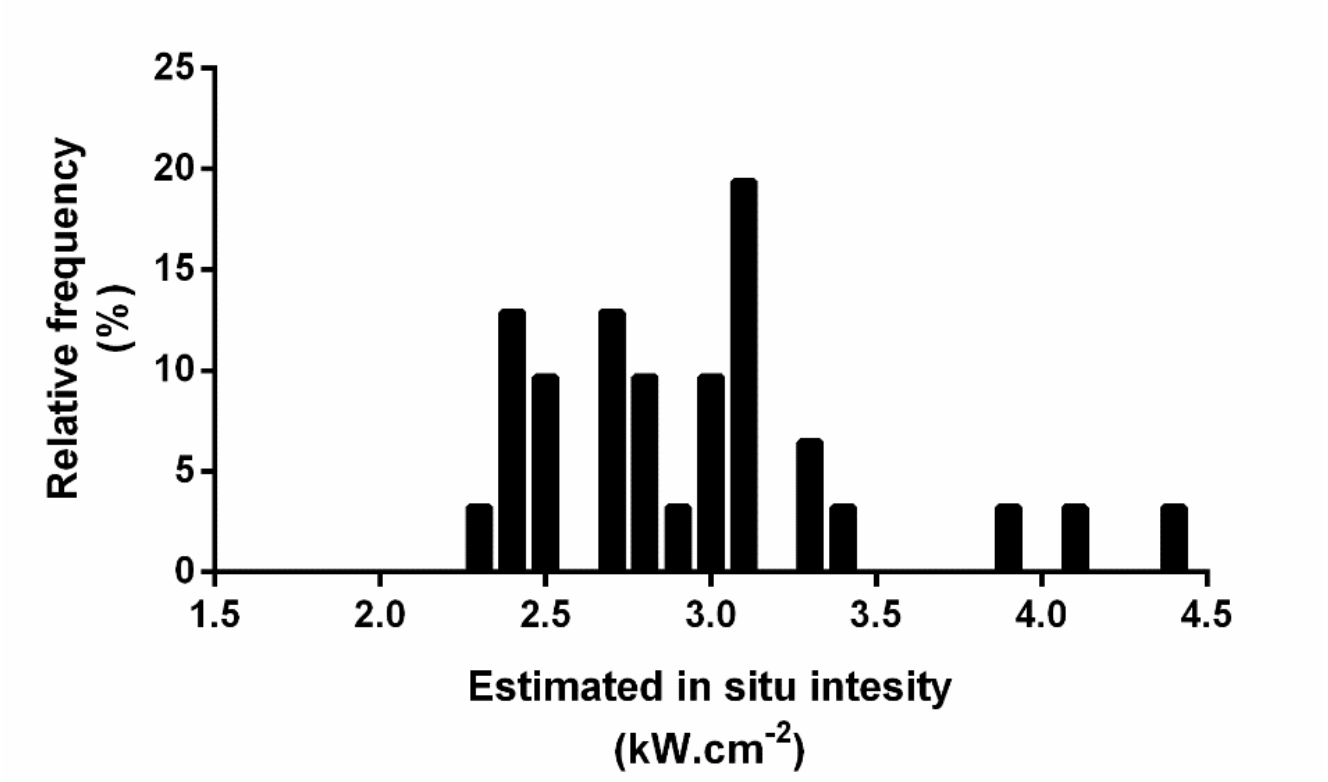

Figure 4.20: Estimated in situ intensity resulting in successful occlusion (Group S).
The histogram shows the relative frequency of estimated in situ intensities which produced successful vascular occlusion using the standard protocol for group S.

After 21 days of follow-up, a total of 34 placentomes with evidence of tissue damage were retrieved at post-mortem examination in animals exposed to HIFU: both the total number and the number per animal matched the number of exposed vascular targets. No damage was seen in the sham exposed placentomes.

Examples of tissue damage in placentomes retrieved on the day of HIFU exposures and after 21 days recovery are compared in Figure 4.21 and Figure 4.22. It is not possible to show the same placentome, excised and bisected immediately after HIFU, and then again after 21 days of healing. However, placentomes treated by HIFU exposure series with similar characteristics in non-recovery animals (Group A or bridging study) and Group S animals are shown in these figures for the purposes of visual comparison only.

While the tissue damage is clearer immediately post HIFU exposures, the presence of damage is still evident after 21 days of healing. However, beyond this, there was little obvious correlation between the visual appearance of the placentome and the exposure conditions; while tissue damage was a sensitive and specific marker for placentomes containing vessels exposed to HIFU, it was not a sensitive or specific marker of vascular occlusion.

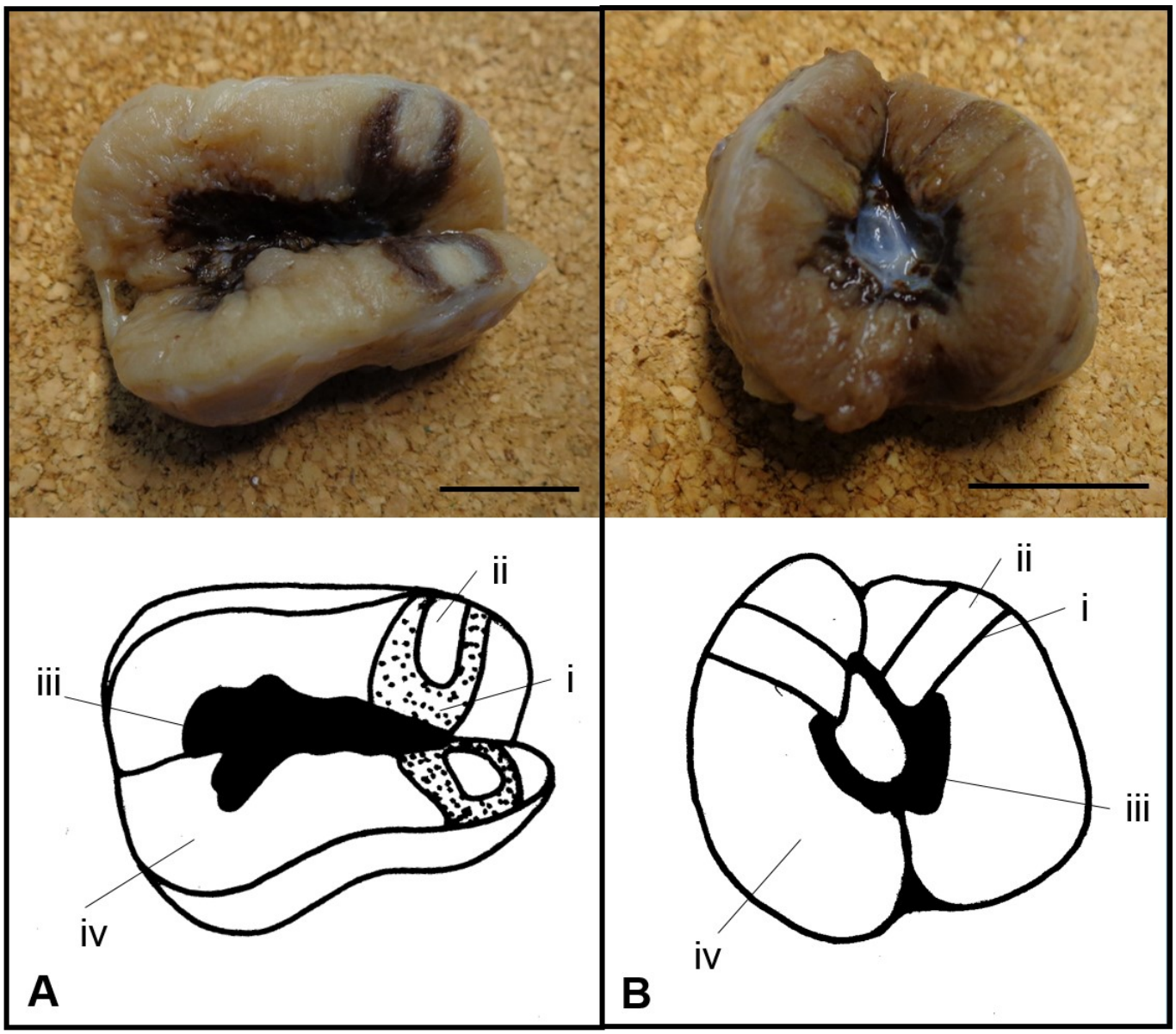

Figure 4.21: Macroscopic tissue changes following HIFU (pallor).
(A) The photograph shows a placentome bisected on the same day as exposure to HIFU, photographed after formalin fixation for 24 h, with an area of tissue pallor surrounded by an area of tissue darkening (Group A, OR638, 115d GA, HIFU exposure series: transuterine, 6 exposures, 2 mm spaced, 5 s duration, estimated in situ intensity 2.7 $kW.cm^{-2}$, target depth 9 mm, echolucent area 0.16 mm^2). (B) The photograph shows a placentome bisected 21 days after exposure to HIFU, photographed after formalin fixation for 24 h, with a less obvious area of tissue pallor which has become soft and yellowed with a small rim of persistent tissue darkening. (Group S, BL89, 128 d GA, HIFU exposure series: transdermal, 5 exposures, 2 mm spaced, 5 s duration, estimated in situ intensity 2.7 $kW.cm^{-2}$, target depth 9 mm, echolucent area 0.21 mm^2). (A,B) The line diagrams represent (i) tissue darkening (ii) tissue pallor (iii) area of materno-fetal exchange surrounding origin of fetal vessels (iv) placental tissue. Scale bars for A and B are 1 cm (photographs and line diagrams to same scale).

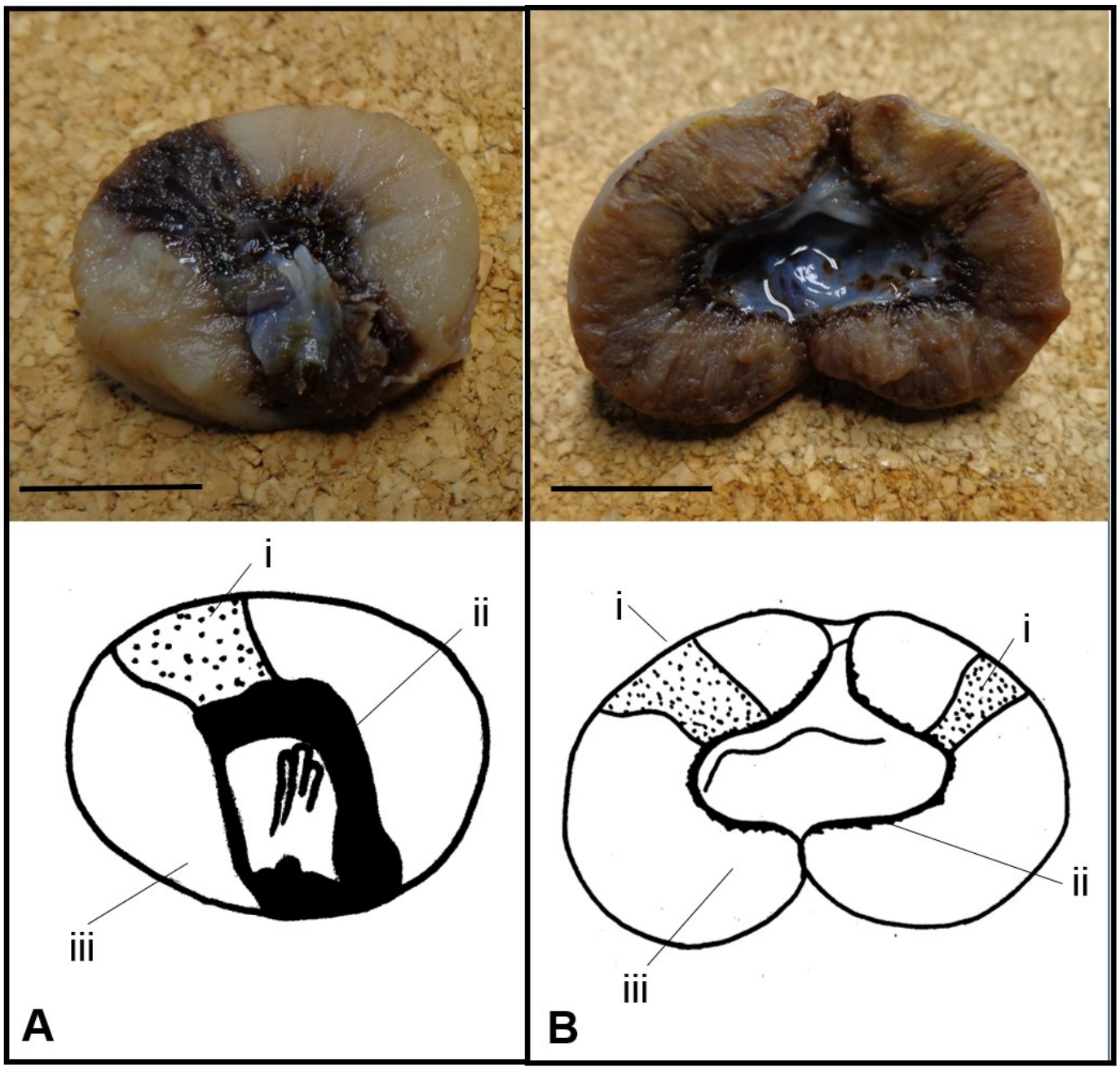

Figure 4.22: Macroscopic tissue changes following HIFU (darkening).
(A) The upper photograph shows a placentome bisected on the same day as exposure to HIFU, photographed after formalin fixation for 24 h, with an area of tissue darkening extending into the origin of the fetal vessels, (Bridging study, BL10, 115 d GA, HIFU exposure series: transdermal, 6 exposures, 2 mm spaced, 5 s duration, estimated in situ intensity 3.5 $kW.cm^{-2}$, target depth 8 mm, echolucent area 0.25 mm^2). (B) The upper photograph shows a placentome bisected 21 days after exposure to HIFU, photographed after formalin fixation for 24 h, with a less obvious area of tissue darkening which has partially resolved over time, (Group S, BL53, 116 d GA, HIFU exposure series: 5 exposures, 2 mm spaced, 5 s duration, estimated in situ intensity 3.3 $kW.cm^{-2}$, target depth 24 mm, echolucent area 0.29 mm^2). (A,B) The line diagrams represent (i) tissue darkening (ii) area of materno-fetal exchange surrounding origin of fetal vessels (iii) placental tissue. Scale bars for A and B are 1 cm (photographs and line diagrams to same scale).

In total, 82 placentomes from Group S animals were examined histologically using H&E stain: 34 with evidence of HIFU damage; 12 undamaged placentomes from animals in which HIFU exposures had been performed, and 36 placentomes from control, sham-HIFU exposed, animals.

Trapped erythrocytes within vessel lumen suggestive of occlusive clot was found in 30/34 placentomes which had been exposed to HIFU; in one placentome the tissue could not be sectioned adequately to visualise the vessels. In 3 vessels where there was no histological evidence of trapped erythrocytes within vessel lumen. There was no evidence of excessive tissue damage in any of the 34 HIFU exposed placentomes examined. The mean diameter of occluded vessels was 1.4 mm (range 0.3 – 3.3 mm).

While histological findings could not be correlated directly to specific placentomes, the number of occluded and non-occluded target vessels per animal matched the number predicted by colour flow Doppler, with the exception of the single animal where once placentome could not be sectioned adequately.

There was no evidence of trapped erythrocytes within vessel lumen or excessive tissue damage within any of the 12 undamaged placentomes of 36 control placentomes examined.

An additional finding, compared to the examination placental vessels within hours of HIFU occlusion, was the presence of vacuolar change around occluded vessels, suggestive of degeneration of the connective tissue surrounding vessels (Figure 4.23c). This was found surrounding occluded vessels in 24/30 placentomes where there was histological evidence of occlusion; there was no evidence of similar vacuolar degeneration surrounding the 3 vessels where occlusion failed, nor surrounding vessel lumen taken from either undamaged (n=12) or sham-HIFU exposed placentomes (n=36).

In 12/30 placentomes (n=2 from each animal) where occlusion and vacuolar degeneration of vessels was suggested by H&E staining, and 6 sham-HIFU exposed placentomes, PTAH staining was performed. All 12 HIFU exposed vessels demonstrated organised fibrin (clot) within the vessel lumen, which was not seen in sham exposed vessels (Figure 4.23d,e). The connective tissue around all 12 occluded vessels stained much more faintly than in control samples, again suggestive of vacuolar change and degeneration of the tissue (Figure 4.23e,f).

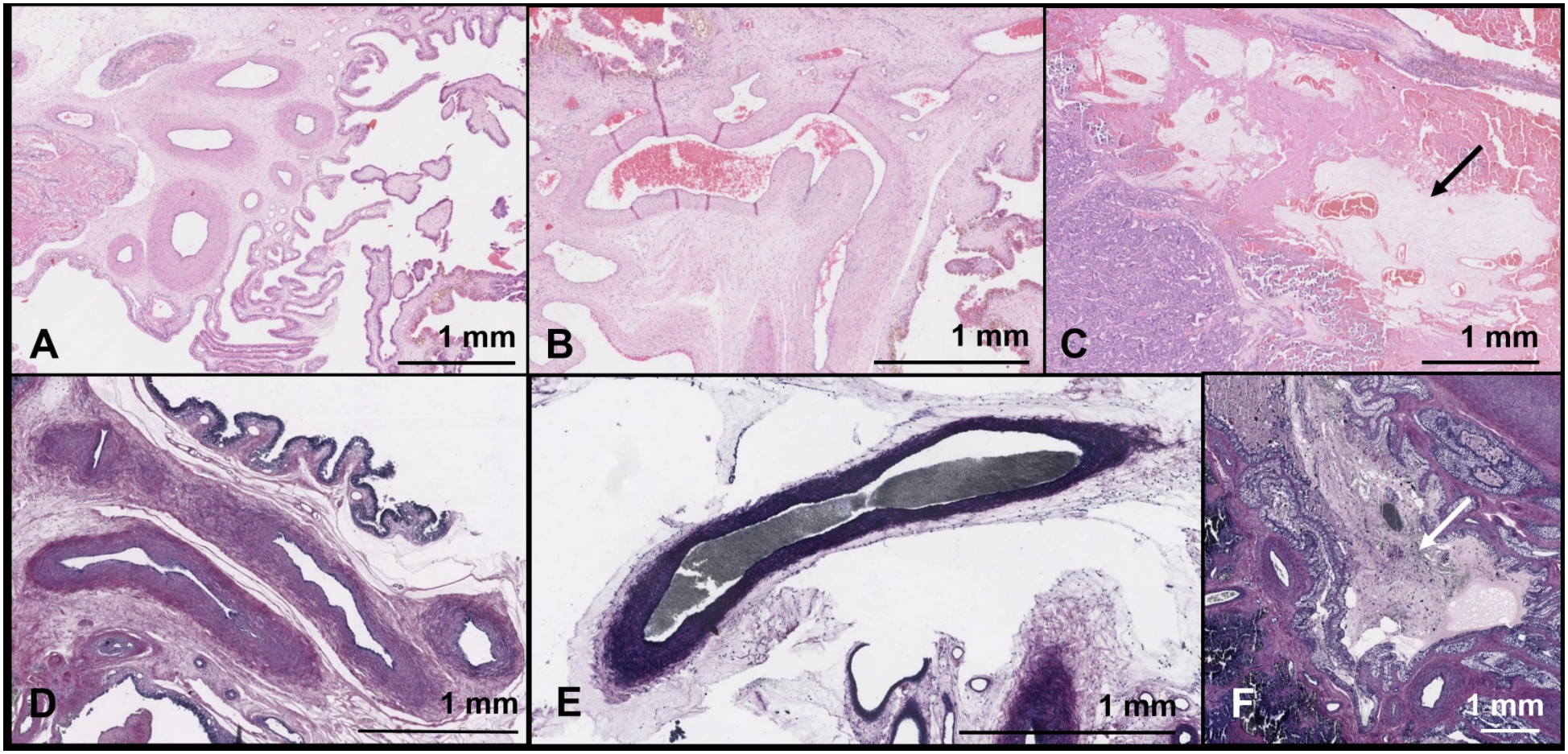

Figure 4.23: Histological confirmation of vascular occlusion after 21 days (Group S).
(A) H&E stain of fetal vessels in a sham exposed placentome. The lumen of the vessels are open and unobstructed, suggesting they remain patent, and the tissue around the vessels shows regular pink staining of normal connective tissue. (B) H&E stain of fetal vessels in an exposed placentome where colour Doppler imaging suggested occlusion. While the vessel lumen is not collapsed, there are trapped erythrocytes within the lumen suggestive of occlusive clot. (C) H&E stain of fetal vessels in an exposed placentome where colour Doppler imaging suggested occlusion; again the lumen are occluded with trapped erythrocytes. The black arrow marks pale, irregular staining in the tissue around the vessels denoting vacuolar degeneration. (D) PTAH stain of fetal vessels in a control placentome. The lumen are open and unobstructed and the connective tissue around the vessels has regular purple staining of normal collagen. (E) PTAH stain of a fetal vessel exposed to HIFU and suggested to be occluded by colour flow Doppler studies. The lumen is stained black, indicating that it is occluded by organised fibrin, a definitive appearance of occlusive clot. (F) PTAH stain of HIFU exposed fetal vessels: there is again black staining in the lumen, but also regions of irregular, pale staining in the collagenous regions surrounding the vessels, matching the H&E finding of vacuolar degeneration.

4.5.2.2 **Iatrogenic harm**

All ewes and fetuses were alive at the end of the planned HIFU exposure series and survived to the end of the 21 d follow-up period. During this period, there were no indicators of maternal pain or distress as a result of the HIFU exposures or maternal skin burns.

There was no evidence of significant maternal injury during the follow-up period as a result of exposure to HIFU. Based on daily systematic observation of maternal movements and gait, pain scores and analgesia requirements, food and fluid intake and passage of urine and faeces there were no complications observed in any animal. Specifically, there was no suggestion in any animal from maternal behaviour or recovery that injury to the spinal cord, bladder or bowel had occurred.

At the time of post mortem examination, there was also no evidence on visual inspection of burns to the rectus sheath or uterus, faecal peritonitis, lesions on the bowel, uroperitoneum lesions on the bladder, or injury extending into the retroperitoneum, although the spine was not formally examined.

There was no evidence of obstetric complications during the follow-up period as a result of exposure to HIFU. Specifically, there were no instances of preterm delivery, preterm rupture of membranes or vaginal bleeding. Non-invasive fetal monitoring with Doppler ultrasound (MCA-PSV, methods described in section 3.6.2) showed no evidence of anaemia in the fetuses following HIFU exposures (Figure 4.24). All fetuses remained in utero at the time of post-mortem, and on visual inspection there was no evidence of fetal burns or damage. There was also no post-mortem evidence of haemorrhage from placental vessels or the umbilical cord, and the fetal haemoglobin concentration of cord blood was not significantly different between sham and HIFU exposed animals at the time of post mortem examination (Figure 4.24).

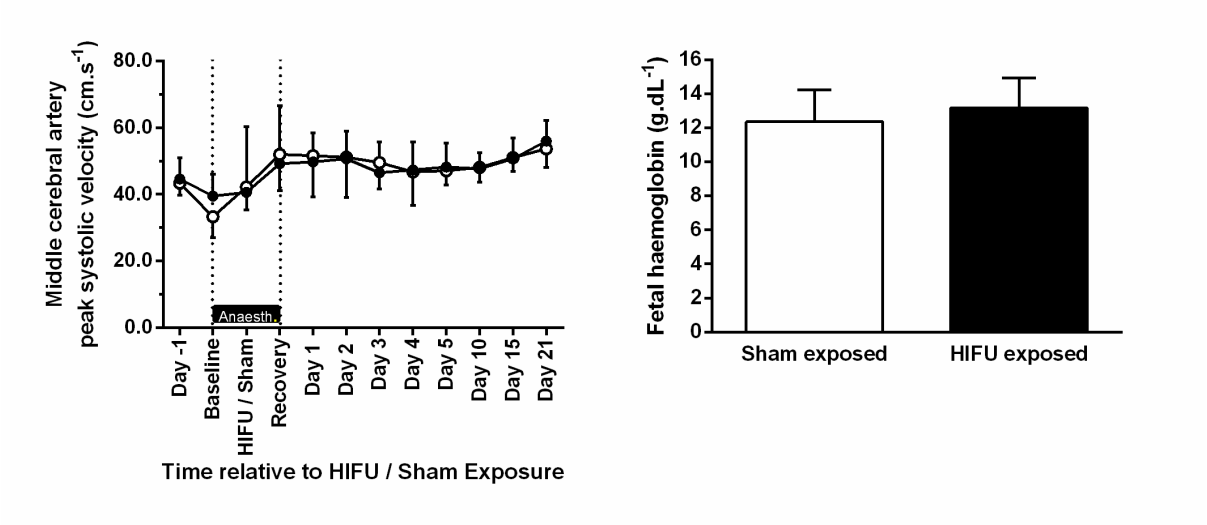

Figure 4.24: Monitoring for fetal anaemia (Group S).
Values represent the mean ± SD of fetal middle cerebral artery peak systolic velocity, a predictor of fetal anaemia in human fetuses, before, during and after HIFU (n=6, closed circles) or sham (n=6, open circles) exposures under general anaesthesia. Dotted lines demarcate the 3 values taken under general anaesthesia; all other measurements were taken in un-anaesthetised animals. Statistical significance was assessed using a repeated measures two-way ANOVA and no differences were found. (B) Values represent the mean ± SD of fetal haemoglobin sample from the umbilical cord at post mortem examination 21 d after HIFU (n=6) or sham (n=6) exposure of placental vasculature. Statistical significance was assessed using a 2-tailed Student's t-test and no differences were found.

The additional findings of the materno-fetal ultrasound studies and fetal post-mortem examination are reported and discussed in chapters 5-8, where groups A, S and R can be compared.

4.5.2.3 **Maternal skin burns**

There were 10 instances of skin erythema and 4 maternal skin burns as a result of a total of 36 HIFU exposure series, giving a rate of 28% for skin erythema (resolution within 24 h) and 11% for skin burns in this group of animals.

There initially appeared to be a tendency for skin burns to occur at higher drive voltages: 3 of 4 burns resulted from exposure series performed at -5 dBm. However, a reduction in drive voltage produced no obvious improvement in skin damage rates: 10/26 (38%) of exposure series at -5 or -6 dBm resulted in some form of skin damage, compared to 4/10 (40%) of exposure series at -7 to -9 dBm. Skin burns occurred when in situ intensities of 2.7 – 4.4 $kW.cm^{-2}$ were delivered to the target tissue; skin erythema occurred when in situ

intensities of 1.3 – 3.4 kW.cm^{-2} were delivered to target tissue, with no obvious pattern to which exposures series resulted in a burn based on this alone.

There was also appeared to be a tendency for skin burns to happen at shallower target depths: 3 of 4 burns were in exposure series with a target depth ≤ 15 mm. In fact, all 4/4 exposures at ≤ 15 mm target depth resulted in a burn; however 10/32 (31%) of skin damage occurred when the target depth was > 15 mm.

Skin damage showed clustering in individual animals, however this no longer appeared related to maternal weight, as the highest rate of skin damage occurred in both the heaviest (50 kg) and lightest (33 kg) ewes. It is possible that differences in skin condition between individual animals played a role that has not be quantified in this study.

A step-wise series of safety measures were introduced to try and reduce the rate of maternal skin burns. The first measure was designed to reduce the skin irritation and erythema which was evident after shaving and depilation. Separation of clipping and chemical depilation by 24-48 h appeared to reduce the degree of, if not totally prevent, skin irritation in all 5 animals in this group where it was performed (Figure 4.25). Reduction of skin irritation by separation of clipping and chemical depilation also appeared to be beneficial in reducing the rate of HIFU skin damage: 7/13 exposure series (54% - including data from the transdermal bridging study) performed after clipping and chemical depilation on the same day resulted in skin damage, compared to 11/32 (34%) when there was a separation of at least 24 hours between the two procedures. However, this was a non-significant reduction (Chi-square test, p=0.23)

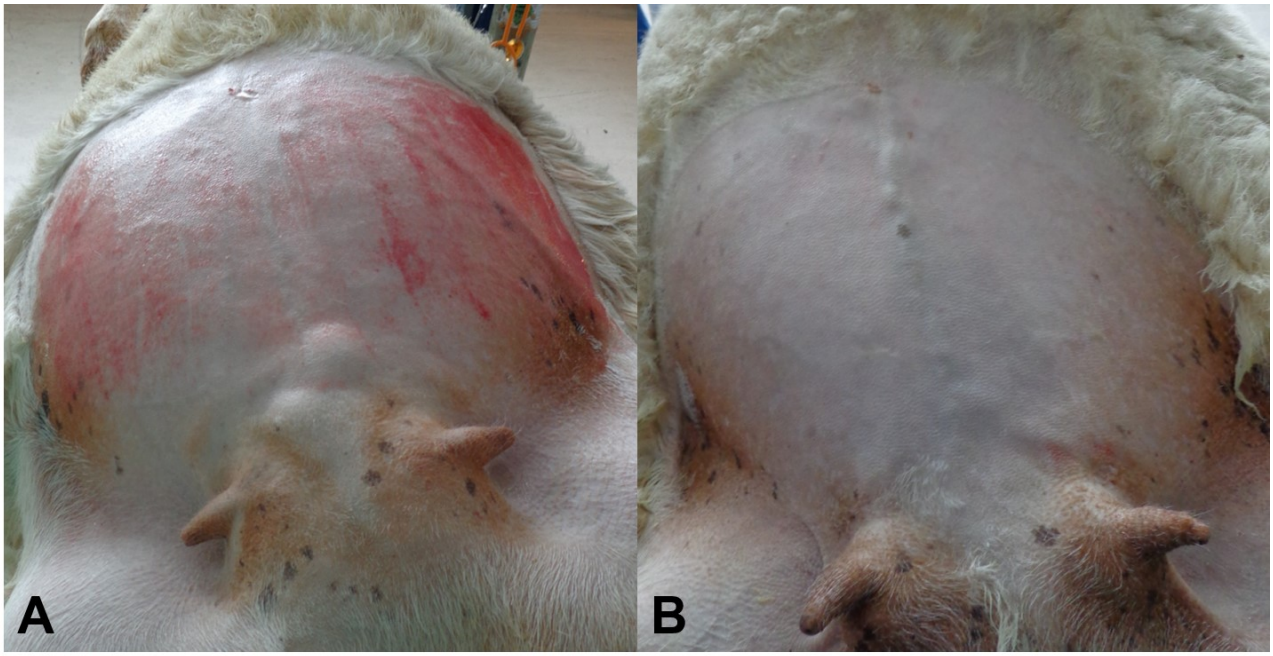

Figure 4.25: Maternal skin irritation from shaving (Group S).
(A) This photograph shows the abdominal skin of an ewe that was shaved and had chemical depilation performed on the same day immediately before any HIFU exposures, with skin irritation evident from the red marks. (B) This photograph shows the abdominal skin of an ewe shaved 48 h before chemical depilation. There is minimal skin irritation in evidence.

The next measure to be introduced was cooling and degassing of the water in the waterbag as described in section 4.5.1.1. Before this was begun 7/12 (58%) of exposure series resulted in skin damage (even when clipping and depilation separated by 24-48 h), compared to 4/18 (22%) of exposure series after it routinely performed. This was a borderline significant reduction (Chi-square test, p=0.04).

When these two interventions are compared together, however they have a clearer value, with a 0.33 relative risk reduction (95% CI 0.12 – 0.94) in the rate of maternal skin burns (Table 4.6).

	Maternal skin damage	No maternal skin damage
Clipping on same day as depilation & Waterbag cooled and degassed before each HIFU exposure series	7	6
Clipping 24-48 h before depilation & Waterbag cooled and degassed at start of HIFU exposures only	4	18

Table 4.6: Effect of interventions to reduce maternal skin burns (Group S).
The table shows the burns resulting from the 13 HIFU exposures series before clipping and depilation were separated and before repeated cooling and degassing of the waterbag was introduced, compared to the 22 HIFU exposure series after both these interventions became part of the safety protocols of Group S. The interventions produced a reduction in risk (Chi-squared test, $p = 0.03$).

The 4 maternal skin burns showed evidence of healing without infection during the 21 d period. The 10 regions of maternal skin erythema (by definition) were not visible by day 1 following HIFU exposures. An example of skin burns and erythema is shown in Figure 4.26. Despite the separation of shaving from chemical depilation by 24 – 48 h in this animal, there is still evidence of some skin damage prior to the start of HIFU exposures, shown with black arrows, numbered 1-8, in the pre-HIFU image.

By the end of the HIFU exposures (post-HIFU image), shaving marks 7-8 have faded, 1-3, 5 and 6 remain unchanged. The original skin mark labelled 4 appears to have become more pronounced, and this was called a region of erythema overlying pre-existing skin damage (causative HIFU exposure series: 6 exposures, estimated in situ intensity 2.4 $kW.cm^{-2}$, 5 s, 2 mm spaced, target depth 20 mm). There is a new raised area demarcated by a black circle – this is the burn which resulted from a HIFU exposure series of 7 exposures, estimated in situ intensity 4.3 $kW.cm^{-2}$, 5 s duration, 2 mm spaced. Due to the targeting error in this placentome, the HIFU energy was delivered only 10 mm beneath the surface of the skin, instead of the intended 24 mm. An enlargement of the burned area, the area of erythema and one of the shaving marks is shown in panel A.

By day 1 post HIFU exposures, the burn (black circle) is still evident and healing has begun, as the area is starting to show fibrinous exudate. Although the angle of the maternal

abdomen is different in the semi-recumbent position to the previous prone positions shown, there does not appear to be any clear evidence of a burn at location 4, supporting its classification as erythema. The shaving mark at location 3 is also starting to scab.

By day 15 post HIFU, the burned area has scabbed over, as has a small area of the shaving mark at location 3. There is no evidence of infection or purulent discharge. While there is still no evidence of skin damage at the site marked 4, the wool is showing an altered pattern of regrowth in this region.

At the time of post-mortem (day 21) the abdomen is again shown with the animal in a prone position. The scab from the burn has detached showing a raised white area where the burn had been, marked by arrow 9; histological examination showed dense scar tissue in this region consistent with the maturational phase of healing of a full thickness burn.

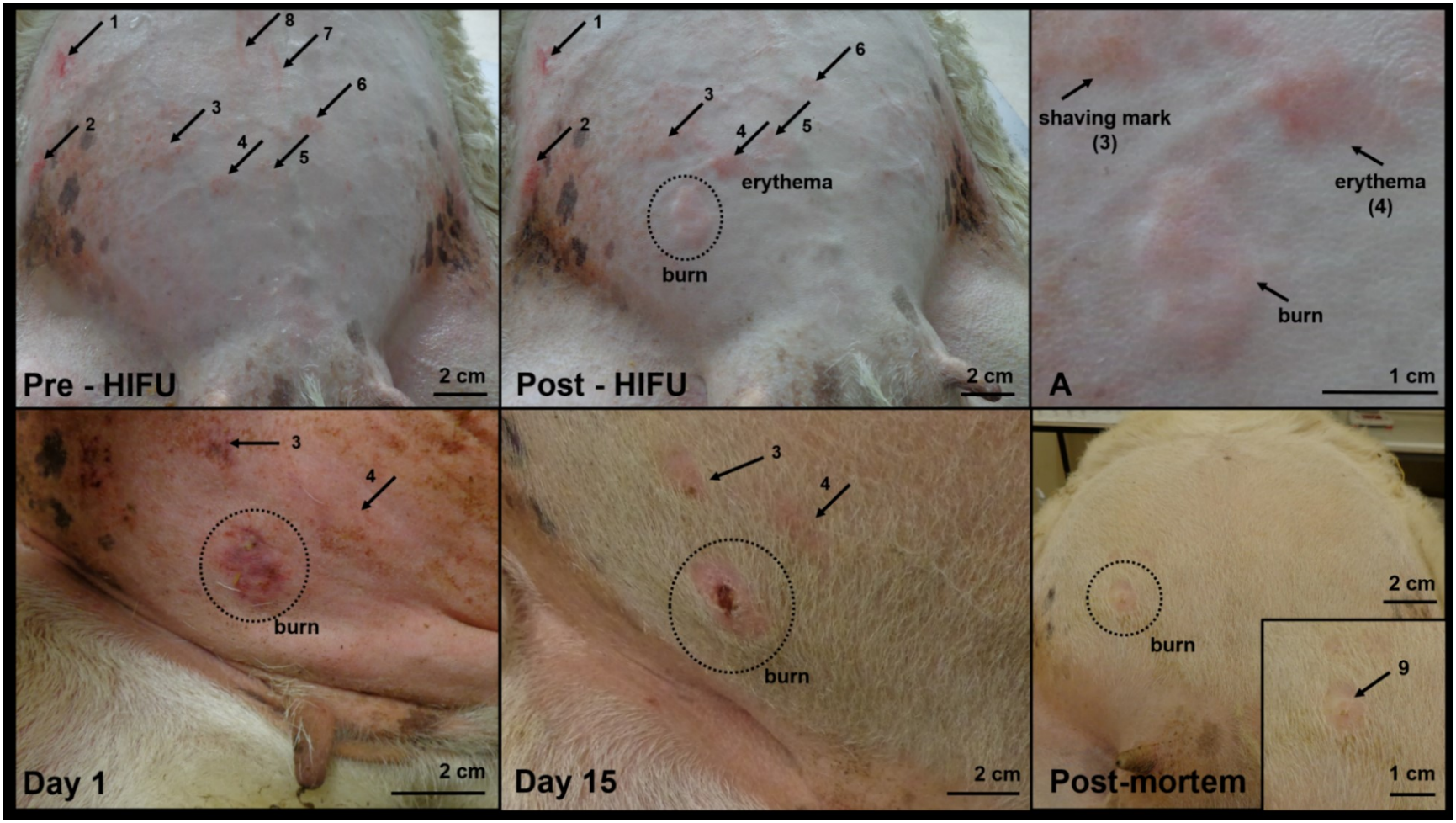

Figure 4.26: Maternal skin burn healing (Group S).
Pre-HIFU: this panel shows the maternal abdomen after shaving and depilation (24 h apart) before exposure to HIFU. Arrows 1-8 mark areas of skin irritation or damage as a result of shaving or chemical depilation. Post HIFU: the maternal abdominal skin is shown after completion of 6 HIFU exposure series. The circled area is a skin burn which was not present before HIFU; the arrow marked 4 shows an area of skin irritation which has enlarged, and appears to be erythema. Areas of skin irritation 1-3 and 5-6 remain unchanged, 7-8 are no longer visible. An enlargement of the new areas of skin damage is shown in panel A. Day 1: the burn has darkened and has a small yellow area of fibrinous exudate. There is now no clear evidence of skin damage at location 4, supporting the classification of erythema; there appears to be an area of persistent skin irritation at location 3, which is starting to develop a fibrinous scab. Day 15: The burned area has formed a fibrinous scab with no sign of infection. A small area of fibrinous scab remains at the area of skin irritation (3); and while there is no skin damage at site 4, the regrowth of hair is altered. Post-mortem: by day 21, the area of skin irritation has healed and the burn is a raised while area of tissue (shown enlarged in the inset, marked by arrow 9).

4.5.3 Transdermal survival study: discussion

In these animals, we were able to once again demonstrate that it was possible to achieve a high rate of placental vascular occlusion (91%) in sheep, using HIFU, this time through intact maternal skin. As previously, identification, targeting and confirmation of occlusion was performed with colour flow Doppler integrated with the HIFU transducer, in vessels of clinical relevant diameters, the importance of which has previously been discussed. While HIFU ablation of placental tissue through intact maternal skin has previously been demonstrated (285, 286), it appears that this was the first demonstration that selective placental vascular ablation during pregnancy could be achieved.

Additionally, for the first time, we were also able to demonstrate survival of mothers and fetus beyond the immediate end of HIFU exposures. All six mothers and fetus who underwent anaesthesia and exposure to HIFU survived without evidence of significant maternal or obstetric complications for a period of three weeks following this. Such survival has not been demonstrated in any other pregnant animal model following HIFU exposure of the placenta (60, 61, 281, 286), although there are 2 case reports in humans of fetal survival and delivery following HIFU energy delivery into the intrauterine space (although not used on placental vessels) (43, 57). This is an advance in demonstrating the potential of HIFU mediated placental vascular occlusion as a therapy suitable for use in human pregnancy.

Overall, the increased safety features in the treatment protocol - the restrictions on maintaining the C-STAR >1, moving the HIFU transducer in only one plane, orthogonal to the direction of sound, starting and ending HIFU exposure series in soft tissue and avoiding in situ intensities > 5.0 $kW.cm^{-2}$ - together meant that there were no further instances of vessel haemorrhage in this animal group. This is despite two technical malfunctions which could have replicated the conditions which resulted in a vascular haemorrhage in the Group A animals (non-movement of the gantry arm and repeated HIFU exposure of the same tissue location). Based on this experience, both these situations were recognised by visually monitoring the gantry arm and ultrasound screen for movement between each HIFU exposure in a series, and were manually stopped before harm occurred. While this system was effective in this circumstance, it was vulnerable to failure through inattention or distraction, and is an area which would require closer regulation in any future, improved HIFU system to be used in this field. An automated confirmation of completed movement and correct positioning of the gantry arm before any HIFU exposure could be delivered would be ideal.

In the pilot, transuterine and transdermal bridging studies, high drive voltages were used to deliver high levels of HIFU energy to the tissue, based on previous studies which had shown that vascular occlusion typically requires such energy levels, with the attendant risk of complications (37, 45). Prior to this phase of the study, there had been only minimal attempts to de-escalate the amount of HIFU energy delivered to the tissues, leading to probable ongoing over-exposure vascular targets, and resulting in unnecessary soft tissue damage. In the Group S animals, driven mainly by a desire to avoid maternal skin burns, there was a reduction in the amount of HIFU energy delivered to tissues, which did not reduce the efficacy of vascular occlusion. In the Group A animals, the median in situ intensity was 5.4 $kW.cm^{-2}$ (IQR 5.1-5.5 $kW.cm^{-2}$); in these Group S animals, the corresponding values were 2.9 $kW.cm^{-2}$ (IQR 2.5 – 3.1 $kW.cm^{-2}$). Accordingly, there was no histological evidence of excessive tissue damage in the exposed placentomes of the Group S animals, although this does not exclude the possibility of healed damage. As such, this is an indicator that the therapeutic window for estimated in situ intensity is lower than had previously been selected, and in the region of 2.5 – 3.5 $kW.cm^{-2}$, although at present there is insufficient evidence to refine this further.

A further consequence of either this reduction in energy delivery to the tissue or imaging through skin (or a combination of both) is that both the presence or absence of hyperecho and structural change within the placentome structure now appear to be less sensitive and specific markers of successful vascular occlusion. This supports the finding that localised, rather than generalised, tissue heating and ablation is compatible with placental vascular occlusion, although the study was not designed in such a way as to allow mechanisms of occlusion to be fully investigated.

This phase of the study was also the first to demonstrate the persistence of vascular occlusion following exposure to HIFU to 21 days. Rather than simply showing trapped erythrocytes within the lumen of exposed vessels and inferring the presence of organised clot (H&E staining), we were also able to show the presence of organised thrombus within exposed vessels at 21 days after HIFU exposures (PTAH staining). This combined with the vacuolar degeneration seen surrounding the vessels matches the previously described sequence of histological changes of occluded vessels following HIFU exposure (35).

One of the outstanding question from the transuterine study was whether using occlusive clotting as the mechanism of vascular occlusion would have a transient or persistent effect. Occlusive clot can lead to permanent vascular occlusion by a process of fibrosis obliterans, or the clot itself can be reabsorbed over time as the vessel recanalises. While there is no fixed time limit over which either process can occur, the presence of organised thrombus in the

presence of vacuolar degeneration is suggestive of the former, rather than the later, process. However, to fully demonstrate the potential of occlusive clot to be useful in human pregnancy, where the interval between HIFU exposures and delivery could be up to 6 months, an animal model with a longer gestational period than the sheep would be required.

A second conclusion drawn from the presence of persistent vascular occlusion to 21 days was that not only were mothers and fetus recovering from anaesthesia and HIFU exposures, they were doing so in the presence of ongoing placental vascular occlusion. This indicates the results presented from Group S in chapters 5-7 are representative of this.

While, as discussed above, there were no significant maternal or fetal injuries or obstetric complications identified, the rate of maternal skin burns continued to be a problem. The incremental protocol changes – reduction in drive voltage, reduction in skin irritation, cooling and degassing of the water in the water bag – did produce a progressive reduction in the rate of skin burns, but were not able to fully prevent skin burns. These are a relatively common complication of HIFU therapies, and had been predicted as the most likely source of iatrogenic harm in these experiments.

As in the transdermal bridging study, the actual rate of maternal skin burns was difficult to properly determine due to the fact that progressive changes to the HIFU treatment protocol were being made to reduce the number of skin burns occurring. For this reason, the overall rate of skin burns does not necessarily reflect the likelihood of skin burns occurring when the final protocol – rather than the initial one – is used, and this will need to be evaluated further in the next group of animals where HIFU was again planned to be applied transdermal.

4.6 Transdermal chronically instrumented recovery study: Group R(ecovery)

Based on the transdermal survival study, we now had an indication that it was feasible to use HIFU through intact maternal abdominal skin with a similarly high degree of efficacy as demonstrated in the prior transuterine studies. These animals also demonstrated that maternal and fetal survival without serious adverse events could be anticipated, although the rate of maternal skin damage remained undesirably high.

We had gained familiarity with the identification of placental vascular targets and planning of HIFU exposure series gained during the Group S animals. The reduction in time required to plan and deliver HIFU exposure series meant that it should now be possible to complete HIFU occlusion of at least 6 placental vessels with the Group R protocol, which allowed 60 minutes to complete this part of the experimental protocol. This protocol also allocated time under anaesthesia to surgical implantation of a limited number (compared to Group A and the Group R control animals) of maternal and fetal vascular catheters and flow probes. This would allow more detailed examination of the maternal and fetal cardiovascular, metabolic and endocrine function to be performed during the recovery phase of these animals, in keeping with the type of information gained from the Group A and Group R control animals.

This animal group also represented the final opportunity to test the efficacy and safety of the most developed version of the HIFU treatment protocol in this study. The previous HIFU treatment protocols had prioritised efficacy over safety, whereas this treatment protocol attempted to balance the two. All the limits on HIFU exposure series previously developed to improve safety were now implemented into this protocol, and no further changes were allowed. The suggested therapeutic window of 2.5 – 3.5 $kW.cm^{-2}$ derived from the experiments in Group S animals (Figure 4.20) was now adopted, and drive voltage was adjusted in real-time to achieve this target. This animal group was also planned to be the largest of any of the animal groups, to provide the greatest amount of data about the efficacy and safety of the most developed HIFU treatment protocol in this study.

Therefore, this phase of the study sought to assess the final transdermal HIFU treatment protocol developed by this study. The key areas to evaluate were:

(i) the efficacy of ultrasound-guided HIFU placental vascular occlusion in the pregnant sheep model;
(ii) the rates and types of maternal and fetal direct iatrogenic harm;

(iii) the rates and types of maternal and fetal indirect iatrogenic harm;

(iv) the time required to plan, perform and complete the planned vascular occlusions.

4.6.1 Methods

In addition to HIFU exposures in these animals (n=6) fetal cardiovascular, metabolic and endocrine wellbeing was assessed by surgically implanted arterial catheters and flow probes following reversal of anaesthesia for 21 days (Figure 3.13). To assess the degree of fetal recovery, they were compared to a control group of pregnant ewes (n=6) who underwent surgical implantation of catheters and flow probes under anaesthesia, before being recovered and monitored for 21 days, but were not exposed to HIFU. These results will be reported and discussed separately in chapters 5-8. These 12 animals will be referred to as 'Group R' in chapters 5-8.

4.6.1.1 **HIFU therapy system**

The system described in section 4.2.1.1 was used.

In all experiments, the water in the water bag was taken cold from the tap and cooled with ice sealed in plastic (so the melting ice water did not mix with degassed water in the bag) and was degassed before each HIFU exposure series.

4.6.1.2 **Animals and surgical methods**

Ten pregnant ewes carrying singleton fetuses at 116.5 ± 1.5 d gestational age were placed under general anaesthesia (sections 3.2.1, 3.2.2). The maternal abdominal skin had been shaved with clippers 24 – 48 hours previously to remove wool.

Following induction of anaesthesia, the skin was washed with iodine scrub solution to remove dirt and lanolin, and washed again with tap water. The remaining hair was chemically depilated (Nair ® hair removal cream, Church & Dwight Co., Kent, UK), the skin was washed for a final time with tap water and coated with degassed water. The waterbag was placed in contact with the maternal skin and trapped air between the plastic and the skin was smoothed out. If the waterbag was repositioned, the layer of degassed water on the skin was replaced, and air pockets were smoothed out again. HIFU exposure series were carried out through intact

maternal skin (see next heading) before any invasive surgical procedures were performed, following the experimental timeline shown in Figure 3.12.

Breath holds were performed during each HIFU exposure series (section 4.2.1.2).

Following completion of all planned HIFU exposures, the maternal skin was cleaned with a chlorhexidine solution (4% chlorhexidine gluconate, 96% ethanol) which was allowed to evaporate before skin incisions were made. Under sterile conditions, a midline laparotomy and hysterotomy was performed to surgically implant fetal arterial catheters and flow probes and an incision in the maternal hindlimb was performed to insert maternal femoral arterial catheters. The underside of the visible rectus sheath and visible surface of the uterus were examined at this time for burns, and were photographed if found. Incisions were closed and the ewes were recovered from anaesthesia (section 3.2.4, 3.2.5). The post-operative care is described in section 3.2.7. Methods for invasive monitoring of materno-fetal wellbeing are described in sections 3.3 - 3.5.

For the next 20 days, ewes were checked daily for signs of maternal pain or distress, infection or poor healing of skin damage, problems with mobility, bladder or bowel function, preterm labour, rupture of membranes or vaginal bleeding. During follow-up, two ewes were removed from the study before the completion of 20 d due to catheter blockage or flow probe failure. One ewe was euthanised for welfare concerns on day 4 post-operative due to colonisation of a fetal arterial catheter with pseudomonas which caused intrauterine infection. A fourth ewe was euthanised for welfare concerns on day 5 post-operative and was found at post-mortem to have a dehiscence of the hysterotomy incision and intra-abdominal amniotic fluid leak. These 4 animals were excluded from Group R follow-up as the complications were recognised post-operative complications, not a result of HIFU exposures. While their cardiovascular, metabolic, endocrine or post mortem data will not be discussed, there was no reason, however, to exclude their data regarding immediate outcomes of HIFU application from this study group, as this did not deviate from planned HIFU delivery experimental protocol.

After the completion of 20 days post-exposure follow-up, the remaining 6 ewes and fetuses were euthanised under schedule one of the UK Animals (Scientific Procedures) Act 1986 for post mortem examination and collection of tissues. A slow intravenous injection into the maternal femoral vein catheter of 120 $mg.kg^{-1}$ pentobarbitone sodium (Pentoject®, Animalcare Ltd., UK) was used for this purpose. Air embolus into the femoral vein was used as a secondary confirmation of death. Maternal and fetal cardiac activity was monitored via the

arterial catheters and cession of cardiac activity was confirmed when asystole was seen on the IDEEQ software.

4.6.1.3 **Vascular targets and HIFU treatment protocol**

HIFU was applied trans-dermally to occlude 6 vessels per animal (n=10).

HIFU exposure series were based on the protocol used in the transdermal survival study: drive voltage -5 to -8 dBm, free field intensity 3.2 – 6.7 $kW.cm^{-2}$, 5 s exposure duration, 5 s intervals between exposures, 2 mm spacing between exposures, placement and number of exposure following the “limited” pattern.

The following safety limits were adopted from the previous treatment protocols: (i) all exposure series were planned to start and finish in placental soft tissue bordering the echo lucent area from which vessels arise; (ii) the ratio of HIFU treatment area to echolucent area of the placentome was planned to be >1; (iii) movement of the mechanical gantry arms was restricted to one direction on an axis orthogonal to the direction of sound; (iv) predicted in situ intensities above 5 $kW.cm^{-2}$ were not planned; (v) vascular targets were not selected if there were fetal parts in the post-focal region, at any distance; (vi) the water in the water bag was cooled and degassed between each HIFU exposure series; and (vii) the depth of the target vessel beneath the skin was used to select the drive voltage, aiming to deliver an in situ intensity 2.5 – 3.5 $kW.cm^{-2}$ (Figure 4.20).

4.6.1.4 **Assessment of treatment success**

Primary confirmation: comparison of pre- and post-HIFU exposure colour flow Doppler imaging for evidence of “no flow” as described in section 4.2.1.4.

Secondary confirmation: identification of occlusive clot within vessel lumen after 20 days in exposed placentomes as described in section 4.5.1.4. No placentomes were taken from the control group, as the completion of this group predated the start of the HIFU study. Retained placental tissues were fixed, sectioned and stained with H&E or PTAH as described in section 4.5.1.4.

4.6.1.5 **Treatment monitoring**

Tissue responses (real-time): as described in section 4.3.1.5.

Offline analysis of saved imaging: as described in section 4.3.1.5.

Identification of fetal position relative to HIFU focus: as described in section 4.3.1.5.

4.6.1.6 **Management of treatment failure**

No changes were made to the methods described in section 4.5.1.6.

4.6.1.7 **Assessment of iatrogenic harm**

Maternal skin burns: These were monitored intraoperatively as described in section 4.4.1.7. These areas were examined again at the end of all HIFU exposure series. It was not possible to monitor the burns thereafter as the maternal abdomen was wrapped in Tubigrip™ (Mölnlycke Health Care Ltd., Oldham, UK) to reduce the risk of midline hernia and the design of the CamDAS jacket did not facilitate access to the maternal abdomen without removal of all monitoring equipment. Any area of skin reddening which resulted from a HIFU exposure series but faded fully by the time the CamDAS jacket was fitted (ca. 2-3 h post-exposures) was classified as erythema; other areas of damage resulting from HIFU exposure which persisted beyond that were classified as skin burns.

A systematic inspection of tissues was performed at post mortem examination and a photographic record was compiled of damage to: (i) maternal skin, (ii) maternal rectus sheath, (iii) anterior and posterior surface of the uterus, (iv) fetal skin (dorsal, ventral, left and right lateral views), and (iv) maternal bladder and bowel. Areas of maternal and fetal skin, rectus and uterus with visual changes suggestive of iatrogenic damage were also collected for histological examination, fixed in formalin, sectioned and stained with H&E as described previously.

4.6.2 Results

4.6.2.1 **Efficacy of vascular occlusion**

Overall, in Group R animals, HIFU mediated vascular occlusion was attempted in 60 placental vessels. The mean depth of the target vessels was 24 mm (SD ± 6 mm), comparable to the animals in the transdermal survival study. Drive voltage ranged from -5 to -8 dBm, and estimated in situ intensities which from 1.8 – 3.9 $kW.cm^{-2}$, and the distribution of estimated in situ intensities which resulted in successful occlusion is shown in Figure 4.27. The median number of exposures required to complete a series was 6 (range 3-7). The median time to complete an HIFU exposure series and determine if occlusion had occurred was 96 s (range 60 – 714 s); the median duration of each breath hold was 56 s (range 24 – 64 s). The median total time to plan, treat and assess if occlusion had occurred of 6 vascular targets, with retreatments if required, in this animal group was 62 min (range 50 – 75 min).

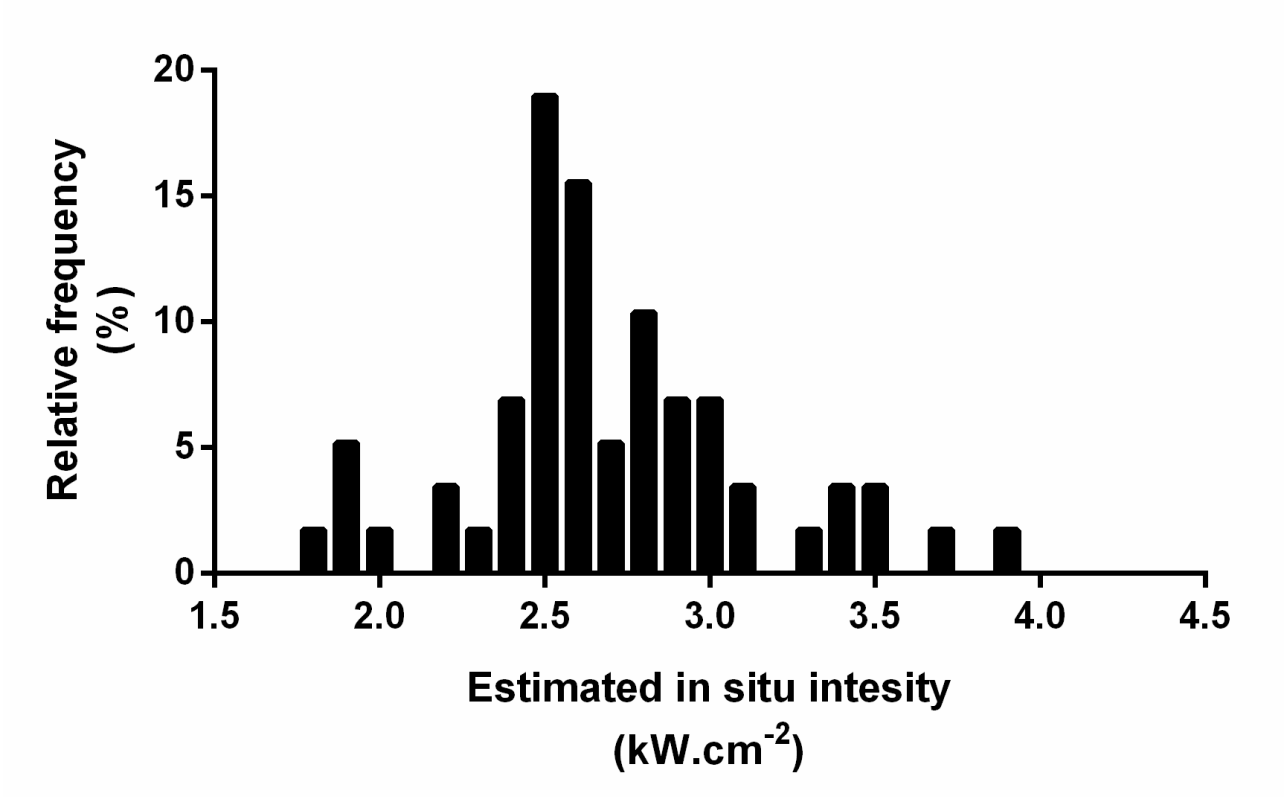

Figure 4.27: Estimated in situ intensity resulting in successful occlusion (Group R).
The histogram shows the relative frequency of estimated in situ intensities which produced successful vascular occlusion using the standard protocol for Group R.

Based on a comparison of pre- and post-HIFU exposure colour flow Doppler imaging, 58/60 vessels were successfully occluded (97%). Of these, 55/60 (92%) vessels were occluded in a single exposure series; a total of 4 retreatments were attempted, of which 3 produced

successful occlusions, giving a total of 64 exposure series. Hyperecho was seen on B-mode ultrasound imaging of HIFU exposures in 56/58 HIFU exposure series resulting in successful vascular occlusion, however it was also seen in 4/6 HIFU exposure series resulting in failed vascular occlusion.

In 3/6 HIFU exposure series which resulted in failed occlusion, there was mistargeting of between 5-10 mm. In all 3 of these vascular targets, a retreatment which corrected this original mistargeting produced successful vascular occlusion.

In 3/6 HIFU exposure series which resulted in failed occlusion (2 in the same vascular target, the original HIFU exposure series and the retreatment) there was no immediate cause for failure identified. One of the three failed occlusions was only recognised by offline analysis of pre- and post-HIFU exposure colour flow Doppler images, so the opportunity to attempt retreatment was missed, as it would not have been contraindicated had it been recognised at the time. All 3 exposure series had an estimated in situ intensity 2.7 – 3.8 $kW.cm^{-2}$, target depth 22 – 27 mm, with exposure series formed of 6-7 exposures. All the C-STARs were >1. However, both vascular targets were in the same animal, and when were retrieved at post mortem were arising near the formed umbilical cord. The vessel diameters measured histologically were 2.4 and 2.8 mm.

A total of 60 placentomes with evidence of tissue damage were retrieved at post-mortem examination, 21 days after HIFU exposures were performed: both the total number and the number per animal matched the number of exposed vascular targets.

In total, 72 placentomes from Group R animals were examined histologically using H&E stain: 60 with evidence of HIFU damage and 12 undamaged placentomes from animals in which HIFU exposures had been performed. There was no placental tissue available from the Group R control animals. Trapped erythrocytes within vessel lumen suggestive of occlusive clot was found in 58/60 placentomes which had been exposed to HIFU. In 2/60 vessels there was no histological evidence of trapped erythrocytes within vessel lumen. These two vessels were found in the animal where colour flow Doppler had identified a failed occlusion in two placentomes. There was no evidence of trapped erythrocytes within vessel lumen taken from either undamaged placentomes. The diameter – measured histologically – of occluded vessels was between 0.4 – 2.9 mm (mean 1.4 mm).

Vacuolar change was found surrounding vessels in 49/58 (85%) placentomes where there was histological evidence of occlusion. There was no evidence of similar vacuolar degeneration

surrounding the 2 vessels where occlusion failed, or surrounding vessels in undamaged placentomes.

In 20/60 placentomes (n=2 from each animal) where occlusion and vacuolar degeneration of vessels was suggested by H&E staining, PTAH staining was performed to identify organised fibrin (clot). All 20 vessels demonstrated organised fibrin (clot) within the vessel lumen, which was not seen in vessels within undamaged placentomes. The connective tissue around all 20 occluded vessels stained much more faintly than in control samples, again suggestive of vacuolar change, loss of collagen and degeneration of the tissue. This was not seen in undamaged placentomes.

4.6.2.2 **Iatrogenic harm**

There was again no evidence of significant maternal injury during the follow-up period as a result of exposure to HIFU. Based on daily systematic observation of maternal movements and gait, pain scores and analgesia requirements, food and fluid intake and passage of urine and faeces there were no complications observed in any animal. Specifically, there was no suggestion in any animal from maternal behaviour or recovery that injury to the spinal cord, bladder or bowel had occurred. The single maternal skin burn healed well without evidence of infection (discussed further in the next section).

At the time of post mortem examination, there was also no evidence on visual inspection of burns to the rectus sheath or uterus, faecal peritonitis, lesions on the bowel, uroperitoneum lesions on the bladder, or injury extending into the retroperitoneum, although the spine was not formally examined.

There was no evidence of obstetric complications during the follow-up period as a result of exposure to HIFU. Specifically, there were no instances of preterm delivery, preterm rupture of membranes or vaginal bleeding. As discussed in the methods (section 4.6.1.2) a full 20 days of follow-up could not be completed in 10 animals: 2 were excluded due to catheter blockage and/or flow probe failure; 2 more were excluded due to recognised post-surgical complications of chronically instrumented fetal sheep preparations. Of the remaining 6 ewes and fetuses, all mothers survived with fetuses alive in utero at the time of post-mortem.

There was also no post-mortem evidence of haemorrhage from placental vessels or the umbilical cord. There had been one uterine burn noted at laparotomy (day 0, discussed further in the next section) which was still evident at day 20 (Figure 4.29b), although its appearance

had changed suggesting healing had taken place. There was no evidence of an open defect in the uterine wall at the site of the burn. The contributory factors to the uterine burn, if any, are unknown.

There was one fetal burn in this group of animals (Figure 4.28). The fetal burn was a result of inadvertent non-adherence to the safety protocols, i.e. not recognising in real-time that ultrasound showed a fetal limb was near the intended vascular target. A series of 5 HIFU exposures with an in situ intensity of 2.4 $kW.cm^{-2}$ was delivered at a depth of 20 mm beneath the surface of the skin and 9 mm (measured parallel to the direction of sound) above the fetal limb which was injured. The burn was full thickness, and there was mild swelling and deformity of the joint evident in comparison to the other hindlimb, with no evidence of infection. This suggests there would have been functional impairment of the joint of uncertain prognosis due to this injury to the fetus. However, as the fetus was euthanised before birth, it was not possible to test this hypothesis, or perform further functional assessment.

The additional findings of the materno-fetal cardiovascular, metabolic, endocrine and fetal post-mortem examination are presented and discussed in chapters 5-8 as part of an integrated consideration (using information from Groups A, S and R) of the effect of HIFU, surgery and anaesthesia on utero-placental function, initiation of fetal defence mechanisms, growth and development.

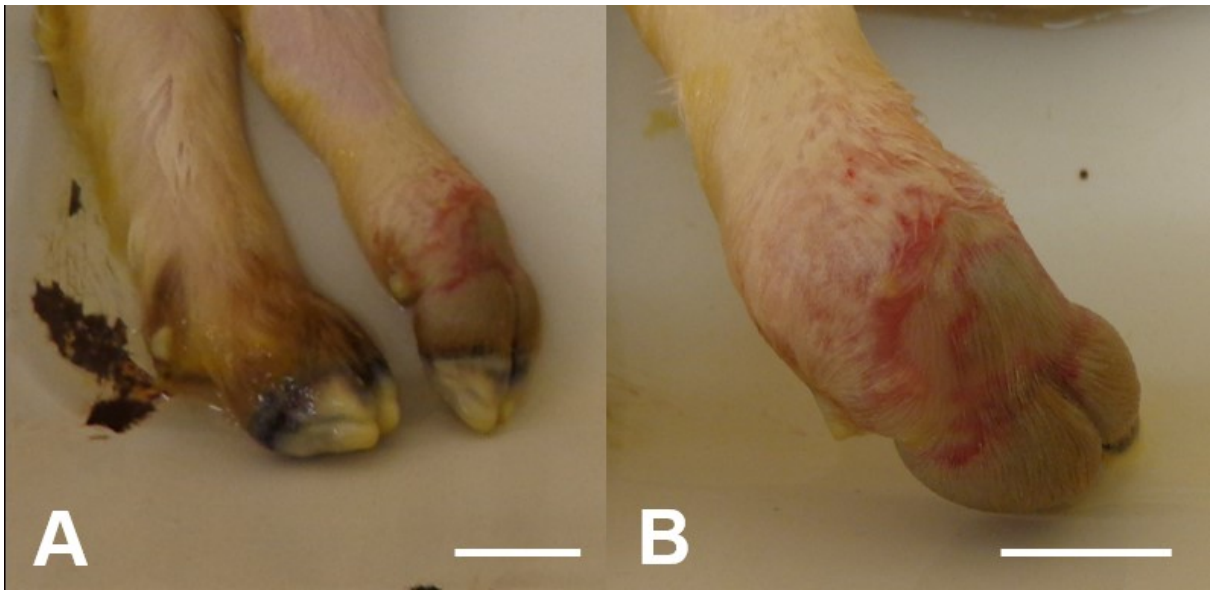

Figure 4.28: Fetal limb injury (Group R).
(A) The photograph shows the fetal hind limbs in comparison, with the one on the left side of the image uninjured and the skin burn evident on the other. (B) The photo graph shows the same burn from the anterior aspect, enlarged. This resulted from 5 HIFU exposures of 2.4 $kW.cm^{-2}$ estimated in situ intensity, 5 s duration, 2 mm spaced, target depth 20 mm. In both cases, the scale bar represents 1 cm.

4.6.2.3 **Maternal burns**

As previously noted, there was one maternal skin burn (rate 2%) and 6 instances of maternal skin erythema, all of which had faded by the end of surgery, (rate 10%) as a result of HIFU exposing 60 vascular targets. These occurred in the first 2 animals in the group; no further protocol changes were made between these animals and the subsequent 8 animals, but there were no further instances of skin damage.

The maternal skin burn resulted from a series of 6 HIFU exposures of 2.6 $kW.cm^{-2}$ at a target depth of 22 mm, comparable to many other exposure series which did not produce a burn. The exposure series which resulted in erythema were all in a single animal, and resulted from each exposure series, 2.4 – 2.6 $kW.cm^{-2}$, 6-7 exposures, target depth 17-32 mm, again comparable to many other exposure series which did not produce this reaction.

There was one uterine burn (rate 2%) noted at the time of laparotomy (Figure 4.29a). This was not repaired at the time of surgery, and there was no evidence of uterine rupture or leak of amniotic fluid. The uterine burn was not attributable to a specific exposure series, as laparotomy was only performed after all HIFU exposures had been completed. The range of in situ intensities of HIFU exposures in this animal was 2.6 – 3.1 $kW.cm^{-2}$, target depths 23 – 40 mm. There was one successful retreatment performed in this animal.

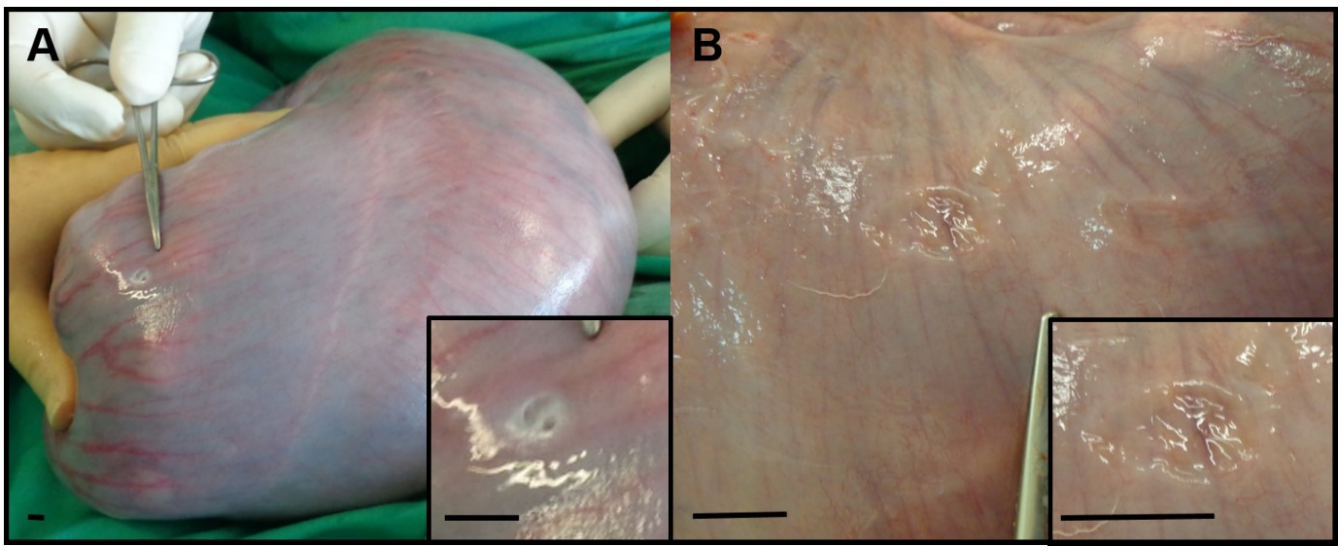

Figure 4.29: Uterine burn (Group R).
(A) The photograph shows a uterine burn immediately following HIFU exposures (noted at subsequent laparotomy – specific HIFU exposure series unknown). The inset shows a close-up of the affected area. (B) The photograph shows the same uterine burn after 21 days, demonstrating healing without rupture; the inset shows a close-up of the damage. The scale bars represent 1 cm.

4.6.3 Transdermal chronically instrumented recovery study: discussion

This group of animals once again provided evidence regarding the efficacy of using HIFU to occlude placental blood vessels in sheep placentae. The occlusion rate remained high (97%) over 60 vascular targets despite a further de-escalation of drive voltage in an attempt to reduce side effects. The median estimated in situ intensity or HIFU exposure series was 2.6 (IQR 2.5 – 2.9) $kW.cm^{-2}$ in this animal group compared to Group S: 2.9 (IQR 2.5 – 3.1) $kW.cm^{-2}$. This not only represents a reduction in the amount of energy delivered to the tissues, but the narrowing of the interquartile range suggests an increased consistency in the amount of energy delivered to tissues, also notable when the relative frequencies of estimated in situ intensities resulting in successful occlusion in Group S (Figure 4.20) and Group R (Figure 4.27) are compared. In fact, in Group R, some successful vascular occlusions were produced with estimated in situ intensities of 1.8 $kW.cm^{-2}$. This suggested the previously therapeutic window of 2.5 – 3.5 $kW.cm^{-2}$ may still represent overtreatment.

The rate of initial HIFU exposure series which produced occlusion was also high: 55/60 (92%). With the reduction in skin burns, however, there were 4 repeat exposures of target vessels following failed occlusion. As previously discussed, 3 of these were to correct mistargeting – effectively exposing a new area of target tissue – and were successful. The fourth repeat exposure was unsuccessful, and it cannot be excluded that this retreatment of the same tissue volume resulted in a uterine burn. Given the cause of the original failure remains unclear, and there was nothing to correct in the application of the HIFU, it is perhaps unsurprising that the repeated treatment of the same vascular target failed. This was one of the larger vessels treated in this, or any group, of animals, but not larger than what had previously been occluded. The C-STAR was 2.9 in this target, and hyperecho was seen, which suggests that with an estimated in situ intensity of 3.2 $kW.cm^{-2}$ delivered, the target should have received sufficient energy. It is possible that a combination of a larger vessel, closer to common umbilical cord meant that the vessel had higher flow than others selected for occlusion, increasing the cooling effect on the tissue, but this remains speculative at best.

Hence, the evidence regarding retreatment following failed occlusions remains mixed and based on small numbers: where there is a clear error to correct, this is likely to be effective and safe, but where there is no apparent cause of failure, delivery of repeated energy to the tissue may be at best ineffective and at worse damaging to surrounding tissues. Given these findings, there is insufficient evidence to make a recommendation regarding retreatment and further investigation is needed.

This animal group provided further evidence regarding survival following HIFU placental vascular occlusion. This group was always going to be high risk: complications with chronically instrumented fetal sheep preparations are recognised, although not widely reported. Postoperative complications such as non-recovery from anaesthesia, haemorrhage, infection and wound dehiscence should be anticipated, akin to any other form of major abdominal surgery. Similarly, invasive monitoring equipment, particularly intravascular lines cannot be maintained indefinitely free of infection or clot in the human clinical setting. However, in the animal setting, repeated anaesthesia to change lines was not permitted under the project licence, and would represent too great a deviation from the experimental recovery protocol to be allowable. For these reasons, 100% survival of this animal group was never anticipated, and was not achieved. However, as explained in section 4.6.1.2, the reasons animals were removed from this group relate to known complications of surgery, post-operative recovery, and the difficulties of keeping intravascular catheters patent, rather than complications of HIFU. While unsatisfactory to have only 6 of 10 animals complete the 20 days follow-up, the evidence from Group S is that, when not subjected to invasive surgical procedures, 100% survival should be anticipated following HIFU exposures.

Another notable feature of the HIIFU exposure series in this group of animals is that there were no system errors. The failed occlusions resulting from mistargeting and the fetal burn were all the result of human errors in target selection in planning of HIFU exposure series. Subjectively, these errors were the result of the increased time pressure to occlude six placental vessels within the allotted 1.5 hours allowed in the experimental timeline. Equally, the lack of system errors was likely the result of increased familiarity with the capabilities and restrictions of the HIFU system, as no software or hardware alterations were made between this and other groups. This meant that the rates of iatrogenic harm are more likely to accurately reflect the risk of complications.

Reassuringly, in this group of animals compared to the previous transdermal bridging and survival groups, the rate of maternal skin burns was reduced. The rate of skin burns was 2% in this group, compared to 11% in Group S. The overall rate of burns and erythema in Group R was 11%. For a common HIFU complication such as superficial skin burns a rate of at least 2%, would not be unreasonable, although 11% would be higher than expected (section 1.2.5). All of the instances of erythema occurred in a single animal in Group R, there was erythema as a result of each exposure, and the reaction was short lived (< 2 h). This raises the possibility that there are unknown conditions which will render individual subjects vulnerable to skin damage regardless of safety limits placed on the application of HIFU.

It remains clear, that despite the safety protocols introduced and the increased experience of application of HIFU to occlude placental vessels, the process of applying HIFU to placental vessels will not be risk free. The risk of uterine and fetal burns cannot be excluded, and skin burns will likely be regarded as the most common complication. In these animals, while there was a uterine burn, it was in one of the animals which completed 20 days follow-up, and it is reassuring that this did not lead to either uterine rupture (although not tested during contractions) or any other obstetric complications. Similarly, the single instance of fetal injury occurred in an ewe which completed 20 days follow-up and the fetus survived for the duration of follow-up, with no indication of the injury from the measures taken until the time of post-mortem examination.

The risk of fetal and maternal injury are not confined to HIFU: both maternal and fetal harm have resulted from fetoscopic laser ablation of placental anastomoses. Combined rates of injury to maternal bowel, uterine blood vessels, trans-placental entry and intra-amniotic haemorrhage of up to 8% are reported (287, 288), although most authors report no significant perioperative complications. As in our study, while these complications were recorded, they did not increase rates of pregnancy loss or affect fetal survival. There are also case reports of fetal injuries to abdominal wall (289) in which the fetuses survived until delivery and a 1-2% incidence of damage to limbs (290). Again, there is uncertainty regarding which injuries can be attributed to ischaemia and which to direct laser damage (291-293), but fetal damage subsequent to accidental laser exposure is at least feasible.

With regards to translation into human studies, this group of animals confirmed the high efficacy of HIFU to occlude placental vessels in sheep. This was achieved at lower estimated in situ intensities than in any other study group, and operator error notwithstanding, mitigated many of the side effects of excessive energy delivery to tissues. The addition of a standard set of safety protocols which did not alter during the study group also contributed to this reduction in iatrogenic harm, though as previously discussed could not remove all risks associated with the procedure. However, collection of data regarding the safety and efficacy of retreatment and exposure conditions which resulted in vascular haemorrhage or fetal injury had been opportunistic in this and all previous study groups. Therefore, while these remain important questions before translation of the technique, the high rates of occlusion and measures introduced to prevent fetal damage or vessel haemorrhage had hampered efforts to collect data in these areas.

4.7 Specific safety study

At the outset of the project, some key concerns regarding safety of HIFU treatment were raised from the review of published literature (section 1.2.5). These concerns regarded:

(i) the safety of repeat HIFU treatments to the same tissue volume;
(ii) the minimum distance required between the HIFU focus and the fetus to prevent post-focal damage;
(iii) the risk of haemorrhage from targeted vessels if exposed but not occluded.

While there had been some opportunistic data collection in these areas in earlier phases of the project, there had a no deliberate attempt to cause iatrogenic harm. These concerns would need to be addressed, not least by regulatory bodies or ethics committees, before considering translating the technique into humans. The aim of this final animal group, therefore, was to provide additional data, by systematically planning exposure series designed to answer these questions, rather than show the efficacy of HIFU as a method of vascular occlusion.

This phase of the project was a late addition to the overall design of work, as the potential of the technique became apparent, and was therefore animal number was particularly limited by both time and financial constraints. As such, the data generated were not exhaustive, but rather to give pilot data for any future human translational project, which would likely include a further pre-clinical safety testing phase of updated equipment and treatment protocols.

4.7.1 Methods

4.7.1.1 HIFU therapy system

The system described in section 4.2.1.1 was used.

In the first 2 of 4 animals in this group, the water in the water bag was taken cold from the tap and cooled with ice sealed in plastic (so the melting ice water did not mix with degassed water in the bag) and was degassed before each HIFU exposure series. In the subsequent 2 of 4 animals, the water was continually cooled and degassed using a water cooling unit (HC-100A, Hailea, Guangdong, China) in conjunction with the previously described degassing system.

4.7.1.2 **Animals and surgical methods**

Four pregnant ewes carrying singleton fetuses at 110.5 ± 5.5 d gestational age were placed under general anaesthesia (sections 3.2.1, 3.2.2).

In the first 1 of 4 animals the uterus was exposed through a midline laparotomy and the surface of the uterus was wet with degassed water, then the waterbag was placed in direct contact with that area. Any pockets of trapped air between the plastic of the waterbag and the surface of the uterus were smoothed out. HIFU exposures were performed through the intact uterine surface; no uterine incisions were performed.

In the remaining 3 of 4 animals the maternal abdominal skin had been shaved with clippers 24 – 48 hours previously to remove wool. Following induction of anaesthesia, the skin was washed with iodine scrub solution to remove dirt and lanolin, and washed again with tap water. The remaining hair was chemically depilated (Nair ® hair removal cream, Church & Dwight Co., Kent, UK), the skin was washed for a final time with tap water and coated with degassed water. The waterbag was placed in contact with the maternal skin and trapped air between the plastic and the skin was smoothed out. If the waterbag was repositioned, the layer of degassed water on the skin was replaced, and air pockets were smoothed out again. HIFU exposure series were carried out through intact maternal skin. In all 3 of these animals, once the placental vessels which could be targeted transdermal had be occluded, a midline laparotomy was performed in order that the uterus could be manipulated. HIFU exposures were then performed transuterine as described in the paragraph above.

Breath holds were performed during each HIFU exposure series (section 4.2.1.2).

All fetuses were assessed with ultrasound at the planned end of the HIFU exposures to determine presence or absence of fetal heart pulsations. Non-invasive maternal recording of maternal heart rate was used to confirm maternal survival to the planned end of the experimental procedure.

On completion of the HIFU exposures the ewe and fetus were euthanised without recovery from general anaesthesia under schedule one of the UK Animals (Scientific Procedures) Act 1986, as per section 4.2.1.2.

4.7.1.3 **Experimental protocol: safety of repeat HIFU treatments of target vessels**

Assessing the safety of repeat HIFU treatments required a two-pronged approach. Thus far in the various study phases, HIFU exposure series had failed to result in vessel occlusion due to targeting or technical errors, or for unknown reasons.

In the event of a targeting or technical error (section 4.2.1.5), it could not be assumed that the planned amount of acoustic energy had been delivered to the target vessel. In some cases, as described, it was likely that either no energy or a reduced amount of acoustic energy had been delivered to the target vessel, due to targeting or technical errors. In these cases, correcting the targeting or technical error should have resulted in acoustic energy being delivered to a different target volume to the first series. While iatrogenic harm could still result from the first HIFU exposure series which had been either planned or delivered incorrectly, there was no logical reason to assume a second exposure series delivered to a different (if nearby) target volume would compound that harm. Data about these kinds of retreatments had been collected opportunistically in the previous transdermal survival, chronically instrumented and transuterine safety and efficacy studies, so it was decided not to simulate this type of failure and retreatment further given the limited availability of resources.

However, in the target vessels where there was no attributable cause for failure, the hypothesis was that the planned acoustic energy had been delivered to the target vessel in full, as no technical or targeting error to prevent this happening could be identified. As the initial HIFU exposure series had been correctly planned, it was delivered again in the same 3D positions as determined by the mechanised gantry arm/positioning system, using 1 dBm higher drive voltage, unless -5 dBm (maximum) had already been used in the first instance, when -5 dBm was used again. This doubling (at least) of acoustic energy delivered to the same target volume had the theoretical potential to cause iatrogenic harm, and more data was needed. As it was not possible to simulate this kind of failed occlusion (by definition, the causes remained unknown) accidental repeat treatment of an already occluded vessel was simulated instead, as a worst-case scenario.

HIFU was applied transuterine to 3 vascular targets in 1 animal and transdermal to 2-3 vascular targets in 3 animals (3 per animal, n=2; 2 per animal, n=1). HIFU exposure series were based on the transdermal chronically instrumented protocol. All the safety limits described in section 4.6.1.3 were adopted, with the exception that the depth of the target vessel beneath the skin was used to select a drive voltage which should deliver exposures of an estimated in situ intensity 3.0 – 4.5 $kW.cm^{-2}$ to the target volume. This was a higher range than in the previous

transdermal studies, but exposures with predicted in situ intensities > 5.0 $kW.cm^{-2}$ were still not planned. HIFU settings used were: drive voltage -5 to -7 dBm, free field intensity 4.1 – 6.7 $kW.cm^{-2}$, 5 s exposure duration, 5 s intervals between exposures, placement of exposures following the "limited" pattern.

A first HIFU exposure series was delivered to the target vessel as per previous studies, and success or failure of vascular occlusion was assessed by comparison of pre- and post-HIFU colour flow Doppler (section 0). "No flow" on post-exposure colour flow Doppler in this setting signified not only that the vessel was occluded, but also that an adequate amount of acoustic energy to occlude a blood vessel had been delivered to the intended target volume. If residual flow was seen following the first HIFU exposure series, that vascular target was retreated, if allowable, as per previous protocols (section 4.5.1.6) and its results were added to the targeting/technical or unknown cause of failed occlusion subgroup as described above.

Following confirmation of "no flow" a second HIFU exposure series was delivered to the target vessel, to simulate accidental repeat treatment of an already occluded vessel. The drive voltage used in the second series was the same as selected for the first. The mechanised gantry arm was used to deliver HIFU exposures to the same 3D position; the gantry arm precision of positioning was better than 1 mm. Colour flow Doppler was then used to assess the vascular target again for any new signals when compared to the previous post-exposure imaging, which could represent haemorrhage. Treatment monitoring was otherwise as described in section 4.3.1.5.

Outcomes of these repeated exposure series were assessed by comparison of pre- and post-first and second HIFU exposure series as described above. A post mortem examination was performed following the end of all planned exposure series in these animals (0.5 – 4 h after the exposure series described) and placentomes which received repeated exposures were examined for any evidence of haemorrhage into surrounding allantoic membranes, excised, bisected and retained for histological examination with H&E stain.

4.7.1.4 **Experimental protocol: safety of HIFU exposures near fetal parts**

Following the demonstration in the pilot study and Group R of the vulnerability of the fetus to post focal HIFU damage, planning HIFU treatments away from fetal parts had been an important safety feature of all subsequent protocols. In our study design this was possible, as the high number of placentomes provided a choice of vascular targets, such that typically 6 could be selected away from the fetus, any placental blood vessel being as suitable a target as

any other. However, the reality of the clinical situation is that the AVAs crossing the placental equator would need to be occluded, not simply the placental blood vessels easiest to target. It was therefore important to understand how close to the fetus the HIFU focus could be targeted before there was evidence of fetal injury. Such information would dictate the exclusion criteria with regard to fetal positioning relative to the target vessels in any future human study.

HIFU was applied transuterine to 15 vascular targets in 3 animals (5 per animal, n=3) and transdermal to 6 vascular targets in 2 animals (3 per animal, n=2). HIFU exposure series were based on the transdermal chronically instrumented protocol. All the safety limits described in section 4.6.1.3 were adopted, with the exception that vascular targets above fetal parts were selected rather than excluded. HIFU settings were: drive voltage -5 to -8 dBm, free field intensity 3.2 – 6.7 $kW.cm^{-2}$, 5 s exposure duration, 5 s intervals between exposures, placement of exposures following the "limited" pattern.

Vascular targets above identifiable fetal parts were selected and HIFU exposure series were planned as per the chronically instrumented protocol. Only one exposure series was performed near the identified fetal part. Success or failure of vascular occlusion was assessed by comparison of pre- and post-HIFU colour flow Doppler (section 4.2.1.4). "No flow" on post-exposure colour flow Doppler signified that an adequate amount of acoustic energy had been delivered to the intended vascular target, and as such implied that any resultant fetal damage was post-focal and not the result of mistargeting.

Offline analysis of saved imaging was performed as described in section 4.3.1.5. The linear distance (parallel to the direction of sound) was measured between the intended target (marked by the ultrasound cursor) and the uppermost surface of the nearest fetal part (section 4.2.1.5); this is reported as the distance to fetus.

Fetuses were examined at post mortem for evidence of burns; sites of potential injuries which had previously been identified on ultrasound and were examined with care. Burns were linked to specific HIFU exposure series in this way. If damage to the fetal skin was found, the skin was excised to examine if there was injury to the underlying tissues. Fetal injuries were then categorised into fetal skin burns – where the injury was confined to the skin – or fetal damage, where underlying tissue was also injured (Figure 4.30). It was not possible to report skin erythema as the experiments were non-recovery and the uterus was not opened until post-mortem, so resolution of erythema had either already occurred by the time of post-mortem examination (and was therefore missed), or was seen as a permanent change without time for healing.

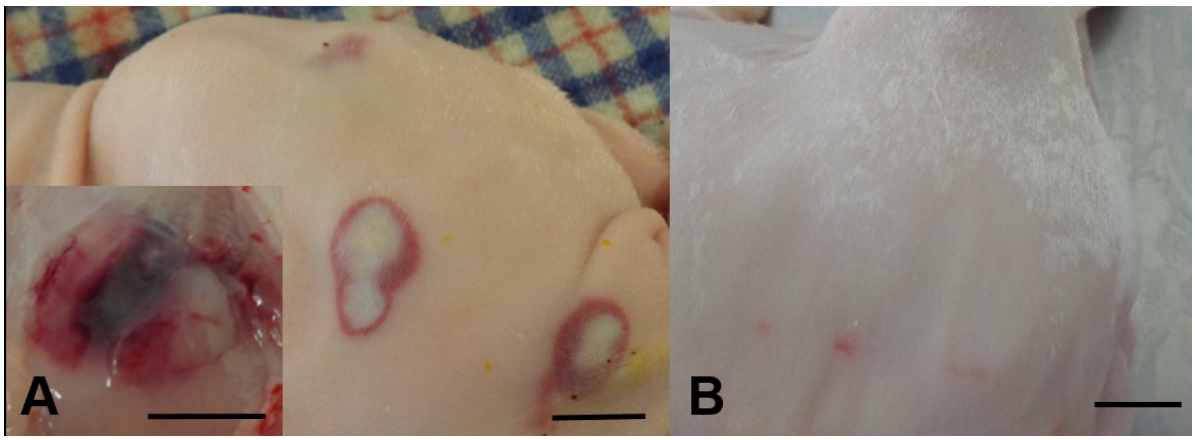

Figure 4.30: Classification of fetal injury.
(A) Photograph showing burns which resulted in injury classified as fetal damage; the inset shows extension of the damage into the subcutaneous tissues and muscles. HIFU exposure series: 6 exposures, estimated in situ intensity 3.6 kW.cm^{-2}, 5 s duration, target depth 7 mm, linear distance from fetus 13 mm. (B) Photograph shows areas of reddening on the skin classified as skin burns, with no damage to underlying tissues. HIFU exposures: 6 exposures, estimated in situ intensity 3.8 kW.cm^{-2}, 5 s duration, target depth 31 mm, linear distance from fetus 22 mm. In all cases the scale bars represent 1 cm.

4.7.1.5 **Experimental protocol to assess risk of vascular haemorrhage**

There were three potential methods by which HIFU exposure of vessels could cause vessel haemorrhage to occur.

The first potential method is the delivery of excessive energy to the vessel, causing vessel wall rupture. Two potential incidences of the had been observed in the pilot study (Figure 4.15a-c) associated with very high in situ intensity exposure series (6.4 and 7.0 kW.cm^{-2}). No further instances of this had been observed since the upper limit of 5.0 kW.cm^{-2} was imposed on planned HIFU exposure series.

The second potential method is repeat exposures of the vessel wall to HIFU causing rupture. This had not been observed in any of the retreatments in the previous animal groups. The risk of retreatment causing haemorrhage will also be further addressed by the experimental protocol described in section 4.7.1.3.

The third potential method is by under-treatment of the targeted vessel, delivering sufficient energy to damage the vessel wall but not enough to result in vascular occlusion. The vascular haemorrhage reported in the Group A animal group was thought to be due to the non-movement of the gantry arm. While the in situ intensity delivered to the tissue in this case (4.9 kW.cm^{-2}) was higher than eventual therapeutic window established in Group R, the C-STAR < 1 due to the technical error, suggesting a spatial under-treatment, which could have caused vessel wall damage without resulting in occlusion. This raised the possibility that the way in which the HIFU energy was applied to the vessel was at least as important as the amount of

energy delivered to the tissue. However, there were other HIFU exposure series with C-STAR < 1 which had not resulted in haemorrhage.

HIFU exposure series which mimicked these undertreatments were therefore planned, with the intention to monitor for signs of haemorrhage by ultrasound imaging.

HIFU was applied transuterine to 9 vascular targets in 3 animals (3 per animal, n=3) and transdermal to 2 vascular targets in 1 animal. HIFU settings used were: drive voltage -5 to -7 dBm, free field intensity 4.1 – 6.7 $kW.cm^{-2}$, 5 s exposure duration, 5 s intervals between exposures, 3 exposures in each series. The 3 exposures were all delivered to the same 3D position in the centre of the echolucent area, resulting in a C-STAR <1. In situ intensities were planned to be in the range 2.5 – 5.0 $kW.cm^{-2}$. Exposures with predicted in situ intensities > 5.0 $kW.cm^{-2}$ were not planned and vascular targets above fetal parts were not selected; no other safety features from previous protocols were adopted.

Pre- and post-HIFU exposure colour Doppler imaging was compared for evidence of persistent, absent or altered colour flow signal following these exposures. A post mortem examination was performed following the end of all planned exposure series in these animals (0.5 – 4 h after the exposure series described) and placentomes which received these “under-treatment” exposures were examined for any evidence of haemorrhage into surrounding allantoic membranes, excised, bisected and retained for histological examination with H&E stain.

4.7.2 Results

4.7.2.1 **Safety of repeat HIFU treatments to the same target volume**

A total of 11 vascular targets were selected. The drive voltages were between -5 to -7 dBm, estimated in situ intensity 3.0 – 4.0 $kW.cm^{-2}$. Exposure series were composed of 6-7 HIFU exposures, 2 mm spaced. The mean depth of the target vessel was 19 mm (SD ± 6 mm). Both in situ intensity and exposure number were at the higher end of previously quoted ranges in the transdermal studies. There were no skin, uterine or fetal burns, or vessel haemorrhages resulting from these exposures.

Of these, 8 repeat HIFU exposure series of the target vessel (3 transuterine, 5 transdermal) – after the first exposure series had resulted in successful vascular occlusion based on colour flow Doppler comparisons – were performed. In 3 targeted vessels (all transdermal), the first exposure series resulted in failed vascular occlusion for unknown reasons, and a second

exposure series at the same or an increased drive voltage (other parameters unchanged) resulted in successful occlusion based on colour flow Doppler comparisons.

Eleven damaged placentomes were retrieved and examined histologically. There was evidence of trapped erythrocytes suggestive of occlusive clot within the lumen of vessels in all 11 placentomes. Tissue changes associated with heat fixation and extravasation were seen in all 11 placentomes, and in 1/11 placentomes was there evidence of tissue boiling and discrete clot formation, despite an estimated in situ intensity of 3.5 $kW.cm^{-2}$. (Figure 4.31). There was no evidence of excessive placental soft tissue damage in the other 10/11 placentomes.

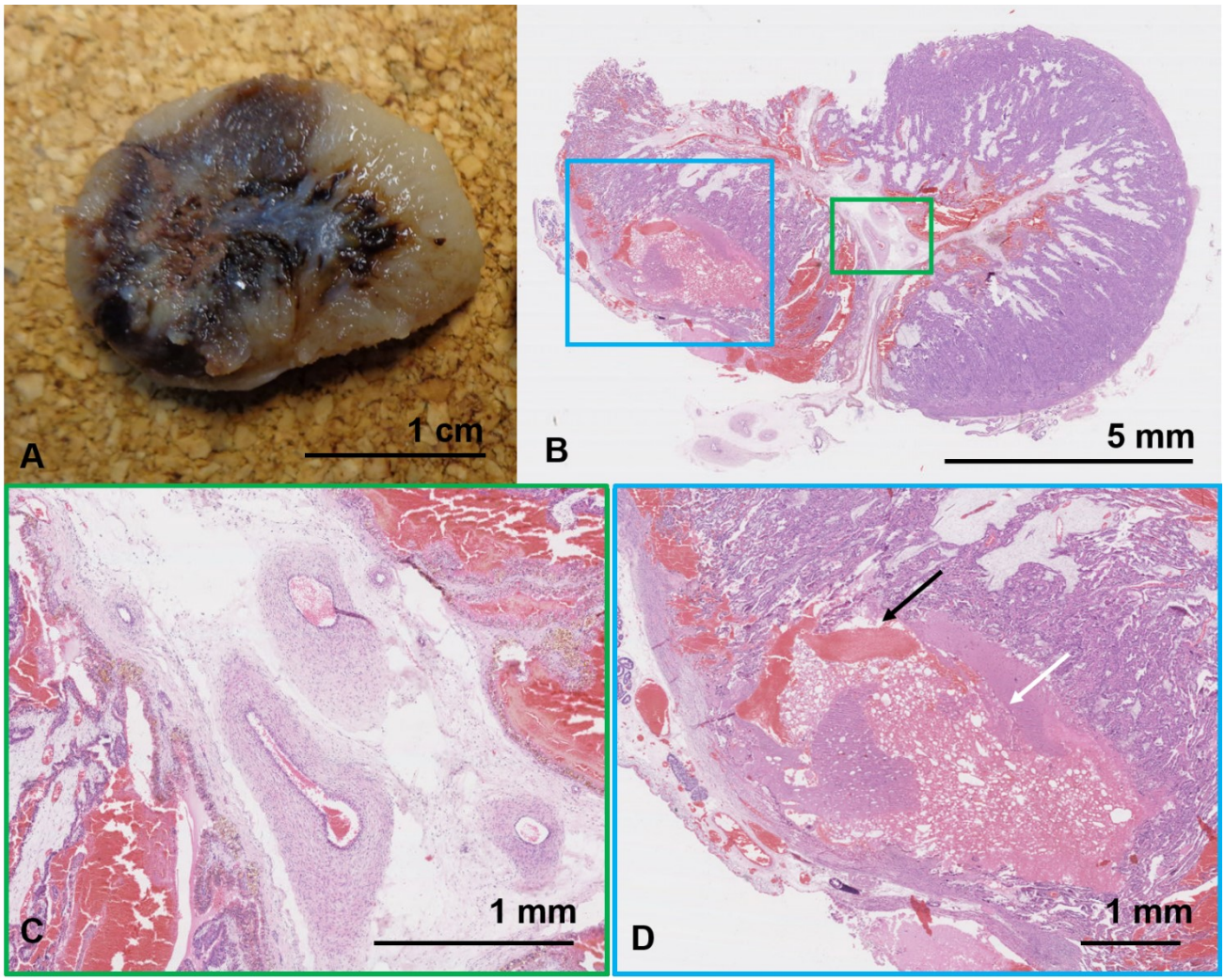

Figure 4.31: Macroscopic and histological consequences of vessel retreatment.
(A) Placentome bisected on the same day as exposure to 2 HIFU exposure series, and photographed after 24 h to improve visual contrast. There is an area of tissue darkening extending into the origin of the placental vessels, with a central area of paling and extensive tissue damage. (B) H&E stained section of tissue from the same placentome. The area in the green box is enlarged in panel (C) and shows trapped erythrocytes within target vessels suggestive of occlusion. The area in the blue box is enlarged in panel (D) and shows an area of tissue boiling (white arrow) and discrete tissue haemorrhage (black arrow) corresponding with the areas showing the greatest visual damage in panel A. The target vessels and placentome were exposed to 2 HIFU exposure series of 6 exposures, estimated in situ intensity 3.5 $kW.cm^{-2}$, 5 s duration, target depth 21 mm.

Study Group	Exposures							Vessel size (mm)	Reason for failure (error type)	Successful retreatment
	Applied through	Exposure series to target	Power (dBm)	In situ Intensity ($W.cm^{-2}$)	Depth of target (mm)	Number of exposures	C-STAR			
A	Uterus	1st	-5.0	5.0	15	5	0.3	1.1	targeting, 10 mm, z axis, 9 mm y axis	
		2nd	-5.0	4.8	17	5	2.5	1.1	-	Yes
		1st	-5.0	5.4	14	5	0.6	2.4	technical: gantry non movement	
		2nd	-5.0	5.4	13	5	1.9	2.4	unable to control haemorrhage	No
		1st	-5.0	4.5	20	6	0.6	2.2	unknown	
		2nd	Not performed - insufficient time in treatment protocol remaining						-	No
		1st	-5.0	5.2	12	3	1.0	1.0	unknown	
		2nd	-5.0	5.5	9	2	0.6	1.0	unknown	No
		1st	-8.0	2.9	5	5	2.0	2.9	targeting: 8mm, y axis	
		2nd	-8.0	2.9	5	6	2.4	2.9	unknown	No
		1st	-8.0	3.2	18	6	6.4	2.1	unknown	
		2nd	Not performed - missed in real time							No
		1st	-7.0	3.1	14	4	5.1	1.0	technical: cavitation in waterbag	
		2nd	-7.0	3.1	15	5	6.6	1.0	-	Yes
S	Skin	1st	-6.0	3.0	17	5	3.2	c	unknown	
		2nd	-6.0	3.1	15	5	3.2	c	-	Yes
		1st	-9.0	1.3	23	4	1.7	0.9	technical: emergency stop activated, drive voltage accidentally set too low	
		2nd	Not performed - skin erythema					-		No
		1st	-7.0	2.4	17	3	1.7	0.7	technical: software crash	
		2nd	Not performed - skin erythema					-		No
		1st	-5.0	4.3	10	7	9.4	0.8	targeting: 14 mm, z axis	
		2nd	Not performed - skin burn					-		No
		1st	-5.0	4.1	30	6	5.0	c	targeting: 10 mm, z axis	
		2nd	-5.0	3.9	40	6	5.0	c	-	Yes
R	Skin	1st	-6.0	2.7	27	7	3.0	c	unknown	
		2nd	-5.0	3.9	22	6	2.5	c	unknown	No
		1st	-5.0	3.8	24	6	2.9	c	unknown	
		2nd	Not performed - missed in real time					c		No
		1st	-6.0	2.5	28	5	3.6	c	targeting: 5 mm axis	
		2nd	-5.0	3.3	23	5	4.2	c	-	Yes
		1st	-5.0	2.4	40	4	0.9	c	targeting: 9 mm, z axis	
		2nd	-5.0	2.7	31	6	1.5	c	-	Yes
		1st	-7.0	2.8	18	6	1.5	c	targeting: 10 mm, z axis	
		2nd	-6.0	3.3	28	6	1.5	c	-	Yes
Specific Safety	Skin	1st	-6.0	2.7	21	6	5.6	3.0	unknown	
		2nd	-6.0	2.7	25	6	5.6	3.0	-	Yes
		1st	-6.0	2.5	29	6	5.0	0.6	unknown	
		2nd	-5.0	2.9	29	6	5.0	0.6	-	Yes
		1st	-6.0	2.3	16	6	2.8	2.3	unknown	
		2nd	-5.0	3.0	17	6	2.8	2.3	-	Yes

Table 4.7: Summary of failed occlusion and retreatments.
The table shows the characteristics of the first and, if attempted, second HIFU exposure series in target vessels from Groups A, S, R and the specific safety group where there was initially a failed occlusion. The reason, if known, for this failed occlusion is given, and whether the retreatment resulted in successful occlusion. Key: 'c' denotes that the histological vessel size could not be linked to a specific HIFU exposure series.

Although these results have previously been described in the relevant sections, the 17 failed occlusions and 11 retreatments in Groups A, S and R animals are tabulated together with the 3 failed occlusions and retreatments in the specific safety group (Table 4.7).

There were 7 failed occlusion which were classified targeting errors. In one a retreatment could not be attempted as a skin burn was present. In the other placentomes 5/6 (83%) of these were successfully occluded after correction of the targeting error.

There were 4 failed occlusions as a result of technical errors, and only 2 were eligible for retreatment: 1/2 (50%) were successfully occluded after correction of the technical error.

Of the remaining 9 failed occlusions, it was not possible to identify a targeting or technical error, and 6 were suitable for retreatment. Of these, 4/6 (67%) were successfully occluded following a repeat HIFU exposure series.

This gives an occlusion rate of 10/14 (71%) following retreatment, and an overall successful occlusion rate following an initial failed occlusion of 10/20 (50%).

There was one fetal burn and one instance of vascular haemorrhage as a result of the exposure series in Table 4.7, and possibly one uterine burn. There was one skin burn and two instances of skin erythema.

4.7.2.2 **Safety of HIFU exposures near fetal parts**

In all groups after the pilot study, exposure series were planned to avoid fetal injury by selecting vascular targets more than 40 mm from fetal parts visible on ultrasound imaging, and excluding vascular targets where this could not be achieved. This was a highly successful strategy in avoiding fetal injury: in 153 HIFU exposure series in 21 animals there was only one recorded accidental fetal injury (rate 0.7%), a burn to the fetal hind limb (Figure 4.28). The fetal hind limb was closer than had been recognised at the time: the fetal distance, measured as described in the methods, was 9 mm from the vascular target.

In this animal group, HIFU mediated vascular occlusion was attempted in 21 vascular targets that were between 4-48 mm above the nearest fetal part. Drive voltages ranged from -5 to -8 dBm; the median estimated in situ intensity was 3.6 $kW.cm^{-2}$ (IQR 2.8 – 4.1 $kW.cm^{-2}$). The median number of exposures in a series was 6 (range 5-6) and the mean depth of the target vessels was 16 mm (SD ± 8 mm). The mean linear distance between the vascular target and

the nearest fetal part was 21 mm (SD ± 10 mm). Based on colour Doppler imaging, successful occlusion was confirmed in all 21/21 vascular targets.

Fetal damage (a burn which involved skin and underlying tissues) was found at post mortem examination in the area of the fetus nearest to 7/21 target vessels. A fetal skin burn (without involving underlying tissues) was found on the nearest fetal part to a further 5/21 target vessels. The relationship of the estimated in situ intensity delivered to the target vessel and the linear distance from the fetus is shown in Figure 4.32. Fetal damage was more likely to occur when the vascular targets were located nearer the fetus, or when higher estimated in situ intensities were delivered to the target tissues. No fetal skin burns or damage resulted from occluding vascular targets more than 25 mm from the fetus; there were no instances of fetal damage resulting when estimated in situ intensities of below 3.0 kW.cm^{-2} were delivered to the tissues.

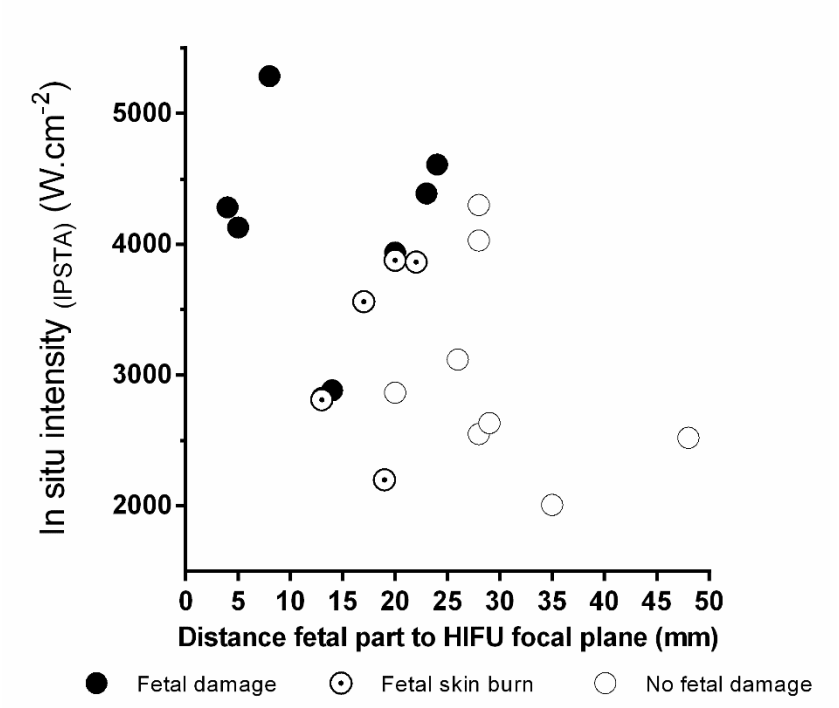

Figure 4.32: Fetal damage relative to distance from HIFU focal plane.
The graph shows type of fetal damage relative to in situ intensity and distance from the fetus (measured parallel to the direction of sound).

4.7.2.3 **Risk of vascular haemorrhage**

A total of 11 vascular targets were included in this subsection of the study (9 transuterine, 2 transdermal). The drive voltages were between -5 to -7 dBm, estimated in situ intensity 2.7 – 5.0 kW.cm^{-2}. Exposure series were composed of 3 exposures, all delivered to the same 3D location with precision of better than 1 mm. The median treatment area ratio was 0.4 (range 0.2

– 0.7). The mean depth of the target vessel was 19 mm (SD ± 6 mm). There were no skin burns in the 2 transdermal exposures, and no uterine or fetal burns resulting from any of these HIFU exposure series.

Based on comparison of pre- and post- colour Doppler imaging, 4/11 (36%) of these HIFU exposure series resulted in successful occlusion and 7/11 (64%) resulted in failed occlusion. There was no evidence of vascular haemorrhage in any of the 4 placentomes where colour Doppler had indicated successful occlusion. There was, however, visual evidence at post mortem (blood in the allantoic membranes) of haemorrhage in 4/7 (57%) vessels where persistent colour flow Doppler signals suggested a failed occlusion.

It was not possible to determine, even on retrospective examination of stored imaging, differences between the persistent colour flow Doppler signal of failed occlusion and vascular haemorrhage in this experimental animal group.

In addition to these 11 deliberate under-exposures, there were 7 undertreated (C-STAR <1) vascular targets in Group A (transuterine). The undertreatment was either due to an error in the movement of the mechanical gantry arm (2/7), or because the planned movement of the gantry arm was parallel, not orthogonal, to the direction of sound (5/7).

The drive voltages of these exposure series were between -5 to -6 dBm, estimated in situ intensity 4.5 – 5.7 $kW.cm^{-2}$. Exposure series were composed of 5-7 HIFU exposures, the mean treatment depth was 14 mm (SD ± 4 mm). None of the undertreatments resulted in uterine or fetal burns. The median treatment area ratio was of these exposure series 0.5 (range 0.2 – 0.9). There was a single instance of vascular haemorrhage (1/7, 14%) in these undertreated vessels.

4.7.3 Specific safety study: Discussion

In Group S and R animals, vascular targets were not selected if there were fetal parts in the post-focal region, at any distance. Based on the ultrasound machine settings for maximum depth, and the offset of the diagnostic ultrasound probe above the maternal uterus or skin, this distance can be estimated to be a minimum of 40 mm linear separation between the HIFU focal zone and the nearest fetal part.

The additional data generated in this specific safety group suggests that HIFU exposure series are likely to result in some form of fetal damage when the separation between the fetus and central point of the HIFU focal zone < 25 mm. Based on Figure 4.32, this threshold was valid

for estimated in situ intensities in the proposed therapeutic window of 2.5 – 3.0 $kW.cm^{-2}$. While it is reasonable to expect that this minimum separation could be reduced at lower estimated in situ intensities, data is lacking to support this in our study. However, Figure 4.32 does suggest the severity of fetal injuries increased with reduction in the separation between fetus and HIFU focal plane, and at higher estimated in situ intensities. There is no published literature with which to compare this study: in Peak et al.(60), there is no report whether the single ablation of placental tissue cause fetal damage, and given that fetal targets were also deliberately ablated, this would have been hard to assess. Caloone et al. (286) report no damage to the fetus in their study ablating areas of a primate placenta during pregnancy, but the position of the fetus in relationship to the HIFU focal plane is not recorded. Similarly, in the human in utero applications of HIFU (43, 57) the target was the acardiac twin, and the proximity of the live twin is not reported, although there was no neonatal injury evident after delivery in either surviving twin.

Regardless of distance or intensity considerations, this subsection of the study serves to clearly demonstrate the severity of the fetal damage that can be cause by HIFU exposures. This study was not designed, nor ethically approved, to investigate the long-term impact of such injuries, the impact of which would likely depend of the area of the fetus affected. However, as discussed in Group R animals, one fetus had a significant injury to the fetal hind-limb, and did not show evidence of fetal distress or compromise as a result. As with other fetal injuries described following fetoscopic laser (289, 290), HIFU injury to the fetus may represent a survivable in utero insult.

These considerations underlie the need for careful case selection, identification of vascular targets, planning of HIFU exposure series and rigorous safety checks to minimise the risk of fetal damage should the technique be translated in to human use. However, the concept that a minimum separation of around 25 mm between the fetus and the HIFU focal plane would be required is not an obvious bar to translating the technique to human pregnancy. The location of the AVAs in relation to the donor twin are likely to be of key importance. The donor twin has limited space in which to move due to oligohydramnios, whereas the polyhydramnios surrounding the recipient twin means it is more likely to be able to move > 25 mm away from the vascular equator.

The minimum separation of 25 mm between HIFU focal plane and nearest fetal part is a finding that is specific to the HIFU transducer used in this study. The source geometry of a HIFU transducer – and so the intensities delivered to the post focal region - is affected by the radius of curvature of the transducer and the presence and size of a central aperture, among other

considerations. This means that in any future study with a different transducer, the minimum separation between HIFU focal plane and the fetus would need to be retested. Human applications of this technique may require a transducer with a longer focal length (implying a wider radius of curvature), or a larger central aperture to allow a larger diagnostic ultrasound probe and better ultrasound imaging of the target.

Overall, as with the consideration of excessive soft tissue damage in the placenta, maternal and uterine burns, it seems that the best strategy to avoid fetal damage is to deliver the minimum amount of ultrasound energy to the target vessel that will achieve occlusion, as far as possible from the fetus. While the distance between the fetus and HIFU plane may be difficult to control, the HIFU energy delivered to the tissues is under direct control of the HIFU operators.

Selection of the "correct" drive voltage at which to expose target vessels, in relation to their characteristics, was a concept that had evolved with successive iterations of the HIFU protocol. Initially, the highest drive voltage that could be generated safely by the HIFU therapy equipment (-5 dBm) was used (Pilot study, Group A) before an upper limit of 5.0 $kW.cm^{-2}$ was introduced to prevent against excessive soft tissue damage (Transdermal bridging study, Group S). To reduce the risk of maternal skin damage, the ratio of drive voltage to target depth was altered in Group R. This was permitted as the therapeutic window of estimated in situ intensity which would result in successful vascular occlusion in Group S (Figure 4.20) was lower than anticipated in the preceding study groups, 2.5 – 3.5 $kW.cm^{-2}$. Finally, because of the findings in group R animals, that the therapeutic window for vascular occlusion is in the region of 2.5 – 3.0 $kW.cm^{-2}$ (Figure 4.27), this ratio of drive voltage to target depth could be further reduced.

This trend to reduction in HIFU energy delivery to the target vessel raises the possibility that some vessels will be incorrectly exposed to sub-therapeutic doses of ultrasound energy, resulting in failed occlusions (although not a spatial under-treatment as defined by the C-STAR). This was not seen in Group R animals, where 92% of vessels were occluded after a single exposure series, compared to 90% in Group A. However, if further reductions in energy delivery are intended, the requirements for retreatments of the same tissue volume may theoretically increase.

As described in section 4.7.1.3, data regarding repeat HIFU exposures of the same target volume had not been opportunistically collected in any of the previous study groups. The findings of this specific safety study suggest that repeat exposures of the same target volume, even when containing blood vessels, does not increase the risk of vascular haemorrhage, or affect an otherwise successful vascular occlusion. It also does not appear to increase the risk

of maternal or fetal injury, although there is a slightly increased risk of excessive tissue damage to the surrounding placental tissue.

This suggests that if there is uncertainty about the correct drive voltage with which to expose the target vessel, a feasible alternative is a cautious approach. This would mean a potentially sub-therapeutic dose of ultrasound energy is used, with the knowledge a retreatment may be required. This may be safer than using a higher dose of ultrasound energy, with attendant increases in risk of maternal and fetal damage, although it would increase the number of HIFU exposures, and the time to complete occlusions. Conversely, the increase in number of HIFU exposures itself may increase the risk of maternal and fetal burns, so the cautious approach may be counter-intuitively more dangerous. We did not have the opportunity to test this hypothesis, which we only generated after the end of the specific safety study, in this project, but this would be an important avenue of investigation in any future pre-clinical or translational study.

Considering the retreatments performed in the first five study groups, which were required by unanticipated failure to produce vascular occlusion, the most amenable to retreatment were those that resulted from targeting errors. Overall, 83% (5/6) of vessels where successfully occluded following a correction of targeting error. While this is based on a small sample, the principle seems sound that these should be the easiest errors to correct. However, these retreatments are also associated with a higher risk of iatrogenic harm: 1 uterine burn, 1 fetal burn and 1 maternal skin burn. This harm is likely to be due to the original mistargeting, but exacerbation of the injury by a second deposition of HIFU energy near the site of the injury cannot be excluded. Therefore, once again, this finding underlies the need for rigorous, and possibly automated, safety checks in the planning and delivery of HIFU exposure series.

Successful occlusion was also possible following correction of a technical error. There were a total of 7 technical errors recorded in this study: 6 were failure of the gantry arm to complete the movements programmed, 1 was a failure to de-gas the water in the water bag adequately, such that cavitation in the waterbag was obvious during the exposures, and minimal energy was delivered to the tissues. Of these technical errors, 4 resulted in failed occlusion; 2 of these were eligible for retreatment (1 gantry failure resulting in haemorrhage, and the exposure series with cavitation in the waterbag). As a result of these technical errors, there were 2 instances of skin damage and 1 instance of vascular haemorrhage (all related to gantry non-movement). As in the discussion of targeting errors, the unplanned delivery of HIFU energy into a single location increased the risks of iatrogenic harm above the background risk.

It should be noted that in Group R, there were no technical errors in a total of 64 HIFU exposure series. Given that 7 technical errors occurred in the preceding 92 exposure series, this is a notable reduction. While it was not a formal safety protocol, we had developed the practice of using a dummy-run of the planned gantry arm movement before the planned HIFU exposure series was delivered. This demonstrates that such a safety check before delivering a HIFU exposure series, perhaps introduced as an automated procedure, should be an effective way of reducing technical errors, and guarding against the related harm and need for retreatment.

Finally, only 60% of vessels were successfully occluded following a first HIFU exposure series which failed for unknown reasons. These HIFU exposure series, unlike the failures resulting from targeting or technical errors, were not associated with any instances of maternal or fetal iatrogenic harm. This suggests that there remain unknown characteristics of vessels which have contributed to the failure of these occlusion, rather than inappropriate delivery of HIFU energy to the tissues. It is possible these vessels may have had higher flow rates, although the diameter of the vessels falls within the range of others successfully occluded, or been nearer larger vessels with a greater cooling effect, although numbers remain too small for a systematic study.

Overall, retreatment appears to be safe, if somewhat less efficacious at producing occlusion than could be expected. The findings of this specific safety study and the opportunistic collection of data regarding retreatments emphasise that the conditions which contributed to the failed occlusion, particularly if an error is recognised, need to be careful considered before embarking on a retreatment. Errors are likely to be a function of the difficultly in targeting a vessel, whether that be related to fetal position, maternal habitus, equipment functionality or time pressures, and these difficulties may contribute to an increased risk of iatrogenic harm and decreased rate of successful occlusion.

The final specific safety concern related to the risk of vascular haemorrhage. The rate of haemorrhage was low in the preceding 5 animal study groups, 3/153 (2%) with only one of those being a proven vascular haemorrhage (1/153, 0.7%). Two haemorrhages occurred in the pilot study, and one in Group A. The risk factors for haemorrhage which were identified were estimated in situ intensities > 6.0 $kW.cm^{-2}$ and undertreatment (as defined by the treatment area ratio) of the vascular target. The eventual therapeutic window of estimated in situ intensity required to achieve successful vascular occlusion fell well below the threshold of 6.0 $kW.cm^{-2}$, and so this had negligible impact on development of the HIUF treatment protocol. The safety protocols introduced into the transdermal bridging study and Group S and R animals prevented these exposure conditions from recurring, and there were no further haemorrhages observed.

These findings are supported by the fact that there was no evidence of anaemia in either the Group S animals (Figure 4.23).

The only circumstance in which vascular haemorrhage appeared to be reproducible was a spatial undertreatment of the vascular target, as defined by the C-STAR. However, even in the specific safety protocol, where these conditions were deliberately replicated, the rate of haemorrhage was 4/11 (36%), which provides some measure of reassurance that haemorrhage is difficult to cause with this application of HIFU. The proposed safety limit to reduce the risk of haemorrhage, that all HIFU exposure series were planned to start and finish in placental soft tissue bordering the echo lucent area from which vessels arise, is made possible by the mechanical gantry arm. While freehand application of the HIFU focus to the tissue would likely lack the precision to form a confluent line of HIFU exposures with millimetre precision, this is well within the capability of the mechanical gantry arm or a robotic arm. While technical errors were encountered in this study, these were issues that could be overcome with improvements to the control software used and the introduction of automated checks that planned gantry arm movements had been made before the HIFU source was fired, not a fault of the gantry system itself.

Our attempts to further investigate the exposure conditions which resulted in vascular haemorrhage, and potentially apply further HIFU treatments to control that haemorrhage, were prevented by the fact that we could not identify vascular haemorrhage using colour flow Doppler. As stated in the results, even on retrospective examination, it was not possible to determine any indicators of haemorrhage using the ultrasound imaging system available. This could have been due to limitations of the ultrasound technology, and so could be improved by use of a different ultrasound system, better attuned to vascular imaging. Equally, the flow from the area of vessel damage may have been sufficiently low flow so as not to show up on colour flow Doppler imaging.

The identification and methods of control of vascular haemorrhage remains a key area for any future pre-clinical or translational study to examine. While, as in previous safety concerns, careful planning of HIFU exposure series and rigorous safety checks to ensure the HIFU energy is delivered to the tissue as planned are an essential part of avoiding iatrogenic harm, it is unreasonable to assume that this alone will prevent vascular haemorrhage.

CHAPTER 5: CARDIOVASCULAR RESPONSES TO HIFU PLACENTAL VASCULAR OCCLUSION

5.1 **Comparison of Group A and Group R animals**

The experimental design required that invasive monitoring of cardiovascular (i) responses to, and (ii) recovery from HIFU placental vascular occlusion were conducted in different animal groups (as discussed in section 2.3). These were Group A(cute) and Group R(ecovery) respectively.

Table 5.1 shows a comparison of demographics and basic maternal cardiovascular status of ewes, subdivided by treatment group, in Group A during the last 30 minutes of the experimental protocol, and in Group R during the first 30 minutes following reversal of anaesthesia. All groups were comparable for maternal weight. The maternal heart rate was not significantly different between any of the groups. The maternal mean arterial pressure was higher in un-anaesthetised animals (Group R) in both sham/control and HIFU exposed animals when compared to the anaesthetised values (Group A).

	Sham/Control		HIFU		*p value*
	Group A	Group R	Group A	Group R	
Weight (kg)	47.6 ± 2.1	42.1 ± 2.7	42.3 ± 3.1	48.7 ± 3.1	ns
Mean arterial pressure (mmHg)	57.6 ± 3.8	90.1 ± 1.4 *	65.3 ± 3.5	82.5 ± 4.9 *	0.002
Heart rate (beats.min^{-1})	95 ± 4	114 ± 3	111 ± 7	101 ± 3	ns

Table 5.1: Maternal cardiovascular comparisons (Group A to R).
Values represent the mean ± SEM of maternal weight on the day of surgery and the mean arterial blood pressure and heart rate during the recovery period (30 min) in group A ewes, and during the first 30 min following the reversal of anaesthesia in group R ewes. Statistical significance was assessed using a one-way ANOVA with post hoc Tukey's test: * denotes a significant difference in HIFU or sham treated animals in group R animals compared to their group A counterparts with *p* values given in the table (ns = not significant, p>0.05).

Table 5.2 shows a comparison of demographics and the cardiovascular status of fetuses, subdivided by treatment group, in Group A during the last 30 minutes of the experimental protocol, and in Group R during the first 30 minutes following reversal of anaesthesia. All groups were comparable for gestational age. The duration of anaesthesia was significantly shorter in Group R control fetuses, for the reasons previously described (section 3.7.3). There were no further differences between fetal mean arterial blood pressure, heart rate, femoral blood flow or vascular resistance.

	Control		HIFU		*p value*
	Group A	Group R	Group A	Group R	
Gestational age (d)	116 ± 2	116 ± 2	116 ± 1	116 ± 1	ns
Total duration of anaesthesia (min)	235 (218 - 270)	145 * (133 - 170)	228 (215 - 247)	238 (211 - 293)	< 0.001
Mean arterial pressure (mmHg)	35.0 ± 2.0	34.8 ± 2.3	39.0 ± 1.4	34.0 ± 0.8	ns
Heart rate (beats.min^{-1})	175 ± 16	192 ± 11	169 ± 10	186 ± 9	ns
Femoral blood flow (ml.min^{-1})	23.2 ± 1.4	26.3 ± 5.1	24.1 ± 1.8	26.9 ± 2.5	ns
Femoral vascular resistance (mmHg(ml.min^{-1})$^{-1}$)	1.9 ± 0.2	1.6 ± 0.3	1.9 ± 0.3	1.5 ± 0.3	ns

Table 5.2: Fetal cardiovascular comparisons (Group A to R).
Values represent the range of fetal gestational age on the day of surgery, the median and range of the total duration of anaesthesia, and the mean ± SEM of fetal mean arterial blood pressure, heart rate, femoral arterial blood flow rate and vascular resistance during the recovery period (30 min) in Group A fetuses, and during the first 30 min following the reversal of anaesthesia in Group R fetuses. Statistical significance was assessed using a one-way ANOVA with post hoc Tukey's test: * denotes a significant difference in HIFU or sham treated animals in group R animals compared to their group A counterparts with *p* values given in the table (ns = not significant, p>0.05).

5.2 **Maternal cardiovascular responses**

5.2.1 Heart rate and blood pressure

Table 5.3 shows that maternal heart rate and mean arterial blood pressure were not affected by exposure to HIFU: the mean values were not different between HIFU and control groups, either while under anaesthesia (Group A) or after 5 days post procedure recovery (Group R). Compared to the un-anaesthetised values in Group R animals, maternal mean arterial blood pressure, but not heart rate, was reduced during the period of anaesthesia preceding the HIFU or sham exposures of placental vasculature in Group A. This reduction was of approximately the same magnitude between treatment groups.

	HIFU		Control	
	Baseline recording (A)	Day 5 post-operative (R)	Baseline recording (A)	Day 5 post-operative (R)
Mean arterial blood pressure (mmHg)	64.5 ± 0.2 *	79.0 ± 1.9	68.1 ± 0.3 *	80.6 ± 0.3
Heart rate (beats.min^{-1})	92.8 ± 0.2	107.0 ± 5.7	96.3 ± 0.2	98.3 ± 5.9

Table 5.3: Baseline maternal mean arterial blood pressure and heart rate.
Values represent the mean ± SEM of maternal mean arterial blood pressure and heart rate during the specified recording periods for HIFU (baseline, n=5; day 5, n=6) and sham/control (baseline and day 5, n=6) treatment groups. Significant differences of the effect of time and treatment group were assessed using a repeated measures two-way ANOVA. No significant differences for the effect of treatment were found, but where authorised post hoc Tukey's tests demonstrated a significant effect of time (* $p<0.001$) during the experimental protocol.

Maternal mean arterial blood pressure and heart rate remained stable (compared to baseline) throughout the application of transuterine HIFU or sham exposures of placental vasculature in Group A animals, and was not different between HIFU and sham exposed animals (Figure 5.1a). In Group S animals, maternal heart rate remained stable during transdermal HIFU or sham exposures, and again was not different between HIFU and sham exposed animals (Figure 5.1b) Similarly, in Group R animals, post-procedure 24-hour averages of maternal heart rate and blood pressure were stable for the duration of the 21 day follow-up period (Figure 5.2).

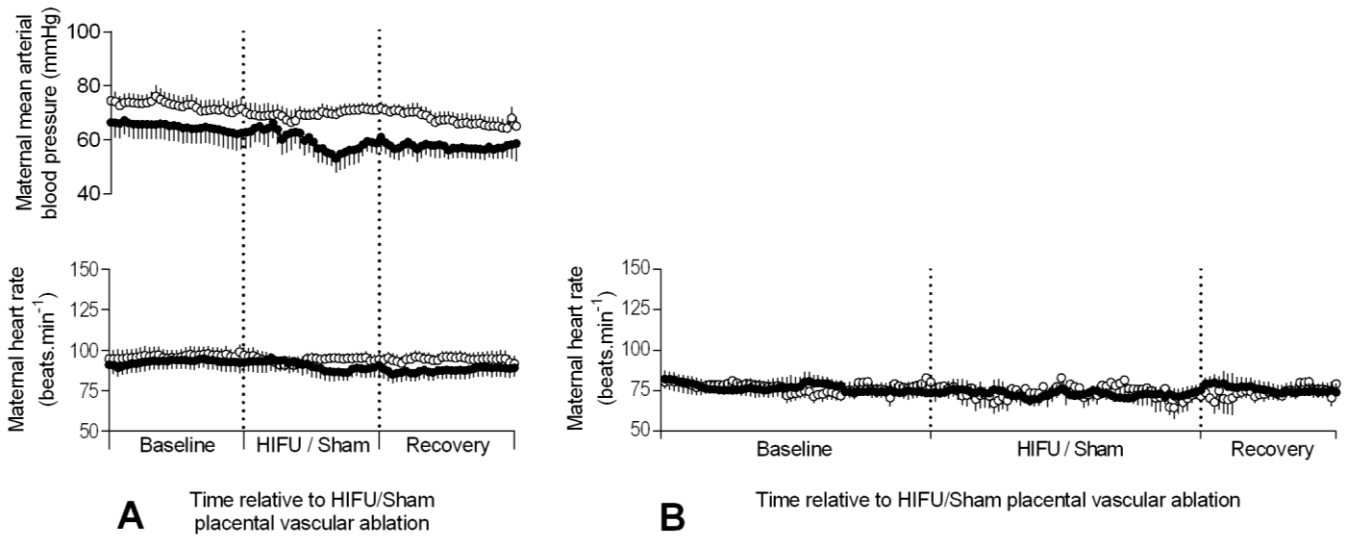

Figure 5.1: Maternal cardiovascular acute responses to HIFU placental vascular occlusion.
(A) Group A animals. Values represent the mean ± SEM of maternal mean arterial pressure and heart rate averaged over sequential 60 s intervals for HIFU (closed circles; n=5) and sham (open circles; n=6) treatment groups, measured from pulsatile flow in the maternal descending aorta arterial catheter. The baseline, HIFU/sham and recovery periods each have a duration of 30 mins, demarcated by dotted lines. (B) Group S animals. Values represent the mean ± SEM of maternal heart rate averaged over sequential 60 s intervals for HIFU (closed circles; n=6) and sham (open circles; n=6) treatment groups, measured non-invasively with a pulse-oximeter. The baseline and HIFU/sham periods have a duration of 60 mins; the recovery period is 30 mins and are demarcated by dotted lines. No significant effects of time or treatment were found using a repeated measures two-way ANOVA.

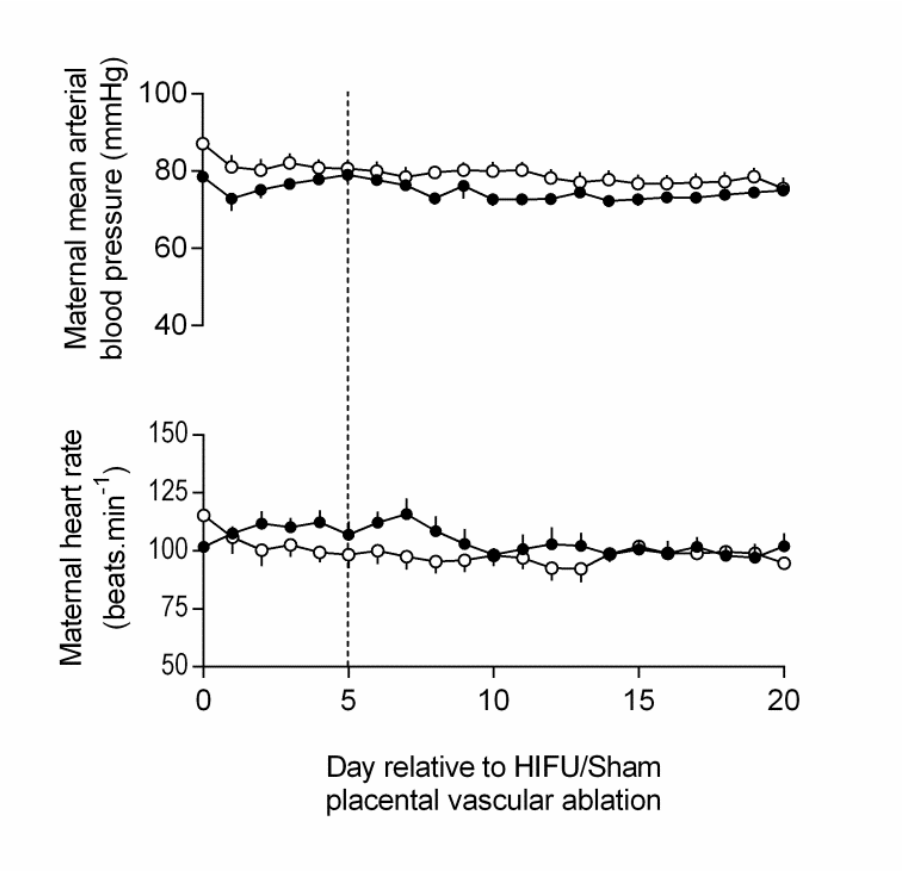

Figure 5.2 Maternal cardiovascular recovery from HIFU placental vascular occlusion.
Group R animals. Values represent the mean ± SEM of maternal mean arterial pressure and heart rate averaged over sequential 24 h intervals for HIFU (closed circles; n=6) and control (open circles; n=6) treatment groups, measured from pulsatile flow in the maternal descending aorta arterial catheter, and compared to the baseline established on day five postoperative (dotted line). No significant effects of time or treatment were found using a repeated measures two-way ANOVA.

5.2.2 Uterine artery blood flow

The mean ± SEM rate of uterine arterial blood flow in Group A ewes was the same in both treatment groups during the baseline recording period. In the HIFU exposed animals uterine blood flow was 285 ± 2 ml.min^{-1} and 276 ± 2 ml.min^{-1} in the sham exposed animals (t-test, p=0.42). During both transuterine HIFU and sham exposures, there was a further reduction in uterine artery blood flow to a nadir of up to 40% below baseline flow rates. The reduction in uterine blood flow had a similar time of onset in both HIFU and sham exposures, and corresponded with the start of a period of gentle uterine manipulation in both treatment groups. The magnitude reduction was not different between treatment groups, and returned to baseline during the recovery period, while still under general anaesthesia (Figure 5.3).

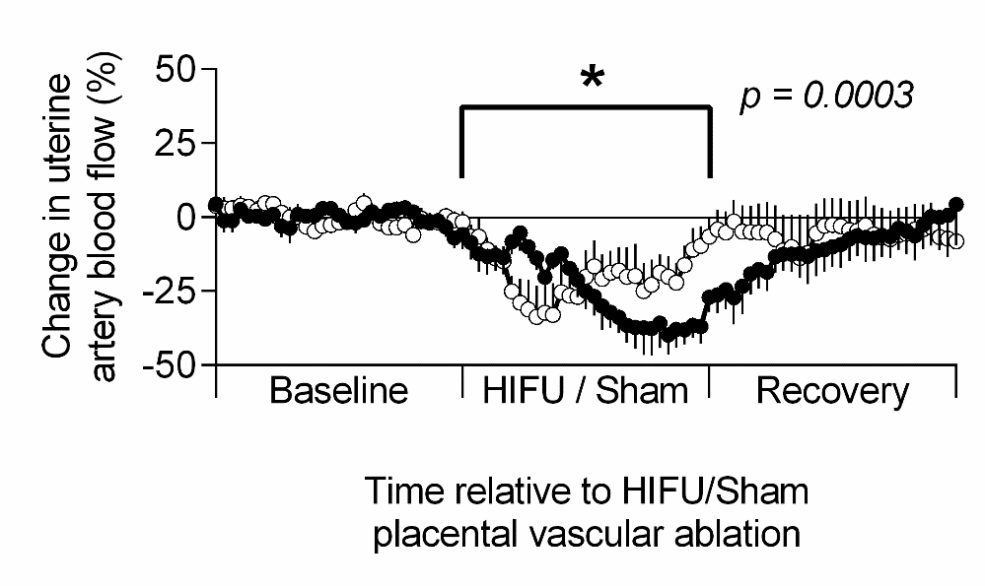

Figure 5.3: Changes in maternal uterine artery blood flow during HIFU or sham exposures.
Group A animals. Values represent the mean ± SEM of percentage change in uterine artery blood flow from baseline during the specified recording periods (each lasting 30 min) for HIFU (closed circles; n=5) and sham (open circles; n=6) treatment groups. Statistical significance was assessed using a repeated measures two-way ANOVA with post hoc Tukey's test; * denotes a significant difference of time with respect to baseline, with the exact *p* value given on the graph. There was no significant effect of treatment.

The decrease in uterine blood flow corresponded with an increase in uterine artery vascular resistance during HIFU or sham exposures in Group A animals (Figure 5.4a). The impact of these changes on substrate delivery will be discussed in chapter 6. Uterine artery vascular resistance was also monitored non-invasively by Doppler ultrasound in Group S animals. UtA-PI was measured before, during and after HIFU or sham exposures of placental vasculature, while the ewe was under general anaesthesia, and at interval during the following 21 d. Figure 5.4b shows the increase in UtA-PI that occurred while under isoflurane anaesthesia, even before the application of HIFU or sham exposures, reflecting a near doubling of the PI values. Uterine artery notching also developed to a variable degree while the ewes were under general anaesthesia (Figure 3.8d), but was not present in un-anaesthetised animals. Uterine artery PI returned to baseline levels by the first post-operative day, and showed no evidence of notching. There were no further changes in UtA-PI with advancing gestational age, or differences in response between treatment groups.

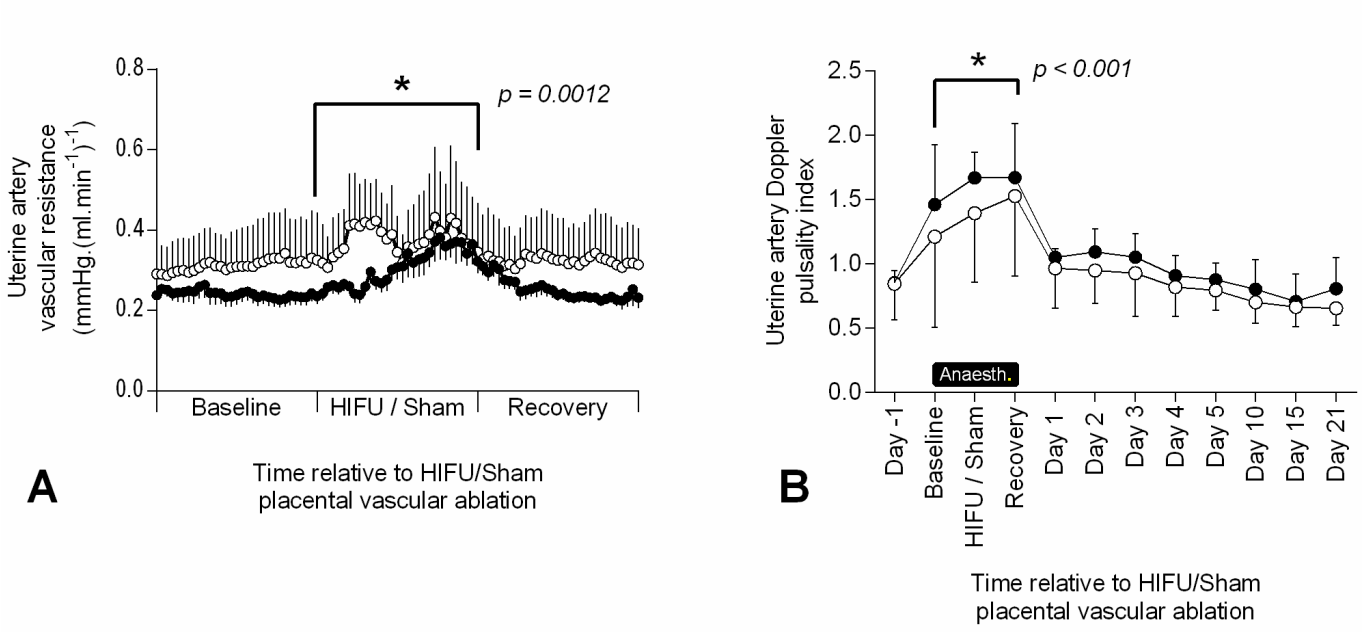

Figure 5.4: Changes in maternal uterine artery vascular resistance.
(A) Group A animals. Values represent the mean ± SEM of maternal uterine artery vascular resistance during the specified recording periods (30 min each) for transuterine HIFU (closed circles; n=5) and sham (open circles; n=6) treatment groups. (B) Group S animals. Values represent the mean ± SD of maternal uterine artery pulsatility index before, during (at approximately 10, 60 and 120 mins of anaesthesia) and after transdermal HIFU (closed circles; n=6) or sham (open circles; n=6) placental vascular occlusion under general anaesthesia. Statistical significance was assessed using a repeated measures two-way ANOVA with post hoc Tukey's test; * denotes a significant difference of time with respect to baseline/day -1, with exact *p* values given on the graph. There was no significant effect of treatment.

5.3 **Fetal cardiovascular responses**

5.3.1 Heart rate and blood pressure

Table 5.4 shows that fetal heart rate, mean pre- and post-ductal arterial blood pressure was not affected by exposure to HIFU: mean values were not different between HIFU and control groups, either while under anaesthesia (Group A) or after 5 days post procedure recovery (Group R). Compared to the un-anaesthetised values in Group R animals, fetal heart rate was reduced during the period of anaesthesia preceding the transuterine HIFU or sham exposures of placental vasculature in Group A. This reduction was of approximately the same magnitude between treatment groups. There was no difference in the un-anaesthetised values for pre-ductal mean arterial pressure in Group R and Group A animals. Post-ductal mean arterial pressure in sham exposed Group A animals was increased compared to un-anaesthetised Group R controls, but there was no difference in the HIFU exposed animals in Groups A and R.

	HIFU		Control	
	Baseline recording (A)	Day 5 post-operative (R)	Baseline recording (A)	Day 5 post-operative (R)
Mean arterial blood pressure: Post- ductal (mmHg)	36.5 ± 0.7	32.5 ± 1.4	45.1 ± 0.5 *	31.0 ± 2.3
Mean arterial blood pressure: Pre- ductal (mmHg)	31.8 ± 4.2	n/a	30.5 ± 1.9	n/a
Heart rate (beats.min^{-1})	167 ± 2 *	187 ± 3	172 ± 2 *	180 ± 3

Table 5.4 Baseline fetal mean arterial pressure and heart rate.
Values represent the mean ± SEM of fetal mean arterial pressure and heart rate during the specified recording periods for HIFU (baseline, n=5; day 5, n=6) and sham (baseline and day 5, n=6) treatment groups. Significant differences of the effect of time and treatment group were assessed using a repeated measures two-way ANOVA. No significant differences for the effect of treatment were found, but where authorised post hoc Tukey's tests demonstrated a significant effect of time (* $p<0.001$) during the experimental protocol.

Fetal mean arterial pressure and heart rate (corresponding to anaesthetised baseline values) remained stable throughout the application of HIFU or sham exposures of placental vasculature in Group A (Figure 5.5a). In Group S animals, there is a fall in fetal heart rate, which occurs during the first 60 minutes of exposure to general anaesthesia. The fetal heart rate was reduced to a similar nadir as seen in Group A animals during the baseline recording period (Figure 5.5b).

After recovery from general anaesthesia, the fetal heart rate in Group R and S animals was not different between treatment groups during the 21 day follow-up period (Figure 5.5b, Figure 5.6). Mean post-ductal arterial blood pressure (Group R) was also not different between treatment groups during follow-up (Figure 5.6).

There was however an effect of gestational age observed during the follow-up period. In Group R animals, the fetal heart rate decreased and the post-ductal mean arterial pressure increased with increasing gestational age. In Group S animals, the fetal heart rate also decreased with increasing gestational age (Figure 5.5b, Figure 5.6).

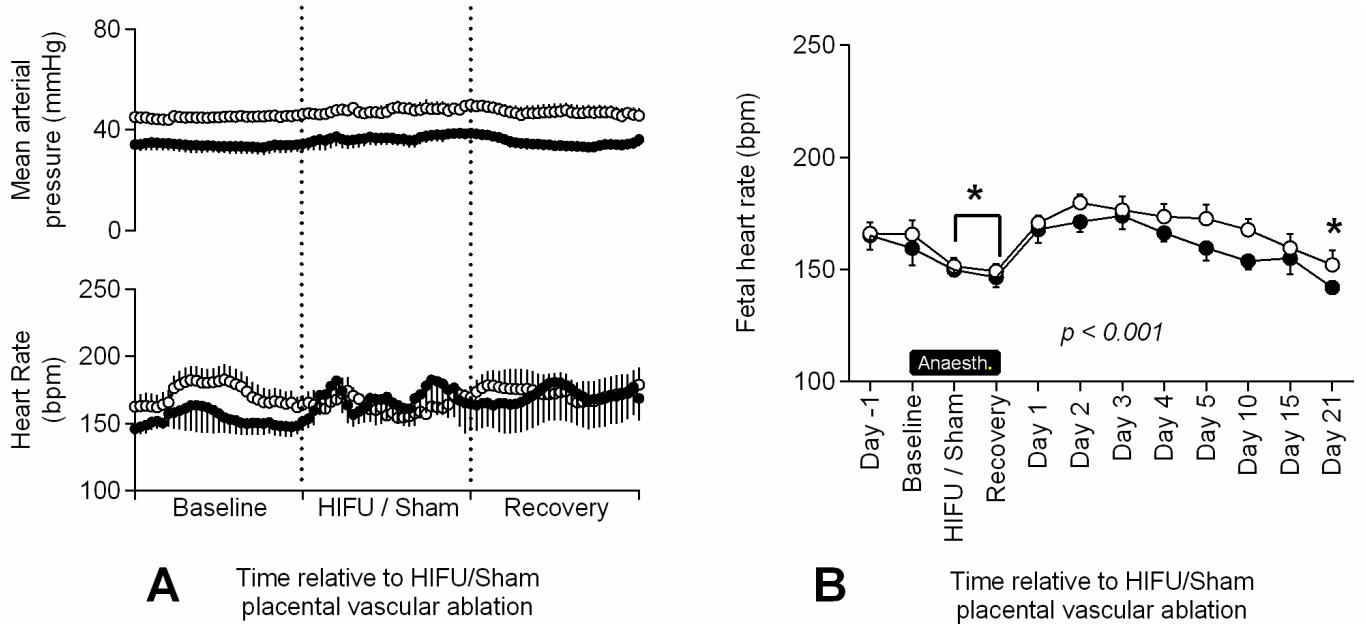

Figure 5.5 Fetal mean arterial pressure and heart rate (intraoperative).
(A) Group A animals. Values represent the mean ± SEM of fetal mean arterial blood pressure and heart rate during the specified recording periods (30 min each) for transuterine HIFU (closed circles; n=5) and sham (open circles; n=6) treatment groups. (B) Group S animals. Values represent the mean ± SD of fetal heart rate before, during (at approximately 10, 60 and 120 mins of anaesthesia) and after transdermal HIFU (closed circles; n=6) or sham (open circles; n=6) treatment groups. Statistical significance was assessed using a repeated measures two-way ANOVA with post hoc Tukey's test; * denotes a significant difference of time with respect to baseline/day -1, with exact *p* values given on the graphs. There was no significant effect of treatment.

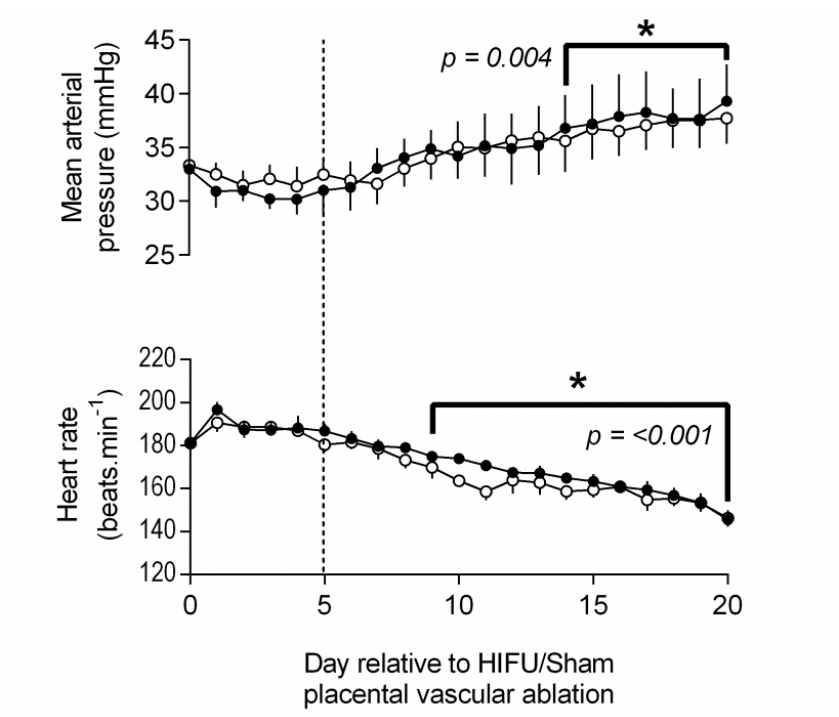

Figure 5.6 Fetal mean arterial pressure and heart rate (follow-up period).
Group R animals. Values represent the mean ± SEM of fetal mean arterial blood pressure and heart rate averaged over sequential 24 h periods following HIFU (closed circles; n=6) or sham (open circles; n=6) placental vascular occlusion and fetal instrumentation under isoflurane anaesthesia. Statistical significance was assessed using a repeated measures two-way ANOVA with post hoc Tukey's test; * denotes a significant difference of time with respect to baseline, with exact *p* values given on the graphs. There was no significant effect of treatment.

5.3.2 Cardiovascular defence mechanisms

At the start of the "baseline" period preceding HIFU or sham exposures of placental vasculature in Group A, fetuses had already undergone a period of general anaesthesia, a period of uterine handling and surgical intervention. Table 5.5 provides a comparison of femoral and carotid arterial blood flow values in comparison to the normal range for gestation derived from un-anaesthetised, chronical instrumented fetal sheep. Femoral vascular resistance is the only measurement which fell outside the normal range.

	Normal range for gestation (95% CI)	Baseline in HIFU group	Baseline in sham group
Femoral artery blood flow ($ml.min^{-1}$)	**28 – 40**	30.3 ± 0.3	29.4 ± 0.6
Femoral vascular resistance ($mmHg.(min.ml^{-1})^{-1}$)	**0.69 – 1.19**	1.2 ± 0.01	1.6 ± 0.01
Carotid artery blood flow ($ml.min^{-1}$)	**58 – 91**	85.6 ± 0.3	87.1 ± 0.9
Carotid artery vascular resistance ($mmHg.(min.ml^{-1})^{-1}$)	**0.24 – 0.66**	0.37 ± 0.01	0.42 ± 0.01
Ratio of carotid to femoral arterial blood flow	**1.5 – 3.0**	3.0 ± 0.01	2.7 ± 0.01

Table 5.5 Normal fetal blood flow dynamics compared to operative baselines.
Group A animals. In the black column, values represent the normal range for gestation, given as a 95% confidence interval, of fetal femoral and carotid artery blood flows and vascular resistances, and the ratio of carotid to femoral blood flow (Derived from experiments performed in the same laboratory (279)). These are compared to the mean ± SEM values during the baseline recording periods for HIFU (n=5) and sham (n=6) treatment groups for the same blood flow measurements. The effect of treatment was assessed between the HIFU and sham groups during the baseline period using a two-tailed student's t-test and no significant differences were found.

During the 30-mintue time period in which HIFU or sham exposures of placental vasculature were performed, there was a reduction in fetal femoral artery blood flow and an increase in femoral artery vascular resistance compared to the baseline, with no difference between treatment groups (Figure 5.7a). These changes occurred in conjunction with the reduction in maternal uterine artery blood flow, and persisted beyond the restoration of maternal uterine artery blood flow to normal. Carotid artery blood flow and vascular resistance again remained stable throughout the duration of the HIFU experimental protocol and no effect of treatment was observed (Figure 5.7b).

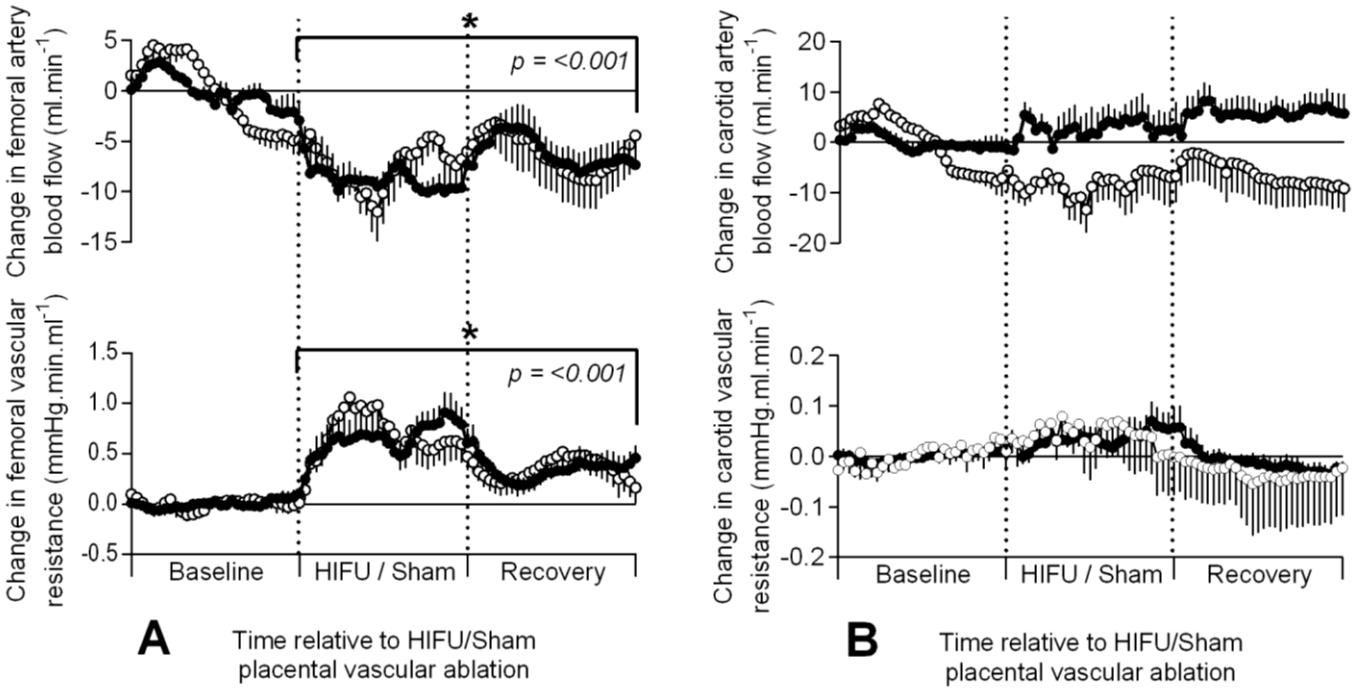

Figure 5.7 Changes in fetal femoral and carotid blood flow and resistance (acute phase).
Group A animals. Values represent the mean ± SEM of absolute change from baseline of (A) fetal femoral blood flow and vascular resistance and (B) fetal carotid blood flow and vascular resistance during the specified recording periods (30 min each) for transuterine HIFU (closed circles; n=5) and sham (open circles; n=6) treatment groups. Statistical significance was assessed using a repeated measures two-way ANOVA with post hoc Tukey's test; * denotes a significant difference of time with respect to baseline, with exact *p* values given on the graphs. There was no significant effect of treatment.

During the post-exposure follow-up period in Group R animals, there was an increase in mean fetal femoral blood flow and pulse pressure with increasing gestation age (Figure 5.8). There was no effect of treatment on these increases. In the first 24 hours of surgical recovery there was an increase in fetal femoral artery vascular resistance. It was no longer statistically increased after this time, but continued to show a trend to decrease for three to four days post procedure, until a stable baseline was formed (Figure 5.8). Carotid artery flow probes were not placed in Group R animals due to the necessity to avoid prolonged anaesthesia by restricting the time allocated to both HIFU and surgical procedures.

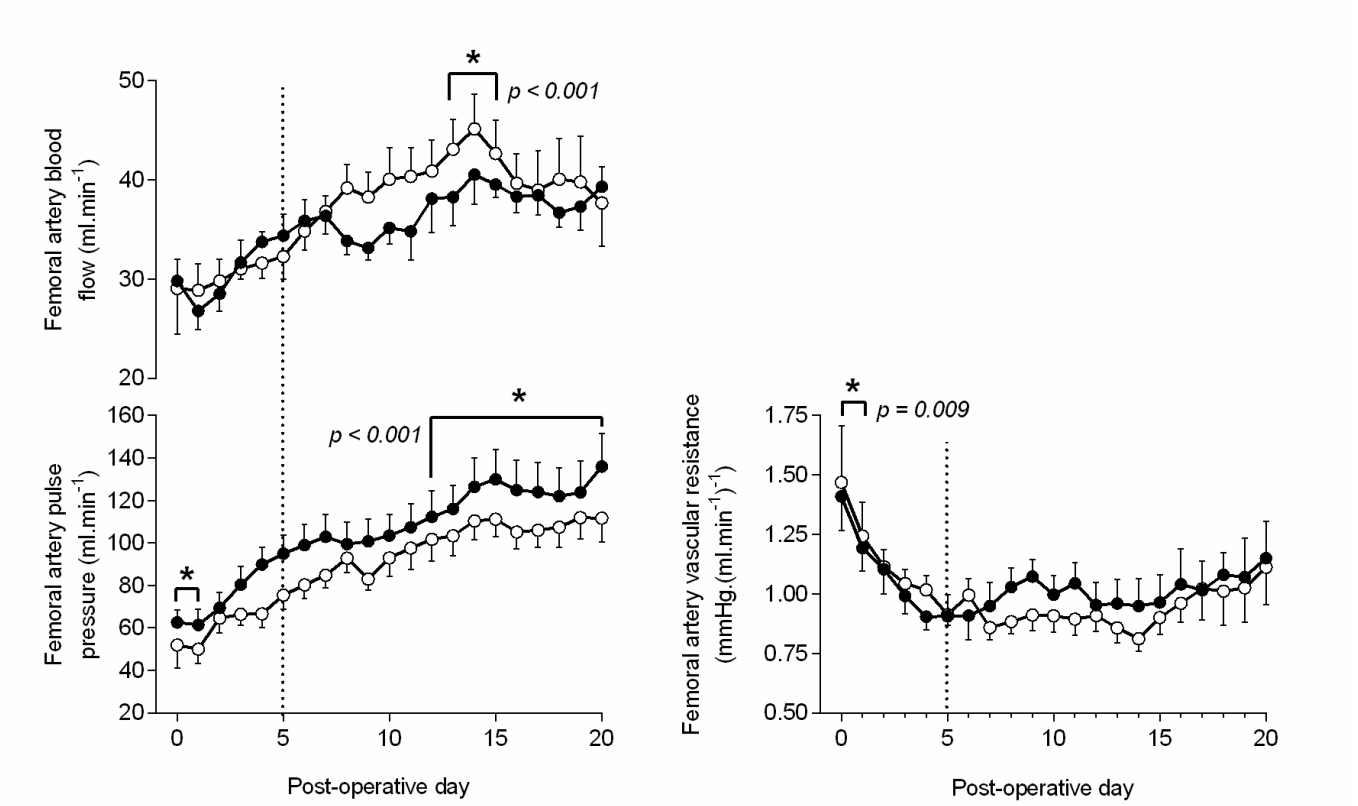

Figure 5.8 Fetal femoral artery flow dynamics after transdermal HIFU/sham exposures (follow-up period). Group R animals. Values represent the mean ± SEM of fetal femoral arterial blood flow, pulse pressure and vascular resistance during the recovery period from HIFU (closed circles; n=5) or sham (open circles; n=6) exposures. The dashed line represents the day five "baseline" against which other values are compared. Statistical significance was assessed using a repeated measures two-way ANOVA with post hoc Tukey's test; * denotes a significant difference of time with respect to baseline, with exact *p* values given on the graphs. There was no significant effect of treatment.

In Group S animals, even in the absence of invasive surgical procedures, and, in the sham animals, in the absence of HIFU exposures, changes in fetal blood flows were noted. Figure 5.9a shows the changes in umbilical artery resistance, reported as PI values. Pre-procedure (24-48 hours), the umbilical artery PI for both groups was < 1.0. Following induction of anaesthesia, there was a progressive rise in the UA-PI with increasing duration of anaesthesia. These changes followed the same pattern as maternal UtA-PI with increasing duration of anaesthesia (Figure 5.4b). Like the changes in fetal femoral artery resistance (Figure 5.8), this elevation in UA-PI was statistically significant for 24 h after the HIFU or sham exposures, and returned to baseline levels over the subsequent 3-4 days, although elevations were not statistically significant during this time. These increases in UA-PI were not different between HIFU and sham treated groups.

Unlike the carotid arterial flow and resistance, which remained stable, (Figure 5.7b), the middle cerebral artery PI did decrease during the period of anaesthesia and HIFU or sham exposures (Figure 5.9). This change was slower to achieve statistical significance than the changes in

uterine and umbilical artery PI. However, the decrease in MCA-PI, and consequently cerebro-placental ratio, persisted for the first 3 days of the follow-up period (Figure 5.9). Again, the timing and magnitude of these changes were not different between HIFU and sham treated groups.

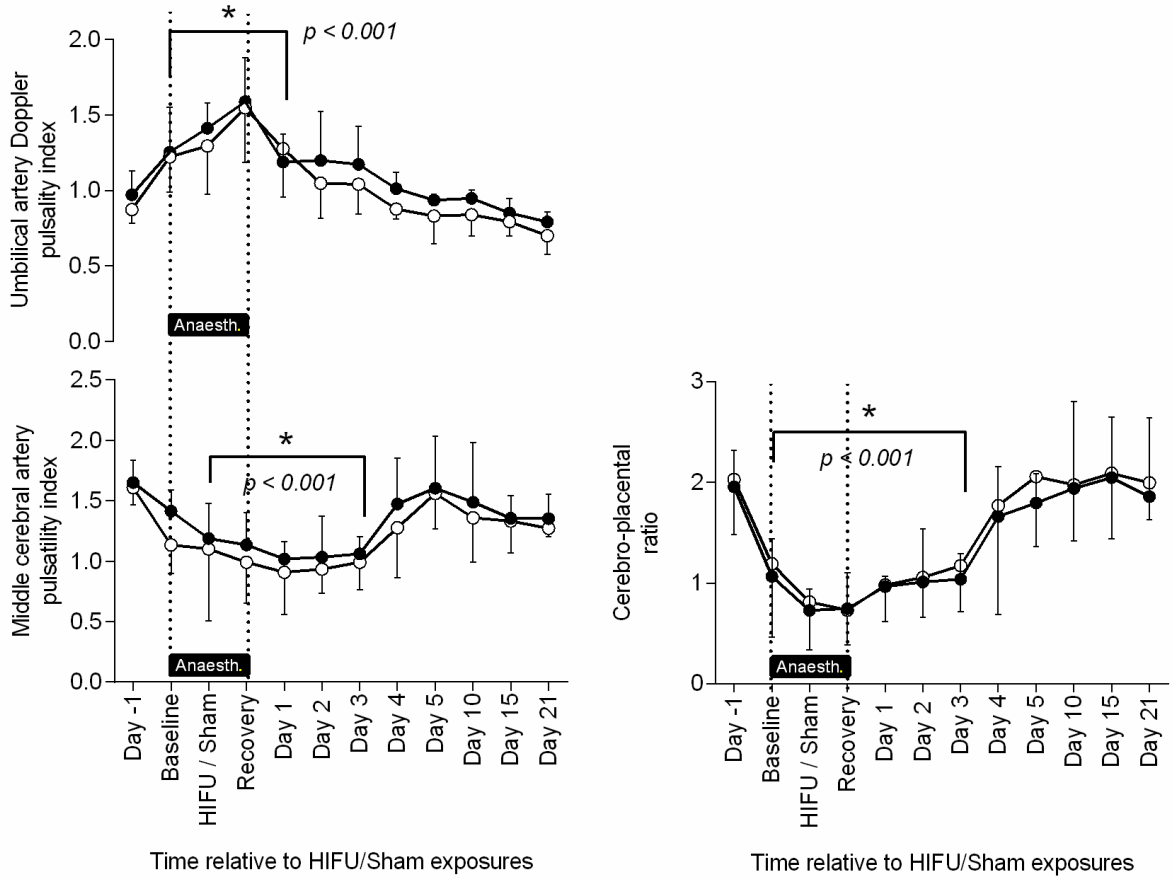

Figure 5.9 Fetal Doppler indices before, during and after HIFU/sham exposures.
Values represent the mean ± SD of fetal umbilical and middle cerebral artery pulsatility index and the ratio of the two, the cerebro-placental ratio, before, during and after transdermal HIFU (closed circles; n=6) or sham (open circles; n=6) non-invasive placental vascular occlusion under anaesthesia. Statistical significance was assessed using a repeated measures two-way ANOVA with post hoc Tukey's test; * denotes a significant difference of time with respect to day -1, with exact p values given on the graph. There was no significant difference of the effect of treatment.

5.4 **Fetal cardiac function**

In addition to in vivo invasive assessment of fetal cardiovascular function in Group A and R animals, fetal echocardiography was performed in Group S animals.

During the period of general anaesthesia, changes in fetal cardiac function were observed, characterised by significant increases in LV-MPI and DV-PIV, compared to the baseline in un-

anaesthetised sheep. Left ventricular EF and FS were unchanged during anaesthesia. There were again no differences between treatment groups in the timing or magnitude of these changes (Figure 5.10).

During the follow-up period, in both treatment groups, LV-MPI remained elevated for the first 24 h. The left ventricular EF was increased during the day 1-2 assessments post HIFU or sham exposures; left ventricular FS was increased during the day 1-4 assessments post HIFU or sham exposures. DV-PIV was not significantly increased following the reversal of anaesthesia (Figure 5.10).

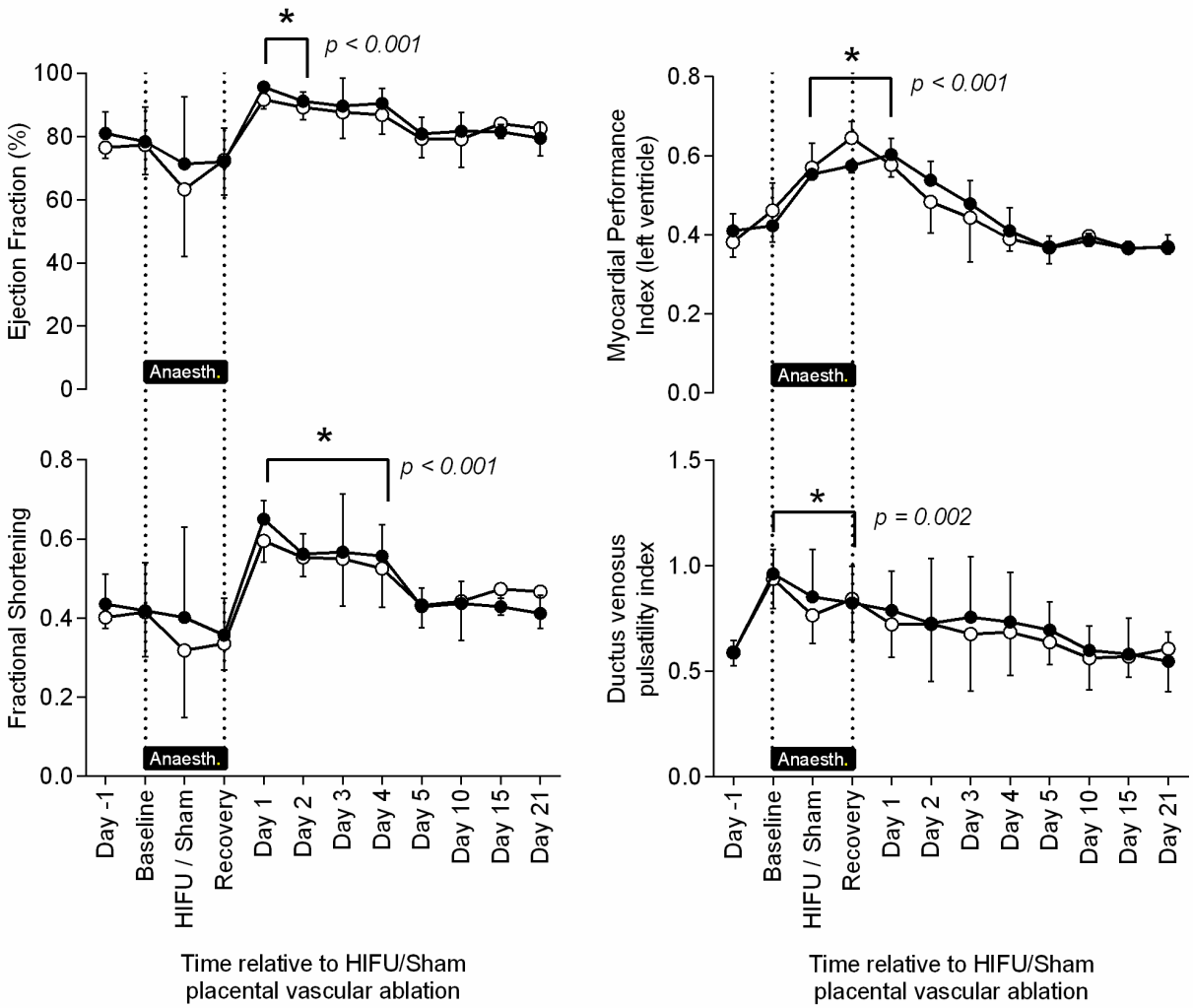

Figure 5.10: Fetal cardiac function (Group S).
Values represent the mean ± SD of fetal cardiac ejection fraction, fractional shortening, left ventricular myocardial performance index and ductus venosus pulsatility index before, during and after transdermal HIFU (closed circles; n=6) or sham (open circles; n=6) exposures. Dotted lines demarcate the measures performed in anaesthetised animals; all other values were in un-anaesthetised animals. Statistical significance was assessed using a repeated measures two-way ANOVA with post hoc Tukey's test; * denotes a significant difference of time with respect to day -1, with exact *p* values given on the graphs. There was no significant effect of treatment.

CHAPTER 6: METABOLIC RESPONSES TO HIFU PLACENTAL VASCULAR OCCLUSION

6.1 Comparison of Group A and Group R animals

The experimental design required that invasive monitoring of cardiovascular and metabolic (i) responses to, and (ii) recovery from, HIFU mediated placental vascular occlusion were conducted in different animal groups (as per section 2.3). These were Group A(cute) and Group R(ecovery) respectively. In the Group R controls, there was no blood sampling of the ewe or fetus performed following reversal of anaesthesia due to a difference in experimental protocols, so the Group A sham animals cannot be compared to Group R controls.

Table 6.1 shows a comparison of the metabolic characteristics of ewes (exposed to HIFU only) in Group A during the last 30 minutes of the experimental protocol, and in Group R during the first 30 minutes following reversal of anaesthesia. With the exception of the arterial partial pressure of oxygen, there were no differences between groups.

	HIFU		*p value*
	Group A	Group R	
P_aO_2 (mmHg)	202 ± 55	109 ± 19 *	< 0.001
Oxyhaemoglobin saturation (%)	102.3 ± 1.4	104.0 ± 0.2	ns
Haemoglobin ($g.dL^{-1}$)	8.6 ± 0.3	7.2 ± 0.7	ns
Glucose ($mmol.L^{-1}$)	2.2 ± 0.2	2.5 ± 0.3	ns
pH	7.51 ± 0.02	7.47 ± 0.02	ns
Arterial base excess ($mmol.L^{-1}$)	7.7 ± 0.7	4.8 ± 1.4	ns
P_aCO_2 (mmHg)	40.5 ± 3.0	37.0 ± 2.6	ns
Arterial lactate ($mmol.L^{-1}$)	1.1 ± 0.2	1.1 ± 1.5	ns
Bicarbonate ($mEq.L^{-1}$)	31.0 ± 1.0	27.8 ± 1.7	ns

Table 6.1: Maternal metabolic status comparisons (Group A to R).
Values represent the mean ± SEM of maternal arterial partial pressure of oxygen (P_aO_2) and carbon dioxide (P_aCO_2), oxygen saturation of haemoglobin, haemoglobin concentration, concentrations of arterial glucose, lactate, bicarbonate and arterial base excess in the descending maternal aorta. Samples were taken either at the end of the recovery period in Group A ewes or within 30 min following the reversal of anaesthesia in Group R ewes. While values for sham treated animals in Group A are available, the corresponding values in Group R control ewes are not, so these comparisons cannot be drawn. Statistical significance was assessed using a two-tailed students' t-test: * denotes a significant difference in HIFU treated animals in Group R animals compared to their Group A counterparts with p values given in the table (ns = not significant, $p > 0.05$).

Table 6.2 shows a comparison of the metabolic characteristics of fetuses (exposed to HIFU) in Group A during the last 30 minutes of the experimental protocol, and in Group R during the first 30 minutes following reversal of anaesthesia. The fetuses of un-anaesthetised ewes in group R have a higher arterial pH, a lower P_aCO_2, show a lesser degree of haemoconcentration and have a higher delivery rate of femoral oxygen and glucose that the fetuses of anaesthetised ewes in Group A.

	HIFU		*p value*
	Group A	Group R	
P_aO_2 (mmHg)	18.4 ± 0.9	19.0 ± 1.7	ns
Oxyhaemoglobin saturation (%)	46.8 ± 2.8	45.7 ± 3.8	ns
Haemoglobin ($g.dL^{-1}$)	11.1 ± 0.2	10.6 ± 0.2 *	0.02
Haematocrit (%)	35.2 ± 0.4	32.6 ± 0.6 *	0.01
Arterial oxygen content ($mmol.ml^{-1}$)	2.2 ± 0.3	3.1 ± 0.2	ns
Femoral oxygen delivery ($mmol.min^{-1}$)	55 ± 8	93 ± 5 *	0.02
Glucose ($mmol.L^{-1}$)	0.8 ± 0.1	0.8 ± 0.1	ns
Femoral glucose delivery ($\mu mol.min^{-1}$)	19 ± 4	22 ± 4	0.02
pH	7.18 ± 0.02	7.24 ± 0.01 *	0.03
Arterial base excess ($mmol.L^{-1}$)	-4.4 ± 0.7	-3.3 ± 1.4	ns
P_aCO_2 (mmHg)	78 ± 7	60 ± 2 *	0.02
Arterial lactate ($mmol.L^{-1}$)	3.0 ± 0.4	2.2 ± 0.2	ns
Bicarbonate ($mEq.L^{-1}$)	24.6 ± 0.2	23.8 ± 1.4	ns

Table 6.2: Fetal metabolic status comparisons (Group A to R).
Values represent the mean ± SEM of fetal arterial partial pressure of oxygen (P_aO_2) and carbon dioxide (P_aCO_2), oxygen saturation of haemoglobin, arterial oxygen content, haemoglobin concentration, haematocrit, concentrations of arterial glucose, lactate, bicarbonate, arterial base excess and femoral arterial oxygen and glucose delivery rates in the fetal ascending aorta (Group A) or descending aorta (GroupR). Samples were taken either at the end of the recovery period in Group A animals or within 30 min following the reversal of anaesthesia in Group R animals. While values for sham treated animals in Group A are available, the corresponding values in Group R control ewes are not, so these comparisons cannot be drawn. Statistical significance was assessed using a two-tailed Student's t-test: * denotes a significant difference in HIFU treated animals in Group R animals compared to their Group A counterparts with p values given in the table (ns = not significant, $p > 0.05$).

6.2 **Maternal substrate availability and delivery**

In Group A ewes, there were no differences in maternal arterial oxygenation, saturation of oxyhaemoglobin or haemoglobin during the acute experimental protocol. In Group S ewes, there were no differences in maternal saturation of oxyhaemoglobin measured non-invasively in animals exposed to HIFU or sham (Figure 6.1). In Group R ewes, maternal oxygenation and haemoglobin was also stable during the five days of postoperative recovery to "baseline" and in the monitoring period to day 21 thereafter, when HIFU exposed animals were compared to the control (Table 6.4).

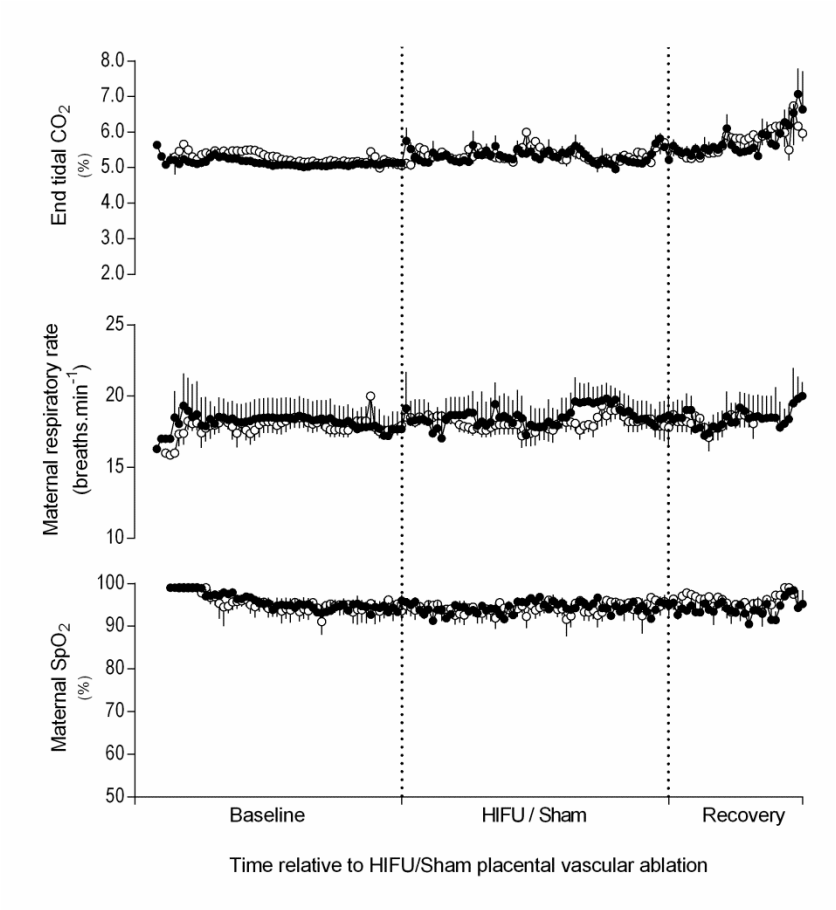

Figure 6.1: Maternal respiratory function under anaesthesia (Group S).
Values represent the mean ± SEM of maternal $EtCO_2$ and respiratory rate measured by capnography, and saturation of maternal haemoglobin with oxygen measured non-invasively with a pulse-oximeter, averaged over sequential 60 s intervals for HIFU (closed circles; n=6) and sham (open circles; n=6) treatment groups. The baseline and HIFU/sham periods have a duration of 60 mins; the recovery period is 30 mins and are demarcated by dotted lines. No significant differences of the effect of time or treatment were found using a repeated measures two-way ANOVA.

Maternal glucose concentration shows a statistically, but not physiologically, significant decrease with increasing duration of the acute experimental protocol, representing a fall

from 2.7 to 2.3 mmol.l^{-1} (Table 6.3). For comparison, the mean values of maternal glucose concentration in the 21 day follow-up period varied between 2.3 and 2.6 mmol^{-1}, showing no statistically significant effect of time or treatment (Table 6.4).

As would be expected, given the reductions in uterine artery blood flow discussed in section 5.2.2, oxygen and glucose delivery by the uterine artery was decreased during HIFU or sham exposures, but was restored to baseline during the recovery phase of the acute protocol (Table 6.3). However, given the maternal super-oxygenation resulting from mechanical ventilation with a high fraction of inspired oxygen, this decrease in oxygenation does not equate to hypoxaemia. Uterine artery flow probes were not placed in Group R HIFU exposed animas due to the necessity to avoid prolonged anaesthesia by restricting the time allocated to both HIFU and surgical procedures, so it is not possible to comment of uterine artery delivery of oxygen and glucose beyond the end of the acute experimental protocol. However, from previously chronically instrumented ovine studies, the normal range of uterine artery oxygen delivery is 83-200 ml.min^{-1} and glucose delivery is 396-1188 µmol.ml^{-1} at approximately this gestational age (unpublished data) (95% confidence intervals), and the values in Table 6.3 fall within this range.

Variable	Group	Baseline (-30 min)	Exposure Series (0 min)	(15 min)	(30 min)	Recovery (60 min)	*p* value (* time)	(† treatment)
P_aO_2 (mmHg)	HIFU	216.0 ± 47.5	200.4 ± 67.3	190.4 ± 74.2	186.2 ± 72.4	218.2 ± 64.2	0.60	0.71
	Sham	198.8 ± 25.4	169.8 ± 22.8	163.8 ± 23.4	183.3 ± 32.3	180.0 ± 26.2		
Oxyhaemoglobin Saturation (%)	HIFU	102.3 ± 1.2	100.1 ± 2.2	97.6 ± 3.0	100.5 ± 1.9	101.9 ± 1.6	0.77	0.96
	Sham	95.1 ± 7.8	102.3 ± 1.3	102.0 ± 1.5	101.3 ± 1.9	102.4 ± 1.1		
Haemoglobin ($g.dL^{-1}$)	HIFU	8.0 ± 0.4	7.8 ± 0.4	8.0 ± 0.5	8.2 ± 0.4	8.5 ± 0.4	0.06	0.14
	Sham	8.9 ± 0.6	8.9 ± 0.6	9.1 ± 0.6	9.4 ± 0.4	9.6 ± 0.5		
Haematocrit (%)	HIFU	0.24 ± 0.01	0.24 ± 0.02	0.25 ± 0.02	0.25 ± 0.01	0.26 ± 0.01	0.00	0.73
	Sham	0.24 ± 0.01	0.24 ± 0.01	0.25 ± 0.01	0.28 ± 0.01 *	0.28 ± 0.01*		
Oxygen content ($ml\ O_2.mL^{-1}$)	HIFU	0.76 ± 0.1	0.71 ± 0.2	0.68 ± 0.2	0.67 ± 0.2	0.77 ± 0.2	0.61	0.77
	Sham	0.71 ± 0.1	0.63 ± 0.1	0.62 ± 0.1	0.68 ± 0.1	0.67 ± 0.1		
Uterine oxygen delivery ($ml.min^{-1}$)	HIFU	203 ± 28	182 ± 49	133 ± 43 *	128 ± 41	202 ± 53	0.00	0.77
	Sham	210 ± 26	197 ± 33	138 ± 20 *	183 ± 15	181 ± 15		
Glucose ($mmol.L^{-1}$)	HIFU	2.6 ± 0.2	2.5 ± 0.2	2.5 ± 0.1	2.5 ± 0.2 *	2.3 ± 0.1 *	<0.001	0.84
	Sham	2.7 ± 0.2	2.5 ± 0.2	2.4 ± 0.2	2.4 ± 0.2 *	2.3 ± 0.2 *		
Uterine glucose delivery ($\mu mol.min^{-1}$)	HIFU	730 ± 55	672 ± 44	485 ± 49 *	477 ± 50 *	617 ± 117	<0.001	0.42
	Sham	812 ± 111	762 ± 121	595 ± 131 *	704 ± 124 *	648 ± 96		

Table 6.3: Maternal substrate availability and delivery during placental vascular exposures (Group A).
Values represent the mean ± SEM of maternal oxygen partial pressure (P_aO_2), oxyhaemoglobin saturation, oxygen content, haemoglobin, haematocrit, glucose concentration in the descending aorta, and uterine artery oxygen and glucose delivery, for animals in the HIFU (n=5) and sham (n=6) treatment groups in each time period of the experimental protocol. Significant differences of the effect of time and treatment group were assessed using a repeated measures two-way ANOVA. No significant differences for the effect of treatment were found (†) but where authorised post hoc Tukey's tests demonstrated a significant effect of time (*) during the experimental protocol, with relevant *p* numbers given in the table.

Variable	Group	Post-operative recovery (day)				Baseline	Monitoring period (day)			*p* value	
		1	2	3	4	Day 5	6-10	11-15	16-20	(* time)	(† treatment)
P_aO_2 (mmHg)	HIFU	96 ± 3	92 ± 6	92 ± 4	89 ± 3	94 ± 3	99 ± 2	93 ± 2	99 ± 1	0.09	0.10
	Control	111 ± 7	105 ± 6	96 ± 3	103 ± 3	100 ± 1	101 ± 3	105 ± 3	97 ± 2		
Oxyhaemoglobin Saturation (%)	HIFU	103 ± 1	102 ± 2	101 ± 1	102 ± 1	103 ± 1	104 ± 1	103 ± 1	104 ± 1	0.71	0.61
	Control	103 ± 1	102 ± 1	102 ± 1	102 ± 1	103 ± 1	103 ± 1	102 ± 1	103 ± 1		
Haemoglobin ($g.dL^{-1}$)	HIFU	10.9 ± 0.3	10.4 ± 0.2	10.2 ± 0.4	10.3 ± 0.5	10.4 ± 0.3	10.5 ± 0.2	10.1 ± 0.2	10.5 ± 0.3	0.12	0.16
	Control	11.2 ± 0.2	10.6 ± 0.2	10.0 ± 0.3	10.0 ± 0.7	9.3 ± 0.4	9.8 ± 0.2	9.7 ± 0.2	9.7 ± 0.1		
Oxygen content (ml $O_2.mL^{-1}$)	HIFU	0.44 ± 0.01	0.42 ± 0.02	0.41 ± 0.02	0.41 ± 0.01	0.42 ± 0.01	0.44 ± 0.01	0.42 ± 0.01	0.44 ± 0.01	0.13	0.47
	Control	0.49 ± 0.03	0.46 ± 0.02	0.43 ± 0.01	0.45 ± 0.02	0.43 ± 0.01	0.44 ± 0.01	0.45 ± 0.01	0.42 ± 0.01		
Glucose ($mmol.L^{-1}$)	HIFU	2.6 ± 0.3	2.3 ± 0.1	2.5 ± 0.2	2.5 ± 0.2	2.4 ± 0.1	2.6 ± 0.1	2.5 ± 0.1	2.3 ± 0.1	0.06	0.78
	Control	2.5 ± 0.2	2.4 ± 0.4	2.5 ± 0.1	2.7 ± 0.1	2.6 ± 0.1	2.7 ± 0.1	2.5 ± 0.1	2.3 ± 0.1		

Table 6.4: Maternal substrate availability following placental vascular exposures (Group R).
Values represent the mean ± SEM of maternal oxygen partial pressure (P_aO_2), oxyhaemoglobin saturation, oxygen content, haemoglobin, haematocrit and glucose concentration in the descending aorta for animals in the HIFU (n=6) and sham (n=6) treatment groups. Values for days one to five following HIFU or sham exposures ("post-operative recovery") are presented as daily means; values for the "monitoring period" are presented as the mean ± SEM of five day values. Before values given in the "monitoring period" were grouped into five-day means they were compared individually to each other and the baseline. Grouping values into five day means did not alter any significant outcomes (or lack thereof), and they are presented grouped for ease of expression. Significant differences of the effect of time and treatment group were assessed using a repeated measures two-way ANOVA. Where authorised, post hoc Sidak's tests demonstrated a significant effect of treatment (†) and post hoc Tukey's tests demonstrated a significant effect of time (*) during the experimental protocol, with relevant *p* numbers given in the table.

6.3 **Fetal substrate availability and delivery**

Carotid arterial oxygen and glucose delivery to the fetal brain remained unaltered during the experimental procedure, despite a reduced partial pressure of oxygen and saturation of oxyhaemoglobin in the fetal blood by the end of the recovery period. Fetuses also showed a trend to haemoconcentration by the end of the recovery period. These changes were present in both the HIFU and sham groups with no effect of treatment seen; additionally, these changes occurred at the same time points for both treatment groups (Table 6.5).

By the first postoperative day, these changes in oxygenation had recovered, and notably the saturation of oxyhaemoglobin of the fetal blood was increased to above baseline levels. This resulted in normalisation of fetal femoral oxygen delivery by the time of the day one samples (Table 6.6), even given the persistence of increased fetal femoral vascular resistance and reduction in pulse pressure noted (Figure 5.8). Fetal femoral oxygen delivery increases with advancing gestational age, related to the previously mentioned increases in femoral arterial blood flow with increasing gestational age (Figure 5.8). There is again no effect of treatment.

Fetal haemoglobin was stable and within the normal range, with no evidence of fetal anaemia or polycythaemia.

Fetal glucose concentration remained unchanged throughout the acute experimental protocol in the Group A animals. Decreases in femoral oxygen delivery were observed in line with the pattern of decreased femoral and maternal blood flows (Figure 5.7). The fetal glucose concentration remained stable throughout the follow-up period, but femoral glucose delivery increased with advancing gestational age, similar to the changes noted with oxygen delivery. As previously, there were no statistically significant differences between treatment groups.

Variable	Treatment group	Baseline (-30 min)	Exposure series (0 min)	(15 min)	(30 min)	Recovery (60 min)	*p* value (* time)	(† treatment)
P_aO_2 (mmHg)	HIFU	25.2 ± 1.1	25.0 ± 2.8	23.8 ± 3.3	23.0 ± 3.2	18.4 ± 0.9 *	< 0.0001	0.21
	Sham	27.2 ± 1.2	28.3 ± 1.2	27.7 ± 1.2	26.3 ± 1.9	22.3 ± 1.9 *		
Oxyhaemoglobin Saturation (%)	HIFU	72.8 ± 1.1	72.3 ± 2.9	69.3 ± 8.3	66.3 ± 7.4	46.8 ± 2.8 *	< 0.0001	0.62
	Sham	70.4 ± 7.5	64.8 ± 2.9	64.3 ± 3.9	63.1 ± 4.7	51.2 ± 9.5 *		
Haemoglobin ($g.dL^{-1}$)	HIFU	10.0 ± 0.2	10.2 ± 0.2	10.7 ± 0.3	11.0 ± 0.5	11.1 ± 0.2 *	0.0026	0.06
	Sham	9.3 ± 0.2	10.5 ± 0.3	9.8 ± 0.2	10.0 ± 0.2	10.7 ± 0.4 *		
Haematocrit (%)	HIFU	0.32 ± 0.01	0.33 ± 0.01	0.34 ± 0.02	0.35 ± 0.01 *	0.35 ± 0.01*	0.03	0.55
	Sham	0.27 ± 0.02	0.34 ± 0.02	0.32 ± 0.02	0.34 ± 0.02 *	0.33 ± 0.03*		
Glucose ($mmol.L^{-1}$)	HIFU	0.70 ± 0.12	0.66 ± 0.14	0.70 ± 0.10	0.83 ± 0.11	0.79 ± 0.13	0.69	0.39
	Sham	0.99 ± 0.17	0.89 ± 0.08	0.86 ± 0.09	0.81 ± 0.11	0.87 ± 0.14		

Table 6.5: Fetal substrate availability during placental vascular exposures (Group A).
Values represent the mean ± SEM of fetal arterial oxygen partial pressure (P_aO_2), oxyhaemoglobin saturation, haemoglobin, haematocrit and glucose concentration in the pre-ductal circulation in animals in the HIFU (n=5) and sham (n=6) treatment groups in each time period of the experimental protocol. Significant differences of the effect of time and treatment group were assessed using a repeated measures two-way ANOVA. No significant differences for the effect of treatment were found (†) but where authorised post hoc Tukey's tests demonstrated a significant effect of time (*) during the experimental protocol, with relevant *p* numbers given in the table.

Variable	Treatment group	Baseline (-30 min)	Exposure Series (0 min)	(15 min)	(30 min)	Recovery (60 min)	*p* value (* time)	(† treatment)
Carotid Arterial Oxygen Delivery ($mmol.min^{-1}$)	HIFU	383 ± 30	374 ± 39	373 ± 41	352 ± 28	283 ± 19	0.21	0.63
	Sham	359 ± 82	361 ± 40	312 ± 37	334 ± 50	281 ± 33		
Femoral Arterial Oxygen Delivery ($mmol.min^{-1}$)	HIFU	116 ± 9	106 ± 13	73 ± 15 *	67 ± 12 *	55 ± 8 *	< 0.0001	0.28
	Sham	114 ± 14	116 ± 13	82 ± 10 *	99 ± 10 *	91 ± 18 *		
Carotid : Femoral Oxygen Delivery Ratio	HIFU	3.1 ± 0.4	3.2 ± 0.2	4.8 ± 0.6	5.2 ± 1.1 *	4.6 ± 0.3	0.04	0.33
	Sham	3.7 ± 1.0	3.3 ± 0.5	4.0 ± 0.7	3.3 ± 0.7	3.0 ± 0.4		
Carotid Arterial Glucose Delivery ($\mu mol.min^{-1}$)	HIFU	61 ± 14	57 ± 16	64 ± 15	77 ± 19	72 ± 13	0.59	0.74
	Sham	78 ± 14	75 ± 12	72 ± 14	67 ± 16	74 ± 19		
Femoral Arterial Glucose Delivery ($\mu mol.min^{-1}$)	HIFU	21 ± 3	19 ± 3	15 ± 2 *	16 ± 3 *	19 ± 4	0.003	0.17
	Sham	30 ± 6	26 ± 3	19 ± 3 *	24 ± 4 *	24 ± 3		
Carotid : Femoral Glucose Delivery Ratio	HIFU	3.0 ± 0.4	2.9 ± 0.3	4.2 ± 0.8 *	4.7 ± 0.7 *	4.0 ± 0.2	0.0004	0.26
	Sham	2.6 ± 0.4	2.7 ± 0.3	3.9 ± 0.7 *	2.9 ± 0.5 *	3.0 ± 0.5		

Table 6.6 Fetal substrate delivery during placental vascular exposures (Group A).
Values represent the mean ± SEM of fetal carotid and femoral arterial oxygen and glucose deliveries and the ratio of both pre- and post-ductal oxygen and glucose delivery for animals in the HIFU (n=5) and sham (n=6) treatment groups in each time period of the experimental protocol. Significant differences of the effect of time and treatment group were assessed using a repeated measures two-way ANOVA. No significant differences for the effect of treatment were found (†) but where authorised post hoc Tukey's tests demonstrated a significant effect of time (*) during the experimental protocol, with relevant *p* numbers given in the table.

Variable	Group	Post-operative recovery (day)				Baseline	Monitoring period (day)			*p* value	
		1	2	3	4	Day 5	6-10	11-15	16-20	(* time)	(† treatment)
P_aO_2 (mmHg)	HIFU	21.8 ± 1.3	20.6 ± 1.7	19.6 ± 2.2	19.0 ± 1.7	20.2 ± 1.5	22.2 ± 0.9	21.2 ± 0.6	20.1 ± 0.4	0.18	0.34
	Control	22.0 ± 0.9	21.2 ± 1.6	18.8 ± 0.5	19.6 ± 0.6	19.4 ± 1.0	19.5 ± 0.6	19.3 ± 0.4	19.5 ± 0.5		
Oxyhaemoglobin Saturation (%)	HIFU	63.7 ± 2.3	55.0 ± 5.3	53.4 ± 6.1	54.5 ± 6.1	57.6 ± 3.5	57.3 ± 1.5	55.8 ± 1.6	55.5 ± 1.0	0.06	0.52
	Control	64.8 ± 2.7	56.9 ± 5.5	49.2 ± 4.1	52.7 ± 4.1	52.9 ± 4.1	54.3 ± 1.7	54.1 ± 1.6	50.5 ± 1.8		
Haemoglobin ($g.dL^{-1}$)	HIFU	9.9 ± 0.8 *	10.1 ± 0.7	9.2 ± 0.7	8.7 ± 0.5	8.6 ± 0.8	9.5 ± 0.4	9.9 ± 0.4	10.6 ± 0.3	0.01	0.38
	Control	10.0 ± 0.5 *	9.2 ± 0.6	8.4 ± 0.4	8.5 ± 0.3	8.7 ± 0.3	8.5 ± 0.3	8.8 ± 0.3	9.2 ± 0.4		
Glucose concentration ($mmol.L^{-1}$)	HIFU	0.95 ± 0.13	0.83 ± 0.09	1.01 ± 0.10	0.93 ± 0.10	0.92 ± 0.10	0.96 ± 0.04	0.90 ± 0.05	0.82 ± 0.03	0.07	0.26
	Control	0.75 ± 0.10	0.83 ± 0.13	0.81 ± 0.10	0.85 ± 0.10	0.97 ± 0.15	0.80 ± 0.04	0.74 ± 0.03	0.70 ± 0.03		
Femoral Arterial Oxygen Delivery ($mmol.min^{-1}$)	HIFU	104.5 ± 8.9	94.7 ± 6.8	90.9 ± 8.6	89.6 ± 9.0	94.0 ± 8.9	124.9 ± 5.5 *	141.1 ± 6.4 *	136.2 ± 7.3 *	0.001	0.31
	Control	105.1 ± 10.7	108.2 ± 13.4	88.4 ± 13.1	101.5 ± 7.8	103.9 ± 3.1	100.6 ± 5.5	121.9 ± 5.5 *	109.5 ± 2.8		
Femoral Arterial Glucose Delivery ($\mu mol.min^{-1}$)	HIFU	27.5 ± 4.5	24.8 ± 3.3	31.2 ± 3.2	29.6 ± 3.6	30.2 ± 4.1	37.3 ± 2.6 *	38.9 ± 2.7 *	33.1 ± 2.3	0.02	0.44
	Control	24.0 ± 4.6	28.1 ± 3.2	29.0 ± 5.9	31.8 ± 4.1	33.0 ± 4.1	30.5 ± 1.5	31.2 ± 1.7	28.6 ± 1.3		

Table 6.7: Fetal substrate availability and delivery following placental vascular exposures (Group R).
Values represent the mean ± SEM of fetal arterial oxygen partial pressure (P_aO_2), oxyhaemoglobin saturation, haemoglobin, haematocrit and glucose concentration in the post-ductal circulation and femoral arterial oxygen and glucose delivery for animals in the HIFU (n=6) and sham (n=6) treatment groups. Values for days one to five following HIFU or sham exposures ("post-operative recovery") are presented as daily means; values for the "monitoring period" are presented as the mean ± SEM of five day values. Before values given in the "monitoring period" were grouped into five-day means they were compared individually to each other and the baseline. Grouping them into five day means did not alter any significant outcomes (or lack thereof) they are presented grouped for ease of expression. Significant differences of the effect of time and treatment group were assessed using a repeated measures two-way ANOVA. No significant differences for the effect of treatment were found (†) but where authorised post hoc Tukey's tests demonstrated a significant effect of time (*) during the experimental protocol, with relevant *p* numbers given in the table.

6.4 **Maternal metabolic by-product clearance**

During the acute experimental protocol in Group A ewes, there were no significant effects due to the duration of anaesthesia or time. There were, however, significant differences in maternal pH and arterial partial pressure of carbon dioxide (P_aCO_2) apparent between the treatment groups, which only reached significance by the end of the exposure series (30 mins) and persisted to the end of the recovery period (60 mins, Table 6.8). These changes in pH are accounted for by the difference in P_aCO_2 levels between the groups, as concentrations of arterial lactate were not different between groups, and did not show elevation during the entire protocol. Conversely, in Group S animals, end tidal expired CO_2 levels remained normal at 5-6% while under anaesthesia (Figure 6.1), only rising during the recovery period when ventilation rates were reduced in preparation for reversal of anaesthesia to promote spontaneous respiratory effort.

There were no differences in maternal P_aCO_2 or pH in Group R ewes on day one post-operative. The pH was higher in Group R controls compared to HIFU exposed animals between days two and five post-operative (Table 6.9). Neither P_aCO_2 nor arterial lactate levels are significantly different between groups, nor were there any differences in arterial base excess or bicarbonate concentration to show differential buffering. Measurement of maternal respiratory rate was part of the daily assessment for pain or distress, and no elevation was noted in either group (data not shown).

Arterial lactate showed elevation on the first post-operative day; this was not significantly different by the second post-operative day and had returned to the normal range for adult pregnant sheep by the third day. Beyond this there were no other differences or trends observed in maternal metabolic by-product clearance once the immediate effect of anaesthesia and surgery had passed.

Variable	Treatment Group	Baseline (-30 min)	Exposure Series (0 min)	(15 min)	(30 min)	Recovery (60 min)	*p* value (* time)	(† treatment)
pH	HIFU	7.51 ± 0.02	7.50 ± 0.03	7.47 ± 0.03	7.49 ± 0.01	7.51 ± 0.02	0.27	0.007
	Sham	7.44 ± 0.01	7.43 ± 0.01	7.42 ± 0.01	7.40 ± 0.02 †	7.40 ± 0.02 †		
Arterial Base Excess ($mmol.L^{-1}$)	HIFU	8.2 ± 0.9	7.6 ± 0.7	7.4 ± 0.8	7.6 ± 0.8	7.2 ± 0.6	0.86	0.16
	Sham	4.8 ± 1.5	5.7 ± 1.1	5.5 ± 1.0	5.7 ± 1.1	5.3 ± 1.3		
P_aCO_2 (mmHg)	HIFU	40.0 ± 1.6	42.0 ± 3.4	43.8 ± 3.7	41.8 ± 1.0	38.6 ± 2.9	0.17	0.048
	Sham	48.7 ± 2.2	49.0 ± 4.0	54.3 ± 2.0	54.3 ± 1.3 †	52.7 ± 1.8 †		
Arterial lactate ($mmol.L^{-1}$)	HIFU	1.2 ± 0.2	1.1 ± 0.2	1.1 ± 0.1	1.0 ± 0.1	1.1 ± 0.2	0.16	0.09
	Sham	0.7 ± 0.1	0.6 ± 0.1	0.6 ± 0.1	0.6 ± 0.1	0.6 ± 0.1		
Bicarbonate ($mEq.L^{-1}$)	HIFU	32.0 ± 1.0	31.8 ± 1.1	31.8 ± 0.8	31.7 ± 0.8	31.0 ± 1.0	0.32	0.84
	Sham	30.8 ± 1.4	31.8 ± 1.4	31.8 ± 1.3	31.8 ± 1.3	31.8 ± 1.3		

Table 6.8: Maternal metabolic by-product clearance during placental vascular exposures (Group A).
Values represent the mean ± SEM of maternal pH, arterial base excess, carbon dioxide partial pressure (P_aCO_2), concentration of lactate and bicarbonate in the descending aorta for animals in the HIFU (n=5) and sham (n=6) treatment groups in each time period of the experimental protocol. Significant differences of the effect of time and treatment group were assessed using a repeated measures two-way ANOVA. No significant differences for the effect of time were found (*) but where authorised post hoc Sidak's tests demonstrated a significant effect of time (†) during the experimental protocol, with relevant *p* numbers given in the table.

Variable	Treatment group	Post-operative recovery (day) 1	2	3	4	Baseline Day 5	Monitoring period (day) 6-10	11-15	16-20	*p* value (* time)	(† treatment)
pH	HIFU	7.47 ± 0.02	7.48 ± 0.01	7.45 ± 0.02	7.48 ± 0.01	7.48 ± 0.01	7.46 ± 0.01	7.46 ± 0.01	7.47 ± 0.01	0.07	0.03
	Control	7.52 ± 0.03	7.55 ± 0.01†	7.53 ± 0.01†	7.55 ± 0.01†	7.54 ± 0.02†	7.49 ± 0.01	7.47 ± 0.01	7.50 ± 0.01		
Arterial Base Excess ($mmol.L^{-1}$)	HIFU	-2.0 ± 0.9	0.8 ± 0.6	0.8 ± 1.1	1.5 ± 0.6	1.3 ± 1.4	0.9 ± 0.7	1.8 ± 0.3	2.3 ± 0.5	0.2	0.07
	Control	2.8 ± 2.0	4.0 ± 2.2	5.5 ± 1.3	4.0 ± 0.4	4.0 ± 0.4	3.0 ± 0.7	2.8 ± 0.5	3.9 ± 0.5		
P_aCO_2 (mmHg)	HIFU	31.0 ± 0.7	32.8 ± 1.1	33.0 ± 1.1	34.0 ± 1.1	34.3 ± 1.8	33.5 ± 0.6	35.8 ± 0.5	36.0 ± 0.6	0.03	0.09
	Control	30.0 ± 0.6	29.5 ± 1.8	32.8 ± 1.1	32.3 ± 0.5	32.0 ± 2.0	32.6 ± 0.8	34.2 ± 0.7	33.4 ± 0.6		
Arterial lactate ($mmol.L^{-1}$)	HIFU	1.15 ± 0.3*	0.63 ± 0.1	0.67 ± 0.1	0.70 ± 0.3	0.62 ± 0.1	0.56 ± 0.1	0.55 ± 0.1	0.49 ± 0.1	0.04	0.92
	Control	1.11 ± 0.3*	1.00 ± 0.3	0.75 ± 0.1	0.41 ± 0.1	0.31 ± 0.03	0.54 ± 0.1	0.53 ± 0.1	0.56 ± 0.1		
Bicarbonate ($mEq.L^{-1}$)	HIFU	21.3 ± 0.5	23.3 ± 0.8	23.0 ± 1.3	23.8 ± 0.5	23.8 ± 1.3	23.2 ± 0.6	24.3 ± 0.4	24.9 ± 0.5	0.2	0.14
	Control	24.0 ± 2.2	25.8 ± 1.8	27.0 ± 1.2	25.2 ± 0.5	25.8 ± 0.6	25.5 ± 0.7	25.3 ± 0.6	26.2 ± 0.5		

Table 6.9: Maternal metabolic by-product clearance following placental vascular exposures (Group R).
Values represent the mean ± SEM of maternal pH, arterial base excess, carbon dioxide partial pressure (P_aCO_2), concentration of lactate and bicarbonate in the descending aorta for animals in the HIFU (n=6) and sham (n=6) treatment groups. Values for days one to five following HIFU or sham exposures ("post-operative recovery") are presented as daily means; values for the "monitoring period" are presented as the mean ± SEM of five day values. Before values given in the "monitoring period" were grouped into five-day means they were compared individually to each other and the baseline. Grouping them into five day means did not alter any significant outcomes (or lack thereof), and they are presented grouped for ease of expression. Significant differences of the effect of time and treatment group were assessed using a repeated measures two-way ANOVA. No significant differences for the effect of time were found (*) but where authorised post hoc Sidak's tests demonstrated a significant effect of time (†) during the experimental protocol, with relevant *p* numbers given in the table.

6.5 **Fetal metabolic by-product clearance**

In Group A fetuses, by the end of the recovery period there was a gradual deterioration in the fetal clearance of metabolic by-products: both P_aCO_2 and arterial lactate concentrations were elevated, leading to the development of a mixed metabolic and respiratory acidosis in the fetuses. There was an elevation in arterial base excess, but no alteration in bicarbonate concentrations. This deterioration occurred at the same rate in both groups, and reached significance by the end of the exposure series (30 min) and continued to worsen until the end of the recovery period (60 min, Table 6.10), after which time the experimental protocol stopped.

Fetuses in Group A had already developed a respiratory acidosis at the start of the baseline (-30 mins), which deteriorated over the subsequent 90 minutes of the experimental protocol (Table 6.8). Fetuses had developed a mixed acidosis by the end of the experimental protocol. The pH values did not fall to levels associated with fetal birth asphyxia (pH < 7.0) in either the sham or HIFU group.

In Group R fetuses, there is evidence of a partial recovery in both groups by day one post-operative, as levels have improved between the end of the recovery period (60 min) and the time of blood sampling the next morning, although there is still a statistically significant mixed respiratory and metabolic acidosis. Fetuses have recovered to baseline by day two post-operative, and remained stable throughout the rest of the post-operative recovery and monitoring periods. The arterial base excess and bicarbonate levels were unremarkable and stable. There were no effects of treatment seen between HIFU exposed and control fetuses.

Variable	Treatment group	Baseline (-30 min)	Exposure series (0 min)	(15 min)	(30 min)	Recovery (60 min)	*p* value (* time)	(† treatment)
pH	HIFU	7.27 ± 0.01	7.28 ± 0.01	7.26 ± 0.02	7.23 ± 0.01 *	7.18 ± 0.02*	< 0.0001	0.02
	Sham	7.21 ± 0.03	7.21 ± 0.02 †	7.18 ± 0.02 †	7.17 ± 0.02 *	7.15 ± 0.03*		
Arterial Base Excess ($mmol.L^{-1}$)	HIFU	-0.4 ± 0.9	-0.2 ± 0.6	-0.6 ± 0.7	-1.8 ± 0.4	-4.4 ± 0.7 *	0.003	0.73
	Sham	-1.2 ± 1.6	-0.8 ± 0.8	-2.2 ± 0.7	-2.3 ± 0.8	-2.5 ± 1.2 *		
P_aCO_2 (mmHg)	HIFU	62.4 ± 3.7	61.8 ± 5.5	70.4 ± 11.4	69.4 ± 7.4	77.6 ± 6.9 *	0.003	0.31
	Sham	73.0 ± 4.3	76.5 ± 2.8	75.8 ± 3.5	75.3 ± 3.9	80.5 ± 5.5 *		
Arterial lactate ($mmol.L^{-1}$)	HIFU	2.3 ± 0.4	2.2 ± 0.3	2.2 ± 0.3	2.8 ± 0.4	3.0 ± 0.4 *	0.0003	0.12
	Sham	1.7 ± 0.2	1.7 ± 0.2	1.8 ± 0.2	1.8 ± 0.2	2.3 ± 0.3 *		
Bicarbonate ($mEq.L^{-1}$)	HIFU	25.6 ± 1.3	26.4 ± 0.8	25.2 ± 0.8	25.0 ± 0.6	24.6 ± 0.2	0.22	0.91
	Sham	27.8 ± 1.7	28.7 ± 0.9	27.5 ± 1.3	27.7 ± 1.2	27.8 ± 0.8		

Table 6.10: Fetal metabolic by-product clearance during placental vascular exposures (Group A).
Values represent the mean ± SEM of fetal pH, arterial base excess, carbon dioxide partial pressure (P_aCO_2), concentration of lactate and bicarbonate in the post-ductal circulation in animals in the HIFU (n=5) and sham (n=6) treatment groups in each time period of the experimental protocol. Significant differences of the effect of time and treatment group were assessed using a repeated measures two-way ANOVA. No significant differences for the effect of treatment were found (†) but where authorised post hoc Tukey's tests demonstrated a significant effect of time (*) during the experimental protocol, with relevant *p* numbers given in the table.

Variable	Treatment group	Post-operative recovery (day)				Baseline	Monitoring period (day)			*p* value	
		1	2	3	4	Day 5	6-10	11-15	16-20	(* time)	(† treatment)
pH	HIFU	7.36 ± 0.02 *	7.33 ± 0.01	7.33 ± 0.02	7.34 ± 0.02	7.33 ± 0.01	7.33 ± 0.02	7.34 ± 0.02	7.35 ± 0.02	<0.001	0.25
	Control	7.39 ± 0.01 *	7.37 ± 0.01	7.36 ± 0.01	7.36 ± 0.01	7.37 ± 0.01	7.33 ± 0.04	7.36 ± 0.01	7.37 ± 0.01		
Arterial Base Excess ($mmol.L^{-1}$)	HIFU	-1.8 ± 0.8 †	-1.6 ± 0.7 †	-3.2 ± 1.5 †	-1.2 ± 2.2	-2.0 ± 1.9 †	-1.1 ± 0.6	-0.8 ± 0.6	0.9 ± 0.5 †	0.06	0.04
	Control	3.4 ± 0.9 †	1.2 ± 1.0 †	2.2 ± 1.6 †	1.6 ± 1.0	4.0 ± 0.7 †	-0.4 ± 0.7	2.5 ± 0.6	4.4 ± 0.4 †		
P_aCO_2 (mmHg)	HIFU	45.2 ± 1.9 *	47.6 ± 2.2	47.6 ± 1.3	49.2 ± 1.1	48.2 ± 0.6	49.8 ± 0.5	49.3 ± 0.4	50.0 ± 0.6	0.03	0.06
	Control	50.7 ± 1.4 *	46.8 ± 1.7	51.7 ± 1.5	49.5 ± 0.9	52.3 ± 1.3	51.7 ± 0.9	53.8 ± 0.9	54.3 ± 0.8		
Arterial lactate ($mmol.L^{-1}$)	HIFU	1.3 ± 0.1 *	1.0 ± 0.1	1.0 ± 0.1	1.0 ± 0.2	0.9 ± 0.1	1.0 ± 0.1	1.0 ± 0.1	1.0 ± 0.1	0.008	0.3
	Control	1.6 ± 0.3 *	1.0 ± 0.1	1.1 ± 0.1	1.0 ± 0.1	1.0 ± 0.1	1.0 ± 0.1	1.1 ± 0.1	1.1 ± 0.1		
Bicarbonate ($mEq.L^{-1}$)	HIFU	22.8 ± 1.1 †	23.4 ± 1.0	22.4 ± 1.1 †	24.4 ± 1.8	23.0 ± 1.4 †	24.1 ± 0.5	24.3 ± 0.5	25.5 ± 0.6 †	0.34	0.03
	Control	28.0 ± 0.7 †	25.8 ± 1.0	27.0 ± 1.7 †	26.4 ± 1.0	29.0 ± 0.7 †	24.8 ± 0.7	27.8 ± 0.6	29.6 ± 0.4 †		

Table 6.11: Fetal metabolic by-product clearance following placental vascular exposures (Group R).
Values represent the mean ± SEM of fetal pH, arterial base excess, carbon dioxide partial pressure (P_aCO_2), concentration of lactate and bicarbonate in the post-ductal circulation in animals in the HIFU (n=6) and sham (n=6) treatment groups. Values for days one to five following HIFU or sham exposures ("post-operative recovery") are presented as daily means; values for the "monitoring period" are presented as the mean ± SEM of five day values. Before values given in the "monitoring period" were grouped into five-day means they were compared individually to each other and the baseline (values shaded grey). Grouping them into five day means did not alter any significant outcomes (or lack thereof), and they are presented grouped for ease of expression. Significant differences of the effect of time and treatment group were assessed using a repeated measures two-way ANOVA. Where authorised, post hoc Sidak's tests demonstrated a significant effect of treatment (†) and post hoc Tukey's tests demonstrated a significant effect of time (*) during the experimental protocol, with relevant *p* numbers given in the table.

CHAPTER 7: FETAL GROWTH AND PHYSIOLOGICAL MATURATION FOLLOWING PLACENTAL VASCULAR OCCLUISON

7.1 Fetal growth

7.1.1 Ultrasound biometry

In Group S, fetal growth was measured non-invasively by ultrasound assessment between the day of exposure to HIFU or sham placental vascular occlusion and the end of the follow-up period, 21 days later. Baseline fetal biometry estimated by ultrasound on the day of HIFU or sham exposures was not different between animals in either treatment group (Table 7.1).

Ultrasound measurement	Sham exposed	HIFU exposed	*p value*
Biparietal diameter (mm)	47.6 ± 5.1	47.5 ± 4.5	0.98
Abdominal circumference (mm)	242 ± 14	233 ± 24	0.44
Femur length (mm)	53.8 ± 9.3	45.8 ± 6.5	0.11
Estimated fetal weight (g)	1080 ± 320	880 ± 250	0.26

Table 7.1 Baseline fetal biometry (Group S).
Values represent the mean ± SD of fetal biparietal diameter, abdominal circumference and femur length measured by ultrasound and estimated fetal weight calculated using the Hadlock (BPD-AC-FL) formula for fetuses in the HIFU (n=6) and sham (n=6) groups, performed on the day of HIFU or sham exposures (day 0). Baseline values in both groups were assessed using a two-tailed student's t-test and no significant differences were found (*p* values shown).

While it was not possible to perform a direct comparison between ultrasound measurements performed at baseline and actual fetal size, there was a strong correlation between ultrasound estimation of fetal biometry on the day of post mortem and the measurements taken within the subsequent hour at necroscopy. The correlations of the data were: BPD, r^2 0.96, $p < 0.001$; AC, r^2 0.94, $p < 0.001$; FL, r^2 0.89, $p < 0.001$; EFW, r^2 0.77, $p < 0.001$. The Bland-Altman Correlation plots (Figure 7.1) show that in addition to being strongly correlated, the 95% limits of agreement suggest a ± 5% difference between ultrasound and necroscopy measurements for BPD, AC and FL. However, the EFW performed worse, with a tendency to under-estimate weight, in smaller fetuses particularly.

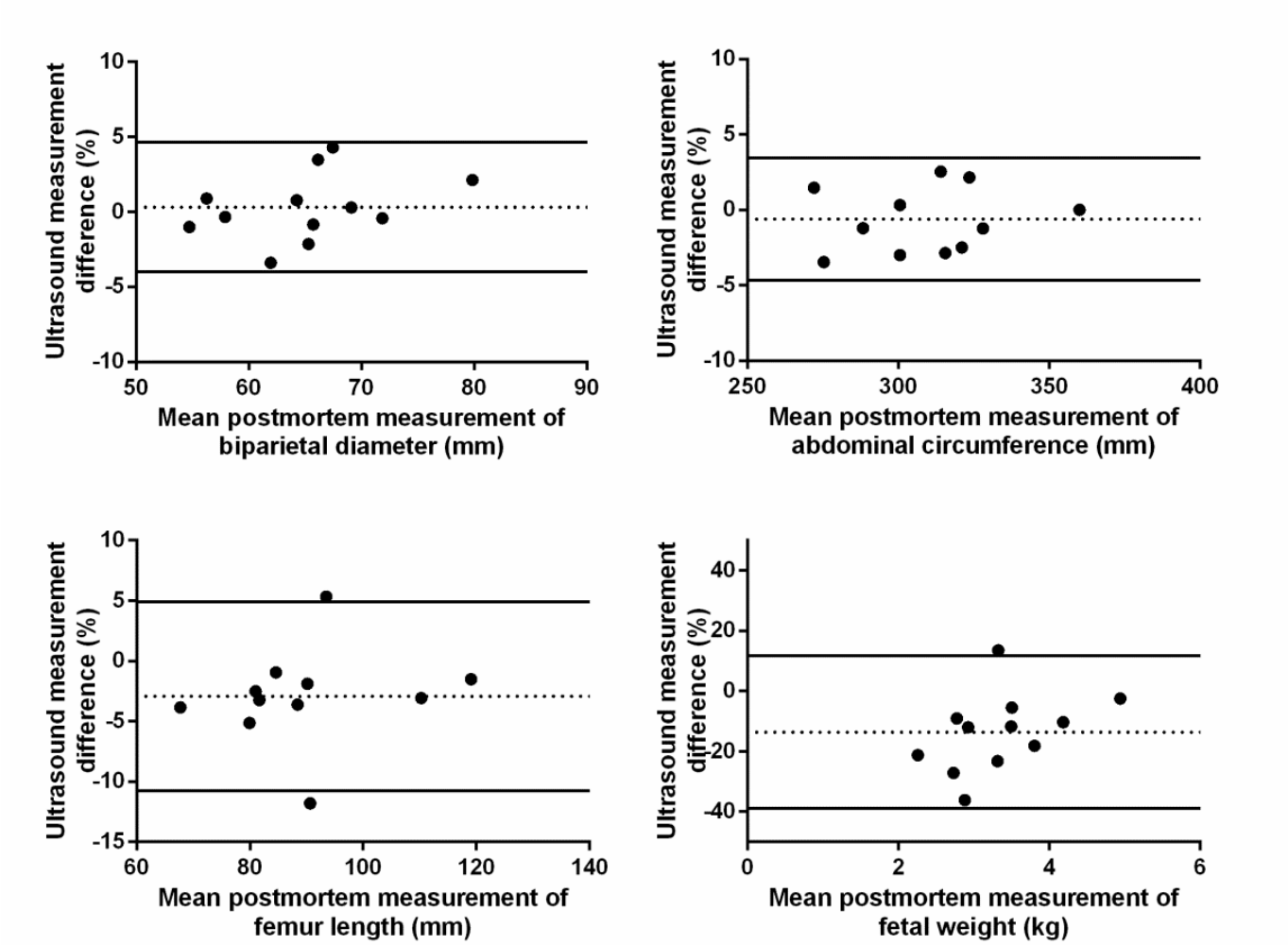

Figure 7.1 Correlation of ultrasound and necroscopy measurements of fetal biometry (Group S).
Bland-Altman Correlation plots of the mean measurement at post-mortem of biparietal diameter (top left), abdominal circumference (top right), femur length (bottom left) and fetal weight (bottom right) compared to the ultrasound percentage difference in measurement. The dashed line represents the bias; the solid lines represent the 95% limits of agreement of the technique.

There appeared to be a linear, rather than curvilinear, relationship between the increases in all four of the ultrasound measurements, relative to advancing gestational age, demonstrated by the scatter plots for these data in Figure 7.2a. In order to account for the greater variation in gestation age at time of HIFU or sham exposure in this group (105-125 days) fetal size is also presented relative to time after HIFU or sham exposure and linear regression was performed on these values (Figure 7.2b). Analysis of covariance (ANCOVA) of the slopes of these regression lines demonstrates that there is no difference between groups (BPD p=0.90, AC p=0.43, FL p=0.77, EFW p=0.34). This is supported by the calculated daily growth rates over full duration of the 21 d follow-up period in presented in Table 7.2, which are not significantly different.

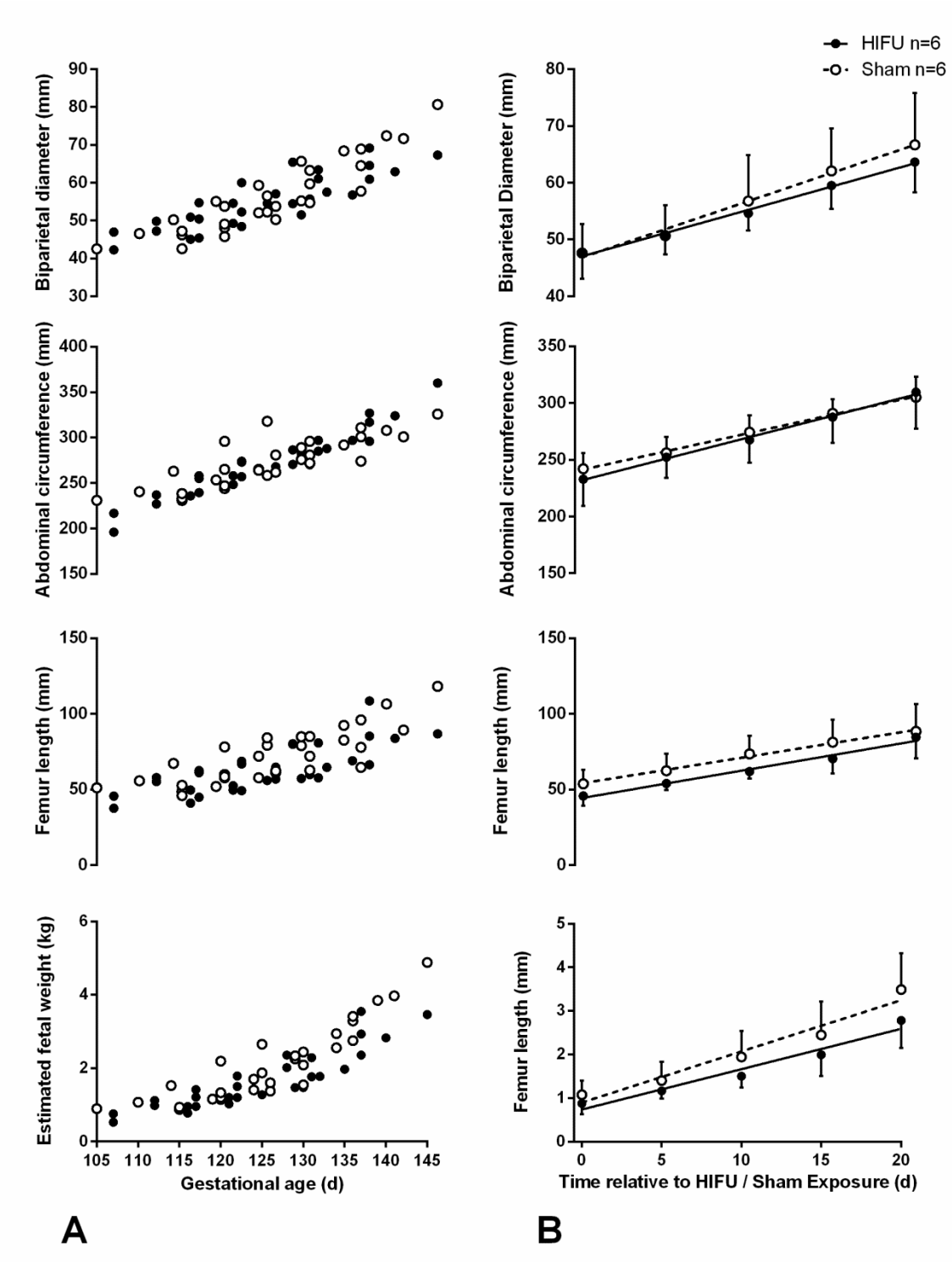

Figure 7.2 Ultrasound measurement of fetal growth (Group S).
(A) Values represent actual ultrasound measurements of fetal BPD, AC, FL and EFW for animals in sham (open circles, n=6) and HIFU (closed circles, n=6) groups relative to gestational age on the day of assessment. (B) Values represent the mean ± SD of fetal BPD, AC, FL and EFW measured by ultrasound relative to the day HIFU (closed circles, n=6) or sham (open circles, n=6) exposures were performed. Linear regression lines (HIFU, solid; sham, dashed) are applied to these graphs. Comparison of slopes was performed by ANCOVA analysis and demonstrated no significant difference; *p* values given in text.

Daily growth rate	Sham exposed	HIFU exposed	*p* value
Biparietal diameter ($mm.d^{-1}$)	0.9 ± 0.3	0.8 ± 0.3	0.37
Abdominal circumference ($mm.d^{-1}$)	3.0 ± 0.9	3.7 ± 0.8	0.21
Femur length ($mm.d^{-1}$)	1.7 ± 0.6	1.8 ± 0.6	0.57
Estimated fetal weight ($g.d^{-1}$)	107 ± 27	90 ± 20	0.26

Table 7.2 Fetal growth rates (Group S).
Values represent the mean ± SD of the calculated fetal growth rate of biparietal diameter, abdominal circumference, femur length (measured) and estimated fetal weight (calculated) for fetuses in the HIFU (n=6) and sham (n=6) groups during the 21 day follow-up period. Rates for both groups were assessed using a two-tailed student's t-test and no significant differences were found (*p* values shown in table).

7.1.2 Size at post mortem

In addition to estimation of fetal growth and size by ultrasound biometry, fetal size was measured at post-mortem in both groups where fetuses were recovered. This confirmed that there were no significant differences between groups exposed to HIFU or sham placental vascular occlusion in the un-instrumented fetuses (Group S, Table 7.3), as suggested by ultrasound estimation of fetal growth (Table 7.2), or the chronically instrumented fetuses (Group R, Table 7.4). Notably, fetal BMI and the ratio of abdominal circumference to biparietal diameter (an index of asymmetric growth) were not different between groups.

The seasonal data for the breeding flock from which the Group S and Group R HIFU ewes were selected was: mean gestational age at delivery: 148 d (range 145-152 d); mean birth weight: 3.9 kg (SD 0.6 kg). Based on this any lamb born with a weight below 2.7 kg at term would be classed as growth restricted. Even given the fact that the lambs in Groups S and R were delivered an average of 10 days before term, no individual lamb weighed less than 2.7 kg.

	Sham exposed	HIFU exposed	*p* value
Maternal weight (kg)	46 ± 2.7	46 ± 1.5	0.99
Gestational age (d)	136.5 ± 2.5	135.3 ± 2.4	0.78
Male : female (fetus) ratio	1:1	1:2	0.26
Fetal weight (kg)	3.8 ± 0.3	3.3 ± 0.2	0.28
Fetal BMI ($kg.m^{-2}$)	15.6 ± 0.6	16.6 ± 0.8	0.40
Crown-rump length (cm)	49.1 ± 1.4	44.8 ± 1.5	0.10
Biparietal diameter (cm)	6.6 ± 0.3	6.4 ± 0.2	0.66
Abdominal circumference (cm)	30.5 ± 0.8	31.3 ± 1.1	0.58
BPD : AC ratio	0.22 ± 0.01	0.21 ± 0.01	0.36
Femur length (cm)	9.2 ± 0.5	8.9 ± 0.5	0.73

Table 7.3: Fetal biometry at post-mortem (Group S).
Values represent mean ± SEM of maternal characteristics and fetal biometry measured at post-mortem, 21 days after HIFU (n=6) or sham (n=6) exposure of placental vasculature and general anaesthesia. Differences between groups were assessed with a two-tailed student's t-test and no significant differences were found (*p* values shown in table).

	Sham exposed	HIFU exposed	*p* value
Maternal weight (kg)	42.1 ± 1.5	51.3 ± 2.1 *	0.01
Gestational age (d)	137 ± 0.2	136 ± 0.4	0.06
Male : female ratio	2:1	1:2	0.47
Fetal weight (kg)	3.3 ± 0.2	3.4 ± 0.1	0.58
Fetal BMI ($kg.m^{-2}$)	17.3 ± 0.8	16.4 ± 0.7	0.46
Crown-rump length (cm)	43.2 ± 0.52	45.5 ± 0.84	0.08
Biparietal diameter (cm)	6.3 ± 0.1	6.7 ± 0.1	0.13
Abdominal circumference (cm)	34.4 ± 2.0	31.8 ± 0.7	0.27
BPD : AC ratio	0.18 ± 0.01	0.21 ± 0.01	0.06
Femur length (cm)	9.8 ± 0.2	9.2 ± 0.3	0.44

Table 7.4: Fetal biometry at post-mortem (Group R).
Values represent mean ± SEM of maternal characteristics and fetal biometry measured at post-mortem, 20 days after HIFU (n=6) or sham (n=6) exposure of placental vasculature, maternal and fetal surgery and general anaesthesia. Differences between groups were assessed with a two-tailed student's t-test and significant differences (denoted with *) were accepted when $p < 0.05$ (*p* values shown in table).

7.1.3 Organ weights

An assessment of fetal organ growth and development was performed in Group S fetuses alone, as these were the only animals in which no surgical procedures were performed. Absolute organ weights and organ weight in relation to fetal body weight were compared between treatment groups, and are presented in Table 7.5. The values show no overall difference between groups, regardless of exposure to HIFU or not.

	Sham exposed	HIFU exposed	*p* value
Brain weight (g)	46.9 ± 2.2	41 ± 2.0	0.10
Brain : body weight ratio	12.6 ± 0.5	12.6 ± 0.9	0.99
Brain : liver ratio	0.55 ± 0.02	0.58 ± 0.04	0.54
Pituitary weight (g)	0.05 ± 0.02	0.07 ± 0.03	0.66
Total lung weight (g)	76.3 ± 4.9	80.5 ± 7.5	0.67
Lung : body weight ratio	20.3 ± 0.5	24.2 ± 1.6	0.06
Heart weigh (g)	23.7 ± 1.7	23.3 ± 1.5	0.85
Heart : body weight ratio	2.58 ± 0.07	2.68 ± 0.25	0.75
Liver weight (g)	86.3 ± 4.0	82.7 ± 4.5	0.08
Liver : body weight ratio	23.5 ± 1.8	22.1 ± 1.4	0.59
Total adrenal weight (g)	0.66 ± 0.13	0.56 ± 0.1	0.59
Adrenal : body weight ratio	0.18 ± 0.04	0.17 ± 0.03	0.93
Pancreas weight	3.06 ± 0.24	2.92 ± 0.27	0.73
Pancreas : body weight ratio	0.82 ± 0.05	0.88 ± 0.07	0.50
Total renal weight (g)	17.6 ± 0.9	19.2 ± 1.4	0.35
Renal : body weight ratio	4.8 ± 0.3	5.7 ± 0.5	0.05
Total peri-renal fat (g)	11.5 ± 1.4	11.2 ± 0.8	0.87
Peri-renal fat : body weight ratio	3.0 ± 0.2	3.4 ± 0.2	0.23

Table 7.5 Fetal organ weights at post-mortem (Group S).
Values represent mean ± SEM of fetal absolute organ weights and relative to body mass measured at post-mortem, 21 days after HIFU (n=6) or sham (n=6) exposure of placental vasculature and general anaesthesia. Differences between groups were assessed with a two-tailed student's t-test and no significant differences were found (*p* values shown in table).

7.2 **Placental size and morphology**

Examination of placental size and development was performed in Group S animals. Total placental weight and placentome number were not different between treatment groups. Total placentome weights and numbers of placentomes within the pregnant horn of the uterus were comparable between both HIFU and sham exposed groups. In both groups, assessed either by total placentome weight or number, there were predominantly type A or B placentomes, and the ratio of A/B types to C/D types was not different between treatment groups (Table 7.6).

	Sham			HIFU			*p* value
Placentome weight							
Total (g)	297.3	±	23.0	285.7	±	21.9	0.75
Pregnant Horn (g)	215.0	±	17.5	245.6	±	20.2	0.32
A or B type (g)	250.2	±	20.1	210.5	±	25.9	0.30
Proportion A or B type of total weight (%)	85.5%	±	6.0%	73.2%	±	7.0%	0.25
C or D Type (g)	47.2	±	20.0	56.8	±	10.0	0.70
Proportion C or D type of total weight (%)	14.5%	±	6.0%	21.8%	±	5.5%	0.44
A or B type : C or D type weight ratio	15.3	±	5.7	6.5	±	2.9	0.21
Placentome number							
Total (g)	83.8	±	6.2	64.3	±	4.5	0.05
Pregnant Horn (g)	57.2	±	5.6	53.7	±	5.5	0.69
A or B type (g)	73.7	±	5.9	54.5	±	5.5	0.06
Proportion A or B type of total number (%)	89.0%	±	5.4%	83.5%	±	4.2%	0.49
C or D Type (g)	10.2	±	5.3	9.0	±	1.9	0.85
Proportion C or D type of total number (%)	11.0%	±	5.4%	15.3%	±	4.2%	0.58
A or B type : C or D type number ratio	27.2	±	14.6	19.1	±	11.9	0.71

Table 7.6: Placentome weight and number at post-mortem (Group S).
Values represent mean ± SEM of weight and number of all placentomes retrieved at post-mortem examination, 21 days after HIFU (n=6) or sham (n=6) exposure of placental vasculature and general anaesthesia. These values have been further subdivided by placentome type (A/B or C/D). The weight and numbers of A/B or C/D subtypes are presented as mean ± SEM, and as percentages of the overall total placentome number or weight in each animal. Differences between groups were assessed with a two-tailed student's t-test and no significant differences were found (*p* values shown in table).

7.3 Fetal maturation

7.3.1 Cortisol

Fetal plasma cortisol concentrations taken under basal conditions in Group R animals were not different between treatment groups at either baseline (day 5) or at the end of the follow-up period (day 20). However, there was a significant increase in plasma cortisol concentrations between 121 ± 2 days gestation age and 136 ± 2 days gestational age (Figure 7.3).

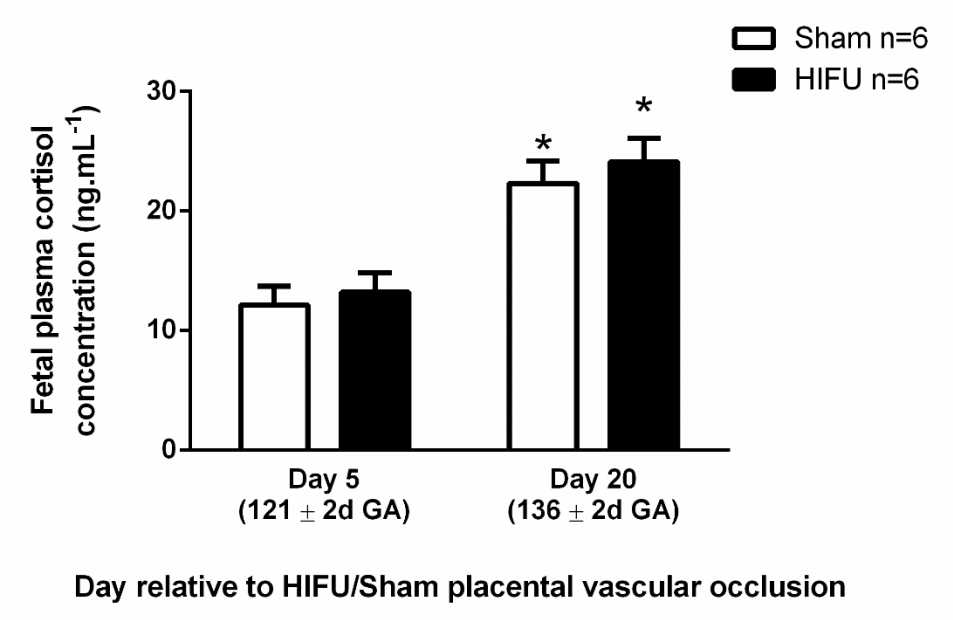

Figure 7.3: Fetal plasma cortisol levels (Group R).
Values represent mean ± SEM of fetal plasma cortisol concentration five and 20 days after surgery in HIFU exposed (n=6) or control (n=6) fetuses. Significant differences: * $p < 0.001$ effect of gestational age, two-way repeated measures ANOVA with Tukey's and Sidak's post Hoc tests. There was no effect of treatment.

7.3.2 Fetal heart rate variability

Fetal heart rate variability was assessed in Group R fetuses between day 3 and day 15 of the follow-up period. A total of 765 fetal heart rate records were analysed (381 control; 384 HIFU). 108 (14%) samples were taken during quite sleep and 428 (56%) were taken in active sleep.

There was no difference between the fetal heart rate or fetal heart rate variability indices at in the baseline measurements (the mean of day 3-5) in either HIFU exposed or control fetuses. There was, however, a significant effect of sleep state on both FHR and FHRV indices in the baseline measurements, which was not dependant on treatment group (Table 7.7).

	Active sleep		Quiet sleep		*p* value	
	Control	HIFU	Control	HIFU	sleep state	treatment
Heart rate (beat.min^{-1})	177 ± 2	181 ± 2	172 ± 2	179 ± 3	0.02 *	0.11
SDNN (ms)	13.2 ± 0.4	12.7 ± 0.6	7.0 ± 0.5	6.6 ± 0.3	< 0.001 *	0.38
STV (ms)	5.6 ± 0.5	6.4 ± 0.9	2.5 ± 0.2	3.1 ± 0.2	< 0.001 *	0.21
Total power (ms^2)	185 ± 15	206 ± 19	50 ± 8	36 ± 3	< 0.001 *	0.81
LF power (ms^2)	75 ± 6	65 ± 9	9 ± 2	8 ± 1	< 0.001 *	0.32
Normalised LF power (nu)	42 ± 1	43 ± 6	30 ± 9	26 ± 3	0.01 *	0.77
HF power (ms^2)	10.7 ± 0.6	8.3 ± 0.8	6.5 ± 0.7	5.5 ± 0.9	0.04 *	0.12
Normalised HF power (nu)	8.7 ± 0.7	8.1 ± 1.3	7.0 ± 1.1	8.4 ± 1.5	0.15	0.60
LF:HF power	6.0 ± 0.5	5.5 ± 0.8	1.3 ± 0.2	1.6 ± 0.3	< 0.001 *	0.91

Table 7.7: Baseline fetal heart rate variability in quiet and active sleep (Group R).
Values represent mean ± SEM of baseline fetal heart rate and indices of fetal HRV in quiet and active sleep in HIFU exposed (n=6) or control (n=6) fetuses. Significant differences: * $p < 0.05$ effect of sleep state, two-way ANOVA. There were no effects of treatment group.

Fetal heart rate was lower in quiet sleep compared to active sleep. SDNN, STV, total power, LF and nLF power, and the LF/HF ratio were higher in active sleep. Absolute HF power is lower in the quiet sleep state compared to active sleep, but there is no difference in the normalised HF power between sleep states.

During the follow-up period during which fetal HRV indices were measured daily, there appeared to be an effect of increasing gestational age, but no apparent effect of exposure to HIFU on the fetuses. In both quiet and active sleep, there was a significant decrease in mean fetal heart rate with advancing gestational age, and corresponding gestational-age dependent increases in the indices of overall variability in the fetal heart rate, SDNN and STV. Total power increased with gestation in active sleep, and showed a trend to increase in quiet sleep (Figure 7.4). For this reason, normalised rather than absolute LF and HF power should be used to assess the relative contribution of the sympathetic (nLF) and parasympathetic (nHF) nervous systems to fetal HRV, as it adjusts for changes in total power with increasing gestational age. With advancing gestation, there was a significant increase in nLF power in active sleep; there was also an increase in nHF power in quiet sleep. The ratio between absolute LF and HF powers remained unchanged with gestation (Figure 7.5).

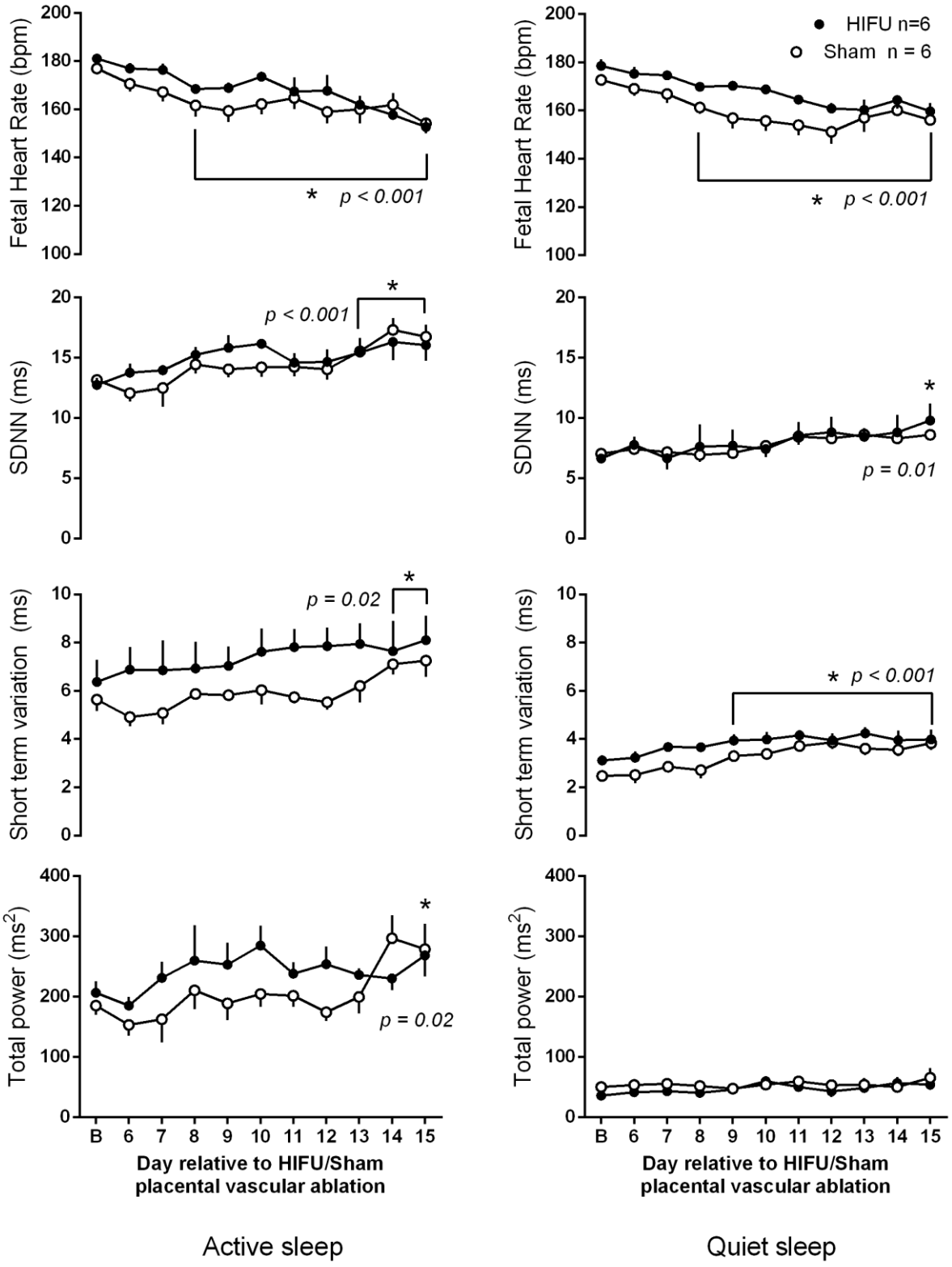

Figure 7.4: Change in fetal heart rate variability indices with gestational age (Group R).
Values represent mean ± SEM of indices of total fetal heart rate variability following HIFU (n=6) or sham (n=6) exposure of placental vasculature, maternal and fetal surgical instrumentation and general anaesthesia. Significant differences of the effect of time and treatment group were assessed using a repeated measures two-way ANOVA. Where authorised, post hoc Tukey's tests demonstrated a significant effect of time (*), with relevant *p* numbers given on the graphs.

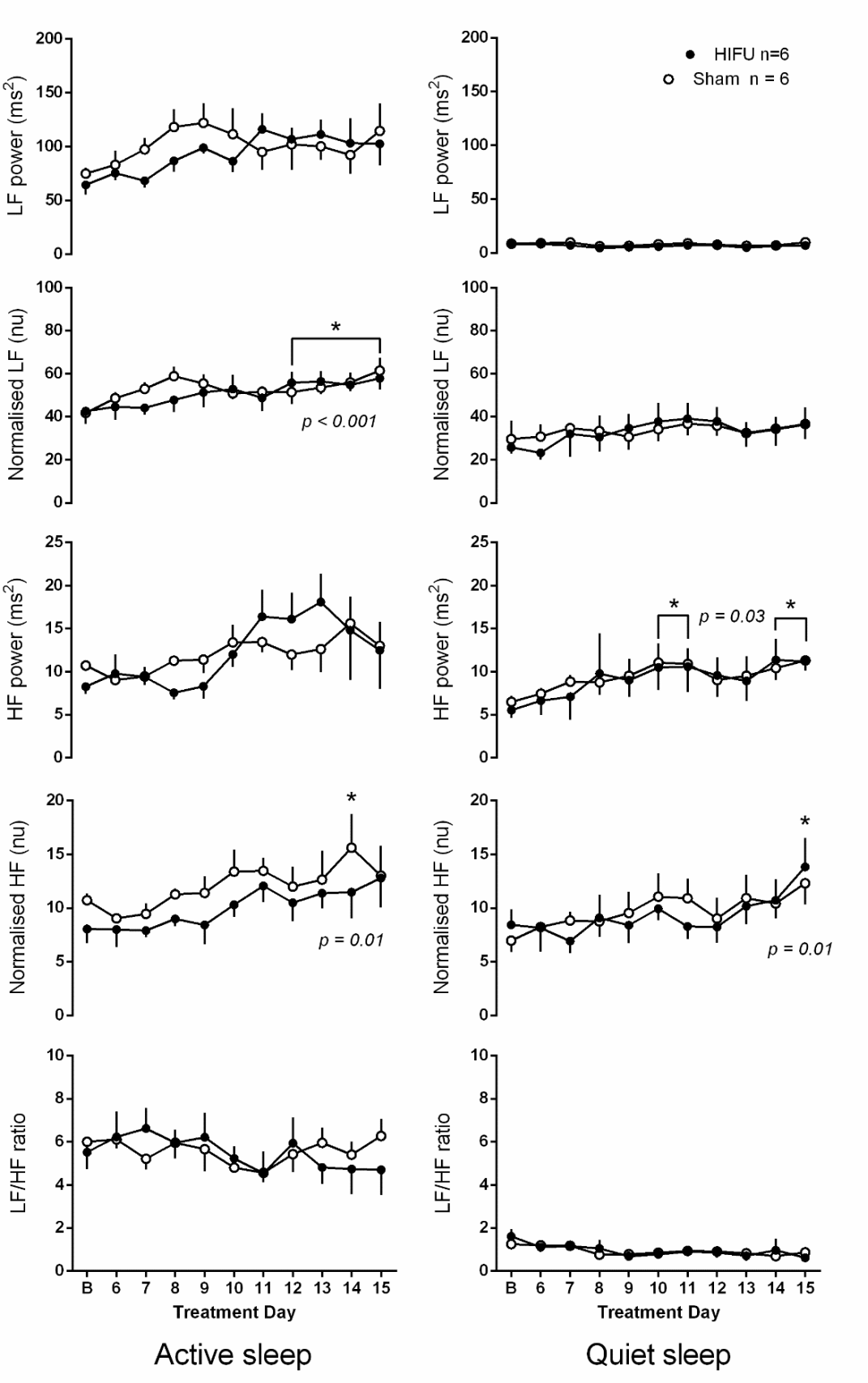

Figure 7.5: Autonomic nervous system contribution to fetal heart rate variability (Group R).
Values represent mean ± SEM of indices of the contribution of the sympathetic and parasympathetic nervous system to fetal heart rate variability following HIFU (n=6) or sham (n=6) exposure of placental vasculature, maternal and fetal surgical instrumentation and general anaesthesia. Significant differences of the effect of time and treatment group were assessed using a repeated measures two-way ANOVA. Where authorised, post hoc Tukey's tests demonstrated a significant effect of time (*), with relevant *p* numbers given on the graphs.

CHAPTER 8: MATERNO-FETAL PHYSIOLOGY DISCUSSION

The text in this chapter is substantially based on a previously published paper, Shaw et al. 2016 (281).

8.1 Maternal physiology

8.1.1 Intraoperative

Maternal physiology was monitored non-invasively in all animals during the intraoperative period to ensure the safe and effective delivery of general anaesthesia and the maintenance of adequate maternal cardiovascular function (as described in section 3.2.2). Additional monitoring of maternal physiology was performed during the application of HIFU or sham treatments in Group A and S animals, to observe the potential effects of HIFU exposures on the ewe in addition to general anaesthesia and/or invasive surgical procedures.

8.1.1.1 Acute maternal responses to HIFU (Group A)

The maternal mean arterial blood pressure and heart rate were measured during the baseline recording period of the Group A animals. Both the baseline blood pressure and heart rate were within the normal ranges for adult Welsh mountain pregnant sheep, although mean arterial pressure was lower than in un-anaesthetised sheep. In contrast, the maternal heart rate was not significantly different between anaesthetised and un-anaesthetised animals (Table 5.1, Table 5.3). While the normal range of mean arterial blood pressure for pregnant ewes is comparable to values for pregnant women, the normal range of resting heart rate is increased by approximately 20 beats per minute in sheep compared to humans (270, 294). The more pronounced depressive effect of isoflurane anaesthesia on mean arterial pressure than heart rate has previously been described (167, 173, 182). The effects of anaesthesia on maternal blood pressure were minimised with maternal positioning to avoid auto-caval compression and infusion of intravenous fluids to increase venous return, both of which were routinely performed in anaesthetised ewes. Therefore, while there was a statistically significant fall in maternal mean arterial pressure, this was not indicative of clinically significant hypotension.

In Group A animals, relative to the baseline recording period, maternal blood pressure and heart rate were stable throughout the acute experimental protocol, whether associated with HIFU or sham treatment (Figure 5.1). Intraoperatively, therefore, while a stable reduction in maternal blood pressure related to general anaesthesia, not HIFU or sham exposures, was noted, the more potentially clinically relevant findings were the changes in maternal uterine artery flow.

In Group A animals, following the completion of surgery, the mean rate of uterine artery blood flow remained within the normal range for pregnant sheep at this gestational age:

230 – 490 ml.min^{-1} (95% CI). This was measured in our laboratory, using similar chronically implanted Transonic flow probes to measure the flow rate of uterine artery blood as were used in the Group A animals in this study (270). However, in the Group A animals, there was a fall in uterine artery blood flow of up to 40% during the treatment phase of the acute experimental protocol, in both HIFU and sham exposed animals (Figure 5.3). This resulted in a corresponding reduction in uterine artery oxygen and glucose delivery to the uterus (Table 6.3).

Maternal super-oxygenation due to mechanical ventilation meant that maternal oxygen availability was high and stable, so even the lowest rate of intraoperative delivery of uterine oxygen remained within the normal range of uterine arterial oxygen delivery in the un-anaesthetised animal (270). Therefore, this change does not represent a hypoxic challenge to the fetus.

The concentration of maternal arterial glucose showed a statistically significant reduction with time during the experimental protocol, unrelated to treatment group. However, both the highest and lowest values still fell within the normal range for an un-anaesthetised sheep (Table 6.4), as did the uterine arterial rate of glucose delivery to the uterus, even during the period of lowest uterine flow (Table 6.3)(270). Again, this does not represent a period of clinically significant glucose inavailability for the fetus.

Hence, these reductions in uterine delivery of oxygen and glucose to the should be seen as secondary to the changes in uterine flow, and not a result of primary substrate inavailability. The reductions were also not sufficient to anticipate severe fetal compromise as a result. There were no significant differences between treatment groups for any of these variables, suggesting that the effect was due to common feature of the experimental protocol – namely, general anaesthesia, maternal surgery, uterine ultrasound imaging or handling – rather than a consequence of the application of HIFU to placental vasculature.

An acute, anaesthetic-related reduction in uterine perfusion, secondary to maternal hypotension and/or bradycardia has been previously linked to isoflurane anaesthesia in sheep (173-175, 181-184). This response was both time- and dose-dependent. All maternal variables recovered to baseline in these studies, at a MAC of 1.5-2.0, within 120 minutes of start of anaesthesia (181, 182). In our experiments, the start of the baseline recording period in Group A animals was between 125 – 180 minutes after the start of anaesthesia, and isoflurane delivery (1.5-2.5% inhaled concentration, equivalent to 1.4 – 2.2 MAC) remained stable throughout the experimental protocol. Accordingly, maternal mean heart rate and uterine arterial blood flow were appeared to have recovered from any acute anaesthetic-related reaction and were within

normal ranges for un-anaesthetised sheep for the duration of the baseline recording period, and were stable during the experimental protocol as previously discussed (Figure 5.1). Therefore, while autoregulatory falls in uterine arterial blood flow are described in response to maternal bradycardia or hypotension, this explanation does not appear to account for the fall in uterine arterial flow observed in Group A animals.

As maternal surgery was also completed by the time of the baseline recording period, in which maternal heart rate and blood pressure were essentially normal, the preceding maternal surgery should not account for the changes seen in uterine artery blood flow. Neither should exposure of the maternal uterus to ultrasound imaging, as this took place during the baseline recording period and the treatment phase, and so preceded the onset of the fall in uterine artery blood flow.

In fact, the fall in uterine artery blood flow coincided with the start of the treatment phase in both HIFU and sham exposed animals, and recovered following the end of the treatment phase. This indicates the most likely cause was the uterine handling needed to alter uterine position and optimise the acoustic window during the treatment phase. This was the only shared feature which started and stopped at those time point in both groups. The effect of direct intraoperative uterine contact and handling on uterine blood flow has not been previously reported. In our experiments, the reduced uterine artery blood flow was associated with an increase in uterine arterial vascular resistance (Figure 5.4a), which may be suggestive of localised vasospasm in response to uterine handling.

This fall in uterine blood flow during HIFU or sham exposures, and the associated changes in oxygen and glucose delivery, therefore appears to be a consequence of the invasive experimental procedures required for this phase of the study protocol. From this point of view, it is not clinically relevant, as the uterus would remain untouched in any potential non-invasive human treatment.

While maternal oxygenation and glucose availability remained clinically stable throughout the experimental protocol, there was a suggestion of differences in the clearance of bi-products of metabolism between treatment groups. By the end of the treatment period, and during recovery period (the last 30 minutes of the 90 minute experimental protocol), there was a significant difference in maternal P_aCO_2 and pH between treatment groups. This was a subtle effect, as compared to baseline, neither animal group developed a statistically significant decrease in pH or elevation in P_aCO_2 (i.e. there was no effect of time). Arterial lactate, bicarbonate concentration and arterial base excess remained unaffected (Table 6.8).

In both treatment groups, at the start of baseline maternal P_aCO_2 levels were elevated above the normal levels for un-anaesthetised sheep, and were not different to each other (Table 6.8, Table 6.9). This elevation in P_aCO_2 would be anticipated for an ewe under prolonged anaesthesia, mechanically ventilated in a recumbent position from previously published literature, due to the accumulation of CO_2 in the dead space of the lungs (182). However, during the treatment period, in HIFU exposed, but not sham exposed ewes, breath holds were performed. In order to maintain oxygenation during the breath holds, ewes in the HIFU exposed arm were pre-oxygenated by hyperventilation, between 4 and 7 times (once preceding each breath hold). This did not occur in the sham exposed groups, as breath holds were viewed to be a part of the HIFU treatment, not an experimental procedure. Hyperventilation is a more effective method of clearing CO_2 from the dead-space in the maternal lungs, compared to standard ventilation. Therefore, in HIFU exposed animals, maternal hyperventilation would have allowed increased clearance of CO_2 from the maternal blood, without accentuating the already pronounced effects of maternal super-oxygenation due to the high fraction of inspired oxygen. This may explain why maternal arterial pH and P_aCO_2 were different between treatment groups only after the treatment period of the experimental protocol.

8.1.1.2 **Acute maternal responses to HIFU (Group S)**

In Group S animals, maternal heart rate and oxygen saturation were monitored with a non-invasive pulse oximeter. End tidal expired CO_2 was monitored by capnography and uterine artery vascular resistance was monitored with Doppler ultrasound, which shows a significant correlation to absolute uterine arterial blood flow in pregnant sheep (295). However, unlike Group A, in Group S preparations, the baseline monitoring period commenced only 4-7 minutes, not 120-180 minutes, after the induction of anaesthesia.

Therefore, it was anticipated that there would be changes in uterine blood flow during the baseline (0-60 mins) and HIFU/sham exposure (60-120 mins) time periods with normalisation following induction of anaesthesia beginning during the recovery period (120-150 mins)(173-175, 181-184). This reduction in uterine flow was anticipated despite the use of maternal tilting to offset auto-caval compression and infusions of crystalloid fluids into the maternal venous circulation, but not confirmed as we did not monitor maternal blood pressure non-invasively.

Maternal heart rate remained stable and within normal limits for an un-anaesthetised ewe throughout the baseline, HIFU/sham and recovery time periods (Figure 5.1b). However, as maternal heart rate had remained stable and normal in Group A ewes, despite a reduction in

mean arterial pressure, this is not indicative of normal blood pressure in Group S ewes. Maternal oxygen saturation, isoflurane usage (1.5 – 2.5% inhaled concentration) and end tidal expired CO_2 also remained stable during all 3 phases of the experimental protocol, suggesting that an appropriate and stable level of general anaesthesia was delivered to the ewes throughout the experimental protocol (Figure 6.1). There was also no direct uterine handling. Matched breath holds (number, spacing and duration) and periods of hyperventilation were applied to both HIFU and sham exposed animals equally in this group.

On this background, evidence of changes in uterine arterial blood flow were still seen. There was an elevation in maternal UtA-PI following the induction of anaesthesia compared to values established in the un-anaesthetised ewe, 24 h earlier (day -1). This elevation of PI was coupled with the development of mild notching in the uterine artery. Considered together, this is suggestive of an increase in uterine artery vascular resistance. The onset of these changes preceded the application of HIFU or sham exposures, or placement of the waterbag on the maternal abdominal skin. The effects were of the same magnitude in both HIFU and sham treated groups (Figure 5.4b), further supporting that this was not a result of exposure to HIFU.

The UtA-PI had normalised by the first postoperative day, compared to the day -1 value, measured again in un-anaesthetised ewes. Both the un-anaesthetised and anaesthetised values for uterine artery PI in sheep, although different to each other, agree with those published elsewhere, which have only reported anaesthetised or un-anaesthetised values, not the change between states (218, 247, 296). This suggests that the increases in UtA-PI are a result of isoflurane anaesthesia, maternal positioning in a recumbent position (head down with a left lateral tilt), or a combination of the two. Regardless of cause, the alterations in uterine artery blood were transient, and fully reversible following the removal of anaesthesia and normal positioning of the ewe.

Whether this increase in resistance was sufficient to produce a clinically significant reduction in uterine arterial flow cannot be quantified by non-invasive measures, and uterine arterial notching is a risk predictor, not a diagnostic feature of utero-placental dysfunction in human pregnancy. As any human HIFU treatment would not be anticipated to be performed under general anaesthesia, there is little clinical importance of this finding to future translational studies.

8.1.2 Post-operative recovery (Groups R and S)

Maternal physiology was monitored for 20-21 days in Group R and S animals following application of HIFU or sham exposures. In Group R ewes, this was achieved by placement of an arterial catheter in the descending maternal aorta. In Group S ewes, uterine artery vascular resistance was monitored with Doppler ultrasound; operative time constraints prevented the placement of a uterine arterial flow probe in the Group R animals. Table 5.1 and Table 6.1 demonstrate that measurements of maternal cardiovascular and metabolic variables at the end of the acute experimental protocols in Group A and R were not significantly different, with the exception of maternal blood pressure, as expected given the previous discussion. Hence, findings of Group A and R, while not derived from the same animals, can be considered relative to each other.

In Group R, maternal mean arterial blood pressure recovered quickly to a stable level following reversal of isoflurane anaesthesia and showed no further changes or effect of treatment over the post-operative period in Group R animals. Maternal mean arterial pressure and heart rate were within the normal ranges for adult Welsh mountain pregnant sheep (270, 294) for the duration of the post-operative recovery (Figure 5.2).

There were no differences observed in maternal oxygenation, haemoglobin, glucose or lactate arterial concentrations between the treatment groups for the duration of the follow-up period. There were also no differences in maternal P_aCO_2, arterial base excess, arterial bicarbonate or lactate concentrations between treatment groups. The differences in maternal pH between treatment groups days 2-5 post-operative, again while statistically significant are not of clinical concern. All maternal pH values remained within the range expected for adult sheep, and do not represent respiratory or metabolic disturbances, based on the normality of the other variables. There was a transient increase in arterial lactate noted on day one post-operative in keeping with recovery from a period of fasting for surgery, which was not different between groups, and not sufficient to produce metabolic acidosis, or require renal buffering.

In Group S, non-invasive monitoring suggested that the uterine artery vascular resistance was normalised within 24 hours of the end of the period of general anaesthesia, both in terms of uterine artery PI (Figure 5.4b) and absence of notching in the pattern of flow, and remained stable for the remainder of the follow-up period. There was no significant change with advancing gestational age, in keeping with previously published values (247)

Together, these observations suggest that HIFU exposures did not compromise maternal physiology during the recovery period. Overall, both sham and HIFU exposed animals recovered well from a variable combination of general anaesthesia, surgery and HIFU occlusion of placental vasculature.

8.2 Fetal physiology

8.2.1 Intraoperative

Fetal physiology was monitored in the intraoperative period and during the application of HIFU or sham treatments in Group A (invasive monitoring) and Group S (non-invasive) fetuses.

8.2.1.1 Acute fetal responses to HIFU (Group A)

The fetal heart rate and mean arterial pressure were within normal ranges during the baseline recording period of the acute HIFU experimental protocol (Group A) for fetal Welsh mountain sheep at this stage of gestation (279). While the normal range of mean arterial blood pressure for fetal sheep is comparable to preterm and term human values at birth (297, 298), the normal range of resting heart rate is increased by approximately 20 beats per minute in sheep compared to the human fetus at a comparable gestational age (132, 279).

In Group A fetuses, unlike the ewes, mean post-ductal arterial blood pressure was not reduced by the effect of general anaesthesia, and was increased in the sham exposed fetuses. Conversely, the fetal heart rate showed a decrease in rate in both the HIFU and sham treated groups compared to un-anaesthetised fetuses (Table 5.2, Table 5.4), suggestive of the known effect of isoflurane type anaesthesia to depress fetal left ventricular cardiac output, certainly by reducing heart rate, and potentially by reducing fractional shortening of the left ventricle (168, 299). Regardless, fetal mean arterial blood pressure and heart rate remained stable throughout the acute experimental protocol and the application of sham or HIFU exposures (Figure 5.5).

Fetal haemodynamic function appeared to be normal during the baseline recording period in Group A animals, even after the preceding period of anaesthesia and invasive surgery, apart from an increase in femoral vascular resistance, a marker of peripheral vascular resistance (Table 5.5). The elevation of femoral vascular resistance occurred in both groups, and the magnitude of increase was greater in the sham exposed group. This increase in peripheral

vascular resistance is the most probable cause of the elevation in fetal mean arterial pressure observed in the sham exposed Group A animals. It is unclear why this response should be more pronounced in sham exposed animals compared to HIFU exposed animals. During this period, there was no evidence of central redistribution of the fetal circulation, as carotid arterial blood flow and vascular resistance remained within normal range, as did the ratio of carotid to femoral blood flow, a suggested index of brain sparing in fetal sheep (269, 300).

In the period of application of HIFU or sham exposures to the uterus, coinciding temporally with the reduction in maternal uterine arterial flow, there was a further increase in fetal femoral vascular resistance. There was a corresponding decrease in femoral arterial blood flow, which persisted beyond the recovery of the maternal uterine arterial flow to its baseline flow rates. There was no change in fetal carotid artery blood flow or vascular resistance during this time (Figure 5.7). These responses were not different between treatment groups, and the only feature of the experimental protocol introduced at this time which was common between the two groups, as previously discussed, was the period of gentle uterine handling.

This differential effect on two elements of the 'fetal brain sparing' response can be explained, as this was a non-hypoxic challenge to the fetus (Table 6.5). Fetal peripheral vasoconstriction, although classically understood as part of the fetal brain sparing response to acute hypoxia (300), can also result from fetal acidosis in the absence of fetal hypoxia (190), primarily mediated by the sympathetic nervous response and maintained by endocrine-mediated fetal stress responses (191). Cerebral vasodilatation in response to acute hypoxia is under paracrine, rather than systemic, control, and so functionally separated from the mechanisms of peripheral vasoconstriction (300). Peripheral vasoconstriction has been described in sheep fetuses as a response to reduced uterine blood flow in the absence of fetal hypoxia (189). An increase in umbilical arterial vascular resistance, and a redistribution of blood to the fetal brain, as a result of uterine surgery in human pregnancy (a non-hypoxic insult) has also been described (188).

Isoflurane sedation does not alter the capacity of fetal sheep to redistribute cerebral and systemic blood flow in response to reduced utero-placental flow or the development of acidosis (184). Given that the delivery of oxygen and glucose to the fetal brain by the carotid artery was preserved within normal limits for the duration of all experiments in Group A animals, hypoxia-induced cerebral vasodilatation would not be expected. Therefore, the increase in the ratio of the carotid to femoral blood flow in the fetus is secondary to the fall in femoral blood flow, not an indication of a classical brain-sparing redistribution of the fetal cardiac output in response to acute fetal hypoxia being represented by cerebral vasodilatation and peripheral vasoconstriction

(301). Therefore, the increased peripheral vascular resistance is most likely as a result of increased sympathetic outflow, potentially as a result of the changes in maternal uterine artery blood flow.

Although fetal oxygenation remained within normal limits for the duration of the procedure, there was a gradual reduction in the fetal P_aO_2, the saturation of oxyhaemoglobin, and delivery of oxygen to the brain between the baseline and recovery periods. These changes were not different between HIFU and sham groups and most likely represent fetal deterioration under anaesthetic rather than an effect of HIFU exposures. With increasing duration of anaesthesia, a mixed respiratory and metabolic fetal acidosis still developed. Placental transfer of oxygen relies on the double Bohr effect, where elimination of CO_2 from the fetal circulation drives maternal oxyhaemoglobin dissociation and increases the affinity of fetal haemoglobin for oxygen (302). Anything that reduces fetal elimination of CO_2, resulting in a fetal respiratory acidosis, paradoxically reduces the availability of maternal oxygen at the placental interface.

Carbon dioxide is generated by the fetus at a steady rate and is eliminated from the fetal circulation by diffusion across the placenta (303). Elevated maternal P_aCO_2 causes steady state equilibration (Fick's first principle) to reset to a higher baseline, eliminating less CO_2 from the fetus (303). Although there was no increase in maternal P_aCO_2 observed during the experimental protocol, the maternal baseline values were above the normal range for non-anesthetised sheep. Ventilating sheep in the recumbent position and their increased alveolar dead space compared to humans make CO_2 elimination from the sheep lungs less effective under anaesthesia (304-306), resulting in a mild maternal respiratory acidosis, as previously described. In our animals, mechanical ventilation was used to maintain the ewes in an isocapnic state despite the need for periods of breath holding, although as previously discussed, the periods of hyperventilation in the HIFU-exposed ewes conferred an advantage in this regard, compared to sham-exposed ewes. This likely accounts for the differences in pH (and in P_aCO_2, although this did not reach significance) seen between sham and HIFU exposed fetuses during the treatment period of the acute experimental protocol, where the sham fetuses experienced a more rapid fall in pH than the HIFU exposed fetuses.

The placental exchange rate of CO_2 is also affected by the supra-physiological P_aO_2 in the mother and fetus. The Haldane effect describes the increased capacity of deoxygenated haemoglobin to buffer CO_2 compared to oxygenated haemoglobin (307), and this has been calculated to account for 46% of placental CO_2 exchange (303). The artificially elevated concentrations of oxygenated haemoglobin in both mother and fetus reduce the magnitude of the Haldane effect in this setting, and so further reduce the fetal elimination of CO_2. Diffusion of

CO_2 across the placenta is limited by uterine blood flow (304) because it is highly soluble (307). Therefore, the additive effects of reduced uterine artery blood flow during the period of uterine manipulation may accelerate the increase in fetal CO_2 accumulation.

Decreases in fetal pH in our results were likely further augmented by the fetal peripheral vasoconstriction that they caused. Lactate is a product of anaerobic respiration and is produced in greater quantities by the under-perfused fetal tissues during peripheral vasoconstriction, particularly by the muscle bulk of the hind limbs (308, 309). In our study, it increased by the recovery period of the experiment, potentially contributing to a mixed respiratory and metabolic acidosis.

A progressive fetal respiratory acidosis and falling P_aO_2 has been reported in the anaesthetised fetus regardless of concomitant operative or experimental procedures (181, 182), and the P_aCO_2 at the end of our recovery period is comparable to other published values for this duration of isoflurane anaesthesia (Appendix I). It could be suggested that these changes in fetal pH, as a result of anaesthesia, are the likely underlying mechanism explaining the trend to reduced fetal oxygenation seen in our studies, and the activation of the sympathetic nervous system to produce peripheral vasoconstriction.

Collectively, these findings suggest that the effects of placental HIFU or sham exposures on the fetal physiology were the result of responses to a uterine vasospasm and the need for mechanical ventilation and general anaesthesia, rather than to a period of acute feta hypoxia, or to HIFU exposures themselves.

8.2.1.2 **Acute fetal responses to HIFU (Group S)**

On the day preceding HIFU or sham exposures, in un-anaesthetised sheep the mean ± SD umbilical artery PI was 1.0 ± 0.2 in the HIFU group and 0.9 ± 0.1 in the sham group. These values are consistent with both expected ranges from published sheep literature and human pregnancy at a corresponding gestational age (247, 310). The mean ± SD of the fetal middle cerebral artery PI was 1.7 ± 0.2 in the HIFU group and 1.6 ± 0.1 in the sham group (Figure 5.9). These were again consistent with the expected ranges from human pregnancy at a corresponding gestational age (222, 226); there is no published data on the expected ranges in sheep.

Following the induction of anaesthesia in Group S animals, there was an increase in UA-PI, which reached significance before the application of either HIFU or sham exposures of placental

vasculature, and continued to rise for the duration of the general anaesthesia. There was also a decrease in MCA-PI which reached significance at the start of the HIFU or sham exposure period and persisted beyond the reversal of anaesthesia. These responses were equal between treatment groups.

The timing the increase in resistance in the umbilical circulation matches the timing of the increase in resistance to flow in the maternal uterine artery seen in Group S ewes, which has previously been discussed as a feature of isoflurane anaesthesia. This response was similar to Group A fetus, where changes in maternal uterine vascular resistance produced changes fetal femoral vascular resistance. Changes in fetal total peripheral resistance have contributions from the systemic vasculature, of which femoral vascular resistance is a measure, as well as from the umbilical-placental vascular bed, of which umbilical artery Doppler PI is a non-invasive measure (311). The umbilical and femoral vascular beds are both sensitive to vasoactive hormones of the sympatho-adrenal and renin-angiotensin systems (312). For this reason, it could be suggested that in the absence of pre-existing utero-placental dysfunction, invasively measured changes in fetal femoral artery vascular resistance should be mirrored by changes in non-invasively calculated umbilical artery PI, especially if the causative mechanism of the changes is circulating vasoactive hormones.

However, unlike Group A animals, where there was no change in carotid blood flow in response to either anaesthesia or HIFU, MCA-PI suggests cerebral redistribution in Group S animals during anaesthesia. While direct observation of arterial oxygenation was not performed in the Group S fetuses, extrapolation from the values for arterial oxygen content and tissue delivery in the Group A fetuses (Table 6.7) would indicate that this was a non-hypoxic period. Therefore, the changes in Group S fetuses appear to simulate classic findings in utero-placental dysfunction and fetal redistribution of blood flow preferentially to the central organs, despite hypoxia not being the underlying cause. This pattern of central redistribution of blood in response to EXIT surgery, in which the fetus was not hypoxic, has been described in humans (188).

It is possible that these fetal defence mechanisms were a response to the reduction in fetal heart rate and depression of cardiac function observed by fetal echocardiography in Group S fetuses. Pre-operatively, in un-anaesthetised fetuses, the values obtained for ductus venosus PIV, left ventricular MPI, FS and EF were broadly comparable to expected values of human fetuses at a comparable gestation (235, 249-252, 255) and sheep (240). However, while anaesthesia alone did not result in a significant reduction in left ventricular ejection fraction or

fractional shortening, it was sufficient to increase left ventricular MPI and ductus venosus PIV during anaesthesia, both markers of decompensation and congestive failure of the fetal heart. This effect was not different between HIFU or sham treated animals (Figure 5.10), but coupled with the reduction in fetal heart rate would reflect a likely reduction in fetal combined cardiac output in both treatment groups. Just as birth asphyxia is recognised to be predominately secondary to failure to deliver oxygen to the fetal brain rather than primary deficit in oxygen availability (313), a reduction in fetal cardiac function may have been sufficient to initiate redistribution of blood flow to the fetal brain.

Collectively, these findings suggest that the effects of placental HIFU or sham exposures on the fetal physiology were the result general anaesthesia, rather than of HIFU exposures themselves.

8.2.2 Post-operative recovery

Fetal physiology was monitored for 20-21 days in Group R and S animals following application of transdermal HIFU or sham exposures (Group A animals were not recovered from anaesthesia).

In Group S animals, the umbilical artery, middle cerebral artery and ductus venosus Doppler PI(V)s and fetal echocardiography were used to monitor the feto-placental circulation after completion HIFU and sham exposures and reversal of anaesthesia.

In Group R animals, this was achieved by placement of a descending aortic (post-ductal) arterial catheter and Transonic femoral arterial flow probe. Operative time constraints prevented the placement of a carotid arterial flow probe and ascending aortic (pre-ductal) catheter in Group R animals.

8.2.2.1 **Group R fetuses**

The main change in the fetal circulation observed in Group A animals was the increase in fetal femoral vascular resistance. In Group R, fetal femoral vascular resistance was also elevated following reversal of anaesthesia (Table 5.2), and remained significantly elevated for the first 24 hours in HIFU exposed or control Group R fetuses. After this, femoral vascular resistance fell back towards baseline until the fifth postoperative day, and the rate or recovery was not different between treatment groups (Figure 5.8). It then remained stable, and within normal

ranges for gestation, while femoral arterial blood flow and amplitude of flow showed increases with gestational age in keeping with previous longitudinal studies (269). It is not possible to comment on carotid arterial flow, as flow probes were not placed in Group R animals.

When the fetal heart rate and blood pressure at the end of the experimental protocol in Group A animals was compared to the heart rate in fetuses immediately following the reversal of anaesthesia, there are no differences (Table 5.2). Fetal heart rate and blood pressure were not different between treatment groups at any point in Group R animals, and fell within normal ranges for gestation. It is well established that fetal arterial blood pressure and heart rate falls with increasing gestational age (314-320), and this occurred in Group R fetuses (Figure 5.6).

As discussed above, in Group A animals by the end of the recovery period, there was a reduction in the partial pressure of fetal arterial oxygen, a mixed respiratory and metabolic acidosis, and evidence of haemoconcentration. Table 6.2 shows that in the Group R fetuses, soon after reversal of anaesthesia, that the pH was higher, and the P_aCO_2 and haematocrit were lower. Fetal P_aO_2 and saturation of oxyhaemoglobin were not different between groups, and both were normal values. The difference in median duration of anaesthesia in these two groups was 10 minutes (Table 5.2) so this is unlikely to account for these differences; similarly, the number of placental vessels occluded was comparable between Groups A and R. It is possible the Group R fetuses were in better condition due to the placement of less arterial catheters and flow probes than in Group A fetuses, or that these changes represent rapid clearance of fetal CO_2 following reversal and anaesthesia and re-establishment of spontaneous maternal ventilation in the standing position.

There are still statistically significant differences in fetal pH, P_aCO_2 and lactate on the first post-operative day. These values are not different to baseline and stable from the second day onwards. Fetal P_aO_2, saturation of oxyhaemoglobin, glucose concentration, and femoral arterial delivery of oxygen and glucose are all normal compared to baseline on the first post-operative day. Femoral arterial oxygen and glucose deliveries show gestational age-related increases, in line with the increases in femoral arterial blood flow.

Hence it appears that resolution of the fetal defence responses, and the consequences of general anaesthesia, noted in Group A animals were also present in Group R animals following the reversal of anaesthesia. These responses recovered quickly and equally in both HIFU exposed and control animals. The expected ontogenic changes in fetal heart rate, blood pressure and femoral blood flow and substrate delivery were seen in both treatment groups, indicating. Hence there is no evidence of chronic fetal cardiovascular compromised or fetal

distress. This is despite the fact that fetuses in the HIFU treated group were exposed to HIFU placental vascular occlusion and a longer duration of anaesthesia than fetuses in the control group, so could have been expected to have a different recovery profile.

8.2.2.2 **Group S fetuses**

The main change in fetal Doppler studies observed intra-operatively in Group S fetuses was an elevation of UA-PI and reduction in MCA-PI, leading to a fall in CPR.

Following the reversal of anaesthesia, the UA-PI remained significantly elevated for the first 24 hours following HIFU or sham exposures. It returned to baseline over the next four days at the same rate in both treatment groups. Following this, umbilical artery Doppler PI showed a tendency to decrease with increasing gestational age following HIFU of sham exposures of placental vasculature, but which like other published values did not show a significant fall in PI at this stage of gestation (205, 247). The values themselves agree well with expected values for sheep fetuses of a comparable gestational age and human fetuses in the third trimester (310). This suggests that there was no clinically significant utero-placental dysfunction acquired as a result of the HIFU occlusion or sham exposures of placental vasculature. These findings also suggest that the resolution of increased fetal peripheral resistance occurred in a stepwise fashion, over the following three to four days, before stabilising at values typical for this stage of gestation in un-anaesthetised sheep (205). This is in keeping with the resolution of a response mediated by vasoactive hormones, rather than progressive fetal deterioration.

Redistribution of blood to the fetal brain as indicated by the reductions in MCA-PI and CPR also continued for 3 days, before they were restored to typical values for human pregnancy at a comparable gestational age, and remained stable (222); there are no published longitudinal values for sheep against which to compare. The magnitude or duration of this redistribution was not different between treatment groups. While not directly comparable, there was no evidence of fetal hypoxia in Group R animals over this same time period, so the underlying cause of this apparent vasodilatation of the cerebral vasculature again appears to be non-hypoxic, but unknown. Due to the lack of carotid artery flow probes it was not possible to correlate MCA Doppler changes between Group R and S animals.

While under general anaesthesia, there was also evidence of reduction in fetal cardiac function, with a lower LV-MPI and DV-PIV. DV-PIV was recovered by the first day post procedure, LV-MPI by the second. However, for the first 1-4 days post procedure in Group S fetuses, the LV-

EF and LV-FS were increased (Figure 5.10), without a corresponding increase in fetal heart rate (Figure 5.5). In terms of timescale, these changes match the period during which an increase in peripheral resistance and central redistribution of blood is observed in the fetus (Figure 5.7, Figure 5.9). This may represent a cardiac contribution to the maintenance of cardiovascular defence mechanisms, although the effectiveness of increasing stroke volume compared to heart rate is thought to be minimal (321, 322). However, recently, two studies of pre-labour cardiac function showed that human fetuses with a lower left ventricular cardiac output were more likely to develop fetal compromise in response to uterine contractions. These fetuses also had the lowest CPRs (323, 324). This suggests, at least in principle, a higher left ventricular cardiac output is beneficial to a fetus undergoing stress and maintaining cerebral redistribution. Regardless, these changes recovered within four days of the exposure to HIFU or sham, and all indices of cardiac function remained stable for the remained of the follow-up period.

Overall, therefore it seems that the fetus can withstand appropriately the challenges of anaesthesia, surgery and of HIFU, and recover rapidly from these events without impact on fetal cardiovascular function or metabolic status. It should be noted that the sheep fetuses were healthy and that the effects on an already compromised fetus with reduced capacity to tolerate intrauterine insults may be different, for example a fetus already affected by TTTS. However, one aim of developing a non-invasive method to divide fetal circulations is to reduce the risks associated with the invasive nature of current therapies and to allow earlier intervention before such fetal compromise occurs.

8.3 **Fetal growth and physiological maturation**

We were able to assess fetal growth velocity in Group S animals by performing non-invasive ultrasound measures of fetal biometry. These studies demonstrated not only consistent growth, which did not differ between treatment groups, but also a linear trend in the pattern of growth (Figure 7.2). This is comparable with other invasive and non-invasive measures of fetal growth reported which show a linear pattern of growth in sheep towards the end of gestation, rather than the curvilinear trends more familiar from human pregnancy (203, 325), a pattern which itself has recently been questioned (326). While standard ultrasound measures of fetal biometry in sheep are not commonly used, they are described in sufficient detail for use in a reproducible fashion.

Furthermore, comparison of post-mortem biometry and ultrasound biometry taken on the same day in this study showed a high level of agreement (Figure 7.1). While there was a tendency to underestimate fetal weight by the formulae used, particularly in lower weights, this is a known feature of Hadlock fetal weight estimation (200). Therefore, while a system optimised for human use might be expected to perform poorly in sheep, the Hadlock formula still outperformed other formulae suggested for specific use in sheep (203).

The rate of fetal growth in late gestation is known to be affected by under or over production of cortisol and its effect on nutrient transfer across the placenta to the fetus (325, 327). Combined, the maintenance of normal growth rate with normal gestational changes in fetal plasma cortisol (Figure 7.3) and stable glucose availability (Table 6.7) strongly suggests that sufficient nutrient transfer across the placenta to meet the fetal requirements was maintained until the time of post-mortem. In addition, there was no evidence of hypoxaemia in the post-ductal circulation (Table 6.7) during the follow-up period, again consistent with the conclusion that no utero-placental dysfunction was induced by HIFU occlusion of placental vessels, or by any other experimental procedure performed in Group R or S animals.

These findings are supported by comparison of post mortem biometry between treatment groups in fetus after 20-21 days of follow-up, which showed that there was no difference in fetal weight, biometry, fat deposition or asymmetric growth at the time of post-mortem (Table 7.3, Table 7.4). While the onset of adverse intrauterine conditions from early or mid-gestation in fetal sheep is well documented to produce a reduction in fetal body weight (328), even apparently significant hypoxic insults in late gestation do not always produce this outcome, although they are associated with asymmetric growth (268, 328, 329).

In Group S, the only animals in which this was measured, showed no differences in absolute fetal organ weights or organ weights as a proportion of total body weight. Notably, there was no difference in adrenal to body weight ratio (Table 7.5), which has previously been shown as the result of short term (3 days) reductions in umbilical artery blood flow (329). Given the transient findings on Doppler ultrasound of redistribution of blood to the fetal brain and an increase in utero-placental resistance, these findings suggest that the degree of the fetal insult was not sufficient to result in any changes in the growth pattern of the fetus or fetal organs. This again supports the idea that there was adequate placental function to maintain fetal growth and development until the time of post mortem.

In the sheep, placental cotyledonary number reaches its maximum at 40 days of gestation; placental weight is maximal at 70 days (330). After this time, placental weight is maintained

until term (331) although remodelling of placentome types can occur to match fetal needs and intrauterine events (332). Placentome morphology is assessed with respect to the degree of eversion of the fetal portion in respect to maternal tissue, and classified as type A (least eversion) to D (most eversion) (160). Towards term, there is a natural reduction in the proportion of type D placentomes resulting from the natural rise in fetal plasma cortisol levels, which is thought to increase glucose delivery to the fetus (327). Adverse intrauterine conditions, such as maternal under or over nutrition, hypoxaemia, reduction in umbilical blood flow, heat exposure and alterations in the activity of cortisol and the renin-angiotensin system have also been shown to influence placental weight and morphology at term (329, 333-337) although results are contradictory as to whether the proportion of type A or type D placentomes are increased by a fetal challenge in late gestation (327, 329).

Reassuringly in Group S animals, the total placental weights were comparable, and the proportion of type A/B and type C/D placentomes were not different between treatment groups, either in terms of number or weight (Table 7.6), similar to previously reported findings for this sheep breed (329). This is potentially unexpected as ablation of six placentomes and occlusion of the blood flow arising here could represent up to a ten percent loss of placental mass, and it might be reasonable to expect some degree of compensation for this loss of blood supply and surface area within the placentome system. This is one area where the sheep placental model, while a good anatomical model of anastomoses in the human monochorionic placenta, is a poorer model of the haemodynamics of twin pregnancy: ideally following occlusion of placental anastomoses the circulation of each twin remains intact with no loss of placental supply. However, it is reassuring to demonstrate that even in the presence of loss of up to 10% of the placental blood supply there is no obvious detrimental effect on fetal growth or placental function. Of course, it should be noted here again, that these were healthy sheep and placentae without pre-existing compromise and the situation in a fetus affected with TTTS may ultimately be different.

In addition to monitoring for gross differences in placental morphology, fetal growth and relative organ size, we also investigated directly for evidence of fetal stress. Elevated fetal plasma cortisol has been reported in sheep fetuses undergoing chronic stress, such as chronic intrauterine hypoxia (338, 339), which is implicated in the persistence of peripheral vascular resistance (301). In Group R animals, we could compare fetal plasma cortisol on day five postoperative, after surgical recovery was completed and all cardiovascular and metabolic variables were normal and stable. At this stage of gestation, fetal plasma cortisol concentrations would still be low, before the cortisol surge that triggers parturition in sheep had

occurred. Accordingly, fetal plasma cortisol levels at this time were around 10 $ng.ml^{-1}$, typical for this gestation (340) and not different between treatment groups, suggesting good recovery from surgery in both groups. At the time of post mortem, 15 days later, cortisol levels were higher, as expected in preparation for delivery, but were again not different between groups. The rise in endogenous cortisol levels approaching term underlies the increase in arterial blood pressure observed in sheep fetuses in late gestation as the sympathetic nervous system matures and begins to establish resting tone (341, 342) and alterations in feta plasma cortisol levels or the activity of the renin-angiotensin system disrupt this pattern of change (340). Accordingly, we could demonstrate progressive increases in mean arterial blood pressure in both treatment groups in fetuses in Groups R (Figure 5.6). Combined, these findings again support the theory that HIFU occlusion of placental vasculature caused no chronic fetal stress in the treated group, and that in fact both groups had recovered well from surgery and tolerated chronic instrumentation well for the duration of the follow-up period.

Finally, the presence of arterial catheters and flow probes allowed the examination of beat-to-beat variation in fetal heart rate to assess the function of the autonomic nervous system in the control of the heart rate (139, 140, 343). Fetuses were predominantly in an active sleep state, which was expected from the observed distribution of fetal behaviour states at these gestational ages (344). Fetuses were highly comparable between treatment groups in both active and quiet sleep (Table 7.7).

Overall variability in the fetal heart rate was greater in active sleep, denoted by a higher mean SDNN and STV in active sleep. Active sleep appears to be a sympathetically dominant state with elevated absolute and normalised LF power compared to the quiet sleep state; the higher ratio of LF to HF power in active sleep also demonstrates this sympathetic dominance. Quiet sleep appears to be a parasympathetically dominant state. However, this appears to be due to withdrawal of sympathetic stimulation rather than parasympathetic nervous system activation, as there is no change in normalised HF power between the sleep states. Given the large difference in total power between sleep states, this would be expected to provide a more comparable measure of the influence of the parasympathetic nervous system between sleep states as it adjusts for the differences in total power (Table 7.7).

During the follow-up period, there were no significant effects of treatment group for any variable of fetal heart rate variability, in either quiet or active sleep states (Figure 7.4, Figure 7.5). Appropriate gestational age-related increases were seen in overall variability (SDNN), the parasympathetic (nHF) and sympathetic (nLF) nervous systems contribution to fetal heart rate variability as both systems matured in the fetuses approaching full term. The STV also

increased in the Group R fetal sheep, in line with expected values from human pregnancy at this gestation (132). These increases can be impaired by fetal growth restriction, and a persistent reduction in STV is a strong indicator of fetal compromise (130), with lower heart rate variability in FGR fetuses resulting from sympathetic suppression (133, 135-138). In experimental fetal sheep, chronic hypoxia has been suggested to decrease the overall fetal heart rate variability, the STV and the sympathetic nervous system contribution to control of fetal heart rate variability (345).

In the present study, there were no changes indicative of chronic stress seen in the animals treated with HIFU. This agrees well with the findings of fetal plasma cortisol and normal ontogenic changes in fetal heart rate, fetal arterial blood pressure and regional blood flow. This suggests, in these fetuses, that the normal pattern of neuro-endocrine development was not affected by the experimental procedures performed, or the application of HIFU to occlude the placental vasculature.

Together, features of consistent fetal growth, normal fetal body size and organ weights at post mortem and an absence of several independent non-invasive and invasive markers of chronic fetal stress provide robust evidence to support that HIFU mediated placental vascular occlusions did not result in fetal compromise.

CHAPTER 9: CONCLUSIONS AND FUTURE WORK

This thesis demonstrates that it is possible to occlude placental blood vessels in the pregnant sheep using non-invasive HIFU. Using an iterative experimental design, we have developed and refined a transuterine, then a transdermal, treatment protocol to deliver HIFU energy into the intra-uterine space, and occlude target placental blood vessels.

This study shows the feasibility of using ultrasound as the imaging modality for vessel targeting and monitoring treatment responses. The final treatment protocol, used in Group R animals, is not yet necessarily fully optimised for use in sheep, and is not optimised for use in human pregnancy. However, to date, it is the first reported use of ultrasound-guided HIFU to selectively occlude placental blood vessels.

Table 9.1 summarises the key findings of the study which specifically demonstrate the feasibility and efficacy of HIFU as a method of non-invasive placental vascular occlusion. These points align to the first hypothesis of the thesis (section 2.2). The occlusion rate in placental blood vessels when transdermal HIFU was applied (as it would be in any potential human therapy) was 97% in the most refined version of the treatment protocol. There was histological evidence that the resultant vascular occlusion persisted for at least 21 days, with changes indicative of fibrosis obliterans in 75% of vascular targets.

Colour flow Doppler ultrasound was also shown to be an accurate method of targeting vascular targets, and confirming occlusion non-invasively. This is of direct clinical relevance, as the only imaging modality which has been used to identify vascular anastomoses in the human monochorionic placenta is ultrasound. Therefore, the imaging modality planned for HIFU guidance in any potential human treatment is ultrasound.

While the efficacy off occlusion appears high in this animal model, the nature of the sheep placenta allowed a multitude of targets, from which the easiest could be selected. However, in a clinical setting, the AVAs causative of TTTS need to be occluded, not simply the easiest vessels to target. Therefore, there still needs to be prospective evaluation of the feasibility of using HIFU to (i) occlude human placental blood vessels, and (ii) occlude selected blood vessels in the monochorionic placenta.

This evaluation will need to include equipment and treatment protocol adaptions to (in outline):

(i) Improve the quality of the imaging to the expected standard for human obstetric applications;
(ii) Address the bioengineering requirements of the transducer, which will need to have a larger central aperture, longer focal length but retain a small and precise focal zone;

(iii) Improve the user interface and system control software to be a more robust system with introduction of automated safety checks prior to the firing of HIFU; and

(iv) Use a more adaptive gantry apparatus to stabilise the HIFU and diagnostic transducers, which could allow for angulation and rotation integrated head to be introduced into treatment protocols.

This list outlines the minimum amount of work which would be required to create a HIFU system suitable for human treatment, and represents a substantial amount of outstanding software and hardware development. As such, while this thesis demonstrates the potential for HIFU to be used in the treatment of TTTS, the research has not yet progressed to a point where human treatment would be feasible or ethical.

Finding of the study	Evidence provided	Thesis section / Reference
Sheep placental blood vessels can be occluded using HIFU.		
Blood vessels of clinically relevant diameters can be occluded non-invasively using HIFU	The diameter of occluded blood vessels in the study (measured histologically) was between 0.4 - 2.9 mm. The quoted diameter of human placental arterio-venous anastomoses is 0.9 - 2.1 mm. Successful occlusion rates: Group A protocol: 93% (n=28/30) Group S protocol: 91% (n=31/34) Group R protocol: 97% (n=58/60)	Lewi *et al.* 2007 (7) Section 4.2.2.1 Section 4.4.2.1 Section 4.5.2.1
Sufficient HIFU energy can be delivered into the intra-uterine space to cause heating effects	Hyperecho (US evidence of tissue heating) observed during HIFU exposures: Group A protocol: 100% (n=28/28) Group S protocol: 84% (n=26/31) Group R protocol: 97% (n=56/58)	Section 4.2.2.1 Section 4.4.2.1 Section 4.5.2.1
HIFU mediated vascular occlusion persists for at least 21 days post exposure	Evidence of trapped erythrocytes (H&E) after 21 days in 88/89 target vessels where colour flow Doppler showed occlusion. Evidence of organised clot (PTAH) after 21 days in 24/24 target vessels examined. Evidence of vacuolar degeneration surrounding target vessels (H&E) in 73/88 (75%) cases where trapped erythrocytes were found.	Section 4.4.2.1 Section 4.5.2.1
Ultrasound guidance is a feasible modality to target and monitor HIFU mediated placental vascular occlusion		
Sheep placental blood vessels of clinically relevant diameters can be identified with colour flow Doppler ultrasound.	Colour flow Doppler signal can be demonstrated arising from the fetal portion of placentomes. The diameters of the targeted vessels (measured histologically) was 0.4 - 2.9 mm.	Figure 4.3 Lewi *et al.* 2007 (7)
Colour flow Doppler ultrasound is a sufficiently accurate method of targeting placental blood vessels to allow HIFU mediated occlusion.	Identified targeting errors resulted in failed occlusion. Discrepancy between the target and HIFU focal plane > 5 mm was sufficient to result in failed occlusions.	Table 4.7
Colour flow Doppler ultrasound is an accurate method of confirming vascular occlusion (rather than identifying transient vascular spasm).	Absent of preserved colour flow Doppler signal can be seen in the target vessel following HIFU exposures. This correlates well with histological findings of entrapped erythrocytes within exposed vessel lumen: True positives: 130/130 True negatives: 9/9 False positives: 0 False negatives: 0 CFD and histology not correlated: 9/148	Figure 4.5, 4.6 and 4.7
Tissue responses to HIFU exposures can be monitored real-time using B-mode ultrasound to identify hyperecho	Hyperecho (US evidence of tissue heating) observed during HIFU exposures: Group A protocol: 100% (n=28/28) Group S protocol: 84% (n=26/31) Group R protocol: 97% (n=56/58)	Figure 4.9

Table 9.1: Key findings of the study: feasibility and efficacy.
The table lists the key findings of the study which align to the first hypothesis, that it is possible to use ultrasound guided HIFU to permanently occlude placental blood vessels. The supporting evidence for the findings is summarised in the table, and the section of the thesis where this evidence is presented or discussed further is also listed.

Prior to this study, the potential for HIFU to cause direct iatrogenic harm to mother, fetus or placenta was suspected based on the known side effect profile of transdermal HIFU. This study has confirmed that maternal, fetal and placental damage can result from the application of HIFU to occlude placental blood vessels. The key points are again summarised in Table 9.2 and Table 9.3, which align to hypothesis 2a (section 2.2).

Overall, the most common adverse event encountered was maternal skin burns in ewes: 6/19 (32%) of ewes experienced a skin burn. In the final version of the treatment protocol 1/10 (10%) experienced a skin burn (2% of HIFU exposure series resulted in burn). While these rates are higher than quoted in retrospective large studies of using a commercially available HIFU system and an established treatment protocol (0.26%, 9988 patients, (107), they are similar to the rates described in prospective smaller scale studies of using HIFU in novel applications (4-10%, 22-80 patients, (108-112, 346, 347). The maternal skin burns healed well with no need for veterinary attention (minor complications (class B) as per SIR guidance (106)), and were well tolerated by the ewes with minimal requirements for analgesia.

The study also reported single instances of a fetal burn (4% fetuses, 1% HIFU exposure series), a uterine burn (6% ewes, 1% transdermal HIFU exposure series) and a placental vascular haemorrhage (4% ewes, 1% HIFU exposure series). All three were likely related to operator or system error, and so should be preventable, but the fetal and uterine burn did occur in the Group R HIFU protocol, i.e. the most refined HIFU treatment protocol.

There were no indications of injury to the maternal bladder, bowel or problems with maternal mobility (nerve or joint injury). There were no instance or preterm rupture of membranes, preterm labour, development of fetal anaemia or intrauterine fetal death related to exposure to HIFU.

Importantly, safety protocols were identified and introduced which reduced the risk of maternal and fetal burns and placental vascular haemorrhage. As previously discussed, there is scope for the safety protocols to be developed further and made more rigorous, potentially with the introduction of automated checks, which may reduce the rate of adverse events further.

Regardless, these rates of adverse events could cast doubt on the suitability of this technique to be adapted to human pregnancy, or to be the subject of a first in human clinical trial. However, the clinical need to test novel agents or technologies with unknown efficacy and safety in rare diseases is a recognised issue in clinical trial methodology. Accordingly, clinical study designs such as the Bryant Day two stage design, are used to evaluate clinical response and toxicity in such challenging circumstances. This study design considers two end-points, both efficacy and

safety, and rejects the new agent or technology if the positive response rate is inadequate, or there the rate of adverse events is excessive. This limits recruitment to the first stage of the study, and prevents recruitment to the larger second stage, until an adequate efficacy and safety have been established. Such a design usually requires one or more positive patient response in around 5-10 patients and limits the rate of adverse events to one or less in around 5-10 patients (348). This allows testing of a novel agents or technologies in rarer disease states, where small numbers of patients are expected to be recruited to the clinical trial. As such, this study design would likely be an ethical way to test HIFU placental vascular occlusion in human subjects, while protecting patients from the risk of excessive adverse events.

Finding of the study	Evidence provided	Thesis section
The risk of maternal skin burns is moderate		
Maternal skin burns were the most common adverse event in the study	Overall, 6/19 (32%) ewes experienced a skin burn. In Group R animals: - 1/10 ewes experienced a maternal skin burn; 1/60 (2%) HIFU exposure series resulted in a maternal skin burn. - 1/10 ewes experiences maternal skin erythema; 6/60 (10%) HIFU exposure series resulted in maternal skin erythema.	Section 4.5.2.3
Careful preparation and cooling of the skin and preservation of the acoustic window appeared to reduce skin burns	Protocol modifications resulted in a 0.33 relative risk (95% CI 0.12-0.94) of maternal skin burns	Section 4.4.2.3 Table 4.6
Healing of maternal skin burns was uncomplicated	No additional procedures (analgesia only) were necessary to aid healing of maternal skin burns	Figure 4.26 Section 4.4.2.3
The delivery of HIFU energy can be modified to reduce the risk of iatrogenic harm		
The depth of the target vessel can be used to determine the drive voltage selected for a HIFU exposure series	The estimated in situ intensity required to produce successful occlusion in sheep placental vessels appears to be between 2.5 - 3.0 kW.cm^2. The depth of the target vessel and the attenuation of overlying tissue can be used to calculate the estimated in situ intensity delivered to the target. This should prevent under- or over- exposure to HIFU energy.	Figure 4.27 Appendix III
The cross sectional area of the region containing the target vessel can be used to plan the number of HIFU exposures in a HIFU exposure series	A C-STAR >1 appears to reduce the risk of failed occlusion and placental vascular haemorrhage. Use of the C-STAR to determine the HIFU treatment area, and so the number of HIFU exposures in a series, should prevent exposure of too large or small an area of placental tissue surrounding the target vessel.	Table 4.3 Section 4.2.2.1 Section 4.6.2.3 Section 4.6.3

Table 9.2: Key findings of the study: direct iatrogenic harm (part 1).
The table lists the key findings of the study which align to the hypothesis 2a: that it is possible to use ultrasound-guided HIFU to permanently occlude placental blood vessels without significant direct iatrogenic harm to the mother or fetus in the pregnant sheep model. The supporting evidence for the findings is summarised in the table, and the section of the thesis where this evidence is presented or discussed further is also listed.

Finding of the study	Evidence provided	Thesis section
The risk of fetal burns is low		
Fetal burns did not occur in the absence errors in HIFU delivery	1/23 (4%) fetuses experience a fetal burn. 1/153 (1%) HIFU exposure series resulted in a fetal burn. The fetal burn was due to a breach of safety protocols	Section 4.6.2.3 Figure 4.28
A minimum safe separation between the fetus and the HIFU focal plane can be established	A minimum separation of >25 mm between the nearest fetal part and the HIFU focal plane appears to be sufficient to prevent fetal injury using this HIFU transducer	Figure 4.32
Fetal burns are a survivable event	The Group R fetus with the burn survived for 20 days of follow-up with no objective indication of fetal compromise until the injury was discovered at post-mortem examination	Section 4.5.2.2
The risk of significant maternal internal injury is low		
There was no evidence of injury to the maternal bladder, bowel or spine	0/32 animals had bladder, bowel of retroperitoneal injury noted at post-mortem examination 0/16 animals recovered from anaesthesia showed evidence of mobility difficulties, or alteration in urinary or bowel function	Section 4.1.2.3 Section 4.2.2.2 Section 4.4.2.2 Section 4.5.2.2
The risk of uterine burns is low	1/18 (6%) ewes experienced an uterine burn when HIFU was applied through intact abdominal skin. 1/103 (1%) transdermal HIFU exposure series resulted in an uterine burn. There was evidence of healing over the course of 20 days and no evidence of uterine rupture at the site.	Section 4.5.2.3 Figure 4.29
The risk of placental vascular haemorrhage following exposure to HIFU is low		
Placental vascular haemorrhage was associated with excessive delivery of HIFU energy	Rates of haemorrhage seen in allantoic membranes, grouped by estimated in situ intensity delivered to the target vessel (all groups, C-STAR >1): ≤ 5.0 kW.cm^2: 0/152 5.0 - 5.9 kW.cm^2: 0/40 6.0 - 6.9 kW.cm^2: 1/2 ≥ 7.0 kW.cm^2: 1/1	Section 4.1.2.3 Figure 4.15
Placental vascular haemorrhage did not occur in the absence errors in HIFU delivery once upper limit for planned in situ intensity introduced	1/23 (4%) ewes experienced placental vascular haemorrhage. 1/153 (1%) HIFU exposure series resulted in a placental vascular haemorrhage. The placental haemorrhage was due a gantry arm movement error.	Section 4.6.2.3 Section 4.6.3
There was no evidence of fetal anaemia following HIFU exposures	In the 12 Group S and R fetuses which completed follow-up, there were no changes in MCA-PSV or haemoglobin noted	Figure 4.24 Table 6.7
Safety protocols to reduce the risk of vascular haemorrhage appeared effective.	There were no instances of vascular haemorrhage when the C-STAR >1 and the in situ intensity <5.0 kW.cm^2	Section 4.6.2.3 Section 4.6.3
Vascular haemorrhage was difficult to provoke	Attempts to create a reproducible vascular haemorrhage model were unsuccessful. Using a C-STAR <1 and in situ intensity < 5.0 kW.cm^2 resulted in a 28% rate of haemorrhage (n=5/18).	Section 4.6.2.3 Section 4.6.3

Table 9.3: Key findings of the study: direct iatrogenic harm (part 2).
The table lists the key findings of the study which align to the hypothesis 2a: that it is possible to use ultrasound-guided HIFU to permanently occlude placental blood vessels without significant direct iatrogenic harm to the mother or fetus in the pregnant sheep model. The supporting evidence for the findings is summarised in the table, and the section of the thesis where this evidence is presented or discussed further is also listed.

At the outset of this study, unlike the potential for direct iatrogenic harm, the potential for indirect materno-fetal harms as a result of HIFU occlusion of placental vessels was unknown, and unreported in published literature. The key points are summarised below, and in Table 9.4 and Table 9.5, which align to hypothesis 2b (section 2.2).

Reassuringly, there was no evidence of maternal cardiovascular or metabolic compromise as a result of HIFU. The mild reduction in maternal blood pressure and tendency to accumulate CO_2 in the blood stream were effects of general anaesthesia, and in agreement with the previously published effects of inhaled isoflurane. The changes in uterine arterial blood flow were also the result of general anaesthesia, with an additive effect of uterine handling in the animals where transuterine HIFU was used. All these effects resolved fully and quickly once uterine handling was stopped, and anaesthesia reversed.

The fetal cardiovascular and metabolic status was similarly unaffected by HIFU, although fetal responses to general anaesthesia, uterine handling and the resultant changes in maternal physiology were more pronounced. While under isoflurane anaesthesia there were reversible reductions in heart rate and cardiac function, and activation of non-hypoxic fetal cardiovascular defence mechanisms, with increases in peripheral vascular resistance and cerebral redistribution of blood flow. Fetuses also became acidotic due to an accumulation of CO_2 and lactate, with a resultant reduction in oxygen levels (not sufficient to result in hypoxaemia) during the period of anaesthesia. These changes recovered at different rates. The majority had normalised by the first day, but all were fully resolved by five days post procedure.

Importantly, all these changes were seen in sham exposed or control animals, with no additive effect of exposure to HIFU. As any human application of HIFU to occlude placental blood vessels – given that it is planned to be a non-invasive therapy – would not involve uterine handling, and is highly unlikely to involve general anaesthesia, these results appear to have little direct clinical relevance.

Maternal and fetal obstetric outcomes were similarly unaltered by HIFU placental vascular occlusion compared to sham exposed animals. Fetal growth and maturation appeared normal, as did placental size and morphology. There was no evidence of chronic stress, from the measures taken in this study, affecting either the fetus or the placenta. While it was not an exhaustive survey of all possible obstetric outcomes, the measures used are those commonly reported in literature to describe complicated pregnancies and chronic distress in fetuses. Given the transient changes in fetal cardiovascular and metabolic status described above, this

is an important confirmation that while there were changes in fetal physiology, these did not appear to constitute a period of fetal distress sufficient to cause lasting harm.

There were also no unanticipated indicators of maternal or fetal harm identified beyond those measured by the planned experimental procedures and described here.

Overall, there is no evidence in this study that HIFU placental vascular occlusion causes acute or chronic (up to 21 days) maternal or fetal compromise, or alters obstetric outcomes. It is true that fetuses affected by TTTS will have a degree of pre-exiting compromise, and that even subtle changes in physiology may have a greater impact on them than the apparently otherwise healthy sheep fetuses used in these experiments. However, currently fetuses showing pathological decompensation resulting from the vascular steal effect of TTTS are the ones in whom fetoscopy and placental vascular ablation are currently performed, and are able to survive this insult. It is not unreasonable to anticipate that HIFU should be at least equally well tolerated, even in a compromised fetus.

Finding of the study	Thesis section
Maternal cardiovascular status is unaffected by exposure to HIFU alone	
Maternal heart rate and blood pressure are stable during the acute application of HIFU	Figure 5.1
Maternal heart rate and blood pressure are stable during recovery from application of HIFU	Figure 5.2
Maternal uterine artery blood flow decreases due to exposure to isoflurane anaesthesia ± uterine handling, not exposure to HIFU	Figure 5.3 Figure 5.4
Maternal uterine artery blood flow is normal and stable during recovery from application of HIFU	Figure 5.4
Fetal cardiovascular status is unaffected by exposure to HIFU alone	
Fetal heart rate and blood pressure are stable during the acute application of HIFU	Figure 5.5
There is evidence of a reversible reduction in fetal heart rate and cardiac decompensation secondary to isoflurane exposure in both sham and HIFU exposed fetuses	Table 5.4 Figure 5.5 Figure 5.10
Fetal heart rate and cardiac function are normal during the recovery period in both sham and HIFU exposed fetuses	Figure 5.5 Figure 5.6 Figure 5.10
There is non-hypoxic, reversible, activation of fetal defence mechanisms in response to isoflurane exposure ± uterine handling. There is an increase in peripheral vascular resistance and a decrease in cerebral vascular resistance, which is equal in sham and HIFU exposed groups	Figure 5.7 Figure 5.9 Table 6.5 Table 6.6
There is no evidence of persistent activation of fetal defence mechanisms or cerebral redistribution during the recovery period in either sham or HIFU exposed animals	Figure 5.8 Figure 5.9
Maternal metabolic status is unaffected by exposure to HIFU	
Maternal oxygenation, glucose availability and pH are stable during the acute application of HIFU exposures	Table 6.3 Table 6.8
The accumulation of carbon dioxide in the maternal arterial blood during prolonged anaesthesia can be offset by an increased ventilatory rate	Table 6.8
Maternal oxygenation, glucose availability and pH are stable during the recovery from application of HIFU exposures	Table 6.4 Table 6.9

Table 9.4: Key findings of the study: materno-fetal compromise (part 1).
The table lists the key findings of the study which align to the hypothesis 2b: that it is possible to use ultrasound guided HIFU to permanently occlude placental blood vessels without significant indirect iatrogenic harm to the mother or fetus in the pregnant sheep model. The section of the thesis where this evidence is presented or discussed further is also listed.

Finding of the study	Thesis section
Fetal metabolic status is unaffected by exposure to HIFU	
There is an equal fall in pH and accumulation of PaCO2 and lactate in sham and HIFU exposed fetuses, related to the length of anaesthesia and activation of fetal cardiovascular defence mechanisms	Table 6.5 Table 6.10
There is a reduction in PaO2 concentrations in both sham and HIFU exposed fetuses related to the developing fetal acidosis. The fall in oxygen levels do not reach the level of hypoxaemia.	Table 6.5
Fetal pH, PaCO2, PaO2, lactate are normal and stable during recovery in both control and HIFU exposed fetuses	Table 6.7 Table 6.11
Glucose availability and haemoglobin concentration are stable during the application of HIFU or sham exposures	Table 6.5
Changes in peripheral oxygen and glucose delivery during the application of HIFU or sham exposures are the result of increases in peripheral vascular resistance	Table 6.5 Table 6.6
Glucose and oxygen delivery are unaffected by treatment group during the recovery period, and show gestational age related increases linked to the increase in fetal femoral blood flow	Table 6.7 Figure 5.8
Maternal and fetal obstetric outcomes are unaffected by exposure to HIFU	
No evidence of preterm rupture of membranes, labour or intrauterine fetal death in the 12/12 ewes which completed the 21 d recovery period	Section 4.4.2.2 Section 4.5.2.2
Total placentome number, weight and placentome subtype distribution equal between sham and HIFU exposed animals	Table 7.6
Fetal growth was normal in sham and HIFU exposed animals, without evidence of asymmetric growth	Figure 7.2 Table 7.2 Table 7.3 Table 7.4 Table 7.5
There was no evidence of a chronic fetal stress (cortisol) response due to exposure to HIFU	Figure 7.3
The autonomic control of heart rate variability developed normally in control and HIFU exposed fetuses	Table 7.7 Figure 7.4 Figure 7.5

Table 9.5: Key findings of the study: materno-fetal compromise (part 2).
The table lists the key findings of the study which align to the hypothesis 2b: that it is possible to use ultrasound guided HIFU to permanently occlude placental blood vessels without significant indirect iatrogenic harm to the mother or fetus in the pregnant sheep model. The section of the thesis where this evidence is presented or discussed further is also listed.

BIBLIOGRAPHY

1. Shaw CJ, ter Haar GR, Rivens IH, Giussani DA, Lees CC. Pathophysiological mechanisms of high-intensity focused ultrasound-mediated vascular occlusion and relevance to non-invasive fetal surgery. J R Soc Interface. 2014;11(95):20140029.

2. Lewi L, Jani J, Blickstein I, Huber A, Gucciardo L, Van Mieghem T, et al. The outcome of monochorionic diamniotic twin gestations in the era of invasive fetal therapy: a prospective cohort study. Am J Obstet Gynecol. 2008;199(5):514.e1-8.

3. Sebire NJ, Snijders RJ, Hughes K, Sepulveda W, Nicolaides KH. The hidden mortality of monochorionic twin pregnancies. Br J Obstet Gynaecol. 1997;104(10):1203-7.

4. Mahieu-Caputo D, Meulemans A, Martinovic J, Gubler MC, Delezoide AL, Muller F, et al. Paradoxic activation of the renin-angiotensin system in twin-twin transfusion syndrome: an explanation for cardiovascular disturbances in the recipient. Pediatr Res. 2005;58(4):685-8.

5. National Institute for Health and Clinical Excellence (2011). Multiple pregnancy: antenatal care for twin and triplet pregnancies (published September 2011). NICE Guidance (CG129).

6. Denbow ML, Cox P, Taylor M, Hammal DM, Fisk NM. Placental angioarchitecture in monochorionic twin pregnancies: relationship to fetal growth, fetofetal transfusion syndrome, and pregnancy outcome. Am J Obstet Gynecol. 2000;182(2):417-26.

7. Lewi L, Cannie M, Blickstein I, Jani J, Huber A, Hecher K, et al. Placental sharing, birthweight discordance, and vascular anastomoses in monochorionic diamniotic twin placentas. Am J Obstet Gynecol. 2007;197(6):587.e1-8.

8. Saunders NJ, Snijders RJ, Nicolaides KH. Twin-twin transfusion syndrome during the 2nd trimester is associated with small intertwin hemoglobin differences. Fetal Diagn Ther. 1991;6(1-2):34-6.

9. Lewi L, Jani J, Cannie M, Robyr R, Ville Y, Hecher K, et al. Intertwin anastomoses in monochorionic placentas after fetoscopic laser coagulation for twin-to-twin transfusion syndrome: is there more than meets the eye? Am J Obstet Gynecol. 2006;194(3):790-5.

10. Lewi L, Deprest J, Hecher K. The vascular anastomoses in monochorionic twin pregnancies and their clinical consequences. Am J Obstet Gynecol. 2013;208(1):19-30.

11. Quintero RA, Morales WJ, Allen MH, Bornick PW, Johnson PK, Kruger M. Staging of twin-twin transfusion syndrome. J Perinatol. 1999;19(8 Pt 1):550-5.

12. Dickinson JE, Evans SF. The progression of disease stage in twin-twin transfusion syndrome. J Matern Fetal Neonatal Med. 2004;16(2):95-101.

13. Senat M-V, Deprest J, Boulvain M, Paupe A, Winer N, Ville Y. Endoscopic Laser Surgery versus Serial Amnioreduction for Severe Twin-to-Twin Transfusion Syndrome. N Engl J Med. 2004;351(2):136-44.

14. Bebbington MW, Danzer E, Moldenhauer J, Khalek N, Johnson MP. Radiofrequency ablation vs bipolar umbilical cord coagulation in the management of complicated monochorionic pregnancies. Ultrasound Obstet Gynecol. 2012;40(3):319-24.

15. Roberts D, Neilson JP, Kilby MD, Gates S. Interventions for the treatment of twin-twin transfusion syndrome. Cochrane Database Syst Rev. 2014;1:CD002073.

16. Walsh CA, McAuliffe FM. Recurrent twin-twin transfusion syndrome after selective fetoscopic laser photocoagulation: a systematic review of the literature. Ultrasound Obstet Gynecol. 2012;40(5):506-12.

17. Robyr R, Lewi L, Salomon LJ, Yamamoto M, Bernard JP, Deprest J, et al. Prevalence and management of late fetal complications following successful selective laser coagulation of chorionic plate anastomoses in twin-to-twin transfusion syndrome. Am J Obstet Gynecol. 2006;194(3):796-803.

18. Baschat AA, Barber J, Pedersen N, Turan OM, Harman CR. Outcome after fetoscopic selective laser ablation of placental anastomoses vs equatorial laser dichorionization for the treatment of twin-to-twin transfusion syndrome. Am J Obstet Gynecol. 2013;209(3):234.e1-8.

19. Slaghekke F, Lopriore E, Lewi L, Middeldorp JM, van Zwet EW, Weingertner AS, et al. Fetoscopic laser coagulation of the vascular equator versus selective coagulation for twin-to-twin transfusion syndrome: an open-label randomised controlled trial. Lancet. 2014;383(9935):2144-51.

20. Burks SR, Ziadloo A, Hancock HA, Chaudhry A, Dean DD, Lewis BK, et al. Investigation of cellular and molecular responses to pulsed focused ultrasound in a mouse model. PLoS One. 2011;6(9):e24730.

21. Cline HE, Schenck JF, Hynynen K, Watkins RD, Souza SP, Jolesz FA. MR-guided focused ultrasound surgery. J Comput Assist Tomogr. 1992;16(6):956-65.

22. Clarke RL, ter Haar GR. Temperature rise recorded during lesion formation by high-intensity focused ultrasound. Ultrasound Med Biol. 1997;23(2):299-306.

23. Shi X, Martin RW, Rouseff D, Vaezy S, Crum LA. Detection of high-intensity focused ultrasound liver lesions using dynamic elastometry. Ultrason Imaging. 1999;21(2):107-26.

24. Responses to cellular injury. In: Underwood JCE, editor. General and systematic pathology. 4th ed. London: Churchill Livingstone; 2004. p. 105.

25. ter Haar GR, Robertson D. Tissue destruction with focused ultrasound in vivo. Eur Urol. 1993;23 Suppl 1:8-11.

26. Susani M, Madersbacher S, Kratzik C, Vingers L, Marberger M. Morphology of tissue destruction induced by focused ultrasound. Eur Urol. 1993;23 Suppl 1:34-8.

27. Fry FJ, Kossoff G, Eggleton RC, Dunn F. Threshold ultrasonic dosages for structural changes in the mammalian brain. J Acoust Soc Am. 1970;48(6):Suppl 2:1413.

28. Winterroth F, Xu Z, Wang TY, Wilkinson JE, Fowlkes JB, Roberts WW, et al. Examining and analyzing subcellular morphology of renal tissue treated by histotripsy. Ultrasound Med Biol. 2011;37(1):78-86.

29. Focused Ultrasound Foundation. State of the Technology. Available from: https://www.fusfoundation.org/the-technology/state-of-the-technology. Last accessed 26.07.2017.

30. Fallon JT, Stehbens WE, Eggleton RC. Effect of ultrasound on arteries. Arch Pathol. 1972;94(5):380-8.

31. Rivens IH, Rowland IJ, Denbow M, Fisk NM, ter Haar GR, Leach MO. Vascular occlusion using focused ultrasound surgery for use in fetal medicine. Eur J Ultrasound. 1999;9(1):89-97.

32. Denbow ML, Rivens IH, Rowland IJ, Leach MO, Fisk NM, ter Haar GR. Preclinical development of noninvasive vascular occlusion with focused ultrasonic surgery for fetal therapy. Am J Obstet Gynecol. 2000;182(2):387-92.

33. Fujiwara R, Sasaki K, Ishikawa T, Suzuki M, Umemura S-i, Kushima M, et al. Arterial blood flow occlusion by high intensity focused ultrasound and histologic evaluation of its effect on arteries and surrounding tissues. J Med Ultrason. 2002;29(3):85-90.

34. Ishikawa T, Okai T, Sasaki K, Umemura S, Fujiwara R, Kushima M, et al. Functional and histological changes in rat femoral arteries by HIFU exposure. Ultrasound Med Biol. 2003;29(10):1471-7.

35. Ichizuka K, Ando S, Ichihara M, Ishikawa T, Uchiyama N, Sasaki K, et al. Application of high-intensity focused ultrasound for umbilical artery occlusion in a rabbit model. Ultrasound Obstet Gynecol. 2007;30(1):47-51.

36. Delon-Martin C, Vogt C, Chignier E, Guers C, Chapelon JY, Cathignol D. Venous thrombosis generation by means of high-intensity focused ultrasound. Ultrasound Med Biol. 1995;21(1):113-9.

37. Hynynen K, Colucci V, Chung A, Jolesz F. Noninvasive arterial occlusion using MRI-guided focused ultrasound. Ultrasound Med Biol. 1996;22(8):1071-7.

38. Mahoney K, Martin H, Hynynen K. Focused ultrasound effects on blood vessels in vivo-limits for vascular interventions. Conf Proc IEEE Ultrasonics Symposium. 2000;2:1405-8.

39. Hwang JH, Vaezy S, Martin RW, Cho MY, Noble ML, Crum LA, et al. High-intensity focused US: a potential new treatment for GI bleeding. Gastrointest Endosc. 2003;58(1):111-5.

40. Ichihara M, Sasaki K, Umemura S, Kushima M, Okai T. Blood flow occlusion via ultrasound image-guided high-intensity focused ultrasound and its effect on tissue perfusion. Ultrasound Med Biol. 2007;33(3):452-9.

41. Hwang JH, Zhou Y, Warren C, Brayman AA, Crum LA. Targeted venous occlusion using pulsed high-intensity focused ultrasound. IEEE Trans Biomed Eng. 2010;57(1):37-40.

42. Yue Y, Chen W, Wang Z. The impact of microbubbles-mediated intermitten HIFU on bloodflow in femoral artery of rabbit. J Biomed Eng. 2010;27(1):58-61.

43. Okai T, Ichizuka K, Hasegawa J, Matsuoka R, Nakamura M, Shimodaira K, et al. First successful case of non-invasive in-utero treatment of twin reversed arterial perfusion sequence by high-intensity focused ultrasound. Ultrasound Obstet Gynecol. 2013;42(1):112-4.

44. Yang FY, Chiu WH, Liu SH, Lin GL, Ho FM. Functional changes in arteries induced by pulsed high-intensity focused ultrasound. IEEE Trans Ultrason Ferroelectr Freq Control. 2009;56(12):2643-9.

45. Hynynen K, Chung AH, Colucci V, Jolesz FA. Potential adverse effects of high-intensity focused ultrasound exposure on blood vessels in vivo. Ultrasound Med Biol. 1996;22(2):193-201.

46. Nizard J, Pessel M, De Keersmaecker B, Barbet JP, Ville Y. High-intensity focused ultrasound in the treatment of postpartum hemorrhage: an animal model. Ultrasound Obstet Gynecol. 2004;23(3):262-6.

47. Kim Y, Nabili M, Acharya P, Lopez A, Myers MR. Microvessel rupture induced by high-intensity therapeutic ultrasound-a study of parameter sensitivity in a simple in vivo model. J Ther Ultrasound. 2017;5:5.

48. Yang R, Griffith S, Rescorla F, Galliani C, Ehrman K, Fry F, et al. Feasibility of Using High Intensity Focused Ultrasound for Treatment of Unresectable Retroperitoneal Malignancies. J Ultrasound Med. 1992;11(3 (Suppl.)):1.

49. Koruth JS, Dukkipati S, Carrillo RG, Coffey J, Teng J, Eby TB, et al. Safety and efficacy of high-intensity focused ultrasound atop coronary arteries during epicardial catheter ablation. J Cardiovasc Electrophysiol. 2011;22(11):1274-80.

50. Jiao J, Wu F, Zou J, Li F, Liu F, Zhao X, et al. Effect of ablations by pulsed versus continuous high-intensity focused ultrasound on isolated perfused porcine liver. South Med J. 2013;33(2):230-4.

51. Vaezy S, Martin R, Yaziji H, Kaczkowski P, Keilman G, Carter S, et al. Hemostasis of punctured blood vessels using high-intensity focused ultrasound. Ultrasound Med Biol. 1998;24(6):903-10.

52. Martin RW, Vaezy S, Kaczkowski P, Keilman G, Carter S, Caps M, et al. Hemostasis of punctured vessels using Doppler-guided high-intensity ultrasound. Ultrasound Med Biol. 1999;25(6):985-90.

53. Zderic V, Keshavarzi A, Noble ML, Paun M, Sharar SR, Crum LA, et al. Hemorrhage control in arteries using high-intensity focused ultrasound: a survival study. Ultrasonics. 2006;44(1):46-53.

54. Vaezy S, Martin R, Schmiedl U, Caps M, Taylor S, Beach K, et al. Liver hemostasis using high-intensity focused ultrasound. Ultrasound Med Biol. 1997;23(9):1413-20.

55. Vaezy S, Martin R, Kaczkowski P, Keilman G, Goldman B, Yaziji H, et al. Use of high-intensity focused ultrasound to control bleeding. J Vasc Surg. 1999;29(3):533-42.

56. Nguyen VP, Kim J, Ha KL, Oh J, Kang HW. Feasibility study on photoacoustic guidance for high-intensity focused ultrasound-induced hemostasis. J Biomed Opt. 2014;19(10):105010.

57. Ichizuka K, Hasegawa J, Nakamura M, Matsuoka R, Sekizawa A, Okai T, et al. High-intensity focused ultrasound treatment for twin reversed arterial perfusion sequence. Ultrasound Obstet Gynecol. 2012;40(4):476-8.

58. Yang R, Reilly CR, Rescorla FJ, Faught PR, Sanghvi NT, Fry FJ, et al. High-intensity focused ultrasound in the treatment of experimental liver cancer. Arch Surg. 1991;126(8):1002-10.

59. Wu F, Chen W-Z, Bai J, Zou J-Z, Wang Z-L, Zhu H, et al. Pathological changes in human malignant carcinoma treated with high-intensity focused ultrasound. Ultrasound Med Biol. 2001;27(8):1099-106.

60. Paek BW, Vaezy S, Fujimoto V, Bailey M, Albanese CT, Harrison MR, et al. Tissue ablation using high-intensity focused ultrasound in the fetal sheep model: potential for fetal treatment. Am J Obstet Gynecol. 2003;189(3):702-5.

61. Kim Y, Gelehrter SK, Fifer CG, Lu JC, Owens GE, Berman DR, et al. Non-invasive pulsed cavitational ultrasound for fetal tissue ablation: feasibility study in a fetal sheep model. Ultrasound Obstet Gynecol. 2011;37(4):450-7.

62. Owens GE, Miller RM, Owens ST, Swanson SD, Ives K, Ensing G, et al. Intermediate-term effects of intracardiac communications created noninvasively by therapeutic ultrasound (histotripsy) in a porcine model. Pediatr Cardiol. 2012;33(1):83-9.

63. Hancock HA, Smith LH, Cuesta J, Durrani AK, Angstadt M, Palmeri ML, et al. Investigations into pulsed high-intensity focused ultrasound-enhanced delivery: preliminary evidence for a novel mechanism. Ultrasound Med Biol. 2009;35(10):1722-36.

64. Lele PP. Production of deep focal lesions by focused ultrasound-current status. Ultrasonics. 1967;5(2):105-12.

65. Burkitt HG, Young B., W. HJ. Circulatory system. In: R. WP, editor. Wheater's functional histology : a text and colour atlas. 3rd ed. Edinburgh: Churchill Livingstone; 1993. p. 140-52.

66. Agah R, Pearce JA, Welch AJ, Motamedi M. Rate process model for arterial tissue thermal damage: Implications on vessel photocoagulation. Lasers Surg Med. 1994;15(2):176-84.

67. Florkin M, H. SE. Comprehensive biochemistry: Extracellular and supporting structures. Amsterdam: Elsevier; 1971.

68. Chen SS, Wright NT, Humphrey JD. Heat-Induced Changes in the Mechanics of a Collagenous Tissue: Isothermal Free Shrinkage. J Biomech Eng. 1997;119(4):372-8.

69. Henderson PW, Lewis GK, Shaikh N, Sohn A, Weinstein AL, Olbricht WL, et al. A portable high-intensity focused ultrasound device for noninvasive venous ablation. J Vasc Surg. 2010;51(3):707-11.

70. Tokarczyk A, Rivens I, van Bavel E, Symonds-Tayler R, ter Haar G. An experimental system for the study of ultrasound exposure of isolated blood. Phys Med Biol. 2013;58(7):2281-304.

71. Moros EG. Physics of thermal therapy: fundamentals and clinical applications. Boca Raton: Taylor and Francis; 2013.

72. DeLia JE, Rogers JG, Dixon JA. Treatment of placental vasculature with a neodymium-yttrium-aluminum-garnet laser via fetoscopy. Am J Obstet Gynecol. 1985;151(8):1126-7.

73. White RA, Kopchok G, Peng SK, Fujitani R, White G, Klein S, et al. Laser vascular welding--how does it work? Ann Vasc Surg. 1987;1(4):461-4.

74. Banga I. Structure and function of elastin and collagen. Budapest: Akadémiai Kiadó; 1966.

75. Martinot VL, Mordon SR, Mitchell VA, Pellerin PN, Brunetaud JM. Determination of efficient parameters for argon laser-assisted anastomoses in rats: Macroscopic, thermal, and histological evaluation. Lasers Surg Med. 1994;15(2):168-75.

76. Landman J, Kerbl K, Rehman J, Andreoni C, Humphrey PA, Collyer W, et al. Evaluation of a vessel sealing system, bipolar electrosurgery, harmonic scalpel, titanium clips, endoscopic gastrointestinal anastomosis vascular staples and sutures for arterial and venous ligation in a porcine model. J Urol. 2003;169(2):697-700.

77. Manouras A, Markogiannakis HE, Kekis PB, Lagoudianakis EE, Fleming B. Novel hemostatic devices in thyroid surgery: electrothermal bipolar vessel sealing system and harmonic scalpel. Expert Rev Med Devices. 2008;5(4):447-66.

78. Harold KL, Pollinger H, Matthews BD, Kercher KW, Sing RF, Heniford BT. Comparison of ultrasonic energy, bipolar thermal energy, and vascular clips for the hemostasis of small-, medium-, and large-sized arteries. Surg Endosc. 2003;17(8):1228-30.

79. Schultz-Haakh H, Li JK, Welkowitz W, Rosenberg N. Ultrasonic treatment of varicose veins. Angiology. 1989;40(2):129-37.

80. Jiang F, He M, Liu YJ, Wang ZB, Zhang L, Bai J. High intensity focused ultrasound ablation of goat liver in vivo: Pathologic changes of portal vein and the "heat-sink" effect. Ultrasonics. 2013;53(1):77-83.

81. Hwang JH, Tu J, Brayman AA, Matula TJ, Crum LA. Correlation between inertial cavitation dose and endothelial cell damage in vivo. Ultrasound Med Biol. 2006;32(10):1611-9.

82. Poliachik SL, Chandler WL, Mourad PD, Ollos RJ, Crum LA. Activation, aggregation and adhesion of platelets exposed to high-intensity focused ultrasound. Ultrasound Med Biol. 2001;27(11):1567-76.

83. Poliachik SL, Chandler WL, Ollos RJ, Bailey MR, Crum LA. The relation between cavitation and platelet aggregation during exposure to high-intensity focused ultrasound. Ultrasound Med Biol. 2004;30(2):261-9.

84. Sakariassen KS, Holme PA, Orvim U, Barstad RM, Solum NO, Brosstad FR. Shear-induced platelet activation and platelet microparticle formation in native human blood. Thromb Res. 1998;92(6 Suppl 2):S33-41.

85. Williams AR, O'Brien Jr WD, Coller BS. Exposure to ultrasound decreases the recalcification time of platelet rich plasma. Ultrasound Med Biol. 1976;2(2):113-8.

86. Rao GH, Smith CM, 2nd, Escolar G, White JG. Influence of heat on platelet biochemistry, structure, and function. J Lab Clin Med. 1993;122(4):455-64.

87. Gershfeld NL, Murayama M. Thermal instability of red blood cell membrane bilayers: temperature dependence of hemolysis. J Membr Biol. 1988;101(1):67-72.

88. Dyson M, Pond JB, Woodward B, Broadbent J. The production of blood cell stasis and endothelial damage in the blood vessels of chick embryos treated with ultrasound in a stationary wave field. Ultrasound Med Biol. 1974;1(2):133-48.

89. ter Haar G, Dyson M, Smith SP. Ultrastructural changes in the mouse uterus brought about by ultrasonic irradiation at therapeutic intensities in standing wave fields. Ultrasound Med Biol. 1979;5(2):167-79.

90. Quick AJ. Hemostasis in surgical procedures. Surg Gynecol Obstet. 1969;128(3):523-32.

91. Discigil B, King RM, Pearson PJ, Capellini VK, Rodrigues AJ, Schaff HV, et al. High-frequency ultrasonic waves cause endothelial dysfunction on canine epicardial coronary arteries. Rev Bras Cir Cardiovasc. 2008;23(2):190-6.

92. Nyborg WLM. Acoustic Streaming. In: Mason WP, editor. Properties of Polymers and Nonlinear Acoustics. Volume 2, Part B. London: Academic Press; 1965. p. 265-331.

93. American College of Surgeons (2008). Advanced Trauma Life Support (Student course manual, 8th Ed.).

94. Laughner JI, Sulkin MS, Wu Z, Deng CX, Efimov IR. Three potential mechanisms for failure of high intensity focused ultrasound ablation in cardiac tissue. Circ Arrhythm Electrophysiol. 2012;5(2):409-16.

95. Chen WS, Shen CC, Wang JC, Ko CT, Liu HL, Ho MC, et al. Single-element ultrasound transducer for combined vessel localization and ablation. IEEE Trans Ultrason Ferroelectr Freq Control. 2011;58(4):766-75.

96. Vaezy S, Shi X, Martin RW, Chi E, Nelson PI, Bailey MR, et al. Real-time visualization of high-intensity focused ultrasound treatment using ultrasound imaging. Ultrasound Med Biol. 2001;27(1):33-42.

97. Sapareto SA, Dewey WC. Thermal dose determination in cancer therapy. Int J Radiat Oncol Biol Phys. 1984;10(6):787-800.

98. Evans N, Kluckow M, Simmons M, Osborn D. Which to measure, systemic or organ blood flow? Middle cerebral artery and superior vena cava flow in very preterm infants. Arch Dis Child Fetal Neonatal Ed. 2002;87(3):F181-4.

99. Hill CR, Rivens I, Vaughan MG, ter Haar GR. Lesion development in focused ultrasound surgery: a general model. Ultrasound Med Biol. 1994;20(3):259-69.

100. Hoerig CL, Serrone JC, Burgess MT, Zuccarello M, Mast TD. Prediction and suppression of HIFU-induced vessel rupture using passive cavitation detection in an ex vivo model. J Ther Ultrasound. 2014;2:14.

101. Henriques FC, Moritz AR. Studies of Thermal Injury: I. The Conduction of Heat to and through Skin and the Temperatures Attained Therein. A Theoretical and an Experimental Investigation. Am J Pathol. 1947;23(4):530-49.

102. Anderson GS. Human morphology and temperature regulation. Int J Biometeorol. 1999;43(3):99-109.

103. Cohen ML. Measurement of the thermal properties of human skin. A review. J Invest Dermatol. 1977;69(3):333-8.

104. Johnson JM, Brengelmann GL, Hales JR, Vanhoutte PM, Wenger CB. Regulation of the cutaneous circulation. Fed Proc. 1986;45(13):2841-50.

105. Heinonen I, Kemppainen J, Kaskinoro K, Knuuti J, Boushel R, Kalliokoski KK. Capacity and hypoxic response of subcutaneous adipose tissue blood flow in humans. Circ J. 2014;78(6):1501-6.

106. Sacks D, McClenny TE, Cardella JF, Lewis CA. Society of Interventional Radiology clinical practice guidelines. J Vasc Interv Radiol. 2003;14(9 Pt 2):S199-202.

107. Chen J, Chen W, Zhang L, Li K, Peng S, He M, et al. Safety of ultrasound-guided ultrasound ablation for uterine fibroids and adenomyosis: A review of 9988 cases. Ultrason Sonochem. 2015;27:671-6.

108. Stewart EA, Gedroyc WM, Tempany CM, Quade BJ, Inbar Y, Ehrenstein T, et al. Focused ultrasound treatment of uterine fibroid tumors: safety and feasibility of a noninvasive thermoablative technique. Am J Obstet Gynecol. 2003;189(1):48-54.

109. Machtinger R, Inbar Y, Cohen-Eylon S, Admon D, Alagem-Mizrachi A, Rabinovici J. MR-guided focus ultrasound (MRgFUS) for symptomatic uterine fibroids: predictors of treatment success. Hum Reprod. 2012;27(12):3425-31.

110. Ikink ME, Voogt MJ, Verkooijen HM, Lohle PN, Schweitzer KJ, Franx A, et al. Mid-term clinical efficacy of a volumetric magnetic resonance-guided high-intensity focused ultrasound technique for treatment of symptomatic uterine fibroids. Eur Radiol. 2013;23(11):3054-61.

111. Voogt MJ, Trillaud H, Kim YS, Mali WP, Barkhausen J, Bartels LW, et al. Volumetric feedback ablation of uterine fibroids using magnetic resonance-guided high intensity focused ultrasound therapy. Eur Radiol. 2012;22(2):411-7.

112. Leon-Villapalos J, Kaniorou-Larai M, Dziewulski P. Full thickness abdominal burn following magnetic resonance guided focused ultrasound therapy. Burns. 2005;31(8):1054-5.

113. Ikink ME, van Breugel JM, Schubert G, Nijenhuis RJ, Bartels LW, Moonen CT, et al. Volumetric MR-Guided High-Intensity Focused Ultrasound with Direct Skin Cooling for the Treatment of Symptomatic Uterine Fibroids: Proof-of-Concept Study. Biomed Res Int. 2015;2015:684250.

114. Stewart EA, Rabinovici J, Tempany CM, Inbar Y, Regan L, Gostout B, et al. Clinical outcomes of focused ultrasound surgery for the treatment of uterine fibroids. Fertil Steril. 2006;85(1):22-9.

115. Bennet L, Gunn AJ. The fetal heart rate response to hypoxia: insights from animal models. Clin Perinatol. 2009;36(3):655-72.

116. Rudolph AM, Heymann MA. Methods for studying the circulation of the fetus in utero. In: P.W. N, editor. Animal models in Fetal Medicine. Amsterdam: Elsevier/North Holland Biomedical Press; 1980.

117. Rudolph AM. Distribution and regulation of blood flow in the fetal and neonatal lamb. Circ Res. 1985;57(6):811-21.

118. Kiserud T. Physiology of the fetal circulation. Semin Fetal Neonatal Med. 2005;10(6):493-503.

119. Segar JL, Merrill DC, Smith BA, Robillard JE. Role of sympathetic activity in the generation of heart rate and arterial pressure variability in fetal sheep. Pediatr Res. 1994;35(2):250-4.

120. Yu ZY, Lumbers ER. Effects of birth on baroreceptor-mediated changes in heart rate variability in lambs and fetal sheep. Clin Exp Pharmacol Physiol. 2002;29(5-6):455-63.

121. Booth LC, Bennet L, Guild SJ, Barrett CJ, May CN, Gunn AJ, et al. Maturation-related changes in the pattern of renal sympathetic nerve activity from fetal life to adulthood. Exp Physiol. 2011;96(2):85-93.

122. Wakatsuki A, Murata Y, Ninomiya Y, Masaoka N, Tyner JG, Kutty KK. Physiologic baroreceptor activity in the fetal lamb. Am J Obstet Gynecol. 1992;167(3):820-7.

123. Hecker JF. Experimental Surgery on Small Ruminants. London: Butterworth and Co. Publishers Limited; 1974. 332 p.

124. Nijhuis JG, Prechtl HF, Martin CB, Jr., Bots RS. Are there behavioural states in the human fetus? Early Hum Dev. 1982;6(2):177-95.

125. Suzuki T, Kimura Y, Murotsuki J, Murakami T, Uehara S, Okamura K. Detection of a biorhythm of human fetal autonomic nervous activity by a power spectral analysis. Am J Obstet Gynecol. 2001;185(5):1247-52.

126. Kimura Y, Okamura K, Watanabe T, Murotsuki J, Suzuki T, Yano M, et al. Power spectral analysis for autonomic influences in heart rate and blood pressure variability in fetal lambs. Am J Physiol. 1996;271:1333-9.

127. Blackwell SC, Grobman WA, Antoniewicz L, Hutchinson M, Gyamfi Bannerman C. Interobserver and intraobserver reliability of the NICHD 3-Tier Fetal Heart Rate Interpretation System. Am J Obstet Gynecol. 2011;205(4):378.e1-5.

128. Grivell RM, Alfirevic Z, Gyte GM, Devane D. Antenatal cardiotocography for fetal assessment. Cochrane Database Syst Rev. 2012;12:CD007863.

129. Pardey J, Moulden M, Redman CW. A computer system for the numerical analysis of nonstress tests. Am J Obstet Gynecol. 2002;186(5):1095-103.

130. Serra V, Moulden M, Bellver J, Redman CW. The value of the short-term fetal heart rate variation for timing the delivery of growth-retarded fetuses. Br J Obstet Gynecol. 2008;115(9):1101-7.

131. Royal College of Obstetricians and Gynaecologists (2013). The Investigation and Management of the Small-for-Gestational-Age Fetus (published March 2013). RCOG Guidance (Green-top Guideline No.31).

132. Serra V, Bellver J, Moulden M, Redman CW. Computerized analysis of normal fetal heart rate pattern throughout gestation. Ultrasound Obstet Gynecol. 2009;34(1):74-9.

133. Ferrario M, Signorini MG, Magenes G. Complexity analysis of the fetal heart rate variability: early identification of severe intrauterine growth-restricted fetuses. Med Biol Eng Comput. 2009;47(9):911-9.

134. Schneider U, Fiedler A, Schroder B, Jaekel S, Stacke A, Hoyer D, et al. The effect of antenatal steroid treatment on fetal autonomic heart rate regulation revealed by fetal magnetocardiography (fMCG). Early Hum Dev. 2010;86(5):319-25.

135. Ohta T, Okamura K, Kimura Y, Suzuki T, Watanabe T, Yasui T, et al. Alteration in the low-frequency domain in power spectral analysis of fetal heart beat fluctuations. Fetal Diagn Ther. 1999;14(2):92-7.

136. Suzuki T, Okamura K, Kimura Y, Watanabe T, Yaegashi N, Murotsuki J, et al. Power spectral analysis of R-R interval variability before and during the sinusoidal heart rate pattern in fetal lambs. Am J Obstet Gynecol. 2000;182(5):1227-32.

137. Graatsma EM, Mulder EJ, Vasak B, Lobmaier SM, Pildner von Steinburg S, Schneider KT, et al. Average acceleration and deceleration capacity of fetal heart rate in normal pregnancy and in pregnancies complicated by fetal growth restriction. J Matern Fetal Neonatal Med. 2012;25(12):2517-22.

138. Huhn EA, Lobmaier S, Fischer T, Schneider R, Bauer A, Schneider KT, et al. New computerized fetal heart rate analysis for surveillance of intrauterine growth restriction. Prenat Diagn. 2011;31(5):509-14.

139. Heart rate variability: standards of measurement, physiological interpretation and clinical use. Task Force of the European Society of Cardiology and the North American Society of Pacing and Electrophysiology. Circulation. 1996;93(5):1043-65.

140. Akselrod S, Gordon D, Ubel FA, Shannon DC, Berger AC, Cohen RJ. Power spectrum analysis of heart rate fluctuation: a quantitative probe of beat-to-beat cardiovascular control. Science. 1981;213(4504):220-2.

141. Pumprla J, Howorka K, Groves D, Chester M, Nolan J. Functional assessment of heart rate variability: physiological basis and practical applications. Int J Cardiol. 2002;84(1):1-14.

142. Malliani A, Lombardi F, Pagani M. Power spectrum analysis of heart rate variability: a tool to explore neural regulatory mechanisms. Br Heart J. 1994;71(1):1-2.

143. Van Laar JO, Porath MM, Peters CH, Oei SG. Spectral analysis of fetal heart rate variability for fetal surveillance: review of the literature. Acta Obstet Gynecol Scand. 2008;87(3):300-6.

144. Peters CH, ten Broeke ED, Andriessen P, Vermeulen B, Berendsen RC, Wijn PF, et al. Beat-to-beat detection of fetal heart rate: Doppler ultrasound cardiotocography compared to direct ECG cardiotocography in time and frequency domain. Physiol Meas. 2004;25(2):585-93.

145. Ferrario M, Magenes G, Campanile M, Carbone IF, Di Lieto A, Signorini MG. Multiparameter analysis of heart rate variability signal for the investigation of high risk fetuses. Conf Proc IEEE Eng Med Biol Soc. 2009:4662-5.

146. Fukushima A, Nakai K, Kanasugi T, Terata M, Sugiyama T. Assessment of fetal autonomic nervous system activity by fetal magnetocardiography: comparison of normal pregnancy and intrauterine growth restriction. J Pregnancy. 2011;2011:218162.

147. Sriram B, Mencer MA, McKelvey S, Siegel ER, Vairavan S, Wilson JD, et al. Differences in the sleep states of IUGR and low-risk fetuses: An MCG study. Early Hum Dev. 2013;89(10):815-9.

148. Sibony O, Fouillot JP, Benaoudia M, Benhalla A, Oury JF, Sureau C, et al. Quantification of the fetal heart rate variability by spectral analysis of fetal well-being and fetal distress. Eur J Obstet Gynecol Reprod Biol. 1994;54(2):103-8.

149. Metsälä T, Siimes A, Välimäki I. The effect of change in sympatho-vagal balance on heart rate and blood pressure variability in the foetal lamb. Acta Physiol Scand. 1995;154(2):85-92.

150. Lumbers ER, Yu ZY. A method for determining baroreflex-mediated sympathetic and parasympathetic control of the heart in pregnant and non-pregnant sheep. J Physiol. 1999;515 (Pt 2):555-66.

151. van Laar JO, Peters CH, Vullings R, Houterman S, Oei SG. Power spectrum analysis of fetal heart rate variability at near term and post term gestation during active sleep and quiet sleep. Early Hum Dev. 2009;85(12):795-8.

152. Koome ME, Bennet L, Booth LC, Davidson JO, Wassink G, Gunn AJ. Ontogeny and control of the heart rate power spectrum in the last third of gestation in fetal sheep. Exp Physiol. 2014;99(1):80-8.

153. Lear CA, Galinsky R, Wassink G, Mitchell CJ, Davidson JO, Westgate JA, et al. Sympathetic neural activation does not mediate heart rate variability during repeated brief umbilical cord occlusions in near-term fetal sheep. J Physiol. 2016;594(5):1265-77.

154. Amoroso EC. Placentation. In: Parkes AS, editor. Marshall's Physiology of Reproduction. 3rd ed. London: Longmans, Green and Co.; 1952.

155. Wooding P, Burton G. Comparative placentation : structures, functions and evolution. Berlin: Springer; 2008.

156. Barry JS, Anthony RV. The pregnant sheep as a model for human pregnancy. Theriogenology. 2008;69(1):55-67.

157. Reproductive Cycles. In: Hafez B, Hafez ESE, editors. Reproduction in farm animals. 7th ed. London: Lippincott Williams and Wilkins; 2000. p. 172-81.

158. Reynolds LP, Borowicz PP, Vonnahme KA, Johnson ML, Grazul-Bilska AT, Wallace JM, et al. Animal models of placental angiogenesis. Placenta. 2005;26(10):689-708.

159. Vonnahme KA, Arndt WJ, Johnson ML, Borowicz PP, Reynolds LP. Effect of morphology on placentome size, vascularity, and vasoreactivity in late pregnant sheep. Biol Reprod. 2008;79(5):976-82.

160. Vatnick I, Schoknecht PA, Darrigrand R, Bell AW. Growth and metabolism of the placenta after unilateral fetectomy in twin pregnant ewes. J Dev Physiol. 1991;15(6):351-6.

161. Baur R. Morphometry of the placental exchange area. Adv Anat Embryol Cell Biol. 1977;53(1):3-65.

162. Harding JE, Jones CT, Robinson JS. Studies on experimental growth retardation in sheep. The effects of a small placenta in restricting transport to and growth of the fetus. J Dev Physiol. 1985;7(6):427-42.

163. Lindsay DR. Reproduction in sheep. Cambridge: Cambridge University Press; 1984.

164. Alexander G. Studies on the placenta of the sheep (ovis aries l.). Effect of surgical reduction in the number of caruncles. J Reprod Fertil. 1964;7:307-22.

165. Hawkins JL, Koonin LM, Palmer SK, Gibbs CP. Anesthesia-related deaths during obstetric delivery in the United States, 1979-1990. Anesthesiology. 1997;86(2):277-84.

166. Hawkins JL. Anesthesia-related maternal mortality. Clin Obstet Gynecol. 2003;46(3):679-87.

167. Okutomi T, Whittington RA, Stein DJ, Morishima HO. Comparison of the effects of sevoflurane and isoflurane anesthesia on the maternal-fetal unit in sheep. J Anesth. 2009;23(3):392-8.

168. Ngamprasertwong P, Michelfelder EC, Arbabi S, Choi YS, Statile C, Ding L, et al. Anesthetic techniques for fetal surgery: effects of maternal anesthesia on intraoperative fetal outcomes in a sheep model. Anesthesiology. 2013;118(4):796-808.

169. Granados MM, Dominguez JM, Fernandez-Sarmiento A, Funes FJ, Morgaz J, Navarrete R, et al. Anaesthetic and cardiorespiratory effects of a constant-rate infusion of alfaxalone in desflurane-anaesthetised sheep. Vet Rec. 2012;171(5):125.

170. Mohamadnia AR, Hughes G, Clarke KW. Maintenance of anaesthesia in sheep with isoflurane, desflurane or sevoflurane. Vet Rec. 2008;163(7):210-5.

171. Hall LW, Clarke KW, Trim CM. Veterinary anaesthesia. London: W.B. Saunders; 2001.

172. Clarke KW. Desflurane and sevoflurane. New volatile anesthetic agents. Vet Clin North Am Small Anim Pract. 1999;29(3):793-810.

173. Palahniuk RJ, Shnider SM. Maternal and fetal cardiovascular and acid-base changes during halothane and isoflurane anesthesia in the pregnant ewe. Anesthesiology. 1974;41(5):462-72.

174. Bachman CR, Biehl DR, Sitar D, Cumming M, Pucci W. Isoflurane potency and cardiovascular effects during short exposures in the foetal lamb. Can Anaesth Soc J. 1986;33(1):41-7.

175. Biehl DR, Yarnell R, Wade JG, Sitar D. The uptake of isoflurane by the foetal lamb in utero: effect on regional blood flow. Can Anaesth Soc J. 1983;30(6):581-6.

176. Gregory GA, Wade JG, Beihl DR, Ong BY, Sitar DS. Fetal anesthetic requirement (MAC) for halothane. Anesth Analg. 1983;62(1):9-14.

177. Gaiser RR, Cheek TG, Kurth CD. Anesthetic management of cesarean delivery complicated by ex utero intrapartum treatment of the fetus. Anesth Analg. 1997;84(5):1150-3.

178. Schwartz DA, Moriarty KP, Tashjian DB, Wool RS, Parker RK, Markenson GR, et al. Anesthetic management of the exit (ex utero intrapartum treatment) procedure. J Clin Anesth. 2001;13(5):387-91.

179. Hirose S, Farmer DL, Lee H, Nobuhara KK, Harrison MR. The ex utero intrapartum treatment procedure: Looking back at the EXIT. J Pediatr Surg. 2004;39(3):375-80.

180. Dahlgren G, Tornberg DC, Pregner K, Irestedt L. Four cases of the ex utero intrapartum treatment (EXIT) procedure: anesthetic implications. Int J Obstet Anesth. 2004;13(3):178-82.

181. McClaine RJ, Uemura K, de la Fuente SG, Manson RJ, Booth JV, White WD, et al. General anesthesia improves fetal cerebral oxygenation without evidence of subsequent neuronal injury. J Cereb Blood Flow Metab. 2005;25(8):1060-9.

182. McClaine RJ, Uemura K, McClaine DJ, Shimazutsu K, de la Fuente SG, Manson RJ, et al. A description of the preterm fetal sheep systemic and central responses to maternal general anesthesia. Anesth Analg. 2007;104(2):397-406.

183. Gaynor JS, Wertz EM, Alvis M, Turner AS. A comparison of the haemodynamic effects of propofol and isoflurane in pregnant ewes. J Vet Pharmacol Ther. 1998;21(1):69-73.

184. Baker BW, Hughes SC, Shnider SM, Field DR, Rosen MA. Maternal anesthesia and the stressed fetus: effects of isoflurane on the asphyxiated fetal lamb. Anesthesiology. 1990;72(1):65-70.

185. Northington FJ, Koehler RC, Traystman RJ, Martin LJ. Nitric oxide synthase 1 and nitric oxide synthase 3 protein expression is regionally and temporally regulated in fetal brain. Brain Res Dev Brain Res. 1996;95(1):1-14.

186. Northington FJ, Tobin JR, Harris AP, Traystman RJ, Koehler RC. Developmental and regional differences in nitric oxide synthase activity and blood flow in the sheep brain. J Cereb Blood Flow Metab. 1997;17(1):109-15.

187. Akata T, Kanna T, Yoshino J, Takahashi S. Mechanisms of direct inhibitory action of isoflurane on vascular smooth muscle of mesenteric resistance arteries. Anesthesiology. 2003;99(3):666-77.

188. Sun L, Tian Z, Moldenhauer J, Khalek N, Martinez-Poyer J, Johnson MP, et al. OP21.02: Acute impact of fetal surgery for myelomeningocele on placental and cerebrovascular circulations [oral presentation]. Ultrasound Obstet Gynecol. 2016;48:119-.

189. Bocking AD, Gagnon R, White SE, Homan J, Milne KM, Richardson BS. Circulatory responses to prolonged hypoxemia in fetal sheep. Am J Obstet Gynecol. 1988;159(6):1418-24.

190. Stein P, White SE, Homan J, Hanson MA, Bocking AD. Altered fetal cardiovascular responses to prolonged hypoxia after sinoaortic denervation. Am J Physiol. 1999;276(2 Pt 2):R340-6.

191. Challis JR, Fraher L, Oosterhuis J, White SE, Bocking AD. Fetal and maternal endocrine responses to prolonged reductions in uterine blood flow in pregnant sheep. Am J Obstet Gynecol. 1989;160(4):926-32.

192. Reynolds JD, Booth JV, de la Fuente S, Punnahitananda S, McMahon RL, Hopkins MB, et al. A review of laparoscopy for non-obstetric-related surgery during pregnancy. Curr Surg. 2003;60(2):164-73.

193. Uemura K, McClaine RJ, de la Fuente SG, Manson RJ, Campbell KA, McClaine DJ, et al. Maternal insufflation during the second trimester equivalent produces hypercapnia, acidosis, and prolonged hypoxia in fetal sheep. Anesthesiology. 2004;101(6):1332-8.

194. Reedy MB, Kallen B, Kuehl TJ. Laparoscopy during pregnancy: a study of five fetal outcome parameters with use of the Swedish Health Registry. Am J Obstet Gynecol. 1997;177(3):673-9.

195. Taylor MJ, Denbow ML, Tanawattanacharoen S, Gannon C, Cox PM, Fisk NM. Doppler detection of arterio-arterial anastomoses in monochorionic twins: feasibility and clinical application. Hum Reprod. 2000;15(7):1632-6.

196. Taylor MJ, Farquharson D, Cox PM, Fisk NM. Identification of arterio-venous anastomoses in vivo in monochorionic twin pregnancies: preliminary report. Ultrasound Obstet Gynecol. 2000;16(3):218-22.

197. Machin GA, Feldstein VA, van Gemert MJ, Keith LG, Hecher K. Doppler sonographic demonstration of arterio-venous anastomosis in monochorionic twin gestation. Ultrasound Obstet Gynecol. 2000;16(3):214-7.

198. Wee LY, Sullivan M, Humphries K, Fisk NM. Longitudinal blood flow in shared (arteriovenous anastomoses) and non-shared cotyledons in monochorionic placentae. Placenta. 2007;28(5-6):516-22.

199. Morel O, Pachy F, Chavatte-Palmer P, Bonneau M, Gayat E, Laigre P, et al. Correlation between uteroplacental three-dimensional power Doppler indices and true uterine blood flow: evaluation in a pregnant sheep model. Ultrasound Obstet Gynecol. 2010;36(5):635-40.

200. Kurmanavicius J, Burkhardt T, Wisser J, Huch R. Ultrasonographic fetal weight estimation: accuracy of formulas and accuracy of examiners by birth weight from 500 to 5000 g. J Perinat Med. 2004;32(2):155-61.

201. Sovio U, White IR, Dacey A, Pasupathy D, Smith GC. Screening for fetal growth restriction with universal third trimester ultrasonography in nulliparous women in the Pregnancy Outcome Prediction (POP) study: a prospective cohort study. Lancet. 2015;386(10008):2089-97.

202. Barbera A, Jones OW, 3rd, Zerbe GO, Hobbins JC, Battaglia FC, Meschia G. Ultrasonographic assessment of fetal growth: comparison between human and ovine fetus. Am J Obstet Gynecol. 1995;173(6):1765-9.

203. Carr DJ, Aitken RP, Milne JS, David AL, Wallace JM. Ultrasonographic assessment of growth and estimation of birthweight in late gestation fetal sheep. Ultrasound Med Biol. 2011;37(10):1588-95.

204. Wallace JM, Milne JS, Redmer DA, Aitken RP. Effect of diet composition on pregnancy outcome in overnourished rapidly growing adolescent sheep. Br J Nutr. 2006;96(6):1060-8.

205. Carr DJ, Aitken RP, Milne JS, David AL, Wallace JM. Fetoplacental biometry and umbilical artery Doppler velocimetry in the overnourished adolescent model of fetal growth restriction. Am J Obstet Gynecol. 2012;207(2):141.e6-15.

206. Giussani DA, Bennet L, Sferruzzi-Perri AN, Vaughan OR, Fowden AL. Hypoxia, fetal and neonatal physiology: 100 years on from Sir Joseph Barcroft. J Physiol. 2016;594(5):1105-11.

207. Alfirevic Z, Stampalija T, Gyte GM. Fetal and umbilical Doppler ultrasound in high-risk pregnancies. Cochrane Database Syst Rev. 2013(11):Cd007529.

208. Neilson JP. Doppler ultrasound. Br J Obstet Gynaecol. 1987;94(10):929-32.

209. Parra-Cordero M, Lees C, Missfelder-Lobos H, Seed P, Harris C. Fetal arterial and venous Doppler pulsatility index and time averaged velocity ranges. Prenat Diagn. 2007;27(13):1251-7.

210. Thompson RS, Trudinger BJ. Doppler waveform pulsatility index and resistance, pressure and flow in the umbilical placental circulation: an investigation using a mathematical model. Ultrasound Med Biol. 1990;16(5):449-58.

211. Al-Ghazali W, Chapman MG, Allan LD. Doppler assessment of the cardiac and uteroplacental circulations in normal and complicated pregnancies. Br J Obstet Gynaecol. 1988;95(6):575-80.

212. Nicolaides KH, Bilardo CM, Soothill PW, Campbell S. Absence of end diastolic frequencies in umbilical artery: a sign of fetal hypoxia and acidosis. Br Med J. 1988;297(6655):1026-7.

213. Bekedam DJ, Visser GH, van der Zee AG, Snijders RJ, Poelmann-Weesjes G. Abnormal velocity waveforms of the umbilical artery in growth retarded fetuses: relationship to antepartum late heart rate decelerations and outcome. Early Hum Dev. 1990;24(1):79-89.

214. Acharya G, Wilsgaard T, Berntsen GK, Maltau JM, Kiserud T. Reference ranges for serial measurements of blood velocity and pulsatility index at the intra-abdominal portion, and fetal and placental ends of the umbilical artery. Ultrasound Obstet Gynecol. 2005;26(2):162-9.

215. Taylor GM, Mires GJ, Abel EW, Tsantis S, Farrell T, Chien PF, et al. The development and validation of an algorithm for real-time computerised fetal heart rate monitoring in labour. Br J Obstet Gynaecol. 2000;107(9):1130-7.

216. Staboulidou I, Wustemann M, Schmidt P, Gunter HH, Hillemanns P, Scharf A. Influence of circadian rhythm on fetal and maternal Doppler parameters--is a diurnal variation detectable? Z Geburtshilfe Neonatol. 2008;212(2):47-52.

217. Nimrod C, Clapp J, Larrow R, D'Alton M, Persaud D. Simultaneous use of Doppler ultrasound and electromagnetic flow probes in fetal flow assessment. J Ultrasound Med. 1989;8(4):201-5.

218. Erkinaro T, Mäkikallio K, Kavasmaa T, Alahuhta S, Räsänen J. Effects of ephedrine and phenylephrine on uterine and placental circulations and fetal outcome following fetal hypoxaemia and epidural-induced hypotension in a sheep model. Br J Anaesth. 2004;93(6):825-32.

219. Galan HL, Hussey MJ, Chung M, Chyu JK, Hobbins JC, Battaglia FC. Doppler velocimetry of growth-restricted fetuses in an ovine model of placental insufficiency. Am J Obstet Gynecol. 1998;178(3):451-6.

220. Barry JS, Davidsen ML, Limesand SW, Galan HL, Friedman JE, Regnault TR, et al. Developmental changes in ovine myocardial glucose transporters and insulin signaling following hyperthermia-induced intrauterine fetal growth restriction. Exp Biol Med. 2006;231(5):566-75.

221. Domínguez E, Rivera Del Álamo MM, Novellas R, Espada Y, Santos L, García F, et al. Doppler evaluation of the effects of propofol, etomidate and alphaxalone on fetoplacental circulation hemodynamics in the pregnant ewe. Placenta. 2013;34(9):738-44.

222. Mari G, Deter RL. Middle cerebral artery flow velocity waveforms in normal and small-for-gestational-age fetuses. Am J Obstet Gynecol. 1992;166(4):1262-70.

223. Mari G, Deter RL, Carpenter RL, Rahman F, Zimmerman R, Moise KJ, Jr., et al. Noninvasive diagnosis by Doppler ultrasonography of fetal anemia due to maternal red-cell alloimmunization. Collaborative Group for Doppler Assessment of the Blood Velocity in Anemic Fetuses. N Engl J Med. 2000;342(1):9-14.

224. Vyas S, Nicolaides KH, Bower S, Campbell S. Middle cerebral artery flow velocity waveforms in fetal hypoxaemia. Br J Obstet Gynaecol. 1990;97(9):797-803.

225. Mari G, Hanif F, Kruger M, Cosmi E, Santolaya-Forgas J, Treadwell MC. Middle cerebral artery peak systolic velocity: a new Doppler parameter in the assessment of growth-restricted fetuses. Ultrasound Obstet Gynecol. 2007;29(3):310-6.

226. Bahlmann F, Reinhard I, Krummenauer F, Neubert S, Macchiella D, Wellek S. Blood flow velocity waveforms of the fetal middle cerebral artery in a normal population: reference values from 18 weeks to 42 weeks of gestation. J Perinat Med. 2002;30(6):490-501.

227. Rizzo G, Capponi A, Arduini D, Romanini C. The value of fetal arterial, cardiac and venous flows in predicting pH and blood gases measured in umbilical blood at cordocentesis in growth retarded fetuses. Br J Obstet Gynaecol. 1995;102(12):963-9.

228. Arduini D, Rizzo G, Romanini C. Changes of pulsatility index from fetal vessels preceding the onset of late decelerations in growth-retarded fetuses. Obstet Gynecol. 1992;79(4):605-10.

229. Dubiel M, Gudmundsson S, Gunnarsson G, Marsal K. Middle cerebral artery velocimetry as a predictor of hypoxemia in fetuses with increased resistance to blood flow in the umbilical artery. Early Hum Dev. 1997;47(2):177-84.

230. Morris RK, Say R, Robson SC, Kleijnen J, Khan KS. Systematic review and meta-analysis of middle cerebral artery Doppler to predict perinatal wellbeing. Eur J Obstet Gynecol Reprod Biol. 2012;165(2):141-55.

231. Baschat AA, Cosmi E, Bilardo CM, Wolf H, Berg C, Rigano S, et al. Predictors of neonatal outcome in early-onset placental dysfunction. Obstet Gynecol. 2007;109(2 Pt 1):253-61.

232. Arbeille P, Patat F, Tranquart F, Body G, Berson M, Roncin A, et al. Doppler examination of the umbilical and cerebral arterial circulation of the fetus. J Gynecol Obstet Biol Reprod. 1987;16(1):45-51.

233. Flood K, Unterscheider J, Daly S, Geary MP, Kennelly MM, McAuliffe FM, et al. The role of brain sparing in the prediction of adverse outcomes in intrauterine growth restriction: results of the multicenter PORTO Study. Am J Obstet Gynecol. 2014;211(3):288.e1-5.

234. Tchirikov M, Rybakowski C, Huneke B, Schroder HJ. Blood flow through the ductus venosus in singleton and multifetal pregnancies and in fetuses with intrauterine growth retardation. Am J Obstet Gynecol. 1998;178(5):943-9.

235. Kessler J, Rasmussen S, Hanson M, Kiserud T. Longitudinal reference ranges for ductus venosus flow velocities and waveform indices. Ultrasound Obstet Gynecol. 2006;28(7):890-8.

236. Bahlmann F, Wellek S, Reinhardt I, Merz E, Steiner E, Welter C. Reference values of ductus venosus flow velocities and calculated waveform indices. Prenat Diagn. 2000;20(8):623-34.

237. Makikallio K, Vuolteenaho O, Jouppila P, Rasanen J. Ultrasonographic and biochemical markers of human fetal cardiac dysfunction in placental insufficiency. Circulation. 2002;105(17):2058-63.

238. Yagel S, Kivilevitch Z, Cohen SM, Valsky DV, Messing B, Shen O, et al. The fetal venous system, Part II: ultrasound evaluation of the fetus with congenital venous system malformation or developing circulatory compromise. Ultrasound Obstet Gynecol. 2010;36(1):93-111.

239. Lees CC, Marlow N, van Wassenaer-Leemhuis A, Arabin B, Bilardo CM, Brezinka C, et al. 2 year neurodevelopmental and intermediate perinatal outcomes in infants with very preterm fetal growth restriction (TRUFFLE): a randomised trial. Lancet. 2015.

240. Panarace M, Garnil C, Cané L, Rodríguez E, Medina M. Echo-Doppler ultrasonographic assessment of resistance and velocity of blood flow in the ductus venosus throughout gestation in fetal lambs. Theriogenology. 2008;70(4):648-54.

241. Cnossen JS, Morris RK, ter Riet G, Mol BW, van der Post JA, Coomarasamy A, et al. Use of uterine artery Doppler ultrasonography to predict pre-eclampsia and intrauterine growth restriction: a systematic review and bivariable meta-analysis. Can Med Assoc J. 2008;178(6):701-11.

242. Lobos H, Rennie JM, Lees C. The natural history of fetal growth restriction in women with abnormal uterine artery Doppler. Prenat Diagn. 2005;25(4):331-2.

243. Ray-Chaudhuri K, Ryder SA, Thomaides T, Mathias CJ. The relationship between blood flow and pulsatility index in the superior mesenteric artery at rest and during constrictor stimuli in normal subjects. J Clin Ultrasound. 1994;22(3):149-60.

244. Saunders HM, Burns PN, Needleman L, Liu JB, Boston R, Wortman JA, et al. Hemodynamic factors affecting uterine artery Doppler waveform pulsatility in sheep. J Ultrasound Med. 1998;17(6):357-68.

245. Gomez O, Figueras F, Fernandez S, Bennasar M, Martinez JM, Puerto B, et al. Reference ranges for uterine artery mean pulsatility index at 11-41 weeks of gestation. Ultrasound Obstet Gynecol. 2008;32(2):128-32.

246. Valino N, Giunta G, Gallo DM, Akolekar R, Nicolaides KH. Uterine artery pulsatility index at 30-34 weeks' gestation in the prediction of adverse perinatal outcome. Ultrasound Obstet Gynecol. 2016;47(3):308-15.

247. Elmetwally M, Rohn K, Meinecke-Tillmann S. Noninvasive color Doppler sonography of uterine blood flow throughout pregnancy in sheep and goats. Theriogenology. 2016;85(6):1070-9.e1.

248. Tutschek B, Schmidt KG. Techniques for assessing cardiac output and fetal cardiac function. Semin Fetal Neonatal Med. 2011;16(1):13-21.

249. Cruz-Martinez R, Figueras F, Bennasar M, Garcia-Posadas R, Crispi F, Hernandez-Andrade E, et al. Normal reference ranges from 11 to 41 weeks' gestation of fetal left modified myocardial performance index by conventional Doppler with the use of stringent criteria for delimitation of the time periods. Fetal Diagn Ther. 2012;32(1-2):79-86.

250. Hernandez-Andrade E, Figueroa-Diesel H, Kottman C, Illanes S, Arraztoa J, Acosta-Rojas R, et al. Gestational-age-adjusted reference values for the modified myocardial performance index for evaluation of fetal left cardiac function. Ultrasound Obstet Gynecol. 2007;29(3):321-5.

251. Van Mieghem T, Gucciardo L, Lewi P, Lewi L, Van Schoubroeck D, Devlieger R, et al. Validation of the fetal myocardial performance index in the second and third trimesters of gestation. Ultrasound Obstet Gynecol. 2009;33(1):58-63.

252. Meriki N, Izurieta A, Welsh AW. Fetal left modified myocardial performance index: technical refinements in obtaining pulsed-Doppler waveforms. Ultrasound Obstet Gynecol. 2012;39(4):421-9.

253. Cruz-Martinez R, Figueras F, Benavides-Serralde A, Crispi F, Hernandez-Andrade E, Gratacos E. Sequence of changes in myocardial performance index in relation to aortic isthmus and ductus venosus Doppler in fetuses with early-onset intrauterine growth restriction. Ultrasound Obstet Gynecol. 2011;38(2):179-84.

254. Benavides-Serralde A, Scheier M, Cruz-Martinez R, Crispi F, Figueras F, Gratacos E, et al. Changes in central and peripheral circulation in intrauterine growth-restricted fetuses at different stages of umbilical artery flow deterioration: new fetal cardiac and brain parameters. Gynecol Obstet Invest. 2011;71(4):274-80.

255. DeVore GR, Siassi B, Platt LD. Fetal echocardiography. IV. M-mode assessment of ventricular size and contractility during the second and third trimesters of pregnancy in the normal fetus. Am J Obstet Gynecol. 1984;150(8):981-8.

256. DeVore GR. Assessing fetal cardiac ventricular function. Semin Fetal Neonatal Med. 2005;10(6):515-41.

257. DeKoninck P, Steenhaut P, Van Mieghem T, Mhallem M, Richter J, Bernard P, et al. Comparison of Doppler-based and three-dimensional methods for fetal cardiac output measurement. Fetal Diagn Ther. 2012;32(1-2):72-8.

258. Mielke G, Benda N. Cardiac output and central distribution of blood flow in the human fetus. Circulation. 2001;103(12):1662-8.

259. Tchirikov M, Strohner M, Scholz A. Cardiac output and blood flow volume redistribution during acute maternal hypoxia in fetal sheep. J Perinat Med. 2010;38(4):387-92.

260. Acharya G, Huhta JC, Haapsamo M, How OJ, Erkinaro T, Rasanen J. Effect of angiotensin II on the left ventricular function in a near-term fetal sheep with metabolic acidemia. J Pregnancy. 2011;2011:634240.

261. Junno J, Bruun E, Gutierrez JH, Erkinaro T, Haapsamo M, Acharya G, et al. Fetal sheep left ventricle is more sensitive than right ventricle to progressively worsening hypoxemia and acidemia. Eur J Obstet Gynecol Reprod Biol. 2013;167(2):137-41.

262. Rossi AC, D'Addario V. The efficacy of Quintero staging system to assess severity of twin-twin transfusion syndrome treated with laser therapy: a systematic review with meta-analysis. Am J Perinatol. 2009;26(7):537-44.

263. DeLia JE, Cukierski MA, Lundergan DK, Kochenour NK. Neodymium:yttrium-aluminum-garnet laser occlusion of rhesus placental vasculature via fetoscopy. Am J Obstet Gynecol. 1989;160(2):485-9.

264. Gayer G, Jonas T, Apter S, Amitai M, Shabtai M, Hertz M. Postoperative pneumoperitoneum as detected by CT: prevalence, duration, and relevant factors affecting its possible significance. Abdom Imaging. 2000;25(3):301-5.

265. Hunter GL. The maternal influence on size in sheep. The Journal of Agricultural Science. 1956;48(01):36-60.

266. Broers P. Compendium of animal reproduction. Boxmeer: Intervet International. 259 p.

267. Gardner DS, Fowden AL, Giussani DA. Adverse intrauterine conditions diminish the fetal defense against acute hypoxia by increasing nitric oxide activity. Circulation. 2002;106(17):2278-83.

268. Brain KL, Allison BJ, Niu Y, Cross CM, Itani N, Kane AD, et al. Induction of controlled hypoxic pregnancy in large mammalian species. Physiol Rep. 2015;3(12).

269. Allison BJ, Brain KL, Niu Y, Kane AD, Herrera EA, Thakor AS, et al. Fetal in vivo continuous cardiovascular function during chronic hypoxia. J Physiol. 2016;594(5):1247-64.

270. Jellyman JK, Gardner DS, Fowden AL, Giussani DA. Effects of dexamethasone on the uterine and umbilical vascular beds during basal and hypoxemic conditions in sheep. Am J Obstet Gynecol. 2004;190(3):825-35.

271. Drost CJ. Vessel diameter-independent volume flow measurements using ultrasound. Proc San Diego Biomed Symp. 1978;17:299-302.

272. Street P, Dawes GS, Moulden M, Redman CW. Short-term variation in abnormal antenatal fetal heart rate records. Am J Obstet Gynecol. 1991;165(3):515-23.

273. Min SW, Ko H, Kim CS. Power spectral analysis of heart rate variability during acute hypoxia in fetal lambs. Acta Obstet Gynecol Scand. 2002;81(11):1001-5.

274. Koome ME, Bennet L, Booth LC, Wassink G, Davidson JO, Gunning M, et al. Quantifying the power spectrum of fetal heart rate variability. Exp Physiol. 2014;99(2):468.

275. Kabaroff L, Boermans H, Karrow NA. Changes in ovine maternal temperature, and serum cortisol and interleukin-6 concentrations after challenge with Escherichia coli lipopolysaccharide during pregnancy and early lactation. J Anim Sci. 2006;84(8):2083-8.

276. Hadlock FP, Harrist RB, Sharman RS, Deter RL, Park SK. Estimation of fetal weight with the use of head, body, and femur measurements - a prospective study. Am J Obstet Gynecol. 1985;151(3):333-7.

277. Bhide A, Acharya G, Bilardo CM, Brezinka C, Cafici D, Hernandez-Andrade E, et al. ISUOG practice guidelines: use of Doppler ultrasonography in obstetrics. Ultrasound Obstet Gynecol. 2013;41(2):233-39.

278. Matthews JN, Altman DG, Campbell MJ, Royston P. Analysis of serial measurements in medical research. Br Med J. 1990;300(6719):230-5.

279. Fletcher AJ, Gardner DS, Edwards CM, Fowden AL, Giussani DA. Development of the ovine fetal cardiovascular defense to hypoxemia towards full term. Am J Physiol Heart Circ Physiol. 2006;291(6):H3023-34.

280. Thakor AS. Nitric Oxide and Antioxidant Modulation of Fetal Cardiovascular, Metabolic and Endocrine Function. University of Cambridge. Thesis/Dissertation.2005.

281. Shaw CJ, Civale J, Botting KJ, Niu Y, Ter Haar G, Rivens I, et al. Noninvasive high-intensity focused ultrasound treatment of twin-twin transfusion syndrome: A preliminary in vivo study. Sci Transl Med. 2016;8(347):347ra95.

282. Sekins KM, Barnes SR, Fan L, Hopple JD, Hsu SJ, Kook J, et al. Deep bleeder acoustic coagulation (DBAC)-Part I: development and in vitro testing of a research prototype cuff system. J Ther Ultrasound. 2015;3:16.

283. Ierullo AM, Papageorghiou AT, Bhide A, Fratelli N, Thilaganathan B. Severe twin-twin transfusion syndrome: outcome after fetoscopic laser ablation of the placental vascular equator. Br J Obstet Gynecol. 2007;114(6):689-93.

284. Lopriore E, Middeldorp JM, Oepkes D, Klumper FJ, Walther FJ, Vandenbussche FP. Residual anastomoses after fetoscopic laser surgery in twin-to-twin transfusion syndrome: frequency, associated risks and outcome. Placenta. 2007;28(2-3):204-8.

285. Bai Y, Luo X, Li Q, Yin N, Fu X, Zhang H, et al. High-intensity focused ultrasound treatment of placenta accreta after vaginal delivery: a preliminary study. Ultrasound Obstet Gynecol. 2016;47(4):492-8.

286. Caloone J, Huissoud C, Vincenot J, Kocot A, Dehay C, Chapelon JY, et al. High-intensity focused ultrasound applied to the placenta using a toroidal transducer: a preliminary ex-vivo study. Ultrasound Obstet Gynecol. 2015;45(3):313-9.

287. Yamamoto M, El Murr L, Robyr R, Leleu F, Takahashi Y, Ville Y. Incidence and impact of perioperative complications in 175 fetoscopy-guided laser coagulations of chorionic plate anastomoses in fetofetal transfusion syndrome before 26 weeks of gestation. Am J Obstet Gynecol. 2005;193(3 Pt 2):1110-6.

288. Middeldorp JM, Lopriore E, Sueters M, Jansen FW, Ringers J, Klumper FJ, et al. Laparoscopically guided uterine entry for fetoscopy in twin-to-twin transfusion syndrome with completely anterior placenta: a novel technique. Fetal Diagn Ther. 2007;22(6):409-15.

289. Liyanage S, Arul GS, Pretlove S, Rasiah SV. PF.41: A surviving case of iatrogenic gastroschisis following laser treatment for twin-twin transfusion syndrome (Poster Presentations). following laser treatment for twin – twin transfusion syndrome. Br J Obstet Gynaecol. 2015(122):54-74.

290. Winer N, Salomon LJ, Essaoui M, Nasr B, Bernard JP, Ville Y. Pseudoamniotic band syndrome: a rare complication of monochorionic twins with fetofetal transfusion syndrome treated by laser coagulation. Am J Obstet Gynecol. 2008;198(4):393.e1-5.

291. Lopriore E, Lewi L, Oepkes D, Debeer A, Vandenbussche FP, Deprest J, et al. In utero acquired limb ischemia in monochorionic twins with and without twin-to-twin transfusion syndrome. Prenat Diagn. 2008;28(9):800-4.

292. Carr SR, Luks F, Tracy T, Plevyak M. Antenatal necrotic injury in severe twin-to-twin transfusion syndrome. A case and review. Fetal Diagn Ther. 2004;19(4):370-2.

293. Schrey S, Huber A, Hecher K, Quintero R, Alkazaleh F, Moise KJ, Jr., et al. Vascular limb occlusion in twin-twin transfusion syndrome (TTTS): case series and literature review. Am J Obstet Gynecol. 2012;207(2):131.e1-10.

294. Jellyman JK, Gardner DS, Edwards CM, Fowden AL, Giussani DA. Fetal cardiovascular, metabolic and endocrine responses to acute hypoxaemia during and following maternal treatment with dexamethasone in sheep. J Physiol. 2005;567(Pt 2):673-88.

295. Abi-Nader KN, Mehta V, Wigley V, Filippi E, Tezcan B, Boyd M, et al. Doppler ultrasonography for the noninvasive measurement of uterine artery volume blood flow through gestation in the pregnant sheep. Reprod Sci. 2010;17(1):13-9.

296. Newnham JP, Kelly RW, Roberts RV, MacIntyre M, Speijers J, Johnson T, et al. Fetal and maternal Doppler flow velocity waveforms in normal sheep pregnancy. Placenta. 1987;8(5):467-76.

297. Hegyi T, Carbone MT, Anwar M, Ostfeld B, Hiatt M, Koons A, et al. Blood pressure ranges in premature infants. I. The first hours of life. J Pediatr. 1994;124(4):627-33.

298. Jones JE, Jose PA. Neonatal blood pressure regulation. Semin Perinatol. 2004;28(2):141-8.

299. Boat A, Mahmoud M, Michelfelder EC, Lin E, Ngamprasertwong P, Schnell B, et al. Supplementing desflurane with intravenous anesthesia reduces fetal cardiac dysfunction during open fetal surgery. Paediatr Anaesth. 2010;20(8):748-56.

300. Giussani DA. The fetal brain sparing response to hypoxia: physiological mechanisms. J Physiol. 2016;594(5):1215-30.

301. Giussani DA, Spencer JA, Moore PJ, Bennet L, Hanson MA. Afferent and efferent components of the cardiovascular reflex responses to acute hypoxia in term fetal sheep. J Physiol. 1993;461:431-49.

302. Johnson MH. Maternal Recognition and Support of Pregnancy. Essential reproduction. 6th ed. Oxford: Blackwell Publishing Ltd; 2007.

303. Hill EP, Power GG, Longo LD. A mathematical model of carbon dioxide transfer in the placenta and its interaction with oxygen. AmJ Physiol. 1973;224(2):283-99.

304. Barnard JM, Chaffin D, Droste S, Tierney A, Phernetton T. Fetal response to carbon dioxide pneumoperitoneum in the pregnant ewe. Obstet Gynecol. 1995;85(5):669-74.

305. Cruz AM, Southerland LC, Duke T, Townsend HG, Ferguson JG, Crone LA. Intraabdominal carbon dioxide insufflation in the pregnant ewe. Uterine blood flow, intraamniotic pressure, and cardiopulmonary effects. Anesthesiology. 1996;85(6):1395-402.

306. Bhavani-Shankar K, Steinbrook RA, Brooks DC, Datta S. Arterial to end-tidal carbon dioxide pressure difference during laparoscopic surgery in pregnancy. Anesthesiology. 2000;93(2):370-3.

307. Gas transport between the lung and the tissues. In: Ganong WF, editor. Review of Medical Physiology. 20th ed. Stamford, Conneticut: McGraw Hill; 2001. p. 644-8.

308. Low JA, Pancham SR, Worthington D, Boston RW. The acid-base and biochemical characteristics of intrapartum fetal asphyxia. Am J Obstet Gynecol. 1975;121(4):446-51.

309. Boyle DW, Meschia G, Wilkening RB. Metabolic adaptation of fetal hindlimb to severe, nonlethal hypoxia. Am J Physiol. 1992;263(5):R1130-5.

310. Acharya G, Wilsgaard T, Berntsen GK, Maltau JM, Kiserud T. Reference ranges for serial measurements of umbilical artery Doppler indices in the second half of pregnancy. Am J Obstet Gynecol. 2005;192(3):937-44.

311. Davidson D. Circulating vasoactive substances and hemodynamic adjustments at birth in lambs. J Appl Physiol. 1987;63(2):676-84.

312. Segar JL, Barna TJ, Acarregui MJ, Lamb FS. Responses of fetal ovine systemic and umbilical arteries to angiotensin II. Pediatr Res. 2001;49(6):826-33.

313. Westgate JA, Wibbens B, Bennet L, Wassink G, Parer JT, Gunn AJ. The intrapartum deceleration in center stage: a physiologic approach to the interpretation of fetal heart rate changes in labor. Am J Obstet Gynecol. 2007;197(3):236.e1-11.

314. Dawes GS, Johnston BM, Walker DW. Relationship of arterial pressure and heart rate in fetal, new-born and adult sheep. J Physiol. 1980;309:405-17.

315. Reeves JT, Daoud FS, Gentry M. Growth of the fetal calf and its arterial pressure, blood gases, and hematologic data. J Appl Physiol. 1972;32(2):240-4.

316. Boddy K, Dawes GS, Fisher R, Pinter S, Robinson JS. Foetal respiratory movements, electrocortical and cardiovascular responses to hypoxaemia and hypercapnia in sheep. J Physiol. 1974;243(3):599-618.

317. Macdonald AA, Colenbrander B, Wensing CJ. The effects of gestational age and chronic fetal decapitation on arterial blood pressure in the pig fetus. Eur J Obstet Gynecol Reprod Biol. 1983;16(1):63-70.

318. Kitanaka T, Alonso JG, Gilbert RD, Siu BL, Clemons GK, Longo LD. Fetal responses to long-term hypoxemia in sheep. Am J Physiol. 1989;256(6 Pt 2):R1348-54.

319. Forhead AJ, Broughton Pipkin F, Taylor PM, Baker K, Balouzet V, Giussani DA, et al. Developmental changes in blood pressure and the renin-angiotensin system in pony fetuses during the second half of gestation. J Reprod Fertil Suppl. 2000(56):693-703.

320. Giussani DA, Forhead AJ, Fowden AL. Development of cardiovascular function in the horse fetus. J Physiol. 2005;565(Pt 3):1019-30.

321. Thornburg KL, Morton MJ. Filling and arterial pressures as determinants of left ventricular stroke volume in fetal lambs. Am J Physiol. 1986;251(5 Pt 2):H961-8.

322. Grant DA, Kondo CS, Maloney JE, Walker AM, Tyberg JV. Changes in pericardial pressure during the perinatal period. Circulation. 1992;86(5):1615-21.

323. Paramasivam G. Ultrasound assessment of fetal cardiac function and risk of adverse obstetric and neonatal outcomes in term fetuses. London: Imperial College London; 2107.

324. Alsolai AA, Bligh LN, Greer RM, Kumar S. Pre-labor fetal cardiac function and its relationship with intrapartum fetal compromise and neonatal status at term. Ultrasound Obstet Gynecol. 2017.

325. Fowden AL, Szemere J, Hughes P, Gilmour RS, Forhead AJ. The effects of cortisol on the growth rate of the sheep fetus during late gestation. J Endocrinol. 1996;151(1):97-105.

326. Papageorghiou AT, Ohuma EO, Altman DG, Todros T, Cheikh Ismail L, Lambert A, et al. International standards for fetal growth based on serial ultrasound measurements: the Fetal Growth Longitudinal Study of the INTERGROWTH-21st Project. Lancet. 2014;384(9946):869-79.

327. Ward JW, Forhead AJ, Wooding FBP, Fowden AL. Functional Significance and Cortisol Dependence of the Gross Morphology of Ovine Placentomes During Late Gestation. Biology of Reproduction. 2006;74(1):137-45.

328. Anthony RV, Scheaffer AN, Wright CD, Regnault TR. Ruminant models of prenatal growth restriction. Reprod Suppl. 2003;61:183-94.

329. Gardner DS, Ward JW, Giussani DA, Fowden AL. The effect of a reversible period of adverse intrauterine conditions during late gestation on fetal and placental weight and placentome distribution in sheep. Placenta. 2002;23(6):459-66.

330. Schneider H. Ontogenic changes in the nutritive function of the placenta. Placenta. 1996;17(1):15-26.

331. Hanson MA, Spencer JAD, Rodeck CH. Fetus and Neonate: Physiology and Clinical Applications. Cambridge: Cambridge University Press; 1995.

332. Kulhanek JF, Meschia G, Makowski EL, Battaglia FC. Changes in DNA content and urea permeability of the sheep placenta. Am J Physiol. 1974;226(5):1257-63.

333. Symonds ME, Heasman L, Clarke L, Firth K, Stephenson T. Maternal nutrition and disproportionate placental-to-fetal growth. Biochem Soc Trans. 1998;26(2):91-6.

334. Steyn C, Hawkins P, Saito T, Noakes DE, Kingdom JC, Hanson MA. Undernutrition during the first half of gestation increases the predominance of fetal tissue in late-gestation ovine placentomes. Eur J Obstet Gynecol Reprod Biol. 2001;98(2):165-70.

335. Wallace JM, Bourke DA, Aitken RP, Palmer RM, Da Silva P, Cruickshank MA. Relationship between nutritionally-mediated placental growth restriction and fetal growth, body composition and endocrine status during late gestation in adolescent sheep. Placenta. 2000;21(1):100-8.

336. Penninga L, Longo LD. Ovine placentome morphology: effect of high altitude, long-term hypoxia. Placenta. 1998;19(2-3):187-93.

337. Bell AW, Wilkening RB, Meschia G. Some aspects of placental function in chronically heat-stressed ewes. J Dev Physiol. 1987;9(1):17-29.

338. Phillips ID, Simonetta G, Owens JA, Robinson JS, Clarke IJ, McMillen IC. Placental restriction alters the functional development of the pituitary-adrenal axis in the sheep fetus during late gestation. Pediatr Res. 1996;40(6):861-6.

339. Simonetta G, Rourke AK, Owens JA, Robinson JS, McMillen IC. Impact of placental restriction on the development of the sympathoadrenal system. Pediatr Res. 1997;42(6):805-11.

340. Forhead AJ, Fowden AL. Role of angiotensin II in the pressor response to cortisol in fetal sheep during late gestation. Exp Physiol. 2004;89(3):323-9.

341. Tangalakis K, Lumbers ER, Moritz KM, Towstoless MK, Wintour EM. Effect of cortisol on blood pressure and vascular reactivity in the ovine fetus. Exp Physiol. 1992;77(5):709-17.

342. Derks JB, Giussani DA, Jenkins SL, Wentworth RA, Visser GH, Padbury JF, et al. A comparative study of cardiovascular, endocrine and behavioural effects of betamethasone and dexamethasone administration to fetal sheep. J Physiol. 1997;499 (Pt 1):217-26.

343. Rosenstock EG, Cassuto Y, Zmora E. Heart rate variability in the neonate and infant: analytical methods, physiological and clinical observations. Acta Paediatr. 1999;88(5):477-82.

344. van Woerden EE, van Geijn HP. Heart-rate patterns and fetal movements. In: Nijhuis JG, editor. Fetal behaviour : developmental and perinatal aspects. Oxford: Oxford University Press; 1992. p. 41-56.

345. Shaw CJ, Allison BJ, Lees CC, Giussani DA. PF.4: Fetal heart rate variability in the chronically hypoxic fetus (Poster Presentations). Br J Obstet Gynaecol. 2015;122:54-74.

346. Leung JH, Yu SC, Cheung EC, Wong AS, Tong MM, Ho SS, et al. Safety and efficacy of sonographically guided high-intensity focused ultrasound for symptomatic uterine fibroids: preliminary study of a modified protocol. J Ultrasound Med. 2014;33(10):1811-8.

347. Rabinovici J, Inbar Y, Revel A, Zalel Y, Gomori JM, Itzchak Y, et al. Clinical improvement and shrinkage of uterine fibroids after thermal ablation by magnetic resonance-guided focused ultrasound surgery. Ultrasound Obstet Gynecol. 2007;30(5):771-7.

348. Bryant J, Day R. Incorporating toxicity considerations into the design of two-stage phase II clinical trials. Biometrics. 1995;51(4):1372-83.

349. Transonic Systems (1997). Transonic Animal Research Flow Meters: T106/206 Operators Manual.

350. Transonic Systems (1995). Unique Features Of Ultrasonic Transit-Time Volume Flowmeters

351. Transonic Systems (2013). Acoustic Couplants for Acute Measurements.

352. Drost CJ, Dobson A, Sellers AF. An implantable transit time ultrasonic flowmeter for long term measurement of blood volume flow. Federation Proceedings. 1984;43(3).

APPENDIX I: REPORTED EFFECTS OF GENERAL ANAESTHESIA ON MATERNAL AND FETAL CARDIOVASCULAR AND METABOLIC VARIABLES

Maternal Mean Arterial Pressure (mmHg)		Duration of exposure to inhaled isoflurane																							
		15-16 minutes			30-32 minutes			45-48 minutes			60-64 minutes			90-96 minutes			120 mintues			180 minutes			240 minutes		
		Mean value	*n*	Reference	Mean value	*n*	Reference	Mean value	*n*	Reference	Mean value	*n*	Reference	Mean value	*n*	Reference	Mean value	*n*	Reference	Mean value	*n*	Reference	Mean value	*n*	Reference
Content of inspired gases	0.5% Isoflurane + oxygen	85	21	Okutomi 2009																					
	Mean of quoted values	**85.0**	**21**																						
	1.0% Isoflurane + oxygen	90	21	Okutomi 2009	91.8	4	Palahniuk 1974				93.2	4	Palahniuk 1974	98.9	4	Palahniuk 1974									
		88.8	4	Palahniuk 1974																					
	Mean of quoted values	**89.8**	**25**		**91.8**	**4**					**93.2**	**4**		**98.9**	**4**										
	1.5% Isoflurane + oxygen	78	21	Okutomi 2009	74.5	6	Palahniuk 1974	81	6	Gaynor 1998	80.3	6	Palahniuk 1974	82.3	6	Palahniuk 1974									
		77.3	6	Palahniuk 1974	78	10	Gaynor 1998				92	8	McClaine 2007												
		65	8	McClaine 2007							80	10	Gaynor 1998												
		76	10	Gaynor 1998																					
	Mean of quoted values	**75.2**	**45**		**76.7**	**16**		**81.0**	**6**		**84.1**	**24**		**82.3**	**6**										
	2.0% Isoflurane + oxygen	70	21	Okutomi 2009	61.1	6	Palahniuk 1974	89.5	8	Biehl 1983	65.2	6	Palahniuk 1974	65	6	Palahniuk 1974	99	8	McClaine 2007	98	8	McClaine 2007	94	8	McClaine 2007
		55.1	6	Palahniuk 1974	86.3	8	Biehl 1983				96	8	Biehl 1983	97.8	8	McClaine 2007									
		83	8	Biehl 1983	58.3	10	Gaynor 1998																		
		60.8	6	Bachman 1986																					
	Mean of quoted values	**69.0**	**41**		**68.3**	**24**		**89.5**	**8**		**82.8**	**14**		**83.7**	**14**		**99.0**	**8**		**98.0**	**8**		**94.0**	**8**	

Maternal Heart Rate (bpm)		Duration of exposure to inhaled isoflurane																							
		15-16 minutes			30-32 minutes			45-48 minutes			60-64 minutes			90-96 minutes			120 mintues			180 minutes			240 minutes		
		Mean value	*n*	Reference	Mean value	*n*	Reference	Mean value	*n*	Reference	Mean value	*n*	Reference	Mean value	*n*	Reference	Mean value	*n*	Reference	Mean value	*n*	Reference	Mean value	*n*	Reference
Content of inspired gases	0.5% Isoflurane + oxygen	120	21	Okutomi 2009																					
	Mean of quoted values	**120.0**	**21**																						
	1.0% Isoflurane + oxygen	119	21	Okutomi 2009	113	4	Palahniuk 1974				116	4	Palahniuk 1974	131	4	Palahniuk 1974									
		72	4	Palahniuk 1974																					
	Mean of quoted values	**111.5**	**25**		**113**	**4**					**116**	**4**		**131**	**4**										
	1.5% Isoflurane + oxygen	117	21	Okutomi 2009	105	6	Palahniuk 1974	97	10	Gaynor 1998	109	6	Palahniuk 1974	114	6	Palahniuk 1974									
		110	6	Palahniuk 1974	96	10	Gaynor 1998				108	8	McClaine 2007												
		95	10	Gaynor 1998	87	8	McClaine 2007				98	10	Gaynor 1998												
	Mean of quoted values	**109.9**	**37**		**95.3**	**24**		**97.0**	**10**		**104.1**	**24**		**114.0**	**6**										
	2.0% Isoflurane + oxygen	115	21	Okutomi 2009	93.7	6	Palahniuk 1974	98.1	8	Biehl 1983	93	6	Palahniuk 1974	96	6	Palahniuk 1974	112	8	McClaine 2007	114	8	McClaine 2007	110	8	McClaine 2007
		91	6	Palahniuk 1974	93.1	8	Biehl 1983				107.5	8	Biehl 1983	106	8	McClaine 2007									
		111	8	Biehl 1983	91	10	Gaynor 1998																		
		102	6	Bachman 1986																					
	Mean of quoted values	**108.8**	**41**		**92.4**	**24**		**98.1**	**8**		**101.3**	**14**		**101.7**	**14**		**112.0**	**8**		**114.0**	**8**		**110.0**	**8**	

Uterine Blood Flow (ml min-1)		Duration of exposure to inhaled isoflurane																							
		15-16 minutes			30-32 minutes			45-48 minutes			60-64 minutes			90-96 minutes			120 mintues			180 minutes			240 minutes		
		Mean value	*n*	Reference	Mean value	*n*	Reference	Mean value	*n*	Reference	Mean value	*n*	Reference	Mean value	*n*	Reference	Mean value	*n*	Reference	Mean value	*n*	Reference	Mean value	*n*	Reference
Content of inspired gases	0.5% Isoflurane + oxygen	378	21	Okutomi 2009																					
	Mean of quoted values	**378.0**	**21**																						
	1.0% Isoflurane + oxygen	390	21	Okutomi 2009	616	4	Palahniuk 1974				654	4	Palahniuk 1974	647	4	Palahniuk 1974									
		580	4	Palahniuk 1974																					
	Mean of quoted values	**420.4**	**25**		**616**	**4**					**654**	**4**		**647**	**4**										
	1.5% Isoflurane + oxygen	350	21	Okutomi 2009	406	6	Palahniuk 1974				434	6	Palahniuk 1974	464	6	Palahniuk 1974									
		400	6	Palahniuk 1974																					
	Mean of quoted values	**361.1**	**27**		**406.0**	**6**		**0.0**	**0**		**434.0**	**6**		**464.0**	**6**										
	2.0% Isoflurane + oxygen	329	21	Okutomi 2009	260	6	Palahniuk 1974				291	6	Palahniuk 1974	313	6	Palahniuk 1974									
		218	6	Palahniuk 1974																					
	Mean of quoted values	**304.3**	**27**		**260.0**	**6**					**291.0**	**6**		**313.0**	**6**										

Table I.i: Reported maternal cardiovascular parameters in pregnant sheep under isoflurane anaesthesia.
The table shows the effect of 0.5-2.0% MAC of isoflurane for a duration of between 15 and 240 minutes on maternal mean arterial blood pressure, heart rate and uterine blood flow in pregnant sheep, reported in 6 studies. The key to the reference is on page 318.

Fetal Mean Arterial Pressure (mmHg)		Duration of exposure to inhaled isoflurane																					
		15-16 minutes			30-32 minutes			45-48 minutes			60-64 minutes			90-96 minutes			120 mintues			180 minutes			240 minutes		
		Mean value	*n*	Reference	Mean value	*n*	Reference	Mean value	*n*	Reference	Mean value	*n*	Reference	Mean value	*n*	Reference	Mean value	*n*	Reference	Mean value	*n*	Reference	Mean value	*n*	Reference
Content of inspired gases	0.5% Isoflurane + oxygen	53	21	Okutomi 2009																					
	Mean of quoted values	**53.0**	**21**																						
	1.0% Isoflurane + oxygen	52	21	Okutomi 2009	47.7	4	Palahniuk 1974				45.8	4	Palahniuk 1974	47.9	4	Palahniuk 1974									
		45.4	4	Palahniuk 1974																					
	Mean of quoted values	**50.9**	**25**		**47.7**	**4**					**45.8**	**4**		**47.9**	**4**										
	1.5% Isoflurane + oxygen	43	21	Okutomi 2009	44.6	6	Palahniuk 1974				44.5	6	Palahniuk 1974	44.9	6	Palahniuk 1974									
		44.8	6	Palahniuk 1974							38	8	McClaine 2007												
		38	8	McClaine 2007																					
	Mean of quoted values	**42.2**	**35**		**44.6**	**6**					**40.8**	**14**		**44.9**	**6**										
	2.0% Isoflurane + oxygen	41	21	Okutomi 2009	35.5	6	Palahniuk 1974	50	8	Biehl 1983	37.8	6	Palahniuk 1974	35.2	6	Palahniuk 1974	39	8	McClaine 2007	41	8	McClaine 2007	40	8	McClaine 2007
		36.4	6	Palahniuk 1974	50.5	8	Biehl 1983				49.2	8	Biehl 1983	50.2	8	McClaine 2007									
		50	8	Biehl 1983	39.2	6	Bachman 1986																		
		40.5	6	Bachman 1986																					
	Mean of quoted values	**42.0**	**41**		**42.6**	**20**		**50.0**	**8**		**44.3**	**14**		**43.8**	**14**		**39.0**	**8**		**41.0**	**8**		**40.0**	**8**	

Fetal Heart Rate (bpm)		Duration of exposure to inhaled isoflurane																					
		15-16 minutes			30-32 minutes			45-48 minutes			60-64 minutes			90-96 minutes			120 mintues			180 minutes			240 minutes		
		Mean value	*n*	Reference	Mean value	*n*	Reference	Mean value	*n*	Reference	Mean value	*n*	Reference	Mean value	*n*	Reference	Mean value	*n*	Reference	Mean value	*n*	Reference	Mean value	*n*	Reference
Content of inspired gases	0.5% Isoflurane + oxygen	164	21	Okutomi 2009																					
	Mean of quoted values	**164.0**	**21**																						
	1.0% Isoflurane + oxygen	165	21	Okutomi 2009	170	4	Palahniuk 1974				160	4	Palahniuk 1974	166	4	Palahniuk 1974									
		160	4	Palahniuk 1974																					
	Mean of quoted values	**164.2**	**25**		**170**	**4**					**160**	**4**		**166**	**4**										
	1.5% Isoflurane + oxygen	158	21	Okutomi 2009	154	6	Palahniuk 1974				152	6	Palahniuk 1974	151	6	Palahniuk 1974									
		166	6	Palahniuk 1974							150	8	McClaine 2007												
	Mean of quoted values	**#REF!**	**27**		**154.0**	**6**					**150.9**	**14**		**151.0**	**6**										
	2.0% Isoflurane + oxygen	145	21	Okutomi 2009	132	6	Palahniuk 1974	156	8	Biehl 1983	142	6	Palahniuk 1974	138	6	Palahniuk 1974	150	8	McClaine 2007	149	8	McClaine 2007	147	8	McClaine 2007
		137	6	Palahniuk 1974	158	8	Biehl 1983				156	8	Biehl 1983	146	8	McClaine 2007									
		166	8	Biehl 1983	122	6	Bachman 1986																		
		142	6	Bachman 1986																					
	Mean of quoted values	**147.5**	**41**		**139.4**	**20**		**156.0**	**8**		**150.0**	**14**		**142.6**	**14**		**150.0**	**8**		**149.0**	**8**		**147.0**	**8**	

Table I.ii: Reported fetal cardiovascular parameters under isoflurane anaesthesia
The table shows the effect of 0.5-2.0% MAC of isoflurane for a duration of between 15 and 240 minutes on fetal mean arterial blood pressure and heart rate, reported in 5 studies. The key to the reference is on page 318.

	Maternal pH	Baseline (pre-ox)			15 min			30 min			45 min			60 min			90 min			120 min			180 min			240 min		
		Mean	SEM	n	Mean	SEM	n	Mean	SEM	n	Mean	SEM	n	Mean	SEM	n	Mean	SEM	n	Mean	SEM	n	Mean	SEM	n	Mean	SEM	n
Isoflurane 1.0%	Palahniuk 1974	7.48	0.01	4	7.55	0.04	4	7.54	0.01	4				7.50	0.02	4	7.40	0.02	4									
	Okutomi 2009	7.52		21	7.48		21																					
	Mean	7.50	0.00160	25	7.52	0.00640	25	7.54	0.01000	4				7.50	0.02000	4	7.40	0.02000	4									
Isoflurane 1.5%	Palahniuk 1974	7.47	0.02	6	7.51		6	7.52		6				7.52		6	7.51		6									
	McClaine 2007	7.50	0.02	8				7.49		8				7.47		8				7.45		8	7.45		8	7.45		8
	Okutomi 2009	7.52	0.02	21	7.47		21																					
	Mean	7.50	0.00437	35	7.49		27	7.51		14				7.50		14	7.51		6	7.45		8	7.45		8	7.45		8
Isoflurane 2.0%	Palahniuk 1974	7.53	0.02	6	7.51		6	7.51		6				7.51		6	7.50		6									
	Biehl 1983	7.48	0.04	8	7.48	0.03	8	7.50	0.02	8	7.50	0.02	8	7.49	0.02	8	7.47	0.03	8									
	Bachman 1986	7.48	0.03	6	7.51		6	7.53		6																		
	Okutomi 2009	7.52	0.02	21	7.46	0.02	21																					
	Mean	7.50	0.00411	41	7.49	0.00089	41	7.51	0.00029	20	7.50	0.00113	8	7.50	0.00049	14	7.49	0.00110	14									

	Maternal PaCO2	Baseline (pre-ox)			15 min			30 min			45 min			60 min			90 min			120 min			180 min			240 min		
		Mean	SEM	n	Mean	SEM	n	Mean	SEM	n	Mean	SEM	n	Mean	SEM	n	Mean	SEM	n	Mean	SEM	n	Mean	SEM	n	Mean	SEM	n
Isoflurane 1.0%	Palahniuk 1974	31.10	1.30	4	29.10	3.40	4	30.20	2.20	4				33.50	1.50	4	34.50	0.02	4									
	Okutomi 2009	29.00	0.80	21	33.00		21																					
	Mean	30.05	2.46592	25	31.05	0.54400	25	30.20	2.20000	4				33.50	1.50000	4	34.50	0.02000	4									
Isoflurane 1.5%	Palahniuk 1974	28.70	1.10	6	32.3		6	32.20		6				32.80		6	34.20		6									
	McClaine 2007	29.00	1.40	8				32.90		8				36.10		8				36.10		8	38.20		8	36.90		8
	Okutomi 2009	29.00	0.80	21	34		21																					
	Mean	28.90	2.00599	35	33.15		27	32.55	0.00000	14				34.45		14	34.20		6	36.10		8	38.20		8	36.90		8
Isoflurane 2.0%	Palahniuk 1974	29.00	1.00	6	32.90		6	31.80		6				33.20		6	33.20		6									
	Biehl 1983	33.30	4.50	8	36.00	0.03	8	28.00	0.02	8	30.00		8	29.00	0.02	8	34.00	0.03	8									
	Bachman 1986	34.00	1.50	6	32.00		6	32.00		6																		
	Okutomi 2009	29.00	0.80	21	35.50		21																					
	Mean	31.33	6.46658	41	34.10	0.00022	41	30.60	0.00029	20	30.00		8	31.10	0.00049	14	33.60	0.00110	14									

Table I.iii: Reported maternal acid-base parameters in pregnant sheep under isoflurane anaesthesia
The table shows the effect of 1.0-2.0% MAC of isoflurane for a duration of between 15 and 240 minutes on maternal pH and P_aCO_2 in pregnant sheep, reported in 5 studies. The key to the reference is on page 318.

	Fetal pH	Baseline (pre-ox)			15 min			30 min			45 min			60 min			90 min			120 min			180 min			240 min		
		Mean	SEM	n	Mean	SEM	n	Mean	SEM	n	Mean	SEM	n	Mean	SEM	n	Mean	SEM	n	Mean	SEM	n	Mean	SEM	n	Mean	SEM	n
Isoflurane 1.0%	Palahniuk 1974	7.34	0.04	4	7.35	0.03	4	7.37	0.02	4				7.33	0.03	4	7.32	0.04	4									
	Okutomi 2009	7.35	0.01	21	7.33		21																					
	Mean	7.35	0.00675	25	7.33	0.00480	25	7.37	0.02000	4				7.33	0.03000	4	7.32	0.04000	4									
Isoflurane 1.5%	Palahniuk 1974	7.38	0.03	6	7.31		6	7.33		6				7.32		6	7.33		6									
	McClaine 2007	7.39		8				7.31		8				7.29		8				7.28		8	7.26		8	7.26		8
	Okutomi 2009	7.35	0.01	21	7.33		21																					
	Mean	7.36	0.00536	35	7.33		27	7.32		14				7.30		14	7.33		6	7.28		8	7.26		8	7.26		8
Isoflurane 2.0%	Palahniuk 1974	7.38	0.02	6	7.29		6	7.30		6				7.29		6	7.26		6									
	Biehl 1983	7.35	0.04	8	7.38		8	7.35		8	7.34		8	7.33		8	7.26		8									
	Bachman 1986	7.34	0.02	6	7.32		6	7.33		6																		
	Okutomi 2009	7.35	0.01	21	7.33		21																					
	Mean	7.35	0.03	41	7.33		41	7.33		20	7.34		8	7.31		14	7.26		14									

	Fetal PaCO2	Baseline (pre-ox)			15 min			30 min			45 min			60 min			90 min			120 min			180 min			240 min		
		Mean	SEM	n	Mean	SEM	n	Mean	SEM	n	Mean	SEM	n	Mean	SEM	n	Mean	SEM	n	Mean	SEM	n	Mean	SEM	n	Mean	SEM	n
Isoflurane 1.0%	Palahniuk 1974	41.40	0.60	4	43.10	4.00	4	41.20	1.80	4				46.20	2.30	4	50.40	4.10	4									
	Okutomi 2009	43.00	1.40	21	45.00		21																					
	Mean	42.74	7.01088	25	44.70	0.64000	25	41.20	1.80000	4				46.20	2.30000	4	50.40	4.10000	4									
Isoflurane 1.5%	Palahniuk 1974	37.30	1.30	6	44.7		6	44.50		6				44.80		6	43.00		6									
	McClaine 2007	37.00	1.20	8				52.40		8				54.30		8				56.90		8	61.60		8	64.00		8
	Okutomi 2009	43.00	1.40	21	46		21																					
	Mean	40.65	4.73105	35	45.71		27	49.01		14				50.23		14	43.00		6	56.90		8	61.60		8	64.00		8
Isoflurane 2.0%	Palahniuk 1974	37.30	1.40	6	43.30		6	42.50		6				41.20		6	44.40		6									
	Biehl 1983	37.00	1.00	8	42.00		8	39.00		8	40.00		8	41.00		8	44.00		8									
	Bachman 1986	37.30	1.10	6	46.80		6	45.10		6																		
	Okutomi 2009	43.00	1.40	21	47.00		21																					
	Mean	40.16	2.58	41	45.45		41	41.88		20	40.00		8	41.09		14	44.17		14									

	Fetal ABE	Baseline (pre-ox)			15 min			30 min			45 min			60 min			90 min		
		Mean	SEM	n	Mean	SEM	n	Mean	SEM	n	Mean	SEM	n	Mean	SEM	n	Mean	SEM	n
Isoflurane 1.0%	Palahniuk 1974	-1.20	2.40	4	-1.90	1.70	4	-1.40	1.40	4				-2.20	1.40	4	-0.90	0.02	4
	Mean	-1.20	2.40000	4	-1.90	1.70000	4	-1.40	1.40000	4				-2.20	1.40000	4	-3.70	0.02000	4
Isoflurane 1.5%	Palahniuk 1974	-2.50	1.40	6	-4		6	-2.50		6				-3.20		6	-3.70		6
	Mean	-2.50	1.40000	6	-4.00		2.4	-2.50		6				-3.20		6	-7.00	0.00000	6
Isoflurane 2.0%	Palahniuk 1974	-2.70	1.80	6	-5.60		-0.6	-5.80		6				-6.50		6	-7.10		6
	Biehl 1983	-1.10	1.50	8	0.10		8	-2.40		8	-2.60		8	-3.20		8	-6.20	0.03	8
	Bachman 1986	-0.60		6	0.30		6	-0.60		6									
	Mean	-1.47	1.74748	20	-1.73		13	-2.93		20	-2.60		8	-4.85		14	-6.65		14

	Fetal PaO2	Baseline (pre-ox)			15 min			30 min			45 min			60 min			90 min		
		Mean	SEM	n	Mean	SEM	n	Mean	SEM	n	Mean	SEM	n	Mean	SEM	n	Mean	SEM	n
Isoflurane 1.0%	Palahniuk 1974	20.90	2.90	4	18.60	3.20	4	17.70	2.00	4				20.20	2.10	4	19.20	2.60	4
	Okutomi 2009	17.00	1.00	21	24.00		21												
	Mean	17.62	3.99200	25	23.14	0.51200	25	17.70	2.00000	4				20.20	2.10000	4	19.20	2.60000	4
Isoflurane 1.5%	Palahniuk 1974	20.50	1.30	6	21.2	1.4	6	21.50		6				22.10		6	21.70		6
	McClaine 2007	20.00	1.20	8															
	Okutomi 2009	17.00	1.00	21	25		21												
	Mean	18.29	2.68646	35	24.16	1.40000	27	21.50		6				22.10		6	21.70		6
Isoflurane 2.0%	Palahniuk 1974	21.80	1.50	6	19.40		6	20.50		6				18.20		6	17.70		6
	Biehl 1983	20.50	1.30	8	26.00		8	24.00		8	24.00		8	24.00		8	25.00		8
	Bachman 1986	22.20	0.83	6	24.00		6	22.30		6									
	Okutomi 2009	17.00	1.00	21	24.00		21												
	Mean	19.15	1.85	41	23.72		41	22.44		20	24.00		8	21.51		14	21.87		14

Table I.iv: Reported fetal acid-base and oxygenation parameters under isoflurane anaesthesia.
The table shows the effect of 1.0-2.0% MAC of isoflurane for a duration of between 15 and 240 minutes on fetal mean arterial blood pressure and heart rate, reported in 5 studies. The key to the reference is on page 318.

LIST OF REFERENCES INCLUDED IN APPENDIX I:

Name in Appendix I	**Number in Bibliography**
Bachman 1986	(174)
Biehl 1983	(175)
Gaynor 1998	(183)
McClaine 2007	(182)
Okutomi 2009	(167)
Palahniuk 1974	(173)

APPENDIX II: TRANSONIC FLOW PROBE PRINCIPALS OF ACTION

Time-transit ultrasonic flow probes make use of upstream and downstream transducers, a known distance apart, with a predefined angle of insonation (R series 45°; S series 65° (349)) and an acoustic reflector in a fixed orientation to calculate the volume of flow through their acoustic window (Figure II). This measurement is independent of the diameter, shape and angulation of the vessel as well as the flow profile of the blood within (271).

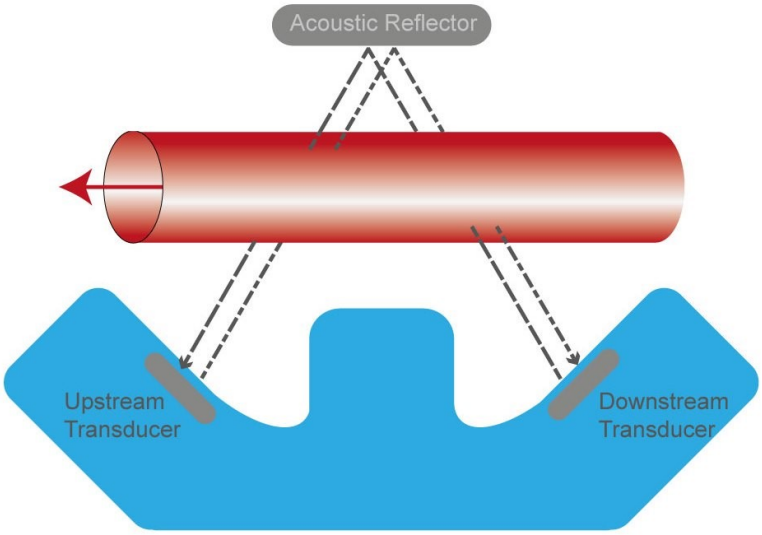

Figure II: Transonic flow probe.
The diagram shows the of path of ultrasound pulse from the up- to the downstream transducer and back, passing through blood vessel in which absolute blood flow will be determined.

The downstream transducer emits and ultrasound pulse which passes through the vessel, before being reflected by the acoustic reflector, passing through the vessel a second time and sensed by the upstream transducer. The time for the ultrasound wave to travel this distance is measured as the downstream transit time (t_{down}). As the ultrasound wave propagates in the same direction as the flow in the vessel it undergoes a phase shift, and the transit time is less than it would be without any flow in the vessel by an amount proportional to the average blood velocity multiplied by the path length over which the velocity is measured. The upstream transducer also emits an ultrasound pulse that is reflected, transects the vessel twice and is sensed by the downstream transducer. In this case, the wave propagates against the direction of blood flow, and so the upstream transit time (t_{up}) is increased from the time without flow in the vessel. Alternating signals are produced by the upstream and downstream transducer at 1ms intervals. The difference between upstream and downstream integrated transit times is therefore a measure of volume flow (reported as $ml.min^{-1}$) through the length of the vessel insonated. Ultrasonic beams which do not intersect the vessel do not contribute to the flow integral (271).

Time-transit ultrasonic flow probes have some advantages over other methods of flow measurement. As each ultrasound signal passes through the vessel twice, angulation of the vessel has negligible effect on the calculation of volume flow, as the increase in one flow vector in the outward path is offset by the corresponding decrease in the flow vector of the return path (unlike Doppler velocimetry where angle of insonation needs to be corrected for). As phase and not frequency shift (unlike Doppler ultrasound velocimetry) is calculated, the flow of liquid, not the passage of erythrocytes is measured, meaning time transit flow probes are unaffected by changes in haematocrit or cell content of the blood (350). They are also able to zero calibrate themselves by sending two consecutive upstream phase measurements without the need for clamping of the vessel to create a situation of no-flow prior to measurement (like electromagnetic flow probes) which reduces the handling of vessels and subsequent vasospasm (280).

When used with a suitable acoustic coupling agent (351) to exclude air from the acoustic window they can be used in the acute setting to monitor arterial flow; for chronic measurement the development of fibrous encapsulation within 7 days of implantation creates a stable pocket filled with tissue fluid which ensures air-free coupling (352). This means they can be implanted loosely around blood vessels, avoiding irritation or constraint of blood vessels and allowing vessel growth in the fetus (280).

APPENDIX III: CRITERIA USED TO IDENTIFY ARTEFACTUAL PHYSIOLOGICAL DATA

Variable	Exclusion criteria			Reason for artefactual data
	If above	If below	Other	
Maternal systolic blood pressure (mmHg)	300	0	If < 5 mmHg different from diastolic blood pressure	Catheter blocked (non pulsatile flow), calibration incorrect, or data cable pin damaged
Maternal diastolic blood pressure (mmHg)	300	0	If < 5 mmHg different from systolic blood pressure	
Maternal heart rate (bpm)	200	0	n/a	Catheter blocked (non pulsatile flow)
Fetal systolic blood pressure (mmHg)	300	0	If < 5 mmHg different from diastolic blood pressure	Catheter blocked (non pulsatile flow), calibration incorrect, or data cable pin damaged
Fetal diastolic blood pressure (mmHg)	300	0	If < 5 mmHg different from systolic blood pressure	
Fetal heart rate (bpm)	300	0	If > 20 bpm difference between FHR derived from catheter and flow probe	
Fetal maximum femoral blood flow ($ml.min^{-1}$)	500	0	If < 5 ml.min-1 different from minimum blood flow	Flow probe transmitting non-pulsatile data (calibration error, data cable damage, poor acoustic window, probe displacement).
Fetal minimum femoral blood flow ($ml.min^{-1}$)	500	0	If < 5 ml.min-1 different from minimum blood flow	
Fetal mean femoral blood flow ($ml.min^{-1}$)	500	0	If < 5 ml.min-1 difference between maximum and minimum blood flow	
Fetal femoral blood flow amplitude ($ml.min^{-1}$)	1000	0	If < 5 ml.min-1 difference between maximum and minimum blood flow	
Amniotic pressure (mmHg)	100	0	If > fetal diastolic blood pressure	Catheter blocked or displaced

Table III: Exclusion criteria for artefactual data.
The table lists the exclusion criteria for maternal and fetal blood pressure and blood flow readings in Group R animals which were determined to be there result of equipment malfunction or incorrect calibration.

APPENDIX IV: HIFU TRANSDUCER CALIBRATION AND ESTIMATION OF IN SITU INTENSITY

Introduction

In situ intensity is an estimate of the actual acoustic energy delivered to the focus per second, accounting for losses (attenuation) in the overlying tissues. It can be estimated by subtracting predicted energy losses (derived from tissue characterisation studies of relevant overlying tissues) from the amount of acoustic energy a HIFU transducer produces at a given drive voltage, the free field intensity. Use of in situ intensity rather than free field intensity essentially corrects for depth of the target tissue and type(s) of overlying tissue, allowing outcomes of individual exposure series to be more readily compared to one-another.

Every HIFU transducer is unique and therefore requires individual calibration to calculate the free-field intensity (a measure of the maximum acoustic energy delivered per second to the focus through a lossless medium) generated by the transducer. **Calibration of the transducer and calculation of free-field intensities for a given drive voltage (the actual setting used on the signal generator to select power level) for the transducer used in this study was performed by Drs Rivens and Civale at the Institute of Cancer Research,** and the final results were supplied to me in order to estimate in situ intensity, as described in the methods section below. The tissue characterisation studies were performed by me, **using a pre-prepared experimental protocol provided by Dr Civale.**

Methods: Calculation of free field intensity from drive voltage

Free-field spatial peak temporal average intensity (I_{SPTA}), measured in $W.cm^{-2}$, was calculated from pressure measured at the focal peak in degassed, deionised water using a calibrated (at the National Physical Laboratories, Teddington) membrane hydrophone (Precision Acoustics, Dorset, UK). Measurements were made over a range of relatively low drive voltages, V_{drive} quantified on a logarithmic dBm scale in order to avoid acoustic cavitation damage to the piezoelectric hydrophone element. An exponential fit to the calculated I_{SPTA} values was used to extrapolate to the free field intensities at the higher drive levels used in the in vivo studies.

Methods: Tissue characterisation

A finite amplitude insertion substitution (FAIS) tissue characterisation system (Figure IV.i) was used to determine the ultrasonic attenuation of relevant tissues for planning of HIFU exposure

conditions and interpretation of vascular occlusion outcomes relative to acoustic energy used. The FAIS system uses a pair of 2.5 MHz weakly focused (20 mm diameter, 100 mm focal length) transducers (Imasonic SA, France) co-axially aligned as a transmitter-receiver pair. Pulsed ultrasound energy was transmitted through water (reference medium) and samples held within a pair of flat, parallel 19 μm thick Melinex membranes (the sample holder windows) and detected by either the "receiver" transducer or, after reflection, by the transmitter. The sample holder position in three orthogonal directions was determined by a motion controller able to move in x, y and z. The offset of the sample from the centre of the sample holder window, the size of the region of tissue to be sampled and of the spacing between measurement points were manually inputted into a custom written tissue characterisation Matlab script GUI (MathWorks, USA). This Matlab interface controlled the FAIS system's motion controller and ultrasonic pulser/receiver (JSR DPR300, Imaginant Inc., USA) and recorded data from a thermocouple (TC01, National Instruments, USA) placed in the water tank adjacent to the sample and the oscilloscope (3205A, PicoTechnology, USA) which measured the reflected and transmitted ultrasound pulses. The software also performed post processing of data acquired to calculate sample thickness, speed of sound, attenuation coefficient ($dB.cm^{-1}.MHz^{-1}$) and frequency dependence of the attenuation coefficient. The software included filters to remove unreliable measurements by ensuring correct echo detection for thickness and therefore sound speed measurements, by filtering out frequency dependent data which were too noisy. It also allowed attenuation level filtering to allow removal of data from the tissue maps which was obtained through water or through the outer edges of the sample where interface effects produced artificially high results. The remaining data in the characterisation maps were used to produce average and standard deviation values for the quantities listed above.

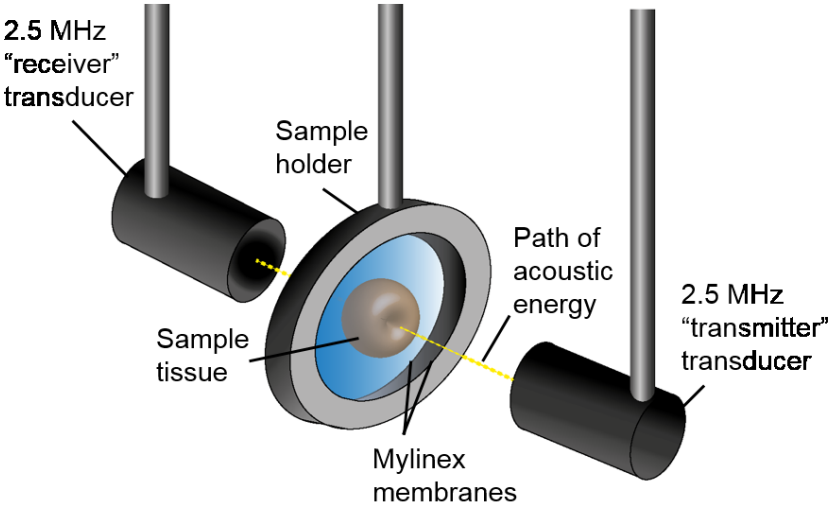

Figure IV.i: FAIS system setup.
The illustration shows the arrangement of a pair of 2.5 MHz transducers co-axially aligned to direct ultrasound energy through the tissue sample, held in degassed water between two 19 μm thick Melinex membranes by the sample holder placed between the transmitter-receiver pair of transducers.

Measurement of the attenuation coefficient, speed of sound and sample thickness were determined in (i) fresh ovine skin with wool and lanolin removed, subcutaneous adipose tissue, rectus sheath and muscles as a composite of layers, (ii) uterus, (iii) placental tissue, and (iv) amniotic fluid. Samples from the maternal abdomen were taken from positions defined as the central, axial or lateral aspects (defined in Figure IV.ii).

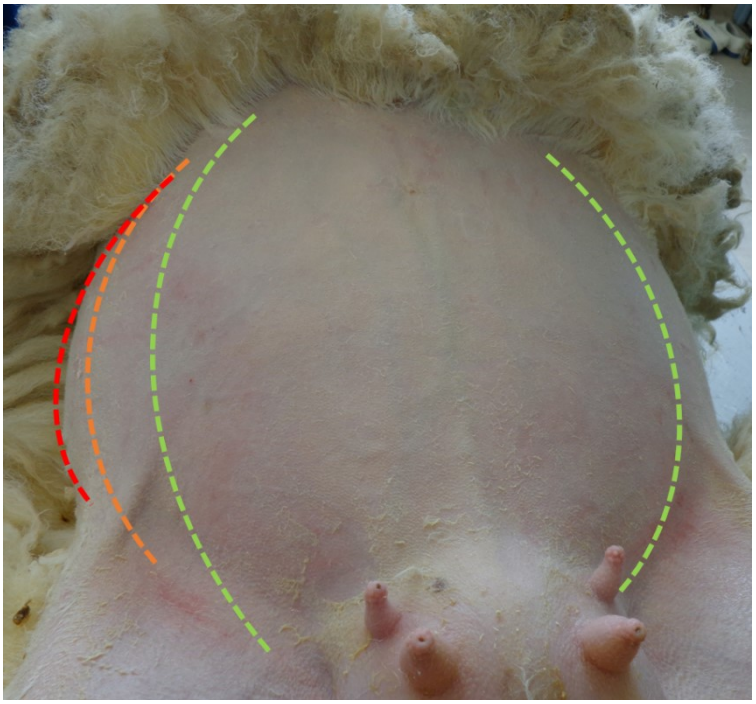

Figure IV.ii: Sheep abdominal regions.
The "central" area of the sheep abdomen is shown demarcated by green lines overlaid on the photographic image. The "axial" area falls between the green and orange lines on both sides (only show on right) and the "lateral" area falls between the orange and red lines on both sides (only shown on right). The sheep abdominal skin has been exposed by shaving with clippers, then 24-48h later washed with iodine to remove dirt and lanolin, chemical depilated to remove short hairs, then washed again with plain water. The upper border of the photo is caudal.

Maternal skin was shaved, washed with iodine, chemically depilated and washed in water to reduce the risk of trapping air bubbles on its surface, which can cause reflection or scattering of HIFU energy, and so introduce measurement artefacts in this setting. Layers of skin, adipose tissue and between one and three layers of muscle (dependant on the location on the maternal abdomen from which the sample was taken) were not separated before testing.

As we needed to know the attenuation of the maternal skin, fat and recuts overlying the uterus to plan in vivo HIFU exposures, measuring the overlying tissue as a composite structure was the most directly relevant way to perform these measurements. Additionally, measuring attenuation in thicker structures is more reproducible than thinner structures, and not separating layers also reduces the risk of trapping air bubble at any of the interfaces, from which air was otherwise excluded, so reducing measurement artefacts.

Each abdominal sample was cut into a rectangular shaped area of even thickness. Placentomes were separated from the uterine tissues prior to measuring; placentomes were categorised by type and their allantoic membranes were removed to reduce the risk of the formation of air pockets, but tested whole. The time between euthanasia of the ewes and the start of tissue characterisation was less than 60 minutes in all cases; however, in some cases tissue samples could not be used due to hardening of the rectus sheath post-mortem.

Results: Free field intensity

Free field intensities were calculated at drive voltages between -22 and -11 dBm. These values are plotted with black symbols in Figure IV.iii, and a line of best fit was applied to them. This equation was then used to extrapolate the free field intensity of drive voltages selected during in vivo studies (-4 to -9 dBm). The degree of uncertainty associated with this was reported as ±10%. For this reason, free field intensities, when reported, are given to 2 significant figures only.

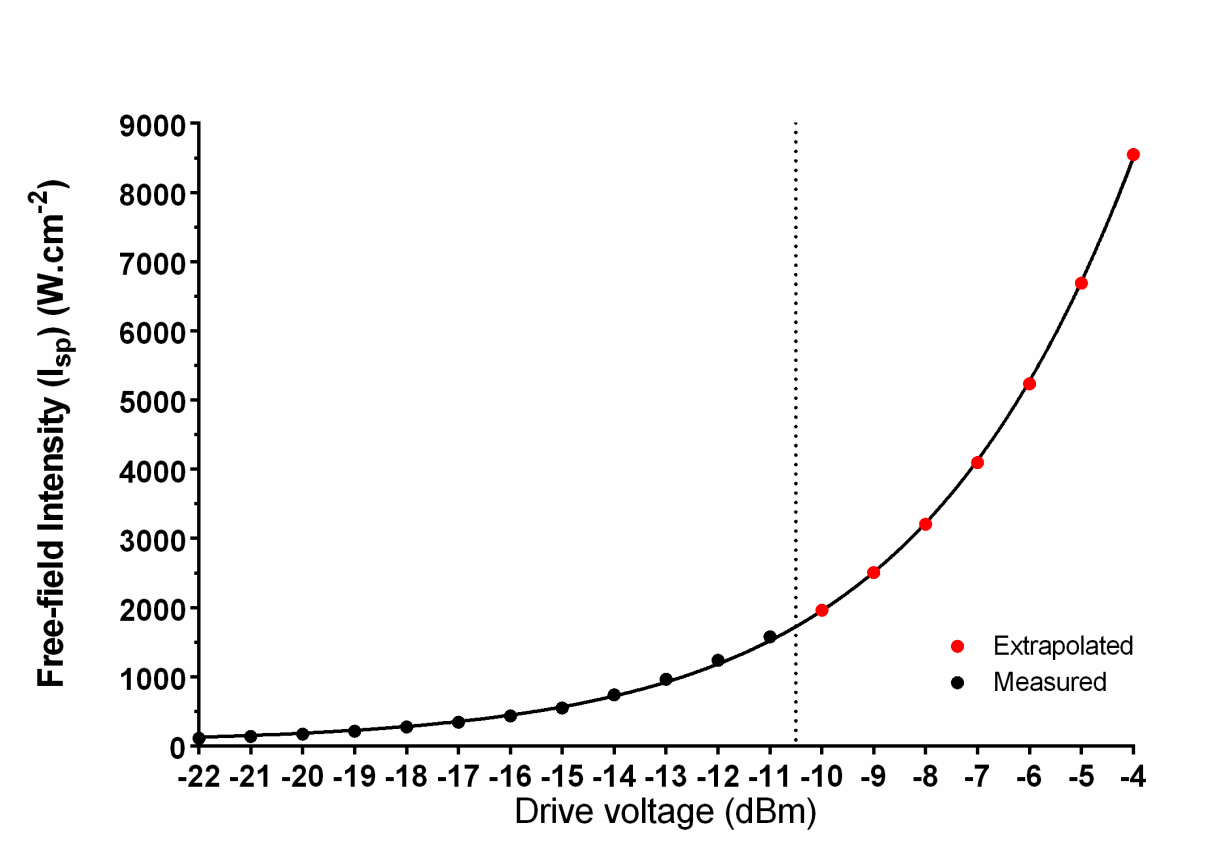

Figure IV.iii: Measured and calculated free field intensities.
The graph shows free field intensities measured by a membrane hydrophone in a deionised, degassed water tank at given drive voltages (n=12, black circles) and the extrapolated values for free field intensity at higher drive voltages based on the curve of best fit (n=7, red circles).

Results: Tissue characterisation

Samples were obtained immediately following euthanasia in nine adult pregnant sheep during the last third of gestation. There were two central, at least two axial and at least one lateral wall tissue sample contributed from each animal (Figure IV.ii). The mean weight of the ewes was 39 kg (SD 8 kg) and ranged from 29 – 54 kg. The results of tissue characterisation of these samples are shown in Table IV.

	Attenuation Coefficient (α) (dB.(cm*MHz)$^{-1}$)	**Exponent of the attenuation coefficient (N)**	**Attenuation at 1.66 MHz (dBm.cm^{-1})**	**Measured thickness (cm)**	**Number of samples**
Skin, subcutaneous adipose tissue, rectus sheath and muscles (central)	0.96 ± 0.20	1.36 ± 0.11	1.91 ± 0.51	0.93 ± 0.09	18
Skin, subcutaneous adipose tissue, rectus sheath and muscles (axial)	1.91 ± 0.53	1.09 ± 0.21	3.32 ± 1.28	1.58 ± 0.10	19
Skin, subcutaneous adipose tissue, rectus sheath and muscles (lateral)	3.05 ± 0.72	0.98 ± 0.40	5.01 ± 2.23	2.28 ± 0.27	11
Uterus	0.29 ± 0.06	1.75 ± 0.17	0.70 ± 0.17	-	24
Placentome (type A/B)	0.34 ± 0.06	1.75 ± 0.22	0.83 ± 0.20	-	28
Placentome (type C/D)	0.30 ± 0.05	1.88 ± 0.32	0.78 ± 0.21	-	16
Amniotic fluid	0.02 ± 0.01	1.05 ± 0.2	0.03 ± 0.01	-	5

Table IV: Tissue characterisation results.
Values represent the mean ± standard deviation of the attenuation coefficient, exponent of the attenuation coefficient and measured thickness of the types of tissue and fluid samples listed. Attenuation at 1.66 MHz is given by $\alpha 1.66^{N}$, for the HIFU transducer used in this study.

Based on this, for transuterine exposures, a weighted average of the calculated attenuation coefficient of the uterus and placental tissues of 0.8 ± 0.2 dB.cm^{-1} (at 1.66 MHz) was used to estimate total energy loss (in dB) between the skin and target region. As the attenuation of water and amniotic fluid were treated as negligible, the following equation was used to estimate energy losses as a result of passing through maternal uterine tissue:

Transuterine energy loss = 0.8 x target depth

However, it should be noted that the error in this calculation arising from the tissue characterisation studies was effectively ±25%, compounded on the ±10% error from conversion of drive voltage to free field intensity. Hence, while estimated in situ intensity is quoted to 2 significant figures, this may still represent a greater degree of accuracy than actually merited. However, quoting to 1 significant figure did not allow sufficient discrimination between the energy levels delivered to tissue.

Tissue characterisation results show that for transdermal exposures, the additional thickness of the rectus sheath and muscles away from the central portion of the sheep abdomen would result in much higher energy losses. If exposures were constrained to the central region only (demarcated in green, Figure IV.ii) a standard value of total attenuation of skin, adipose tissue and rectus sheath and muscle of 1.9 ± 0.5 $dB.cm^{-1}$ (at 1.66 MHz) could be anticipated in addition to the attenuation from the uterus and placentomes. Again, this shows a degree of uncertainty in this result of ±25%. However, using the value of 1.9 $dB.cm^{-1}$ for the attenuation of skin, fat and rectus and a value of 0.8 $dB.cm^{-1}$ for the attenuation of uterus and placental tissue, the following equation can be used to estimate energy losses in transdermal exposures:

Trans-dermal energy losses = 0.8(target depth – 0.9) + (1.9 x 0.9)